1,4-DIHYDROPYRIDINES AS VERSATILE REAGENTS IN PHOTOCHEMICAL CARBON-CARBON BOND-FORMING PROCESSES

Nurtalya Alandini

UNIVERSITAT ROVIRA i VIRGILI

1,4-Dihydropyridines as Versatile Reagents in Photochemical Carbon-Carbon Bond-Forming Processes

NURTALYA ALANDINI

DOCTORAL THESIS
2020

UNIVERSITAT ROVIRA I VIRGILI
1,4-DIHYDROPYRIDINES AS VERSATILE REAGENTS IN PHOTOCHEMICAL CARBON-CARBON BOND-FORMING PROCESSES
Nurtalya Alandini

UNIVERSITAT ROVIRA I VIRGILI
1,4-DIHYDROPYRIDINES AS VERSATILE REAGENTS IN PHOTOCHEMICAL CARBON-CARBON BOND-FORMING PROCESSES
Nurtalya Alandini

Nurtalya Alandini

1,4-Dihydropyridines as Versatile Reagents in Photochemical Carbon-Carbon Bond-Forming Processes

Doctoral Thesis

Supervised by Prof. Paolo Melchiorre

ICIQ – Institut Català d'Investigació Química

UNIVERSITAT ROVIRA i VIRGILI

Tarragona

2020

UNIVERSITAT ROVIRA i VIRGILI

ICIQ Institut Català d'Investigació Química

Prof. Paolo Melchiorre, ICREA Research Professor & ICIQ Group Leader

I STATE that the present study, entitled "1,4-Dihydropyridines as Versatile Reagents in Photochemical Carbon-Carbon Bond-Forming Processes", presented by NURTALYA ALANDINI for the award of the degree of Doctor, has been carried out under my supervision at the Institut Català d'Investigació Química (ICIQ).

Tarragona, June 1st 2020

Doctoral Thesis Supervisor

Prof. Paolo Melchiorre

UNIVERSITAT ROVIRA I VIRGILI
1,4-DIHYDROPYRIDINES AS VERSATILE REAGENTS IN PHOTOCHEMICAL CARBON-CARBON BOND-FORMING PROCESSES
Nurtalya Alandini

Acknowledgements

This thesis has benefited greatly from the support of many people, some of whom I would like to thank here.

First of all, I would like to express my deepest gratitude to Prof. Paolo Melchiorre for giving me the opportunity to be part of his research group and for providing endless support and guidance during my PhD.

I am very grateful to the past and present members of the Melchiorre group. Thanks to Dr. Bertrand Schweitzer-Chaput, Dr. Giacomo Crisenza, Daniele Mazzarella, Pablo Bonilla, Dr. Catherine Holden, Dr. Giulio Goti, Dr. Zhong-Yan Cao, Dr. Sara Cuadros, , Eduardo de Pedro, Dr. Tamal Ghosh, Dr. Eva Raluy, Emilien Le Saux, Adriana Faraone and Davide Spinnato for the support and friendship. Special thanks to Dr. Luca Buzzetti for the help and fruitful discussion about chemistry and many other things during my PhD. To Eugenio Gandolfo for being the support system and always be there when needed. I would also like to thank the people I have shared projects with: Dr. Cristofer Pezzetta, Dr. Charlie Verrier, Dr. Hamish Hepburn, Dr. Alberto Vega-Penaloza and Prof. Dr. Gianfranco Favi. I would like to express my gratitude for Dr. Lorna Piazzi, Maria Checa, and Nuria Planella for the administrative support and to Dr. Laia Cuesta for the support around the laboratory.

Very special thanks to Dr. Robert Davidson and Prof. Dr. Giacomo Bergamini, who kindly accepted and support me to conduct my secondments in Dr. Reddy's Laboratories and University of Bologna. I would like to thank all the research support units at ICIQ, in particular the NMR staff, the spectroscopy unit, the chromatography unit and the high-throughput experimentation unit.

Finally, deepest gratitute to my family and friends who always provide me constant support from thousand miles away over these past years.

Support from the European Union's Horizon 2020 Research and Innovation Program under the Marie Sklodowska-Curie Actions H2020-MSCA-ITN-2016-722591 (PHOTOTRAIN).

List of Publications

Some of the results presented in this thesis have been published:

- Verrier, C., Alandini, N., Pezzetta C., Moliterno, M., Buzzetti, L., Hepburn, H. B., Vega-Peñaloza, A., Silvi, M. and Melchiorre, P., "Direct Stereoselective Installation of Alkyl Fragments at the β-Carbon of Enals via Excited Iminium Ion Catalysis". *ACS Catalysis*, **2018**, *8*, 1062-1066.

- Alandini, N., Buzzetti, L., Favi, G., Schulte, T., Candish, L., Collins, K. D., and Melchiorre, P., "Amide Synthesis by Nickel/Photoredox-Catalyzed Direct Carbamoylation of (Hetero)Aryl Bromides". *Angew. Chem. Int. Ed.*, **2020**, *59*, 5248-5253.

UNIVERSITAT ROVIRA I VIRGILI
1,4-DIHYDROPYRIDINES AS VERSATILE REAGENTS IN PHOTOCHEMICAL CARBON-CARBON BOND-FORMING PROCESSES
Nurtalya Alandini

Untuk Ayah dan the Bona Girls.

Table of Contents

Chapter I

General Overview

1.1. Photochemistry

Light initiates many chemical reactions that occur in the biological system and in nature. Through photosynthesis, plants harvest the energy of light to convert raw materials into chemical energy in the form of carbohydrates. This natural process has long inspired scientists, in particular chemists, to use light as an abundant energy source to induce chemical reactions. Although scattered reports on the photochemical reactivity of organic molecules had been very early documented,[1] it was not until the beginning of the 20th century that photochemistry was considered as an independent branch of chemistry.[2] In pioneering studies, Giacomo Ciamician and Paul Silber extensively investigated the behavior of organic substances towards sunlight and thereby established the field of organic photochemistry.[3]

Today, the conceptual foundations of photochemistry are firmly established. The field of photochemistry concerns chemical reactions promoted by the absorption of light. Therefore, photochemistry deals with the reactivity of molecules in their electronically excited states. Absorption of a photon of suitable energy – typically of visible or ultraviolet (UV) light – by a molecule, promotes the transition of an electron from the highest occupied molecular orbital (HOMO) to the lowest unoccupied orbital (LUMO, Figure 1.1a).[4] This implies that the molecule passes from its ground state to an electronically excited state (Figure 1.1b). Because light excitation causes changes in the electronic structure of a molecule, its chemical and physical properties in the excited state can be significantly different from that of the ground state. Thus, light-mediated chemistry can offer interesting new reactivity patterns that are unavailable under thermal activation.

[1] a) Roth, H. D., "The Beginnings of Organic Photochemistry", *Angew. Chem. Int. Ed.* **1989**, *28*, 1193. b) König, B., "Chemical Photocatalysis", Berlin/Boston, Walter de Gruyter GmbH, 2013.
[2] Albini, A., "Photochemistry: Past, Present and Future", Berlin Heidelberg, Springer-Verlag, 2016.
[3] a) Ciamician, G., Silber, P., "Chemische Lichtwirkungen" *Ber. Dtsch. Chem. Ges.* **1910**, *43*, 45. b) Ciamician, G., "The Photochemistry of the Future", *Science*, **1912**, *926*, 385.
[4] Balzani, V., Ceroni, P., Juris, A., "Photochemistry and Photophysics: Concept, Research and Applications", Weinheim, Wiley-VCH, 2014.

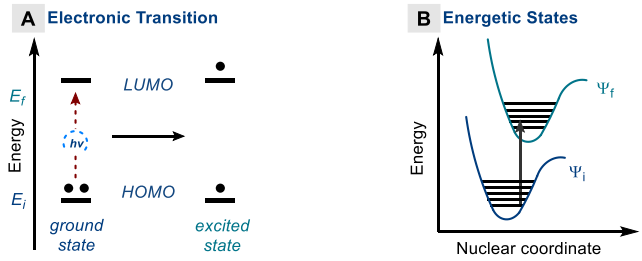

Figure 1.1. a) Energy of the absorbed photons promotes the transition of an electron from the highest occupied molecular orbital (HOMO) to an unoccupied orbital (LUMO) providing access to an b) electronically excited state Ψ_f.

Photochemical transformations can proceed according to two main activation strategies: *i*) by direct photoexcitation of substrates or intermediates, or *ii*) by employing light-absorbing catalysts that, upon excitation, can activate achromatic substrates. In the former case, a substrate directly participates in the light-absorption and can access its electronically excited state. These excited molecules are both better electron donors and electron acceptors than in the ground state and can engage in single-electron transfer (SET) events with other reaction components. For example, 1,4-dihydropyridine derivatives **1**, potent hydride donors in the ground state, can switch on new reactivity patterns upon light excitation and become strong SET reductants. In the excited state, **1*** ($E^*(\mathbf{1}^{\bullet+}/\mathbf{1}^*) \approx -2.28$ V vs SCE) is capable to reduce α-bromo ketones **2** to the corresponding ketones **3** (Scheme 1.1.).[5]

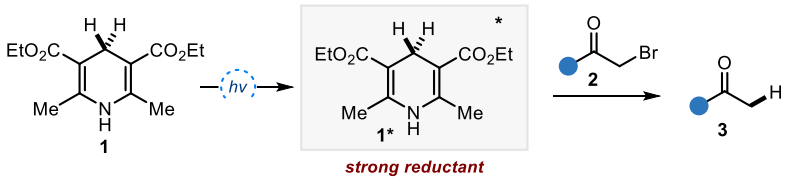

Scheme 1.1. SET reduction of α-bromo ketones **2** by the excited 1,4-dihydropyridine **1***.

Similarly, light irradiation of reaction intermediates can promote them to the excited states, from where they can activate other substrates.[6] As an example of this activation strategy, our research laboratories recently exploited the light excitation of chiral enamines, organocatalytic intermediates with a known nucleophilic character in the ground state, to

[5] Jung, J., Kim, J., Park, G., You, Y., Cho, E. J., "Selective Debromination and α-Hydroxylation of α-Bromo Ketones Using Hantzsch Esters as Photoreductants", *Adv. Synth. Catal.* **2016**, *358*, 74.
[6] Holden, C. M.; Melchiorre, P., "Photochemistry and Excited-State Reactivity of Organocatalytic Intermediates" Photochemistry, **2020**, *47*, 344.

drive the asymmetric functionalization of aldehydes (Scheme 1.2.).[7] The enamine intermediate **I**, generated upon condensation of an aldehyde **4** with the chiral secondary amine **7**, is primarily understood as a nucleophile in the ground state.[8] Upon absorption of near UV light ($\lambda \approx 400$ nm), the enamine can populate its excited states to become a potent SET reductant ($E^*(\mathbf{I}^{\bullet+}/\mathbf{I}^*) \approx$ -2.50 V, vs Ag/AgCl, NaCl sat). SET reduction of suitable acceptors, such as diethyl bromomalonate **5**, generates the open-shell radical species **II**. At the same time, the ground-state nucleophilic chiral enamine **I** provides effective stereochemical control over the ensuing trap of the electrophilic radical **II**. Conceptually, this study demonstrated that the synthetic potential of organocatalytic intermediates is not limited to the ground-state domain, but could also be extended by exploiting their photochemical behavior.[9] This discovery has enabled new means to generate radicals under mild conditions and employ them in asymmetric catalytic transformations.

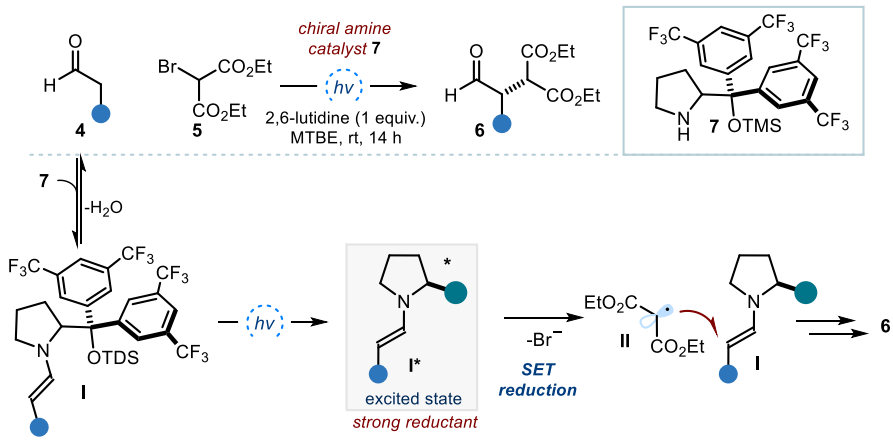

Scheme 1.2. Direct photoexcitation of enamines **I** generates a strong reductant **I*** that facilitates SET reduction of bromomalonates **5** to form radical **II**. TMS: trimethyl silyl.

Iminium ions are other classical organocatalytic intermediates with established electrophilic reactivity in the polar domain.[10] In analogy to enamines, iminium ions can also absorb light to reach an excited state and unveil a completely new reactivity. Specifically, excited iminium ions become strong oxidants, and this behavior can be exploited to generate radicals and

[7] Silvi, M.; Arceo, E.; Jurberg, I. D.; Cassani, C.; Melchiorre, P. "Enantioselective Organocatalytic Alkylation of Aldehydes and Enals Driven by the Direct Photoexcitation of Enamines" *J. Am. Chem. Soc.,* **2015**, *137*, 6120.
[8] Mukherjee, S., Yang, J. W., Hoffmann, S., List, B., "Asymmetric Enamine Catalysis", *Chem. Rev.* **2007**, *107*, 5471.
[9] Silvi, M., Melchiorre, P., "Enhancing the Potential of Enantioselective Organocatalysis with Light", *Nature*, **2018**, *554*, 41.
[10] Erkkilä, A., Majander, I., Pihko, P. M., "Iminium Catalysis", *Chem. Rev.* **2007**, *107*, 5416.

catalyze enantioselective transformations that are not achievable using thermal pathways. An example of this photochemical reactivity is depicted in Scheme 1.3.[11] Condensation of aromatic enals **8** with a chiral amine catalyst converts achromatic substrates into colored iminium ions **III**. Excitation with visible light ($\lambda \approx 420$ nm) turns the iminium ion **III**, which is electrophilic in the ground state, into a strong oxidant **III*** ($E^*(\mathbf{III}^{\bullet+}/\mathbf{III}^*) \approx +2.40$ V, vs Ag/AgCl, in CH_3CN). The chiral excited intermediate **III*** triggers the formation of benzyl radical **IV** through an SET oxidation of benzyl silane **9**. This event furnishes the 5π-electron β-enaminyl radical **V** and the benzyl radical **IV**, which is generated upon irreversible fragmentation of the carbon-silicon bond in **9**. Subsequent intermolecular radical coupling of the chiral β-enaminyl radical **V** and **IV** forms a new carbon-carbon bond while forging the stereogenic center in the β-functionalized aldehyde product **10**. This protocol enabled the direct enantioselective β-functionalization of enals with poor nucleophilic substrates **9**, that are unsuitable for ground-state iminium ion chemistry.

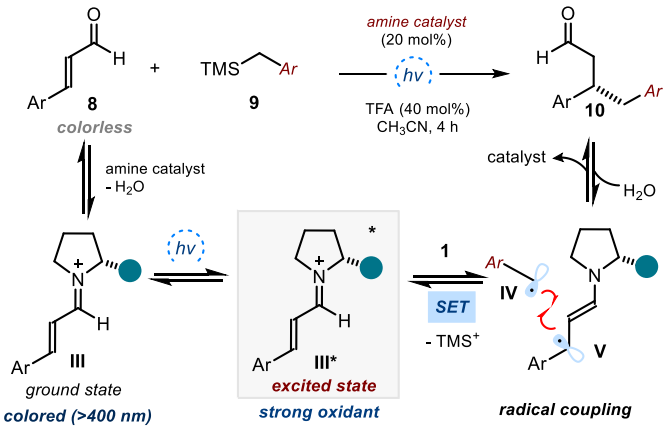

Scheme 1.3. Direct excitaton of chiral iminium ion **III** enables the stereocontrolled β-funtionalization of enals **8** with non-nucleophilic benzylsilanes **9**.

An alternative photochemical strategy capitalizes upon the use of a light-absorbing catalyst (*photocatalyst*) to accelerate a chemical reaction. These photocatalysts can harvest the energy of visible-light photons and activate achromatic organic substrates, reagents or secondary catalysts through either energy transfer or electron transfer mechanisms.[12] The field of *photoredox catalysis* uses an excited photocatalyst (PC*) to activate substrates through an SET event. This allow the formation of highly reactive open-shell intermediates under mild

[11] Silvi, M.; Verrier, C.; Rey, Y. P.; Buzzetti, L; Melchiorre, P., "Visible-light Excitation of Iminium Ions Enables the Enantioselective Catalytic β-Alkylation of Enals" *Nat. Chem.*, **2017**, *9*, 868.
[12] Fagnoni, M., Dondi, D., Ravelli, D., Albini, A., "Photocatalysis for the Formation of the C-C Bond", *Chem. Rev.* **2007**, *107*, 2725.

conditions.[13] The electronically excited photocatalysts are better reductants and oxidants than in the ground state and therefore can interact with a ground-state molecule through an oxidative or a reductive quenching cycle (Figure 1.2.). In the oxidative quenching cycle, the PC* acts as a reductant, giving an electron to a suitable acceptor (A) *via* an SET event. This process delivers the radical anion of the acceptor $A^{\bullet-}$ and the oxidized form of the PC ($PC^{\bullet+}$). The latter is an oxidant and may accept an electron from a donor (D), thereby regenerating the ground-state photocatalyst PC while completing the photoredox catalytic cycle. Alternatively, in the reductive quenching cycle, the PC* acts as a strong oxidant facilitating an SET oxidation of a suitable electron donor (D). This event provides the radical cation of the donor ($D^{\bullet+}$) and the reduced form of the photocatalyst $PC^{\bullet-}$. The later acts as a reductant and can give an electron to an acceptor (A) restoring the ground state PC. The resulting radical intermediates formed upon the SET processes from the photoredox catalyst can undergo subsequent transformations to afford the final reaction products.

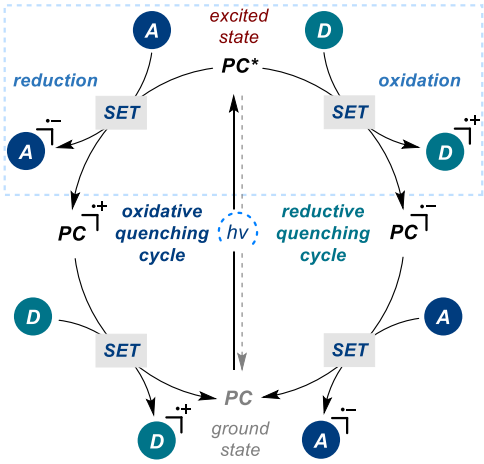

Figure 1.2. Quenching cycles in photoredox catalysis.

Many of the most commonly used visible-light photocatalysts are ruthenium and iridium polypyridyl complexes. A classical example is tris(bipyridine)ruthenium(II) complex ($Ru(bpy)_3^{2+}$). The ability of these metal complexes to function as visible-light photocatalysts has been extensively studied for applications in material and inorganic chemistry.[14] In the

[13] a) Shaw, M. H., Twilton, J., MacMillan, D. W. C., "Photoredox Catalysis in Organic Chemistry", *J. Org. Chem.* **2016**, *81*, 6898., b) Tucker, J. W., Stephenson, C. R. J., "Shining Light on Photoredox Catalysis: Theory and Synthetic Applications", *J. Org. Chem.* **2012**, *77*, 1617.

[14] a) Meyer, T. J., "Chemical Approaches to Artificial Photosynthesis", *Acc. Chem. Res.* **1989**, *22*, 63. b) Takeda, H., Ishitani, O "Development of Efficient Photocatalytic Systems for CO_2 Reduction Using Mononuclear and Multinuclear Metal Complexes Based on Mechanistic Studies", *Coord. Chem. Rev.*, **2010**, 254, 346. c) Sun Y., Giebink, N., Kanno, H., Ma, B., Thompson, M. E., Forrest, S. R., "Management of Singlet and Triplet Excitons for Efficient White Organic Light-Emitting Devices", *Nature* **2006**, 440, 908.

context of organic synthesis, the applications of these photocatalysts date back to the work of Kellogg in 1978.[15] However, it took three decades for the chemistry community to recognize the synthetic power of photoredox catalysis. The simultaneous studies from Yoon,[16] MacMillan[17] and Stephenson[18] in 2008 and 2009 are considered the dawn of photoredox catalysis (Figure 1.3.). In subsequent years, this field has experienced a rapid growth, providing synthetic chemists with powerful strategies for the activation of small molecules and for the discovery of novel bond-disconnections under exceptionally mild conditions.

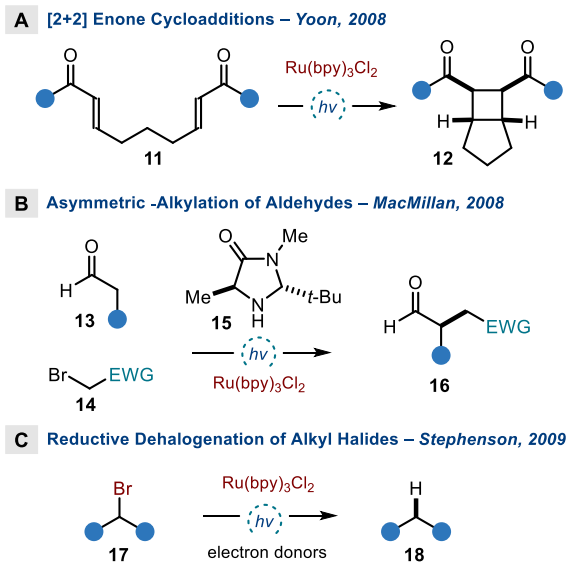

Figure 1.3. Pioneering reports that conceptualized the modern field of photoredox catalysis: a) photocatalytic [2+2] enone cycloaddition reported by Yoon; b) photocatalytic asymmetric α-alkylation of aldehydes reported by MacMillan. c) Photocatalytic reduction of alkyl halides reported by Stephenson.

The mild reaction conditions and broad functional group tolerance offered by photoredox catalysis allow its merger with other catalytic activation modes. This dual catalytic strategy has given rise to new transformations that are difficult to achieve using either catalyst system independently. The merger of photocatalysis and transition-metal catalysis, termed

[15] Hedstrand, D. M., Kruizinga, W. H., Kellogg, R. M. "Light Induced and Dye Accelerated Reductions of Phenacyl Onium Salts by 1,4-Dihydropyridines", *Tetrahedron Lett.* **1978**, 19, 1255.
[16] Ischay, M. A., Anzovino, M. E., Du, J., Yoon, T. P., "Efficient Visible Light Photocatalysis of [2+2] Enone Cycloadditions", *J. Am. Chem. Soc.* **2008**, *130*, 39, 12886.
[17] Nicewicz, D. A., MacMillan, D. W. C., "Merging Photoredox Catalysis with Organocatalysis: The Direct Asymmetric Alkylation of Aldehydes", *Science* **2008**, *322*, 77.
[18] Narayanam, J. M. R., Tucker, J. W., Stephenson, C. R. J., "Electron-Transfer Photoredox Catalysis: Development of a Tin-Free Reductive Dehalogenation Reaction", *J. Am. Chem. Soc.* **2009**, *131*, 8756.

metallaphotoredox catalysis,[19] has provided an additional tool for the development of new synthetic methodologies, allowing the direct coupling of non-traditional reaction partners.[20] In this strategy, the photoredox catalyst plays different key roles: *i*) it is responsible for the mild generation of reactive radicals from the substrates, and *ii*) it modulates the redox properties of the transition-metal complex through electron- or energy transfer processes. In 2014, two back-to-back publications from the Molander group[21] and from the MacMillan and Doyle research groups[22] demonstrated the feasibility of combining photoredox catalysis with nickel catalysis for the construction of C(sp^2)-C(sp^3) bonds (Scheme 1.6). Classic methods for C(sp^3)-fragment coupling are complicated by the competing β-hydride elimination of alkyl-metal complexes.[23] The MacMillan and Doyle collaboration demonstrated that the combination of iridium-based photoredox catalyst with a nickel catalyst allows the decarboxylative coupling of readily accessible alkyl carboxylic **19** acids with aryl bromides **21**. It is proposed that photoexcited iridium catalyst promotes the SET oxidation of the carboxylic acid **19** to form oxygen-centered radical, which upon decarboxylation generates C(sp^3)-centered radicals **VI**. Concomitantly, the nickel catalyst activates the aryl bromides and directs the reactivity towards the coupling of the radical intermediates, thus leading to the formation of cross-coupling products **22**. Concurrent with this report, the Molander group disclosed an alternative strategy using alkyl trifluoroborate salts **20** as radical coupling partners. This methodology overcame the challenge of a slow rate of transmetallation in traditional alkyl-boron cross-coupling reactions.

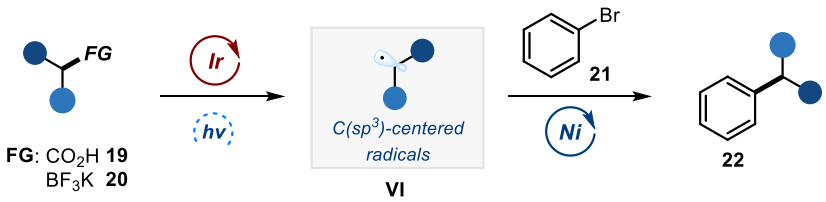

Scheme 1.4. Pioneering works on the combination of nickel catalysis and photoredox catalysis for the radical C(sp^2)-C(sp^3) cross-coupling reactions.

[19] Skubi, K. L., Blum, T. R., Yoon, T. P., 'Dual Catalysis Strategies in Photochemical Synthesis" *Chem. Rev.* **2016**, *116*, 17, 10035.
[20] Twilton, J., Le, C., Zhang, P., Shaw, M. H., Evans, R. W., MacMillan, D. W. C., "The merger of transition Metal and Photocatalysis", *Nat. Rev. Chem.,* **2017**, *52*, 1.
[21] Tellis, J. C., Primer, D. N., Molander, G. A., "Single-Electron Transmetalation in Organoboron Cross-Coupling by Photoredox/Nickel Dual Catalysis", *Science* **2014**, *345*, 433.
[22] Zuo, Z., Ahneman, D.T., Chu, L., Terret, J. A., Doyle, A. G., MacMillan, D. W. C., 'Merging Photoredox with Nickel Catalysis: Coupling of α-Carboxyl Sp^3-Carbons with Aryl Halides', *Science* **2014**, *345*, 437.
[23] Cárdenas, D. J., "Towards Efficient and Wide-Scope Metal-Catalyzed Alkyl-Alkyl Cross-Coupling Reactions", *Angew. Chem. Int. Ed.* **1999**, *38*, 3018.

In the span of only few years, metallaphotoredox catalysis has allowed major progresses in the field of cross coupling chemistry, providing non-traditional disconnections suitable for the development of new transformations. Chemists in drug discovery laboratories have also started to adopt this powerful strategy for the construction of compounds of pharmaceutical relevance.[24]

The reactivity concepts and the photochemical strategies described above have laid the foundations for developing the chemistry discussed in this doctoral thesis. Herein, I briefly detail the general objectives of my research endeavours.

1.2. General Objectives and Summary

The main objective of this doctoral studies was to implement photochemical strategies suitable for developing useful synthetic transformations that are not achievable via established thermal approaches. In particular, I investigated and exploited the unique ability of 4-substituted-1,4-dihydropyridines (DHPs) **23** to form carbon-centered radicals **VII** under mild conditions (Figure 1.4). Specifically, I used two different photochemical strategies to activate DHPs: *i*) by employing the excited-state reactivity of either a chiral organocatalytic intermediate or an external photoredox catalyst; and *ii*) through the direct visible-light-excitation of the 1,4-dihydropyridines, which produced the desired carbon-centered radicals. The resulting radicals have been then used to design useful synthetic processes.

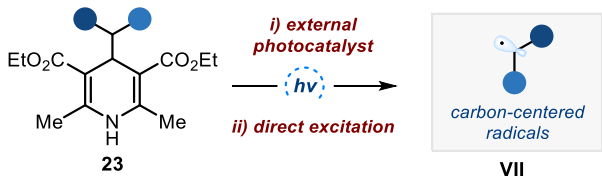

Figure 1.4. Photochemical activation of 4-substituted-1,4-dihydropyridines **23** for the generation of carbon-centered radicals **VII**.

1.2.1. Enantioselective β-Alkylation of Enals via Excited Iminium Ions

In chapter III, I discuss the asymmetric β-alkylation of enals using 4-alkyl-1,4-dihydropyridines (alkyl-DHPs, **24**) as alkyl radical precursors (Scheme 1.5.). The direct stereoselective introduction of alkyl fragments at the β-position of α,β-unsaturated aldehydes is a difficult target. Previous catalytic enantioselective conjugate addition methods based on organometallic reagents were complicated by the competing 1,2-addition reactions. Our strategy relied on the ability of photo-excited chiral iminium ions **III** to act as an SET oxidant.

[24] Blakemore, D. C., Castro, L., Churcher, I., Rees, D. C., Thomas, A. W., Wilson, D. M., Wood, A., "Organic Synthesis Provides Opportunities to Transform Drug Discovery", *Nat. Chem.* **2018**, *10*, 383.

Oxidative activation of alkyl-DHPs **24** afforded the alkyl radicals **VI**. The subsequent stereoselective radical coupling between the radicals **VI** and the chiral 5π-β-enaminyl radical **V** led to the enantioenriched chiral β-alkylated aldehydes **25** upon hydrolysis of the resulting enamine intermediate.

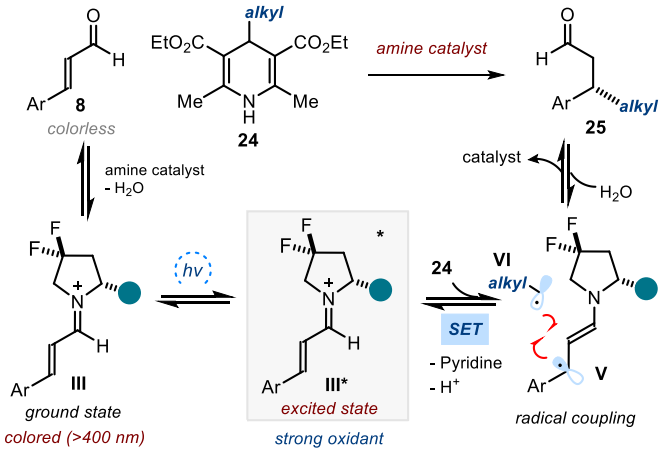

Scheme 1.5. Excited iminium ions trigger the installation of simple alkyl groups at the β-carbon of enals.

This work was undertaken in collaboration with Dr. Mauro Moliterno and Dr. Mattia Silvi, who conducted the initial studies, Dr. Charlie Verrier, who participated in the initial optimization process, and Dr. Cristofer Pezzetta, who carried out part of the reaction scope. Dr. Luca Buzzetti and Dr. Alberto Vega-Peñaloza participated in the preliminary investigations about the role of alkyl-DHPs and Dr. Hamish B. Hepburn synthesized part of the starting materials. I performed extensive method development and investigated the generality and the scope of the photochemical organocatalytic protocol.

1.2.2. Amide Synthesis by Photochemical Nickel-Catalyzed Carbamoylation of Aryl Bromides

Chapter IV details a photochemical strategy for catalytic amide synthesis *via* nickel-catalyzed carbamoylation of aryl bromides using 4-carbamoyl-1,4-dihydropyrines **26** (carbamoyl-DHP) as carbamoyl radical sources. The carbamoyl radicals were generated by two different approaches: *i*) upon direct excitation of the carbamoyl-DHP substrate **26**, or *ii*) by using an external photoredox catalyst.

The first approach (Scheme 1.8.) exploits the selective excitation of carbamoyl-DHP **26** to form a strong SET photoreductant **26***. This excited-state reactivity could be used to reduce the nickel catalyst by SET. At the same time, the resulting radical cation of **VIII** collapsed to

deliver carbamoyl radicals **IX**. The dual reactivity profile of excited carbamoyl-DHPs served to develop a photochemical nickel-catalyzed cross-coupling reaction with aryl bromides **21**.

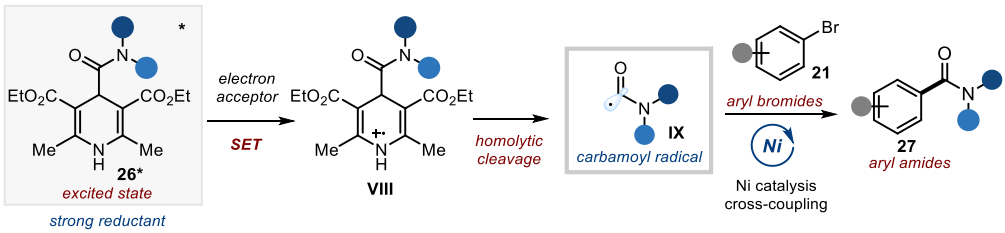

Scheme 1.6. Carbamoyl-DHPs as carbamoyl radical precursors for the synthesis of aryl amides.

A second Ni-cross coupling strategy for amide synthesis exploited the merger of photoredox catalysis and nickel catalysis (Scheme 1.7.). The method's mild reaction conditions make it tolerant to sensitive functional groups and allow the installation of an amide scaffold within pharmaceutically relevant heterocycles. This catalytic approach for the synthesis of amides could effectively complement traditional catalytic amidation processes or carbonylation chemistry, without the need to use excessive drying agents or gaseous carbon monoxide, respectively.

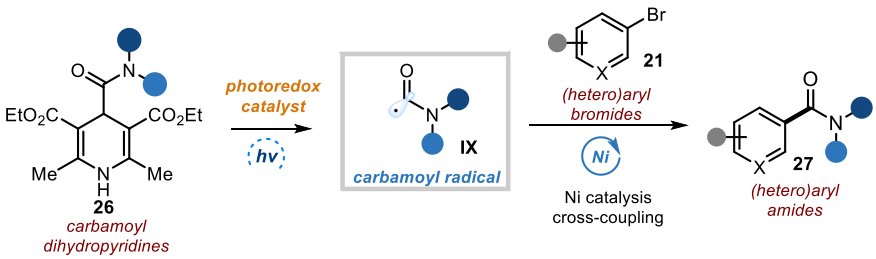

Scheme 1.7. Amide synthesis enabled by the combination of nickel catalysis and photoredox catalysis.

This work was undertaken in collaboration with Dr. Luca Buzzetti, who was involved in the discovery of the reaction and the preliminary studies, with Prof. Dr. Gianfranco Favi, who was involved in the optimization process and the synthesis of the radical precursors, and with the industrial collaborators at *Bayer AG Pharmaceuticals*, Mr. Tim Schulte, Dr. Lisa Candish and Dr. Karl D. Collins, who were involved in the expansion of the reaction scope and performed the large scale reaction. I led the optimization campaign and investigated the reaction scope.

Chapter II

The Chemistry of 1,4-Dihydropyridines

This doctoral study has largely used 1,4-dihydropyridines (DHPs) as versatile reagents to develop new photochemical processes. Therefore, the aim of this chapter is to provide the readers with a general overview of the properties and reactivity of 1,4-dihydropyridines. In particular, I will discuss the different reactivity patterns available to DHPs in their ground state and excited state (Figure 2.1).

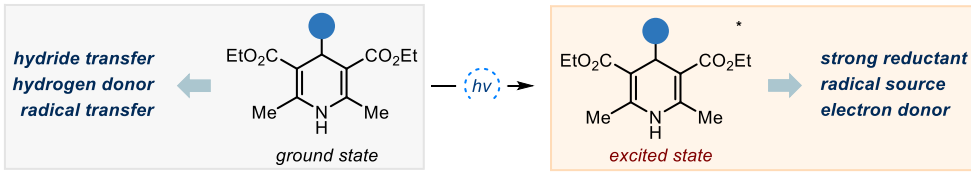

Figure 2.1. Reactivity of 1,4-dihydropyridines in the ground state and in the excited state.

2.1. Properties and Reactivity of DHPs in the Ground State

2.1.1. General Properties

1,4-dihydropyridines **4** (DHPs) were first synthesized by Artur Hantzsch in 1881 through a multicomponent condensation of an aldehyde **1**, two equivalents of β-ketoesters **2** and ammonium acetate **3** (Scheme 2.1.).[1] These molecules, also referred to as Hantzsch esters, were initially prepared as intermediates for the synthesis of pyridines through oxidative aromatization.

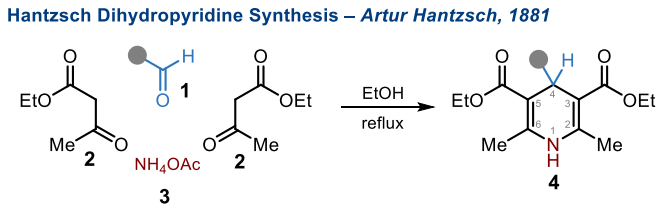

Scheme 2.1. First synthesis of Hantzsch esters by Artur Hantzsch.

[1] A. Hantzsch, A., "Condensationsprodukte Aus Aldehydammoniak und Ketonartigen Verbindungen", *Ber. Dtsch. Chem. Ges.* **1881**, 14, 2, 1637.

The high stability of 1,4-dihydropyridines can be attributed to the hyperconjugation between the π-electron system and the nitrogen lone pair.[2] Moreover, the presence of electron withdrawing groups (EWG) at the 3- and 5-positions stabilizes the molecule by extending the conjugation. This stability means that DHPs **4** are generally easily handled and stored. Dihydropyridines are analogues of cyclohexadienes (CHDs). Both compounds are especially prone to aromatization and are often employed as H-atom donor.[3] However, DHPs are more convenient to prepare and avoid the hazardous Birch reduction or alkylation in ammonia required for the typical preparation of CHDs.

The dihydropyridine scaffold is widely present in pharmaceutical and biological compounds. Its derivatives exhibit important pharmacological properties and are commonly used as calcium channel blockers to treat high blood pressure and other cardiovascular diseases (Figure 2.2).[4]

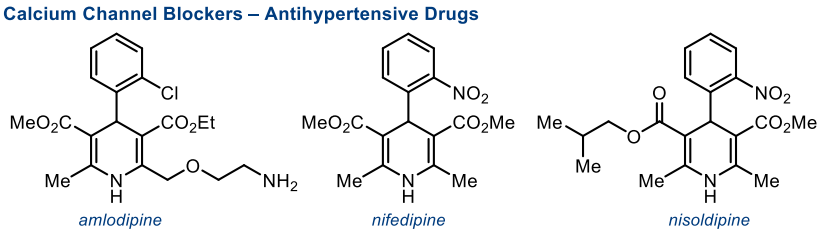

Figure 2.2. Calcium schannel blockers containing dihydropyridine scaffold.

Moreover, Hantzsch dihydropyridines are also synthetic analogue of nicotinamide adenine dinucleotide (NADH) or its phosphate (NADPH).[5] This enzyme cofactor is present in all living cells and plays an important role in the cell metabolism, acting as reductants by transferring hydride ions to the surrounding substrates. This process is referred to as *transfer hydrogenation*, and it is accomplished by the coexistence of a redox couple: the oxidized form NAD^+ **5**, which can accept electrons from a reductant, and the reduced form NADH **6**, which can donate electrons to an acceptor (Scheme 2.2.).

[2] Eisner, U., Kuthan, J., "Chemistry of Dihydropyridines", *Chem. Rev.* **1972**, 72, 1, 1-42.
[3] Walton, J. C., Studer, A., "Evolution of Functional Cyclohexadiene-Based Synthetic Reagents: The Importance of Becoming Aromatic", *Acc. Chem. Res.* **2005**, *38*, 10, 794.
[4] Lavilla. R, "Recent Developments in the Chemistry of Dihydropyridines", *J. Chem. Soc. Per. Trans. 1*, **2002**, 9, 1141.
[5] Stout, D. M., Meyers, A. I., "Recent Advances in the Chemistry of Dihydropyridines", *Chem. Rev.* 82, **1982**, *2*, 223.

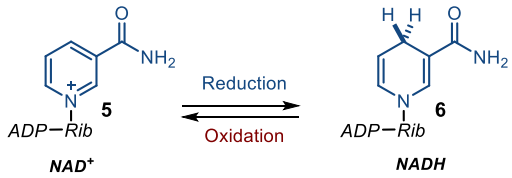

Scheme 2.2. The two oxidation states of NAD. Rib: ribose. ADP: adenine diphosphate.

2.1.2. 1,4-Dihydropyridines as Biomimetic Hydride Sources

The recognition of NADH as bioreductants have inspired chemists to employ DHPs as hydride sources for the reduction of unsaturated functionalities.[6] Driven by the aromatization energy, DHPs in their ground state can be easily oxidized to the corresponding pyridines while donating a hydride (H^-) to a suitable electrophile. Since the dihydropyridine H-DHP **7** has two hydrogen atoms (at the 1- and 4-positions) to lose, several studies have been conducted to determine which hydrogen atom is first transferred during the hydride transfer reactions. [7] Zhu, Cheng and co-workers investigated the hydride transfer mechanism from H-DHP **7** to an α,β-unsaturated ester **8** (Scheme 2.3.).[8] Through kinetic and thermodynamic investigations, they concluded that the reduction of **8** was initiated by one-step hydride migration from the C4-position of H-DHP **7** to the benzylic carbon of substrate **8**. Subsequent proton transfer from the *N*-position of **I** to the carbanion **II** delivered the reduction product **10** and the corresponding pyridine **9**.

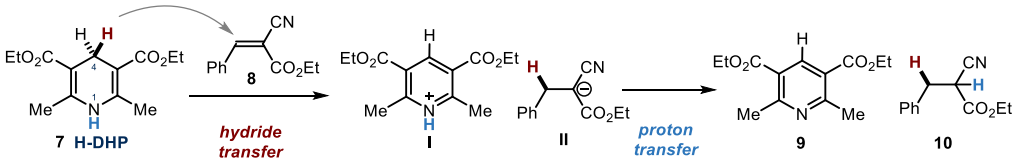

Scheme 2.3. Mechanism of hydride transfer from H-DHP **7** to α,β-unsaturated ester **8.**

In recent years, dihydropyridines have been widely used as reducing agents in organocatalytic enantioselective reactions. In 2005, Rueping and co-workers reported the asymmetric transfer

[6] Rueping, M., Dufour, J., Schoepke, F. R., "Advances in Catalytic Metal-Free Reductions: From Bio-inspired Concepts to Applications in the Organocatalytic Synthesis of Pharmaceuticals and Natural Products", *Green Chem.* **2011**, 13, 1084.

[7] Selected examples: a) Zhu, X.-Q., Liu, Y.-C., Cheng, J.-P., "Which Hydrogen Atom Is First Transferred in the NAD(P)H Model Hantzsch Ester Mediated Reactions via One-Step and Multistep Hydride Transfer?", *J. Org. Chem* **1999**, *64*, 25, 8980. b) Zhao, B., Zhu, X., Lu, Y., Xia, C.-Z., Cheng, J.-P., "Kinetic and Mechanistic Investigation on the Oxidation of Hantzsch 1,4-Dihydropyridines with the Tropylium Cation: A Model for NADH Oxidation", *Tetrahedron Lett.,* **2000**, *41,* 257.

[8] Zhu, X.-Q., Liu, H.-L., Yuan, P.-W., Liu, Y., Cao, L., Cheng, J.-P., "A Detailed Investigation into the Oxidation Mechanism of Hantzsch 1,4-Dihydropyridines by Ethyl α-Cyanocinnamates and Benzylidenemalononitriles", *J. Chem. Soc., Perkin Trans. 2,* **2000**, 1857.

hydrogenation (ATH) of imines with H-DHP **7** in the presence of catalytic amounts of chiral phosphoric acids **13**.[9] Using the chiral phosphoric acid (*R*)-**13a**, *N*-protected-arylmethylamines **12** could be prepared in good yields and enantioselectivity (Scheme 2.4.). The authors proposed that the protonation of imine **11** by the chiral phosphoric acid **13** delivers a chiral electrophilic iminium ion pair **III**. Subsequent hydride transfer from H-DHP **7** to the iminium ion yields the chiral amine **12** along with the pyridinium salt **IV**, which undergoes proton transfer to liberate the catalyst. In an independent report, the group of List demonstrated that, by employing the more sterically demanding *TRIP* phosphoric acid (**13b**), the enantioselectivity could be improved while using a lower catalyst loading.[10]

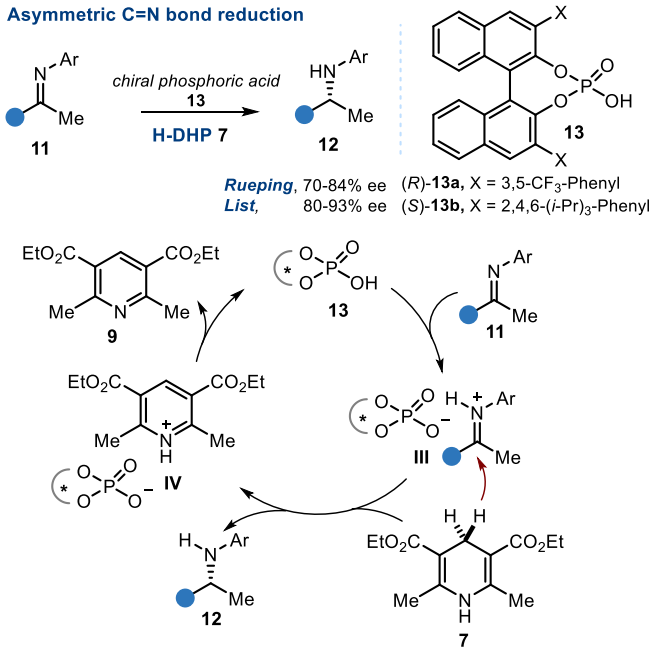

Scheme 2.4. Chiral phosphoric acid-catalyzed enantioselective reduction of imines.

In 2005, the groups of MacMillan[11] and List[12] independently reported the iminium ion-mediated asymmetric transfer hydrogenation of α,β-unsaturated aldehydes **14** with H-DHP **7**. Using chiral amine catalyst **16** and H-DHP **7**, various β-disubstituted enals **14** could be

[9] Rueping, M., Sugiono, E., Azap, C., Theissman, T., Bolte, M., "Enantioselective Brønsted Acid Catalyzed Transfer Hydrogenation: Organocatalytic Reduction of Imines", *Org. Lett.,* **2005**, *7*, 17, 3781.
[10] Hoffmann, S., Seayad, A. M., List, B., "A Powerful Brønsted Acid Catalyst for the Organocatalytic Asymmetric Transfer Hydrogenation of Imines", *Angew. Chem. Int. Ed.* **2005**, *44*, 7424.
[11] Ouellet, S. G., Tuttle, J. B., MacMillan, D.W. C., "Enantioselective Organocatalytic Hydride Reduction", *J. Am. Chem. Soc.* **2005**, *127*, 1, 32.
[12] Yang, J. M., Hechavarria Fonseca, M. T., Vignola, N., List, B., "Metal-Free, Organocatalytic Asymmetric Transfer Hydrogenation of α,β-Unsaturated Aldehydes", *Angew. Chem. Int. Ed.* **2005**, *44*, 108.

converted to the corresponding saturated aldehydes **15** in high yields and excellent enantioselectivities (Scheme 2.5.).

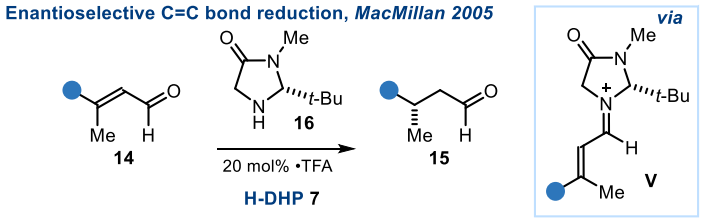

Scheme 2.5. Iminium ion-mediated asymmetric transfer hydrogenation of enals **14.**

This protocol is characterized by an enantio-convergent pathway, since the geometry of the double bond within the enal substrates **14** has no influence on the enantioselectivity of the final products. It was proposed that the (*E*)- and (*Z*)-iminium ions **V** are in fast equilibrium via the dienamine intermediate **VI** (Scheme 2.6.), which serves as a vehicle of interconversion. The subsequent rate-determining hydride transfer from H-DHP **7** proceeds much faster with the (*E*)-**V** isomer ($k(E) > k(Z)$) and, therefore, one enantiomer of the saturated aldehyde product can be predominantly formed. This feature allows the use of starting materials with low geometric purity, which enhances the practical utility of this asymmetric reduction.

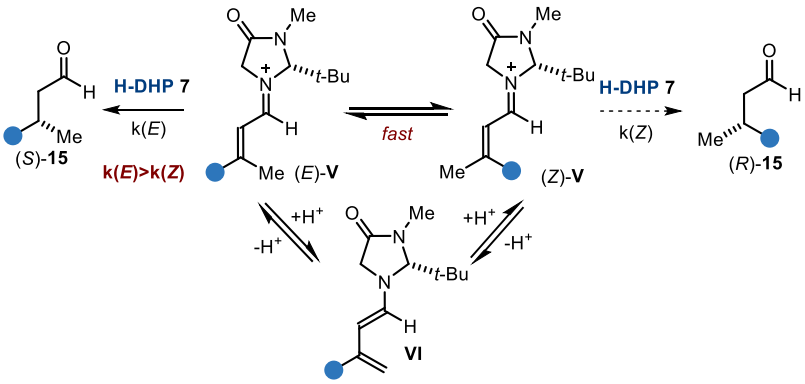

Scheme 2.6. Enantioconvergence in the iminium-ion-mediated asymmetric transfer hydrogenation reduction of enals with H-DHP **7**.

2.1.3. 4-Alkyl-1,4-dihydropyridines as Alkyl Transfer Reagents

In addition to serving as a hydride source, dihydropyridines in their ground state can also function as alkyl transfer reagents when they are decorated with easily fragmenting alkyl groups (benzyl, secondary and tertiary alkyl moieties) at the C4-position. In 2013, the group

of Tang reported the Lewis acid-catalyzed transfer alkylation of imines **16** with 4-alkyl-1,4-dihydropyridines **17** (alkyl-DHPs), allowing the formation of new C–C bonds leading to amine products **18** (Scheme 2.7.).[13] The authors proposed a concerted mechanism proceeding through the cleavage of the alkyl group to generate a nearly-instantaneous carbanion, which could sequentially add into the imine substrate **16**. Reactions in the presence of radical scavengers or an excess of Brønsted acid delivered the desired product without any effect on the yield, which excluded the possibility of a radical or a free carbanion-based mechanism.

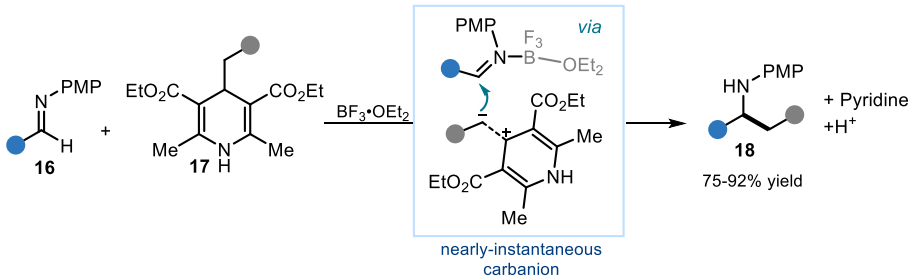

Scheme 2.7. Alkyl-DHPs **17** as alkylation reagents in the Lewis acid catalyzed alkylation of imines.

2.1.4. 1,4-Dihydropyridines as Electron- and Hydrogen Atom Donors

Recently, the chemistry of 1,4-dihydropyridines has found application in the rapidly expanding field of photoredox catalysis.[14] Because of its low oxidation potential (E^{ox} ~ 0.8-0.9 V), H-DHP **7** can indeed act as a single-electron donor in the ground state (Scheme 2.8.). For example, **7** can undergo single-electron transfer (SET) oxidation from a photo-excited photocatalyst (PC*) to deliver the radical cation **VII** and the reduced form of the photocatalyst (PC^{-}). The radical cation **VII** can also donate a hydrogen atom to another substrate, delivering the corresponding pyridinium **19**. Therefore, **7** has been successfully used in photoredox processes with the dual consecutive role to initiate reductive quenching cycles of photoredox catalysts and as an hydrogen atom source.[15]

[13] Li, G., Chen, R., Wu, L., Fu, Q., Zhang, X., Tang, Z., "Alkyl Transfer from C–C Cleavage", *Angew. Chem. Int. Ed.* **2013**, *52*, 32, 8432.
[14] Huang, W., Cheng, X., "Hantzsch Esters as Multifunctional Reagents in Visible-Light Photoredox Catalysis", *Synlett* **2017**, 28, 2, 148.
[15] a) Zhu, X.-Q., Li, H.-R., Li, Q., Ai, T., Lu, J.-Y., Yang, Y., Chen, J.-P., "Determination of the C4–H Bond Dissociation Energies of NADH Models and Their Radical Cations in Acetonitrile", *Chem. – Eur. J.* 2003, *9*, 4, 871. b) Roth, H. G., Romero, N. A., Nicewicz, D. A., "Experimental and Calculated Electrochemical Potentials of Common Organic Molecules for Applications to Single-Electron Redox Chemistry", *Synlett* **2016**, *27*, 5, 714.

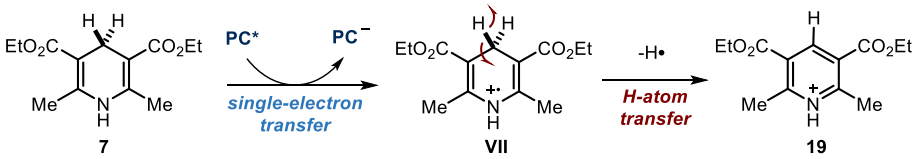

Scheme 2.8. H-DHP **7** serves as electron and hydrogen atom donor in the ground state.

In this context, the group of Stephenson demonstrated that the DHP **7**/trialkylamine **20** combination is an effective electron donor/hydrogen atom donor system for the reductive dehalogenation of organic halides (Scheme 2.9.).[16] This reaction is proposed to start with the SET from H-DHP **7** to the excited Ru(II) to form a highly reducing Ru(I) and the radical cation **VII**. Reduction of carbon-halogen bonds in **21** by Ru(I) generates the alkyl radicals **VIII**, which are capable of abstracting a hydrogen from the radical cation **VII** affording the reduced products **22**.

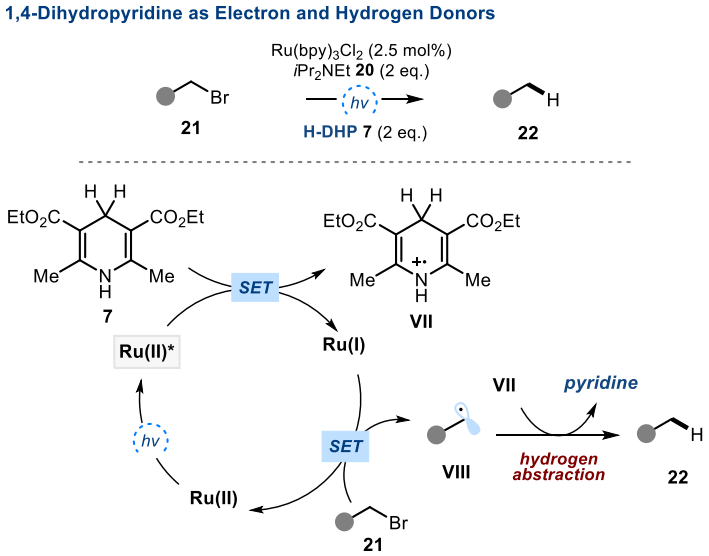

Scheme 2.9. Hantzsch dihydropyridine as an electron and a hydrogen atom donor.

2.1.5. 1,4-Dihydropyridines as Radical Precursors

More recently, alkyl-DHPs were also used as alkyl radical precursors in photoredox catalytic processes. SET oxidation of alkyl-DHPs **23** by an excited photocatalyst generates the unstable

[16] Narayanam, J. M. R., Tucker, J.W., Stephenson, C. R. J., "Electron-Transfer Photoredox Catalysis: Development of a Tin-Free Reductive Dehalogenation Reaction", *J. Am. Chem. Soc.* **2009**, *131*, 25, 8756.

radical cation **IX**, which can undergo C–C fragmentation delivering carbon-centered radical **X** and the corresponding pyridine (Scheme 2.10.).[17]

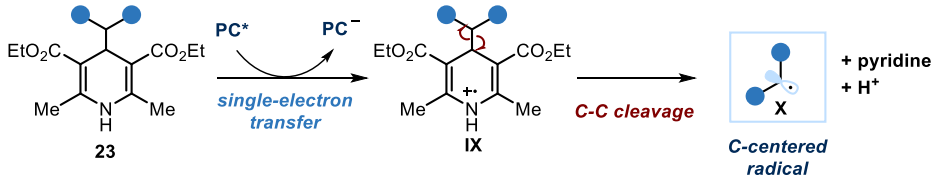

Scheme 2.10. Generation of alkyl radicals from 4-alkyl-DHPs **23** upon SET oxidation.

This reactivity was exploited by the Molander laboratories to develop a nickel/photoredox catalytic process for the construction of C(sp^2)–C(sp^3) bonds (Scheme 2.11.).[18]

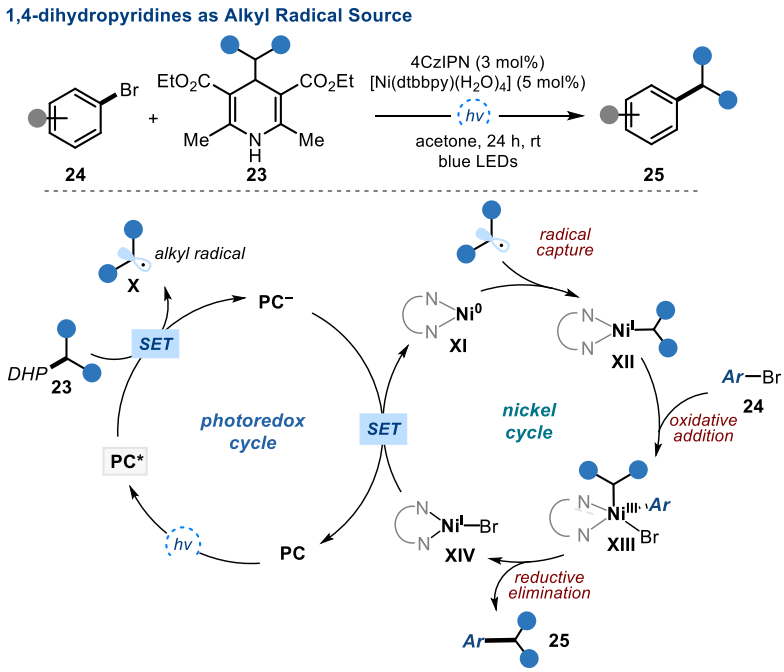

Scheme 2.11. Alkyl-DHPs **23** as radical precursors in Ni/photoredox radical cross-coupling reaction.

This reaction starts with excitation of the organic photocatalyst 1,2,3,5-tetrakis(carbazol-9-yl)-4,6-dicyanobenzene (4CzIPN, **PC**) via visible-light irradiation, which generates the excited state **PC***. This triggers the SET oxidation of the alkyl-DHPs **23**. The ensuing radical

[17] Wang, P. Z., Chen, J. R., Xiao, W. J., "Hantzsch Esters: An Emerging Versatile Class of Reagents in Photoredox Catalyzed Organic Synthesis", *Org. Biomol. Chem.* **2019**, *17*, 29, 6936.
[18] Gutiérrez-Bonet, Á., Tellis, J. C., Matsui, J. K., Vara, B. A., Molander, G. A., "1,4-Dihydropyridines as Alkyl Radical Precursors: Introducing the Aldehyde Feedstock to Nickel/Photoredox Dual Catalysis", *ACS Catal.* **2016**, *6*, 12, 8004.

cation affords the alkyl radical **X** upon C–C fragmentation. Subsequent capture of the radical **X** by the Ni(0) complex **XI** affords intermediate **XII**, which undergoes oxidative addition with aryl halides **24** to yield the high-valent Ni(III) complex **XIII**. Reductive elimination delivers the cross-coupled product **25** and the Ni(I) complex **XIV**, which is then reduced by the reduced form of the photocatalyst **PC**$^-$ to generate both the Ni(0) catalyst **XI** and the ground-state photocatalyst **PC**. Molander also recently demonstrated the compatibility of this process with DNA-encoded library synthesis.[19]

N-substituted dihydropyridines could also be employed as a source of nitrogen-centered radicals.[20] Studer and co-workers reported the hydroamination of olefins employing *N*-aminated Hantzsch dihydropyridine **26** as the radical source (Scheme 2.12.). The reaction proceeds by abstraction of a hydrogen atom from **26** by the thiyl radical **XV**, facilitating aromatization via N–N bond cleavage. Subsequent intermolecular addition of the *N*-centered radical **XVII** to an olefin **27** leads to the corresponding alkyl radical **XVIII**, which can abstract H-atom from thiophenol **29** to afford the product **28** and regenerate PhS• **XV**.

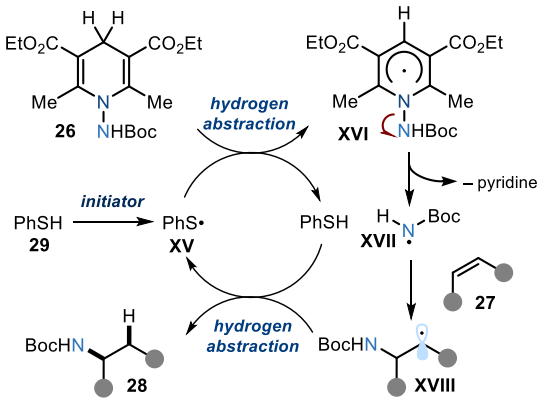

Scheme 2.12. Radical transfer hydroamination using *N*-aminated dihydropyridine **26** as the N-centered radical precursor.

2.2. Properties and Reactivity of DHPs in the Excited State

Since the discovery of NADH and its role in biological systems, model compounds that mimic this coenzyme have been developed and explored in a variety of transfer hydrogenation reactions.[21] However, these thermal reactions have mostly relied on the ability of dihydropyridines to serve as a hydride (H^-) source, thus only electrophilic compounds could

[19] Phelan J. P., Lang, S. B., Sim., J., Berritt, S., Peat, A. J., Billings, K., Fan, L., Molander, G. A. "Open-Air Alkylation Reactions in Photoredox-Catalyzed DNA-Encoded Library Synthesis", *J. Am. Chem. Soc.* **2019**, 141, 8, 3723.
[20] Guin, J., Frölich, R., Studer, A., "Thiol-Catalyzed Stereoselective Transfer Hydroamination of Olefins with N-Aminated Dihydropyridines", *Angew. Chem. Int. Ed.* **2008**, *47*, 779.
[21] Eisner, U., Kuthan, J. "Chemistry of Dihydropyridines". *Chem. Rev.* **1972**, 71, 1.

be employed.[22] The excited-states properties of 1,4-dihydropyridine derivatives have provided new reactivity frameworks to extend the scope of the hydride transfer reactions. Early studies were reported by Kurz in 1961, who described the photochemical reduction of bromotrichloromethane **30** with H-DHP **7** (Scheme 2.13.).[23] This reaction occurs through the photoexcitation of **7** and delivered the corresponding pyridine **9** and chloroform **31** as the products. However, the authors did not discuss the reaction mechanism and, therefore, the role of the excited DHP **7*** remained uncertain.

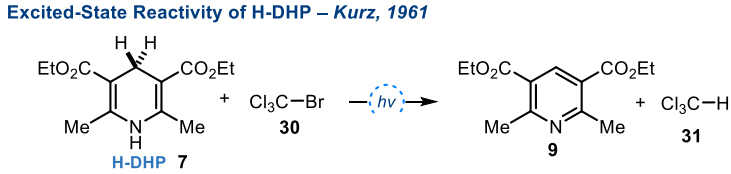

Scheme 2.13. Discovery of the excited-state reactivity of H-DHP **7**.

More than 20 years later, Fukuzumi conducted a thorough investigation on light-induced dehalogenation of benzyl halides in the presence of an NADH model compound 1-benzyl-1,4-dihydronicotinamde (BNAH, **32**, Scheme 2.14).[24]

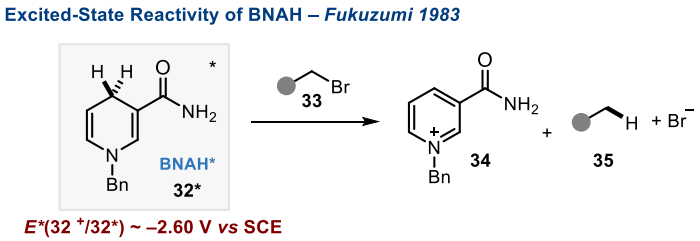

Scheme 2.14. Reduction of benzyl bromides from the excited BNAH **32.**

By means of kinetic analysis and spectroscopic techniques, it was established that the excited states of the BNAH **32** could act as strong photoreductants and mediate the SET reduction of

[22] Sammes, J. D., Widdowson, D. A. "Hydrogen Transfer in NADH Models. An Intramolecular Photochemical Redox Reaction", *J. Chem. Soc., Chem. Comm.*, **1972**, 18, 1023,
[23] Kurz, J. L., Robert Hutton, R., Westheimer, F. H., "The Photochemical Reduction of Bromotrichloromethane by Derivatives of 1,4-Dihydropyridine", *J. Am. Chem. Soc.* **1961**, 83, 584.
[24] a) Fukuzumi, S., Hironaka, K., and Tanaka, T., "Photoreduction of Alkyl Halides by an NADH Model Compound. An Electron-Transfer Chain Mechanism", *J. Am. Chem. Soc.* **1983**, 105, 14, 4722. b) Fukuzumi, S., Inada, O., Suenobu, T., "Mechanisms of Electron-Transfers Oxidation of NADH Analogues and Chemiluminescence. Detection of the Keto and Enol Radical Cations", *J. Am. Chem. Soc.* **2003**, *125*, 4808.

various electron acceptors. Since then, many methods have been developed in which the photochemistry of DHPs was exploited for the reduction of various acceptors.[25]

These findings have prompted the group of Cho to investigate the photochemical properties of Hantzsch dihydropyridine H-DHP **7** by means of electrochemical and spectroscopic analysis.[26] The ground-state oxidation potential of 0.79 V and the band gap energy of 3.07 eV were used to calculate the excited-state redox potential of H-DHP **7*** ($E^*(7^{\bullet+}/7^*) \approx -2.28$ V vs SCE, Figure 2.3.).[27] This indicated that, in the excited state, H-DHP **7*** becomes a very strong SET reductant.

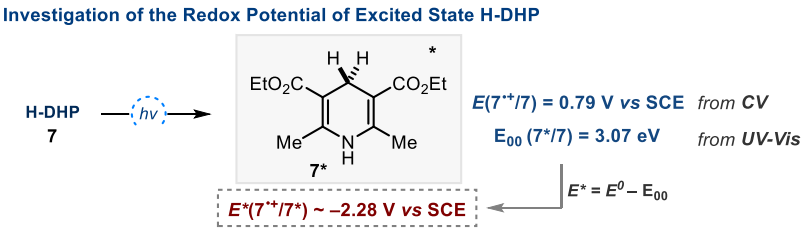

Figure 2.3. Determination of the excited-state redox potential of H-DHP **7**.

In the work reported by Cho, the ability of the excited-state H-DHP to function as reductant elicited the reductive debromination of α-bromo ketones **36** (Scheme 2.15.). Photoexcitation of **7** induces an SET-based reductive cleavage of **36**, forming a radical cation **VII** and α-keto radical **XIX**. This radical **XIX** abstracts a hydrogen from **VII** or H-DHP **7**, which delivers the reduced product **37**.

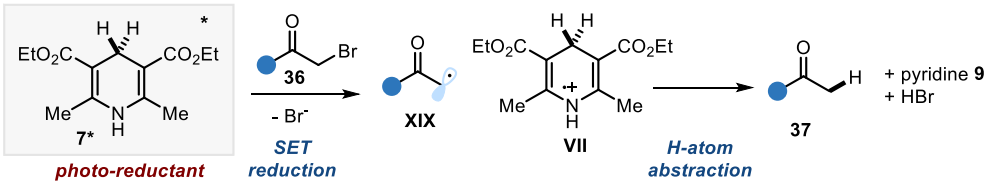

Scheme 2.15. Reductive debromination of α-bromo ketone **32** using H-DHP **7** as photoreductant.

[25] Selected examples: a) Jin, M.-Z., Yang, L., Wu, L.-M., Liu, Y.-C., Liu, Z.-L., "Novel Photoinduced Aromatization of Hantzsch 1,4-dihydropyridines" *Chem. Commun.* **1998**, 2451. b) Zhang, J., Jin, M.-Z., Zhang, W., Yang, L., Liu, Z.-L "Photoinduced Transformation of α,β-epoxyketones to β-hydroxyketones by Hantzsch 1, 4-dihydropyridine" *Tetrahedron Lett.* **2002**, *43*, 9687.
[26] Jung, J., Kim, J., Park, G., You, Y., Cho, E. J., "Selective Debromination and α-Hydroxylation of α-Bromo Ketones Using Hantzsch Esters as Photoreductants", *Adv. Synth. Catal.* **2016**, *358*, 74–80.
[27] Calculated using the Rehm-Weller equation; Rehm, D., Weller, A., "Kinetics of Fluorescence Quenching by Electron and H-atom Transfer", *Isr. J. Chem.* **1970**, *8*, 259

The photochemistry of NADPH was recently exploited by the Hyster group for the development of enzyme-catalyzed enantioselective radical dehalogenation of halolactones (Scheme 2.16.).[28]

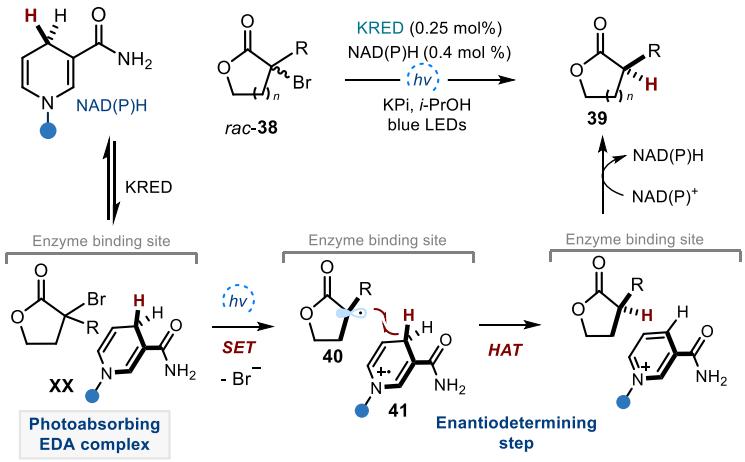

Scheme 2.16. Combination of enzyme catalysis with the photochemistry of NADH enables the enantioselective debromination of bromolactones.

The racemic lactone **38** and the cofactor NADPH are brought in close proximity through non-covalent interactions within the active site of a ketoreductase (KRED) enzyme, where they can form an electron donor-acceptor (EDA) complex. [29] This complex, which arises from the ground-state association between the electron-rich NADPH (donor) and the electron-poor halolactones **38** (acceptor), can absorb light in the visible region.[30] Irradiation of the EDA complex **XX** triggers an SET to substrate **38** to form the prochiral radical intermediate **40** upon reductive cleavage of the substrate C-Br bond. Subsequent hydrogen atom transfer (HAT) from the radical cation **41** drives the formation of the reduced chiral product **39**. The enzyme secured a high stereocontrol during this radical step. Finally, the $NADP^+$ is reduced by either isopropyl alcohol or a glucose dehydrogenase, thereby completing the catalytic cycle.

Inspired by the work of Hyster, the group of Chen showed that H-DHP **7** could also serve as an electron-donor molecule in EDA complex formation with electron-poor

[28] Emmanuel, M. A., Greenberg, N. R., Oblinsky, D. G., Hyster, T. K., "Accessing Non-Natural Reactivity by Irradiating Nicotinamide-Dependent Enzymes with Light", *Nature* **2016**, 540, 414.
[29] Crisenza, G. E. M., Mazzarella, D., Melchiorre, P., "Synthetic Methods Driven by the Photoactivity of Electron Donor-Acceptor Complexes", *J. Am. Chem. Soc.* **2020**, *142*, 5461.
[30] Although NADPH itself can absorb light in the visible region (until around 410 nm), a shift to longer wavelength (redshift) was observed in the absorbance spectrum of NADPH when the bromolactone was added to the system. This potentially indicates the formation of an EDA complex between the substrate and NADPH.

N-alkokyphthalimides **42**, which enabled the generation of alkyl radicals (Scheme 2.17.).[31] Visible-light irradiation of the EDA complex **XXI** triggers an SET step that delivers the phthalimide anion **45**, an alkoxy radical **XXII** and the DHP radical cation. Extrusion of formaldehyde from **XXII** generates the alkyl radical **X**, which can be trapped by allyl phenyl sulfone **43** through a Giese-type addition to afford products **44**.

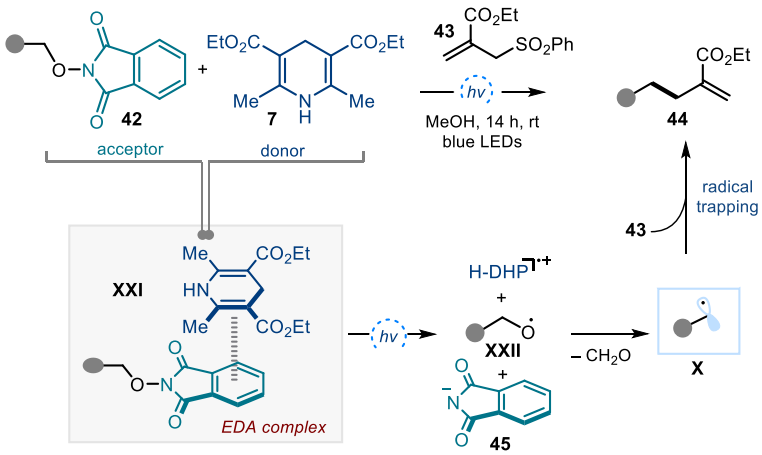

Scheme 2.17. H-DHP **7** forms an EDA complex with *N*-phthalimides **42** for the generation of alkyl radicals.

Recently, our group has demonstrated that 4-alkyl-1,4-dihydropyridines **23** (alkyl-DHPs) can absorb light and exhibit a dual reactivity profile in the excited state (Scheme 2.18.).

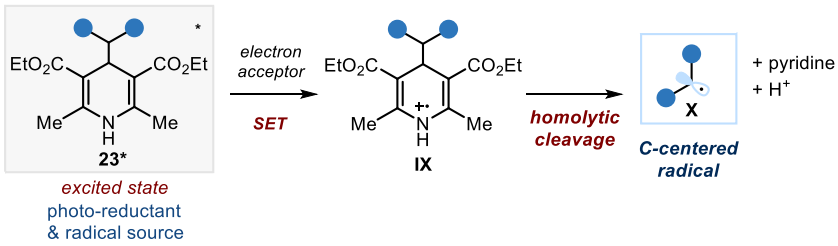

Scheme 2.18. Photo-excited 4-alkyl DHP **23** as strong reductants and alkyl radical sources.

Upon light excitation (λ = 405 nm), and in analogy to the H-DHP analogue, 4-alkyl-DHPs become strong photo-reductants **23***. They can therefore effectively engage in SET processes with an acceptor to deliver the radical cation **IX**. The unstable **IX** can then undergo homolytic

[31] Zhang, J., Li, Y., Xu, R., Chen, Y. "Donor–Acceptor Complex Enables Alkoxyl Radical Generation for Metal-Free C(Sp^3)–C(Sp^3) Cleavage and Allylation/Alkenylation', *Angew. Chem. Int. Ed.* **2017**, *56*, 12619.

cleavage to deliver the carbon-centered radicals.[32] Thus, the excited alkyl-DHPs can simultaneously serve as both a strong SET reductant and as a radical precursor.

The dual reactivity profile of the photo-excited **23** was exploited to trigger a nickel-catalyzed C(sp^2)–C(sp^3) cross coupling without the need of an exogenous photoredox catalyst (Scheme 2.19.). The reaction started with the direct excitation of alkyl-DHP **23** to yield **23***, which is responsible for the reduction of the Ni(II) precatalyst to Ni(0) complex **XI** via a sequential SET reduction. Concomitantly, aromatization of the radical cation **IX** delivers the pyridine and the alkyl radical **X**, which is then intercepted by the Ni(0) complex **XI**. The resulting alkyl-Ni(I) complex **XII** undergoes oxidative addition to the aryl bromide **24** to yield the Ni(III) complex **XIII**.[33] Subsequent reductive elimination delivers the desired cross-coupled product **25** and the Ni(I) complex **XIV**, which upon SET reduction from another molecule of **23*** generates the active Ni(0) complex **XI** and another C(sp^3) radical **X**.

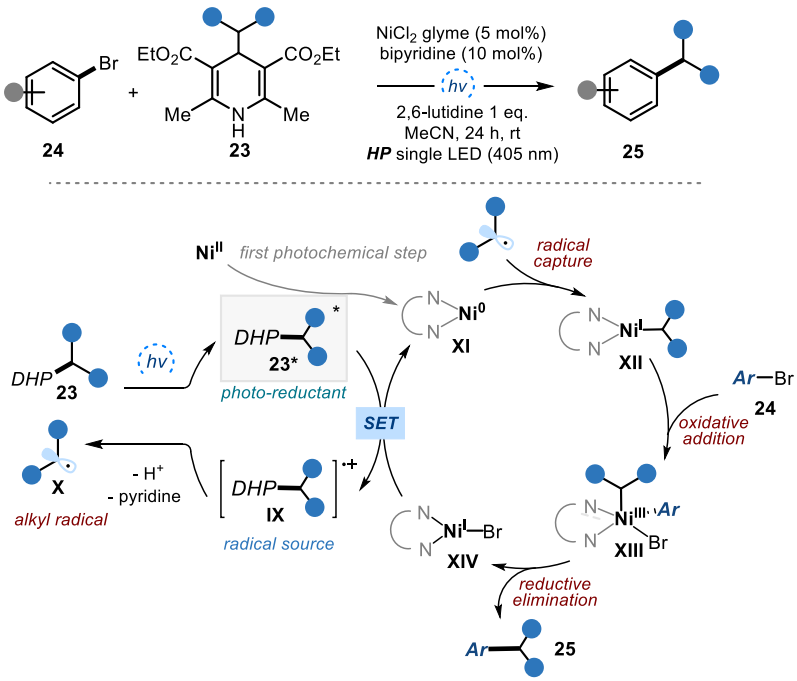

Scheme 2.19. The excited-state reactivity of alkyl-DHPs **23** triggers a nickel-catalyzed radical cross-coupling reaction without the need of external photocatalysts.

[32] Buzzetti, L., Prieto, A., Roy, S. R., Melchiorre, P., "Radical-Based C–C Bond-Forming Processes Enabled by the Photoexcitation of 4-Alkyl-1,4-Dihydropyridines", *Angew. Chem. Int. Ed.* **2017**, *56*, 15039.
[33] Alternatively, the alkyl radical can combine with the oxidative addition complex aryl-Ni(II) to give the Ni(III) complex **XIII** prior to reductive elimination step. For a review: Diccianni, J. B., Diao, T., "Mechanisms of Nickel-Catalyzed Cross-Coupling Reactions", *Trends Chem.* **2019**, *1* (9), 830.

In this doctoral thesis, I have developed photochemical processes that capitalized upon the multifaceted reactivity of 1,4-dihydropyridines, and their tendency to serve as carbon-centered radical precursors, electron donor, and photoreductant. Specifically, in the chemistry discussed in Chapter III, alkyl-DHPs in the ground-state served as electron donors and alkyl radical precursors to develop the stereoselective β-alkylation of α,β-unsaturated aldehydes under excited iminium ion-mediated catalysis. Finally, Chapter IV describes the use of 4-carbamoyl-1,4-dihydropyridines (carbamoyl-DHPs) in both their ground state and excited state for the generation of carbamoyl radicals. This reactivity has been applied to develop a photochemical strategy for amide synthesis.

Chapter III

Stereoselective β-Alkylation of Enals *via* Excited Iminium Ion Catalysis

Target

Exploiting the excited-state reactivity of catalytically generated chiral iminium ions to develop asymmetric β-alkylation of α,β-unsaturated aldehydes.

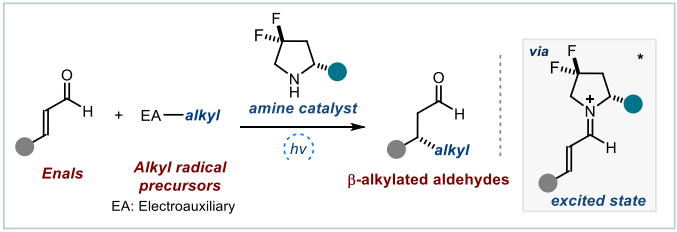

Tool

Using the oxidative power of excited-state chiral iminium ions to generate alkyl radicals from readily available precursors, and their ability to intercept radicals in a stereoselective fashion.[1]

3.1. Introduction and Target of the Project

Chiral iminium ions, generated by condensation of a chiral primary or secondary amine catalyst with an α,β-unsaturated ketone or aldehyde, have been widely used to catalyze the preparation of enantioenriched chiral molecules. Since the pioneering work in 2000 by MacMillan on iminium ion activation,[2] a plethora of enantioselective catalytic transformations has been developed. Nevertheless, it was only recently that iminium ion-mediated catalysis found application in enantioselective photochemistry. This approach can open new reaction pathways that are unavailable to ground-state reactivity (Scheme 3.1).

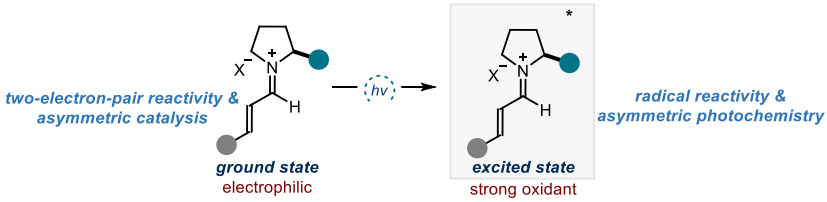

Scheme 3.1. Different reactivities of iminium ion in the ground state (left) and excited state (right).

[1] The project discussed in this chapter was conducted in collaboration with Dr. Charlie Verrier, Dr. Cristofer Pezzetta, Dr. Mauro Moliterno, Dr. Luca Buzzetti, Dr. Hamish B. Hepburn, Dr. Alberto Vega-Peñaloza and Dr. Mattia Silvi. I was involved in the final reaction optimization and investigated the scope of the reaction. Part of the study has been published: Verrier, C., Alandini, N., Pezzetta, C., Moliterno, M., Buzzetti, L., Hepburn, H. B., Vega-Peñaloza, A., Silvi, M., Melchiorre, P., "Direct Stereoselective Installation of Alkyl Fragments at the β-Carbon of Enals via Excited Iminium Ion Catalysis" *ACS Catal.* **2018**, 8, 2, 1062.

[2] Ahrendt, K. A., Borths, C. J., MacMillan, D. W. C., "New Strategies for Organic Catalysis: The First Highly Enantioselective Organocatalytic Diels–Alder Reaction", *J. Am. Chem. Soc.* **2000**, *122*, 17, 4243.

In nature, human vision is elicited by the absorption of visible-light by an iminium ion, formed upon condensation of 11-*cis*-retinal with the lysine residue of opsins.[3] Inspired by this mechanism, the Melchiorre group recently demonstrated that visible-light irradiation of transiently generated electron-poor chiral iminium ions could generate strong oxidants **I*** (Scheme 3.2.).[4] These excited-state intermediates **I*** are capable of facilitating the single-electron transfer (SET) oxidation of organosilanes **1** to generate benzyl radicals **II**. Subsequent stereoselective coupling of **II** with the chiral 5-π electron system **III**, arising form SET reduction of **I***, delivers the enantioenriched β-benzylated products **2**. Remarkably, silanes **1** are poor nucleophiles that could not react with the electrophilic ground-state iminium ion trough a classical polar pathway.

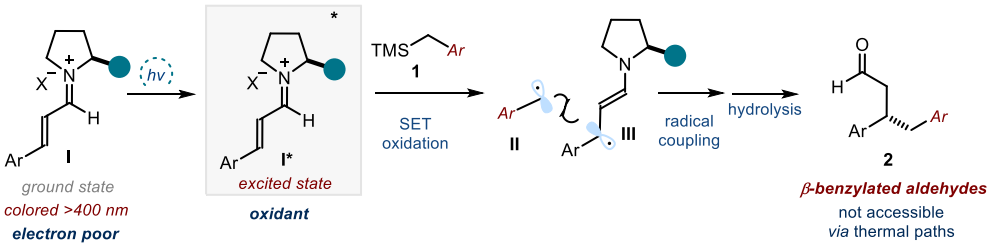

Scheme 3.2. Visible-light excitation turns an iminium ion **I** into a strong oxidant **I*** that can trigger SET oxidation of organosilanes **1** to form benzyl radicals. The ensuing stereocontrolled radical coupling forges a new stereogenic center with high fidelity; SET: single-electron transfer

To expand the synthetic utility of this photochemical activation mode in enantioselective organocatalysis, we investigated other radical precursors that could effectively engage in excited-state iminium ion-mediated transformations. As a design plan, we realized that these precursors should possess redox properties that match the oxidative power of the excited-state iminium ions **I***. Following this idea, we identified alkyltrifluoroborate salts **4** and 4-alkyl-1,4-dihydropyridines **5** (alkyl-DHPs) as suitable electron donors and alkyl radical precursors (Scheme 3.3.). This knowledge allowed us to develop the enantioselective β-alkylation of α,β-unsaturated aldehydes **3** using the photochemistry of iminium ions. This transformation overcame the need for stabilized benzyl and α-heteroatom radicals, which were used in our original studies,[4] since simple alkyl fragments could be stereoselectively introduced at the β-positions of enals. The development of this system is detailed in this chapter.

[3] Ernst, O. P., Lodowski, T. D., Elstner, M., Hegemann, P., Brown, L. S., Kandori, H., "Microbial and Animal Rhodopsins: Structures, Functions, and Molecular Mechanisms", *Chem. Rev.*, **2014**, *114*, 1, 126.
[4] Silvi, M., Verrier, C., Rey, Y. P., Buzzetti, L., Melchiorre, P., "Visible-Light Excitation of Iminium Ions Enables the Enantioselective Catalytic β-Alkylation of Enals", *Nat. Chem.* **2017**, *9*, 868.,

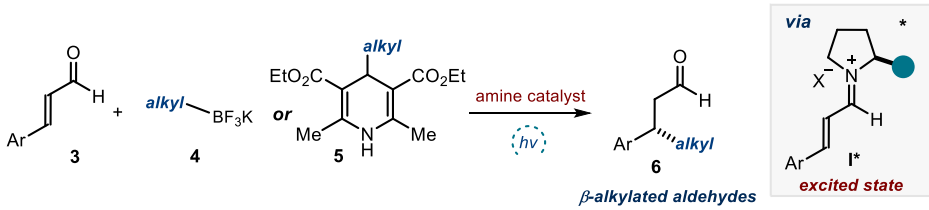

Scheme 3.3. Photo-excited chiral iminium ions **I*** enables the stereoselective installation of alkyl fragments at the β-carbon of enals **3**.

The following sections will detail the scientific background and the previous studies that were essential to the development of this research project.

3.1.1. Iminium Ion-Mediated Catalysis

Iminium ion-mediated catalysis provides a general and effective strategy to activate α,β-carbonyl compounds.[5] This activation mode involves the reversible condensation of a chiral amine catalyst **7** with an α,β-unsaturated carbonyl substrate **3** to furnish electron-deficient iminium intermediate **I** (Scheme 3.4).[6] The lowest unoccupied molecular orbital (LUMO) of the iminium ion **I** is lower in energy than the original unsaturated carbonyl **3**, resulting in enhanced electrophilicity. Therefore, the iminium ion in the ground state is a good electrophile, which is susceptible to a nucleophilic attack.

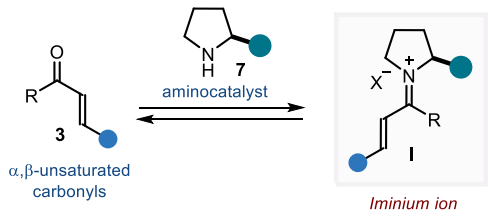

Scheme 3.4. Iminium ion-mediated catalysis – LUMO lowering activation strategy.

In 2000, MacMillan conceptualized the iminium ion formation as a general organocatalytic mode for substrate activation (Scheme 3.5.).[2] This seminal work described the first organocatalytic Diels-Alder reaction mediated by iminium ion **IV** formed upon condensation of the chiral imidazolidinone catalyst **10** with an enal **8**. This electron-poor olefin (**IV**), acting as a dienophile, reacts with a diene **9** to afford cyclic products **11** with a good level of enantio- and diastereo-selectivity.

[5] Erkkilä, A., Majander, I., Pihko, P. M., "Iminium Catalysis", *Chem. Rev.* **2007**, *107*, 12, 5416.
[6] Dalko, P. I., "Comprehensive Enantioselective Organocatalysis" 2013, Wiley-VCH Verlag.

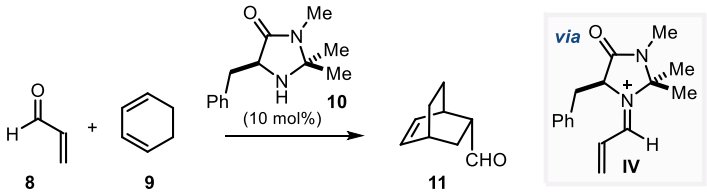

Scheme 3.5. Iminium ion-mediated asymmetric [4+2]-cycloaddition.

The generality and simplicity of the concept ignited the quest for other iminium ion-mediated asymmetric transformations, which allowed the stereoselective β-functionalization of enals (Figure 3.1.).[6] These transformations often offer complementary approach to well-established metal-catalyzed asymmetric conjugate addition reactions. The iminium-mediated reactions generally involve the addition of soft nucleophiles at the β-carbon of the unsaturated carbonyls, delivering the enantioenriched β-functionalized products after subsequent hydrolysis of the catalyst-bound products.

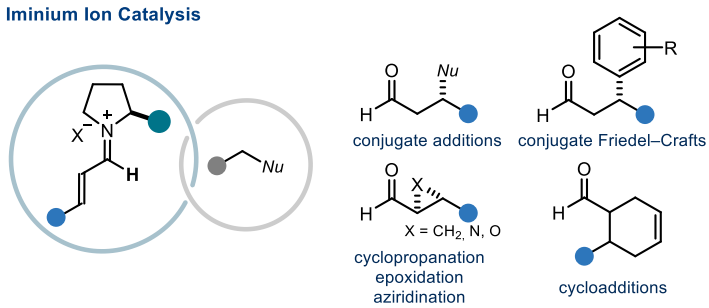

Figure 3.1. Reaction of iminium ions with nucleophiles leading to a wide array of asymmetric cycloadditions and β-functionalization products.

The success and expansion of iminium ion-mediated catalysis can be attributed to the design of new chiral secondary amine catalysts. To secure a high level of reactivity and stereoselectivity, some requirements must be fulfilled: *i*) these chiral amine catalysts should facilitate efficient condensation with the enals in a reversible manner; *ii*) the catalysts must be able to control the iminium ion geometry, while *iii*) providing enantiofacial discrimination of the prochiral π-system by selective shielding one face. Since the *Z*-form of the C=C double bond is highly unfavorable, the catalyst should exert geometry control of the iminium ion by defining the C=N double bond and the sigma bond between the two unsaturations (*s-cis* and *s-trans* isomers, Figure 3.2.). Due to the steric repulsion between the alkene and the methylene protons or the bulky substituents of the chiral catalyst, the *s-cis* conformation (Figure 3.2a) is

highly unfavored.[7] The same factor accounts for the geometry of the C=N double bond, which induces a preference for the *E* geometry. This implies that the most favorable iminium ion conformation is *s-trans*(*E*)-**I** (Figure 3.2b).[8]

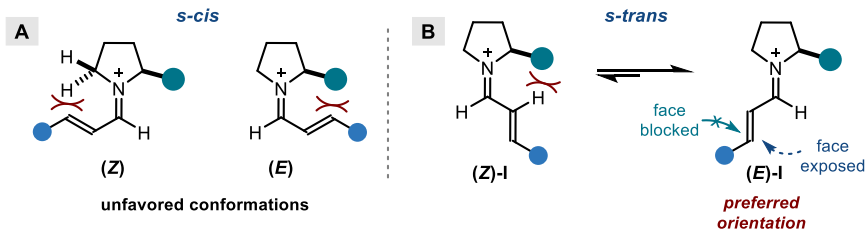

Figure 3.2. Role of chiral amine catalysts in iminium ion-mediated catalysis – steric control approach.

The more effective chiral secondary amines, which possess all these features, are the diarylprolinol silyl ethers, independently developed by Jørgensen[9] and Hayashi,[10] and the aforementioned MacMillan's imidazolidinones (Figure 3.3).

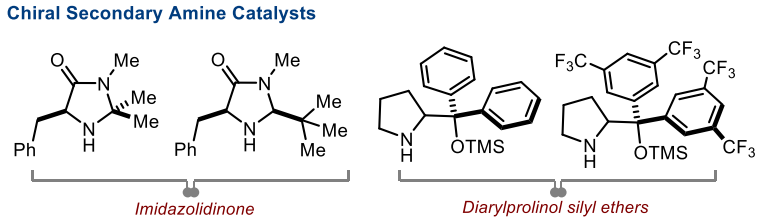

Figure 3.3. Selected examples of chiral secondary amine catalysts.

These catalysts served to develop a variety of highly enantioselective β-functionalization of enals. The nature of these amine catalysts also affects the electrophilicity of the iminium ion intermediate. The group of Mayr has conducted kinetic studies to quantify the electrophilicities of chiral iminium ion intermediates, generated from classical amine

7 Grošelj, U., Seebach D., Badine, D. M., Schweizer, W. B., Beck, A. K., Krossing, I., Klose, P., Hayashi, Y., Uchimaru, T., "Structures of the Reactive Intermediates in Organocatalysis with Diarylprolinol Ethers" Helv. Chim. Acta, 2009, 92, 1225

8 Seebach, D., Gilmour, R., Grošelj, U., Deniau, G., Sparr, C., Ebert, M.-O., Beck, A. K., McCusker, L. B., Šišak, D., Uchimaru, T., "Stereochemical Models for Discussing Additions to α-β-Unsaturated Aldehydes Organocatalyzed by Diarylprolinol or Imidazolidinone Derivatives – Is There an (E)/(Z)-Dilemma?" *Helv. Chim. Acta*, **2010**, *93*, 603.

9 Franzén, J., Marigo, M., Fielenbach, D., Wabnitz., T. C., Kjærsgaard, A., Jørgensen, K. A., "A General Organocatalyst for Direct α-Functionalization of Aldehydes: Stereoselective C−C, C−N, C−F, C−Br, and C−S Bond-Forming Reactions. Scope and Mechanistic Insights", *J. Am. Chem. Soc.* **2005**, *127*, 51, 18296.

10 Hayashi, Y., Gotoh, H., Hayashi, T., Shoji, M., "Diphenylprolinol Silyl Ethers as Efficient Organocatalysts for the Asymmetric Michael Reaction of Aldehydes and Nitroalkenes", *Angew. Chem. Int. Ed.* **2005**, *44*, 4212.

catalysts and cinnamaldehyde (Figure 3.4.).[11] The electrophilicity parameter (*E*) defines the tendency of these intermediates towards the attack of nucleophiles. Notably, intermediates derived from diarylprolinol and imidazolidinone catalysts showed highest electrophilicities, which explained their superior reactivity and utility for the asymmetric functionalizations of enals.

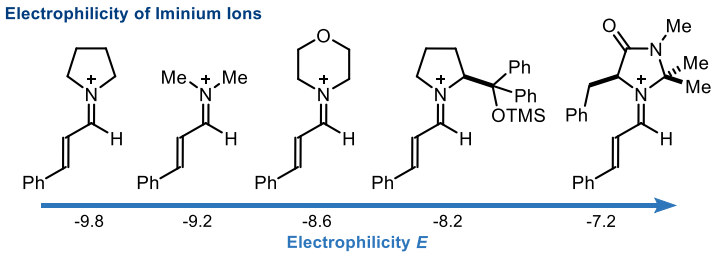

Figure 3.4. Electrophilicity of various iminium ions.

3.1.2. Excited-State Reactivity of Chiral Iminium Ions

The merge of organocatalysis and photochemical reactivity has opened the possibility to further expand the synthetic potential of iminium ion-mediated transformations.[12] The Melchiorre group recently disclosed that catalytic chiral iminium ions have the capacity to absorb visible light. This excitation turns a simple electrophilic compound in the ground state into a strong oxidant in the excited state.[4] In fact, the internal energy of a molecule is increased upon absorption of photonic energy, and therefore it can reach an excited state. In this new electronic configuration, the excited-state molecule increases its ability to donate and accept electrons – this means that, at the same time, an excited molecule is a better oxidant and a better reductant than in the ground state.

As described in Figure 3.5., a comparison of the electron affinity (EA) and ionization potential (IP) of an excited-state diamagnetic molecule with those in the corresponding ground-state shows that the EA of the excited molecule is higher than in the ground state, while the IP is lower.[13] From a thermodynamic point of view, the addition of an electron to half-filled highest occupied molecular orbital (HOMO) of the excited molecule is more exothermic than its addition to the lowest occupied molecular orbital (LUMO) in the ground state. At the same time, removing an electron from the excited state is less endothermic than removing it from

[11] Lakhdar, S., Tokuyasu, T., Mayr, H., "Electrophilic Reactivities of α,β-Unsaturated Iminium Ions" *Angew. Chem. Int. Ed.* **2008**, *47*, 45, 8723.
[12] Selected reviews: a) Silvi, M., Melchiorre, P., "Enhancing the Potential of Enantioselective Organocatalysis with Light", *Nature* **2018**, *554*, 41. b) Zou, Y.-Q., Hörmann, F. B., Bach, T., "Iminium and Enamine Catalysis in Enantioselective Photochemical Reactions" *Chem. Soc. Rev.* **2018**, *47*, 278.
[13] Pitre, S. P., McTiernan, C. D., Scaiano, J. C., "Understanding the Kinetics and Spectroscopy of Photoredox Catalysis and Transition-Metal-Free Alternatives", *Acc. Chem. Res.* **2016**, 49, 6, 1320.

the ground state. For these reasons, a molecule becomes both a better reductant and oxidant in its excited state.

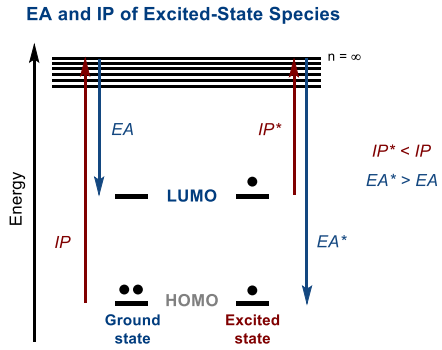

Figure 3.5. Excited-state molecules have a higher electron affinity (EA) and a lower ionization potential (IP) than in the ground state.

The reactivity of preformed, stoichiometric achiral iminium ions in the excited state was initially studied by Mariano in the 1980s.[14] These early studies established that the iminium ion photochemistry is dominated by SET processes. Upon light absorption, iminium ions become strong oxidants and their redox potential reaches E^{red} > 3 V (Figure 3.6.), making them capable to oxidize various electron-donors, including olefins and arenes.

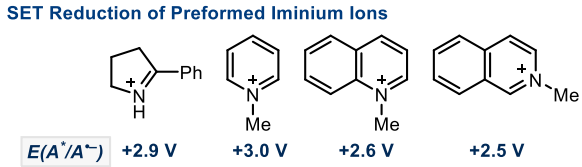

Figure 3.6. Excited-state reduction potential of various preformed iminium ions.

Capitalizing upon this reactivity, our group successfully translated this concept into a catalytic asymmetric regime. This approach has opened up new reaction pathways that are unavailable to ground-state reactivity of iminium ions. Specifically, we have used this strategy for the asymmetric catalytic β-benzylation of enals (Scheme 3.6.). The formation of the chiral iminium ion **I** upon condensation of a chiral aminocatalyst with cinnamaldehyde **3** results in the bathochromic shift of the absorption band into the visible region of the electromagnetic spectrum and in an increase of the molar absorption coefficient. Irradiation of the iminium intermediate **I** with violet light induces a ππ* transition, generating an excited state **I*** which

[14] Mariano, P. S., "The Photochemistry of Iminium Salts and Related Heteroaromatic Systems", *Tetrahedron* **1983**, *39*, 3845.

functions as a strong oxidant (E^{red} ($\mathbf{I}^*/\mathbf{I}^{\bullet-}$) ≈ +2.30 V vs Ag/Ag^+ in CH_3CN).[15] This species could trigger the formation of benzylic radical **II** through an SET oxidative cleavage of the silicon–carbon bond within benzyl trimethylsilane **1**. The subsequent stereoselective coupling between **II** and the chiral 5π-electron β-enaminyl radical **III**, generated from $\mathbf{I}^*$ upon SET, led to the direct β-benzylation of enals **2**.

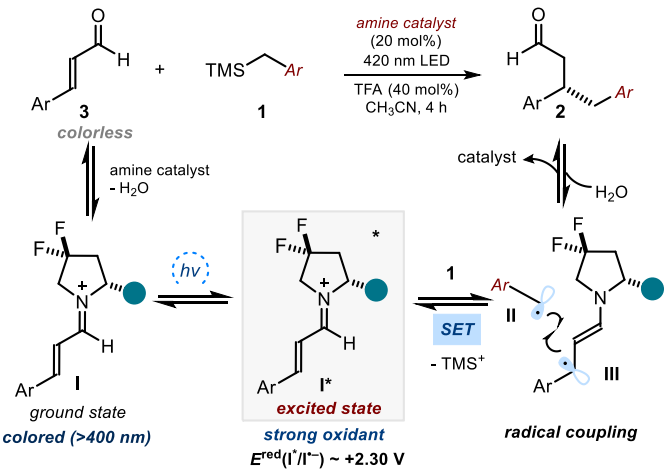

Scheme 3.6. Enantioselective β-benzylation of enals *via* excited-state iminium ion catalysis.

Essential to the success of this strategy was the design of a new class of chiral aminocatalysts that secured the reproducibility of the reaction while providing high enantioselectivity (Scheme 3.7.). The incorporation of geminal fluorine atoms on the pyrrolidine scaffold enhances the stability of the ground-state amine catalysts towards oxidation by the excited-state iminium ion. The introduction of fluorine atoms is a widely used strategy in medicinal chemistry to lower the tendency of a compound toward enzymatic oxidation.[16] Moreover, fluorine atoms are known to reduce the basicity of amines.[17] The fluorinated catalysts **B** and **C** showed higher oxidation potential than the Jørgensen's diarylprolinol silylether progenitors **A**. As a consequence of a much higher stability under the oxidative conditions of the reaction, they greatly outperformed the Jørgensen catalyst **A** in terms of catalytic activity and enantioselectivity.

[15] The excited-state redox potential of iminium ion **I** has been approximated on the basis of spectroscopic and electrochemical measurement and applying the Rehm-Weller theory, see Ref. 4. Rehm, D., Weller, A. "Kinetics of Fluorescence Quenching by Electron and H-Atom Transfer" *Isr. J. Chem*., **1970**, *8*, 259.
[16] Müller, K., Faeh, C., Diederich, F., "Fluorine in Pharmaceuticals: Looking Beyond Intuition", *Science* **2007**, *317*, 5846, 1881.
[17] Morgenthaler, M., Schweizer, E., Hoffmann-Röder, A., Benini, F., Martin, R., Jaeschke, G., Wagner, B., Fischer, H., Bendels, S., Zimmerli, D., Schneider, J., Diederich, F., Kansy, M., Müller, K., "Predicting and Tuning Physicochemical Properties in Lead Optimization: Amine Basicities", *ChemMedChem* **2007**, *2*, 1100.

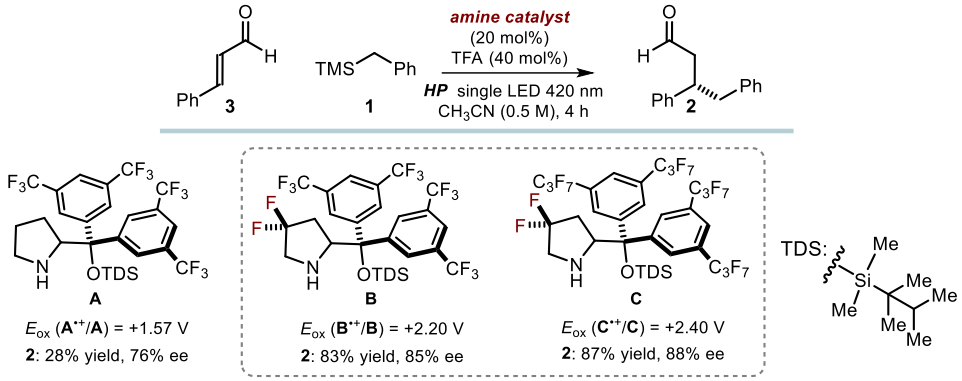

Scheme 3.7. Comparison of the redox properties of the pyrrolidine-based catalysts **A**, **B** and **C** and their catalytic activity in the photochemical β-benzylation of cinnamaldehyde. TDS: thexyl-dimethylsilyl.

3.2. Target of the Project

The aim of the project is to further expand the scope of the excited-state iminium chemistry for the development of novel enantioselective transformations, which could not be accessed through classical ground-state reactivity. Specifically, we sought to exploit the properties of the excited-state iminium ion to promote the stereoselective installation of simple and non-stabilized alkyl fragments at the β-position of enals (Scheme 3.8.). The original methodology, based on the use of alkyl silanes[4] was limited to the generation of either benzyl radicals or radicals stabilized by an adjacent heteroatom. This encouraged us to identify alternative alkyl radical precursors **12** with redox properties that match the oxidative capability of excited-state iminium ions **I***. SET oxidation of these precursors would generate alkyl radicals **V**, which could be stereoselectively coupled with the chiral β-enaminyl radical **III**. Subsequent hydrolysis of enamine intermediate **VI** affords the enantioenriched chiral aldehydes **6** and liberates the amine catalyst.

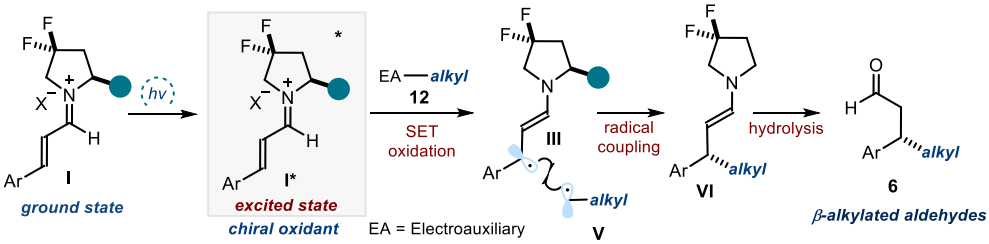

Scheme 3.8. Enantioselective installation of non-stabilized alkyl fragments at the β-carbon of enals through photoexcitation of iminium ions. EA: electroauxiliary.

The enantioselective β-alkylation of enals with simple alkyl fragments is a challenging process for a variety of reasons. Despite major advances in the development of asymmetric conjugate addition reactions using organometallic reagents, applying this strategy to α,β-unsaturated aldehydes has proven difficult.[18] The main issue lies in the high reactivity of the aldehyde moiety, which enables a competing addition to the carbonyl substrate, leading to a mixture of 1,2- and 1,4-addition adducts (Scheme 3.9a). This regioselectivity issue was highlighted by Bräse, who reported that the catalytic addition of diethyl zinc to enals proceeds with high enantioselectivity but poor 1,4/1,2 selectivity (ranging from 4:1 to 1:1).[19] Subsequent studies by Alexakis showed that a chiral copper catalyst could facilitate the addition of both dialkyl zinc and Grignard reagents to enals.[20] While the former reacted with high 1,4-regioselectivity with moderate stereocontrol, Grignard reagents afforded highly enantioenriched β-substituted enals along with the 1,2-addition adducts.

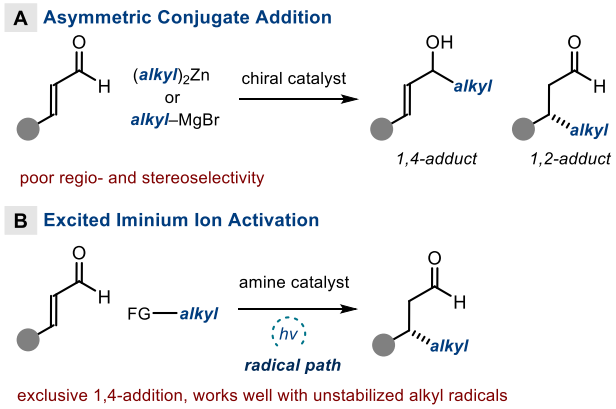

Scheme 3.9. a) Asymmetric conjugate addition reactions with organometallic reagents or metal catalysts for the β-alkylation of enals. b) This work: excited iminium-ion mediated β-alkylation of enals.

We surmised that the excited-state reactivity of iminium ions might provide an effective strategy to close this gap in synthetic methodology (Scheme 3.9b).

[18] Córdova, A., "Catalytic Asymmetric Conjugate Reactions", 2010 Wiley-VCH Verlag.
[19] a) Bräse, S., Höfener, S., "Asymmetric Conjugate Addition of Organozinc Compounds to α,β-Unsaturated Aldehydes and Ketones with [2.2]Paracyclophaneketimine Ligands without Added Copper Salts" *Angew. Chem. Int. Ed.* **2005**, *44*, 7879. b) Ay, S. Nieger, M., Bräse, S., "Co-Metal-Free Enantioselective Conjugate Addition Reactions of Zinc Reagents", *Chem. Eur. J.* **2008**, *14*, 11539.
[20] Palais, L., Babel, L., Quintard, A., Belot, S., Alexakis, A., "Copper-Catalyzed Enantioselective 1,4-Addition to α,β-Unsaturated Aldehydes", *Org. Lett.* **2010**, *12*, 1988. b) Goncalves-Contal, S., Gremaud, L., Palais, L., Babel, L., Alexakis, A. "Copper-Catalyzed Enantioselective Conjugate Addition to α,β-Unsaturated Aldehydes with Various Organometallic Reagents", *Synthesis* **2016**, *48*, 3301.

3.3. Results and Discussion

Excited-state iminium ions are very strong oxidant (E^{red} ($\mathbf{I}^*/\mathbf{I}^{\bullet-}$) ≈ +2.30 V vs Ag/AgCl)[15] and are capable to accept an electron from donor compounds. Looking for suitable radical precursors, we focused on a selection of substrates that can fulfill two requirements: *i*) these substrates should readily donate an electron to the photoexcited iminium ion, and *ii*) they should easily undergo fragmentation after SET to prevent a possible unproductive back-electron transfer (BET) to occur, thereby providing the desired alkyl radicals. We envisioned that the introduction of an electro-auxiliary (EA) group within the redox partner could fulfill these requirements.[21] EA groups are functional groups that facilitate SET processes by modulating the redox potentials of the substrates. In addition, the EA groups can favor the formation of desired radicals by undergoing a facile irreversible fragmentation. In the original study, the TMS group within the benzyl silane substrate played exactly this role. We envisioned that alkyltrifluoroborate salts and 4-alkyl-1,4-dihydropyridines (alkyl-DHPs, Figure 3.7.) could serve as suitable alkyl radical precursors and electron donors for the enantioselective β-alkylation process. These substrates, compared to alkyl silanes, are bench-stable and can be prepared from readily accessible precursors.

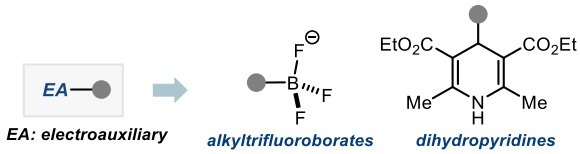

Figure 3.7. Selected alkyl radical precursors.

3.3.1. Alkyltrifluoroborate Salts as Radical Precursors

Organotrifluoroborates have been widely used as an alternative to boronic acids, boronate esters and organoboranes in Suzuki-Miyaura and other transition-metal catalyzed cross-coupling reactions.[22] Because of their tetracoordinate nature, trifluoroborate salts can be considered as the protected forms of boronic acid. Contrary to other organoboron reagents, trifluoroborate salts are bench stable and easily handled. Organotrifluoroborates can also serve as carbon-centered radical precursors under oxidative conditions.[23] Because of their low

[21] Yoshida, J., Kataoka, K., Horcajada, R., Nagaki, A., "Modern Strategies in Electroorganic Synthesis", *Chem. Rev.* **2008**, *108*, 2265.
[22] Molander, G., A., Ellis, N., "Organotrifluoroborates: Protected Boronic Acids That Expand the Versatility of the Suzuki Coupling Reaction", *Acc. Chem. Res.* **2007,** *40*, 275.
[23] Selected examples: a) Sorin, G., Mallorquin, R. M., Contie, Y., Baralle, A., Malacria, M., Goddard, J.-P., Fensterbank, L., "Oxidation of Alkyl Trifluoroborates: An Opportunity for Tin-Free Radical Chemistry", *Angew. Chem., Int. Ed.* **2010**, *49*, 8721. b) Molander, G. A., Colombol, V., Braz, V. A., "Direct Alkylation of Heteroaryls Using Potassium Alkyl- and Alkoxytrifluoroborates", *Org. Lett.* **2011**, *13*, 1852.

oxidation potentials, they are useful reagents for photoredox processes.[24] The first photoredox generation of alkyl radicals from the corresponding alkyl trifluoroborates was reported by Koike and Akita in 2012 (Scheme 3.10.).[25]

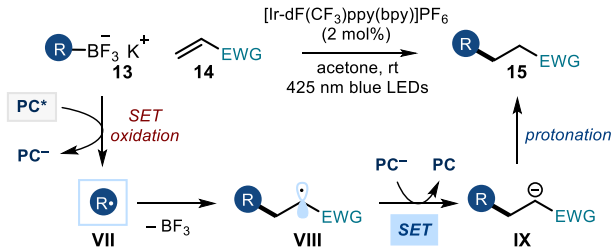

Scheme 3.10. Photoredox catalysis in the oxidation of alkyltrifluoroborate salts **13** and the generation of alkyl radicals.

The trifluoroborate salts **13** were used as alkyl radical precursors for the development of a Giese-type addition reaction. The alkyl radical, formed upon SET oxidation of **13** from an excited iridium-based photocatalysts (PC^*), reacts with electron-deficient alkenes **14**. The resulting radical intermediate **VIII** then undergoes SET reduction by the reduced photocatalyst (PC^-) to form the anionic intermediate **IX**, which after protonation furnishes the Giese-type product **15**. Recently, organotrifluoroborates have been extensively used as radical precursors in photoredox processes, including in Ni/photoredox dual catalytic processes.[26]

Motivated by these precedents, we anticipated that alkyl trifluoroborate salts could be suitable radical precursors for the enantioselective β-alkylation process and would provide the desired alkyl radicals upon SET oxidation by the photo-excited iminium ion. We started out our investigations by synthesizing potassium *iso*-propyltrifluoroborate salt **18** from readily available *iso*-propylmagnesium bromide **16** and trimethyl borate **17** (Scheme 3.11.).[27] We then determined the electrochemical property of **18** by conducting cyclic voltammetry (CV) experiments. Substrate **18** has an oxidation potential $E^{ox}(\mathbf{18}^{\bullet+}/\mathbf{18})$ = +1.72 V (vs Ag/AgCl), a value which falls within the oxidative capability of the excited-state iminium ion (E^{red} ($\mathbf{I}^*/\mathbf{I}^{\bullet-}$) ≈ +2.30 V vs Ag/AgCl).

[24] Koike, T., Akita, M., "Combination of Organotrifluoroborates with Photoredox Catalysis Marking a New Phase in Organic Radical Chemistry", *Org. Biomol. Chem.* **2016**, *14*, 6886.
[25] Yasu, Y., Koike, T., Akita, M., "Visible Light-Induced Selective Generation of Radicals from Organoborates by Photoredox Catalysis", *Adv. Synth. Catal.* **2012**, *354*, 3414.
[26] Tellis, J. C., Kelly, C. B., Primer, D. N., Jouffroy, M., Patel, N. R., Molander, G. A., "Single-Electron Transmetalation via Photoredox/Nickel Dual Catalysis: Unlocking a New Paradigm for Sp^3–Sp^2 Cross-Coupling", *Acc. Chem. Res.* **2016**, *49*, 1429.
[27] Dreher, S. D., Dormer, P. D., Sandrock, D. L., Molander, G. A., "Efficient Cross-Coupling of Secondary Alkyltrifluoroborates with Aryl Chlorides – Reaction Discovery Using Parallel Microscale Experimentation", *J. Am. Chem. Soc.* **2008**, *130*, 9257.

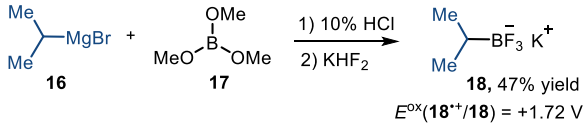

Scheme 3.11. Synthesis of *iso*-propyl potassium trifluoroborate salt **18.**

Encouraged by this observation, we began our investigation using cinnamaldehyde **3** as the model substrate, the difluorinated amine catalyst (*S*)-**B** (20 mol%) and trifluoroacetic acid (TFA, 40 mol%) as co-catalyst, which was needed to promote the formation of the iminium ion intermediate (Scheme 3.12.). The reaction was conducted in CH_3CN at room temperature under irradiation by a single violet high-power light-emitting diode (HP LED, λ_{max} = 420 nm) with an irradiance of 40 mW/cm^2, as controlled by an external power supply (full details of the experimental set up are discussed below, Figure 3.8.).

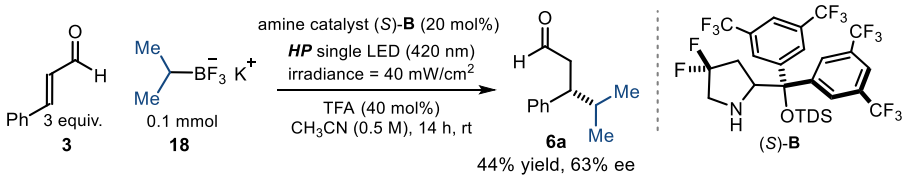

Scheme 3.12. β-alkylation of cinnamaldehyde **3** with *iso*-propyl trifluoroborate salt as the radical source.

After 14 hours of irradiation, we obtained the desired alkylated product **6a** in 44% yield and 63% ee, proving the feasibility of the reaction. We wondered whether the lower reactivity, compared to the β-benzylation reaction using benzyl silane (83% yield, 85% ee), is attributed to the nature of the radical generated upon SET oxidation. In this reaction, the resulting *iso*-propyl radical is less stabilized than the benzyl radical and can undergo undesired side reactions.[28] To verify this hypothesis, we performed the reaction using benzyl potassium trifluoroborate salt **19** as radical precursor and we obtained the benzylated product **2** in 40% yield and 70% ee (Scheme 3.13.). This result suggests that the lower reactivity observed with trifluoroborate salts was not ascribed to the nature of the generated radical, but on the nature of the precursor instead.

[28] Griller, D., Ingold, K. U., "Persistent Carbon-Centered Radicals", *Acc. Chem. Res.* **1976**, *19*, 13.

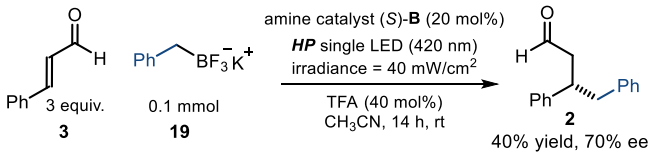

Scheme 3.13. β-Benzylation of cinnamaldehyde **3** with benzyl trifluoroborate salt **19** as the radical source.

An aspect to consider when using alkyl trifluoroborates as radical precursors is the side product formed upon oxidative fragmentation. Specifically, a strong Lewis acid, boron trifluoride (BF_3), is generated. In the presence of water, BF_3 reacts to produce a mixture of boric acid ($B(OH)_3$) and fluoroboric acid (HBF_4).[29] We wondered whether the formation of HBF_4 could be the reason for the low reactivity observed. We first made sure that this acid could not replace TFA as co-catalyst in the β-benzylation of enals with benzyl silane, since we did not observe any product formation.[30] We then used trifluoroacetate salts to quench the generated HBF_4 and generate TFA. However, these attempts met with failure as we observed lower reactivity (Table 3.1., entry 2-4). Moreover, using one equivalent of TFA did not bring about any significant improvement in terms of yield (entry 5).

Table 3.1. Screening of additives.

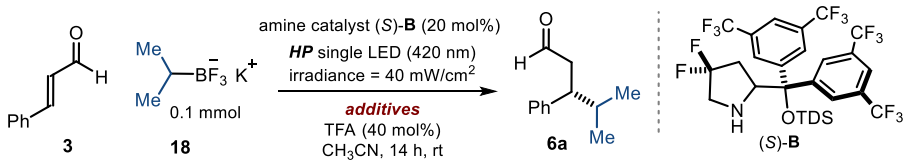

entry	additives	yield (%)[a]
1	-	44
2	LiTFA	25
3	CsTFA	traces
4	TBATFA	10
5	1 equiv. TFA	47

Reactions performed on a 0.1 mmol scale using 3 equiv. of **3** in CH_3CN (0.5 M) under illumination by a single high-power (HP) LED (λ_{max} = 420 nm). [a] Yield of **6a** determined by ^1H NMR analysis of the crude mixture using 1,3,5-trimethoxybenzene as an internal standard**.** TFA: trifluoroacetate or trifluoroacetic acid. TBA: tetrabutylammonium. TDS: thexyl-dimethylsilyl.

We then continued our investigation by evaluating the reaction temperature. For this experiment, we assembled a reliable reaction set-up that enables irradiation of the reaction

[29] Wamser, C. A., "Equilibria in the System Boron Trifluoride-Water at 25°", *J. Am. Chem. Soc.* **1951**, *73*, 409.
[30] Unpublished result.

mixture at low temperatures. As illustrated in Figure 3.8, an aluminium block with an inlet and an outlet was connected to a chiller, in order for a refrigerating liquid to circulate and control the temperature within the aluminium block. This piece was placed on top of an HP LED and separated by a 3D-printed holder, where a reaction vessel could be accommodated. This plastic support secured a constant distance of 1 cm between the light source and the bottom of the reaction vessel. This setup secured a reliable control of the reaction temperature and of irradiation, which was modulated by an external power supply and measured using a photodiode light detector at the start of each reaction.

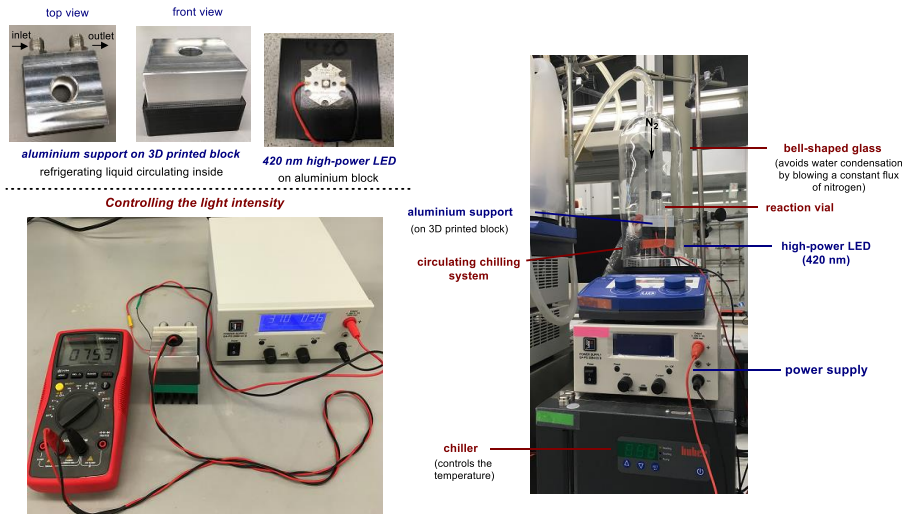

Figure 3.8. Detailed set-up and illumination system. The light source for illuminating the reaction vessel consisted in a 420 nm high-power single LED. The use of chiller allows the control of temperature.

Lowering the temperature to 0° C slightly increased the reaction yield and the enantiomeric excess (Table 3.2, entry 1). Better results in terms of yield and enantioselectivity were obtained when conducting the reaction at –10 °C, which delivered the product **6a** in 55% yield and 78% ee (entry 2). A cation exchange from potassium to tetrabutylammonium (E^{ox} (**20**$^{\bullet+}$/**20**) = +1.65 V vs Ag/AgCl) greatly increased the solubility of the trifluoroborate reagent. However, the tetrabutylammonium substrate **20** offered a similar reactivity as the K analogue **18** in the enantioselective photochemical β-alkylation of **3** (entry 3). The chiral amine (*S*)-**C**, bearing bulkier perfluoro alkyl group at the aromatic ring, exhibited lower reactivity and similar control of the stereoselectivity (entry 4).

Table 3.2. Evaluation of reaction temperature.

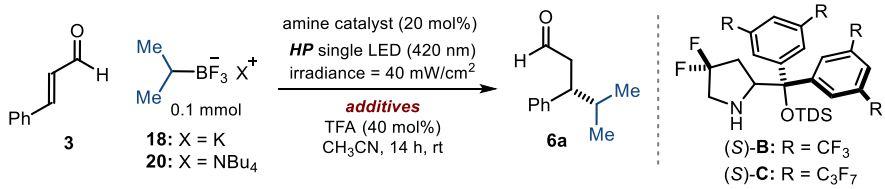

entry	catalyst	radical precursor	Temperature (°C)	yield (%)[a]	ee (%)
1	B	18	0	50	70
2	B	18	–10	55	78
3	B	20	–10	58	79
4	C	18	–10	39	80

Reactions performed on a 0.1 mmol scale using 3 equiv. of **3** in CH_3CN (0.5 M) under illumination by a single high-power (HP) LED (λ_{max} = 420 nm). [a] Yield of the isolated **6a.**

Generally, we observed full conversion of the trifluoroborate salts at the end of these experiments. Attempts to preserve the starting material were unsuccessful: screening of other reaction parameters, including solvents, acid co-catalysts and additives, did not lead to any improvement. Despite extensive efforts, the reaction using trifluoroborates did not offer synthetically useful results. Therefore, we decided to focus on other alkyl radical precursors for the development of the enantioselective photochemical β-alkylation of enals.

3.3.2. 4-Alkyl-1,4-dihydropyridines (Alkyl-DHPs) as Alkyl Radical Precursors

4-Alkyl-1,4-dihydropyridines (alkyl-DHPs) are known to generate alkyl radicals upon SET oxidation.[31] The formation of alkyl radicals from alkyl-DHPs was first reported by the group of Wu, who used electron spin resonance (ESR) spectroscopy analysis to firmly confirm the generation of open-shell intermediates.[32] SET oxidation of 4-*iso*-propyl- and 4-*iso*-butyl-DHP with nitrosonium tetrafluoroborate $NOBF_4$ delivered the corresponding isopropyl and isobutyl radicals. The relatively low oxidation potentials of alkyl-DHPs allowed their extensive use for the generation of C(sp^3)-centered radicals in photocatalytic processes (Scheme 3.14.). In a typical process, the alkyl-DHPs **5** undergo SET oxidation from an excited photocatalyst (**PC***) to deliver the unstable radical cation **X**. This species then undergoes

[31] Wang, P.-Z., Chen, J.-R., Xiao, W.-J., "Hantzsch Esters: An Emerging Versatile Class of Reagents in Photoredox Catalyzed Organic Synthesis", *Org. Biomol. Chem.* **2019**, *17*, 6936.
[32] Wu, L.-M., Chen, W., Liu, Z.-L. "Stable Free Radicals Generated during the Oxidation of 4-Alkyl Hantzsch 1,4-Dihydropyridines with Nitrosonium – EPR Evidence", *Res. Chem. Intermediat.* **2001**, *27*, 219.

irreversible C–C bond fragmentation to provide the pyridine **21** and the key carbon-centered radical **V**, which can be trapped by a suitable acceptor.

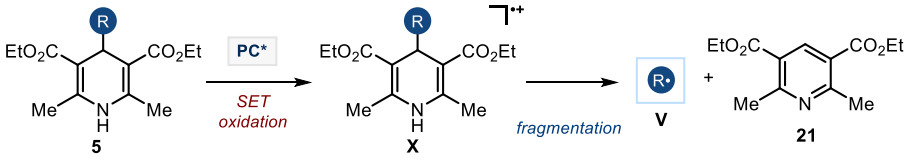

Scheme 3.14. SET oxidation of alkyl-DHP generates alkyl radicals.

We surmised that the excited-state iminium ion **I*** could act as the photo-oxidant to promote the SET oxidation of the alkyl-DHP **5** and generate the alkyl radical **V** (Scheme 3.15.). The tendency of dihydropyridines to aromatize and afford pyridines would hamper the possible unproductive BET process, thus facilitating the stereoselective installation of alkyl fragments at the β-position of enals.

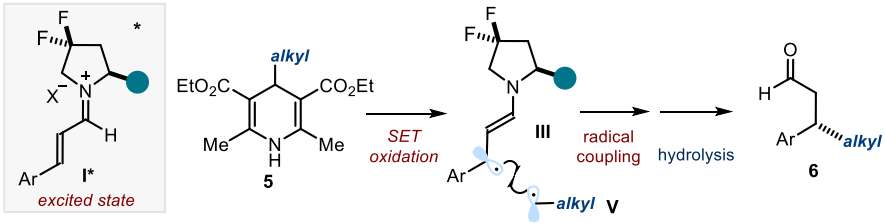

Scheme 3.15. Alkyl-DHPs **5** as radical precursors in the photochemical β-alkylation of enals using the exacted-state reactivity of iminium ions.

We started our investigation by synthesizing the alkyl-DHPs through the condensation of an aldehyde **22** with ethyl acetoacetate **23** and ethyl aminocrotonate **24** in the presence of a catalytic amount of tetrabutylammonium hydrogensulfate (Scheme 3.16.).[33] The alkyl-DHPs **5** were obtained as light yellow solid in moderate yields. Those substrates are stable to air and moisture and can be easily handled. However, they are sensitive to light, and therefore they need to be stored in containers wrapped with aluminium foil and stored in a dark place to avoid decomposition.

[33] Gutiérrez-Bonet, Á., Tellis, J. C., Matsui, J. K., Vara, B.A., Molander, G. A., "1,4-Dihydropyridine as Alkyl Radical Precursors: Introducing the Aldehyde Feedstock to Nickel/Photoredox Dual Catalysis", *ACS Catal.* **2016**, *6*, 12, 8004.

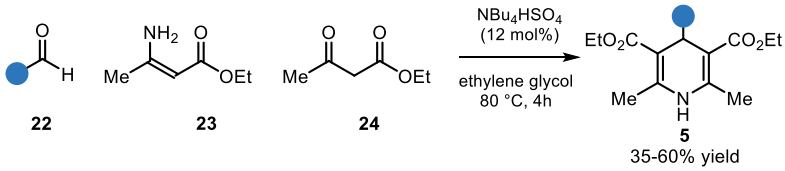

Scheme 3.16. Synthesis of 4-alkyl-1,4-dihydropyridine **5**.

We then selected the *iso*-propyl derivative **25** as the model substrate, which was electrochemically characterized (Figure 3.9.). Cyclic voltammetry measurement of **25** indicated an irreversible oxidation peak $E_p^A = E_{ox}$ (**25**$^{\bullet+}$/**25**) = +1.41 V and thereby confirmed the ability of alkyl-DHPs to serve as suitable electron donor for photo-excited iminium ion chemistry.

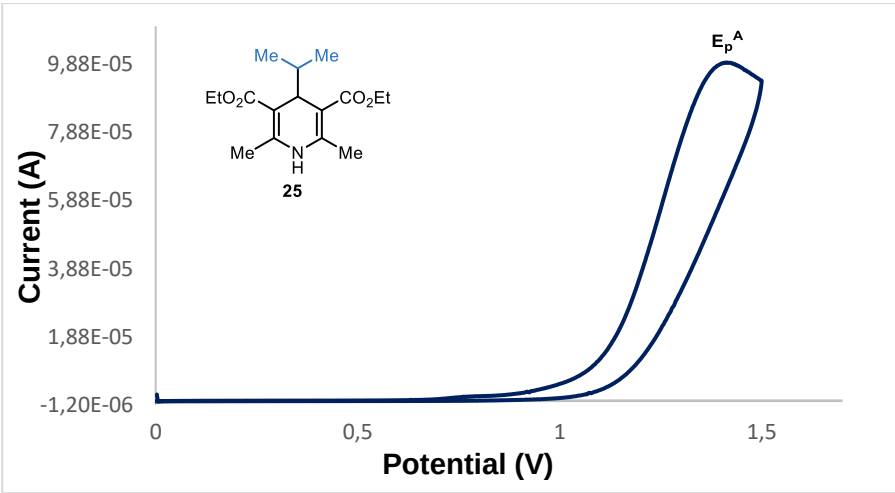

Figure 3.9. Cyclic voltammogram of **25** [0.03 M] in [0.1 M] $TBAPF_6$ in CH_3CN. Sweep rate: 20 mV/s. Pt electrode working electrode, Ag/AgCl (KCl 3.5M) reference electrode, Pt wire auxiliary electrode. Irreversible oxidation. $E_p^A = E_{ox}$ (**25**$^{\bullet+}$/**25**) = +1.41 V; E_p^A is the anodic peak potential, while E_{ox} value describes the electrochemical properties of **25**.

3.3.3. Reaction Optimization

To test the feasibility of the photochemical β-alkylation reaction with alkyl-DHPs, we submitted substrate **25** to the reaction conditions previously used for the *iso*-propyltrifluoroborate salt. The reaction was performed under 420 nm irradiation (irradiance of 40 mW/cm^2) in CH_3CN at –10 °C, in the presence of 3 equiv. of cinnamaldehyde **3**, 20 mol% of catalyst **B**, and 40 mol% of TFA (Table 3.3.)

Table 3.3. Optimization studies using 4-isopropyl-DHP as the radical precursor

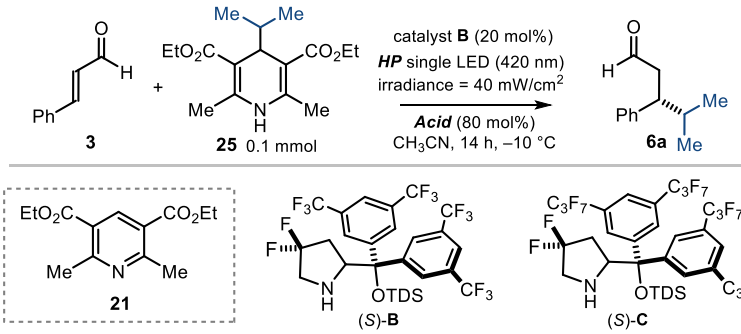

entry	catalyst	TFA (mol%)	yield (%)[a]	ee (%)
1	**B**	40	70	80
2	**B**	80	91	80
3	**C**	80	59	87
4[b]	**C**	80	83	86

Reactions performed in CH_3CN (0.5 M) on a 0.1 mmol scale using 3 equiv. of **3** under illumination by a single high-power (HP) LED (λ_{max} = 420 nm). [a] Yield of the isolated **6a.** [b] Performed in a 2:1 CH_3CN/perfluorohexane (C_6F_{14}) solvent mixture (0.33 M). TDS: thexyl-dimethylsilyl.

After 14 hours of irradiation, the desired β-alkylated product **6a** was obtained in 70% yield and 80% ee when using catalyst (*S*)-**B** (entry 1). The reactivity was greatly improved by increasing the amount of TFA to 80 mol% (entry 2). The chiral amine catalyst (*S*)-**C**, possessing bulkier substituents, was suitable for improving the enantiocontrol, but at the expense of reactivity (entry 3). Finally, increasing the concentration of the reaction system secured a better reactivity, delivering the β-alkylated aldehyde **6a** in 83% yield and 86% ee (entry 4). The use of perfluorohexane as co-solvent was necessary to improve the catalyst's solubility.

Further screening of Brønsted acid co-catalysts (Table 3.4.) showed that benzoic acid, acetic acid and triflic acid were not competent acids (entries 1-3). The desired product **6a** was formed in moderate yield and selectivity when using perchloric, *p*-toluenesulfonic, and tetrafluoroboric acids (entries 4-6). Clearly, trifluoroacetic acid provided the best results in terms of reactivity and enantiocontrol (entry 7).

Table 3.4. Screening of acid co-catalysts.

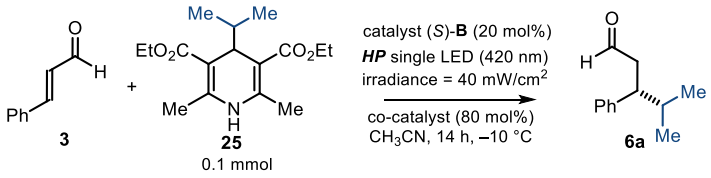

entry	acid	Yield **6a** (%)[a]	ee (%)
1	Benzoic Acid	< 5	-
2	Acetic Acid	< 5	-
3	Triflic Acid	6	-
4	Perchloric Acid	65(58)[b]	63
5	Tosylic Acid	66(55)[b]	68
6	Tetrafluoroboric Acid	73(67)[b]	67
7	Trifluoroacetic Acid	91[c]	80

Reactions performed in CH_3CN (0.5 M) on a 0.1 mmol scale using 3 equiv. of **3** under illumination by a single high-power (HP) LED (λ_{max} = 420 nm). [a] Yield of **6a** was determined by ^1H NMR analysis of the crude mixture using trichloroethylene as an internal standard. [b] Number in parenthesis indicates the yield of the isolated **6a** after chromatographic purification on silica gel. [c] Yield of the isolated **6a**.

3.3.4. Scope of the Reaction

With the best reaction conditions in hand (Table 3.3., entry 4), we next demonstrated the generality of the β-alkylation process by performing reactions with various alkyl-DHPs and cinnamaldehyde derivatives (Scheme 3.17.). Both linear and cyclic radicals could be successfully introduced at the β-carbon of cinnamaldehyde **3**, exclusively leading to the 1,4-adducts with generally good yields and stereocontrol (**6a-m**). Heterocycles, including a tetrahydropyran (**6f**) and a piperidine (**6g**) moiety, could be installed at the β-position with good stereocontrol. Sterically demanding fragments were accommodated well, as demonstrated by the *tert*-butyl moiety (**6h**). In this case, we use the corresponding trifluoroborate salts as the radical precursor since the corresponding DHP was not easily accessible. The use of DHP reagents bearing a chiral alkyl fragment delivered the formation of adducts **6i-m**, which have two vicinal stereogenic centers, with high enantiomeric excess, albeit with a poor diastereomeric ratio. Interestingly, alkyl fragments bearing both alkene and aromatic moieties could be installed, leading to the corresponding products **6j-m**. Primary radicals could also participate in this stereoselective coupling reaction when adorned with a stabilizing α-oxygen atom, providing the products **6n** and **6o**.

As for the scope of enals **3**, different substituent at the β aromatic moiety could be accommodated well, regardless of their electronic and steric properties and the position on the phenyl ring. The β-alkylation products **6p-v** were formed with exclusive 1,4-selectivity, in moderate to good yields and with good stereocontrol.

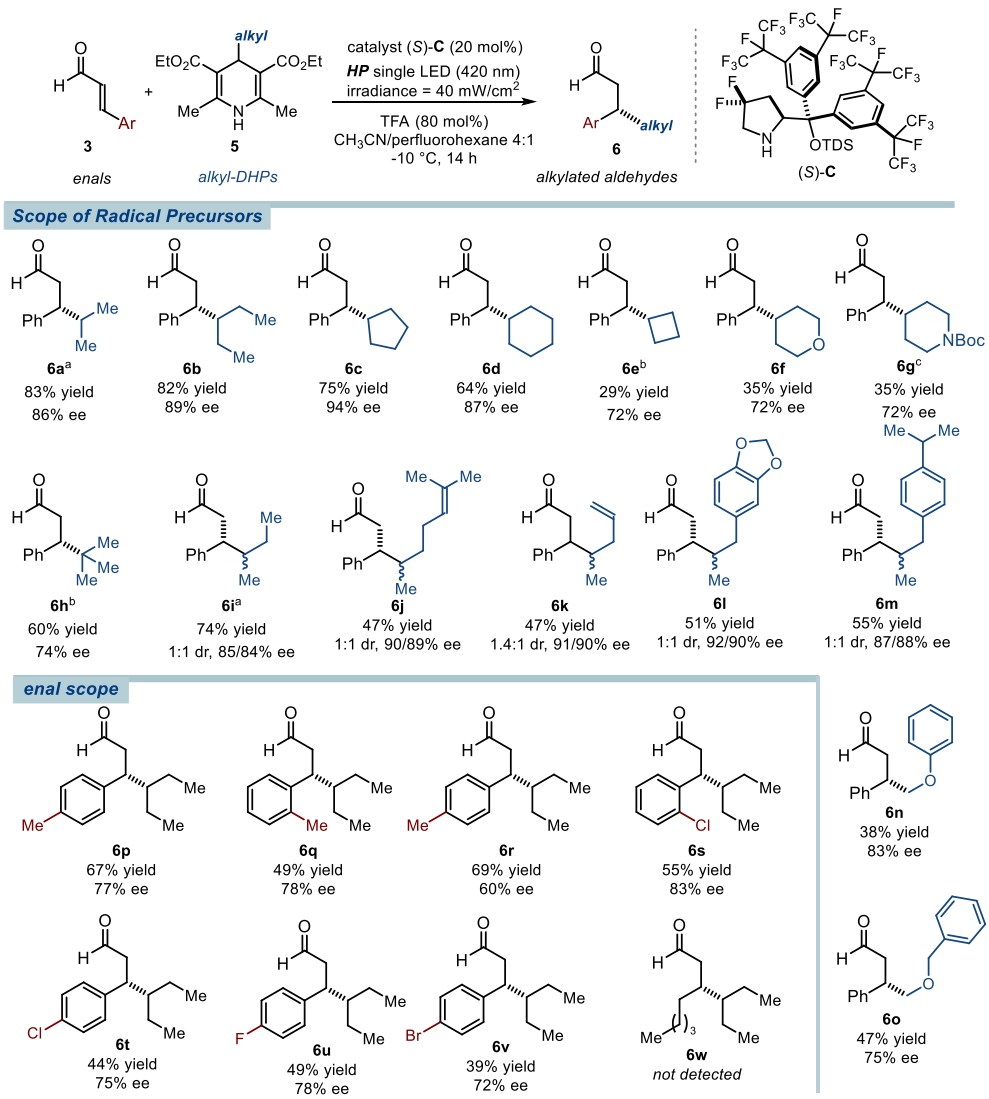

Scheme 3.17. Survey of the enals **3** and the 4-alkyl-1,4-dihydropyridines **5** that can participate in the photochemical catalytic strategy for the asymmetric installation of alkyl fragments at the β position of enals. Reactions performed on a 0.1 mmol scale over 14 hours in a 4:1 CH_3CN/perfluorohexane (C_6F_{14}) solvent mixture (0.5 mL) using 3 equiv. of **3** and an irradiance of 40 mW/cm². Yields and enantiomeric excesses of the isolated products are indicated below each entry. [a] Performed in a 2:1 CH_3CN/C_6F_{14} solvent mixture (0.3 mL). [b] Performed using 40 mol% of TFA and the corresponding tetrabutylammonium trifluoroborate as the radical precursor. [c] Performed in dichloromethane using catalyst (*S*)-**B** and 100 mol% of TFA. TDS: thexyl-dimethylsilyl.

As a limitation of the method, the presence of a linear alkyl substituent at the β position of enals **3** completely inhibited the reaction (adduct **6w**). A possible rationalization for this lack of reactivity is the inability of the iminium ions derived from aliphatic enals (e.g. octenal) to absorb light in the visible region. We therefore performed the β-alkylation reaction of octenal

3a using a high-power black light LED (λ_{max} = 365 nm, Scheme 3.18.), a wavelength which could be absorbed by the aliphatic iminium ion. For this experiment, we used potassium *iso*-propyl trifluoroborate salt **18** as the radical precursor since the DHP derivative can absorb light at this wavelength and undergo decomposition (Chapter 2.2.). Unfortunately, we could not detect the desired β-alkylation product **6a**.

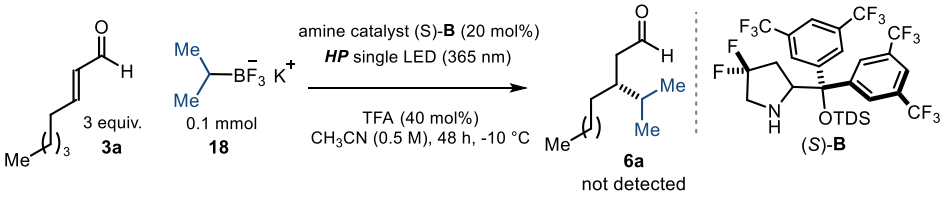

Scheme 3.18. Evaluating the reactivity of octenal **3a** in the photochemical β-alkylation reaction.

Based on this result, a plausible explanation is that aliphatic enals **26** may form an extended enamine (dienamine) **XI** upon reaction with the amine catalyst **7**, which changes its electronic nature. Although the dienamine intermediate **XI** can absorb visible light,[34] it would become a strong reductant in the excited state and therefore could not trigger the SET oxidation of the radical precursor (Scheme 3.19.).

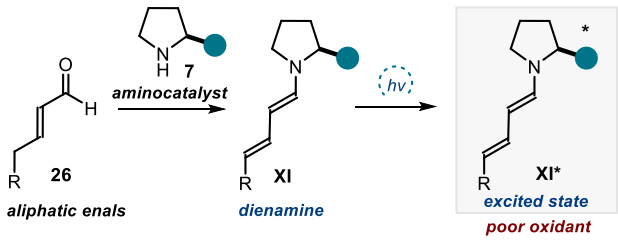

Scheme 3.19. Formation of dienamine intermediate **XI** from aliphatic enals **26** and aminocatalyst **7**.

3.3.5. Functionalization of Glycosides

To further expand the synthetic utility of the methodology, the optimized conditions were applied to the stereocontrolled preparation of saccharide-containing aldehydes (Scheme 3.20). The 1,4-dihydropyridine substrate bearing a galactosyl moiety **27** was easily prepared from the corresponding protected sugar.

[34] Silvi, M., Arceo, E., Jurberg, I. D., Cassani, C., Melchiorre, P., "Enantioselective Organocatalytic Alkylation of Aldehydes and Enals Driven by the Photoexcitation of Enamines", *J. Am. Chem. Soc*, **2015**, *137*, 6120.

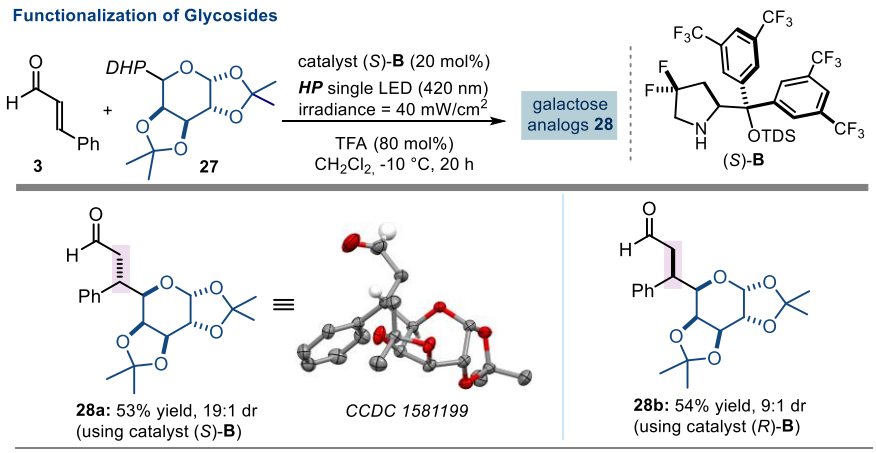

Scheme 3.20. Stereocontrolled synthesis of saccharide-containing aldehydes. The configuration of the stereocenter highlighted in pink is dictated by the chiral aminocatalyst **B**.

The reaction with **27** delivers the target adducts **28** in good yields and high stereocontrol. The reactions were performed with both enantiomers of the chiral organic catalyst **B**, providing access to different diastereoisomers of the galactose derivatives (adducts **28a** and **28b**). These results indicate that the chiral catalyst governs the stereoselectivity of the process and can overwrite the inherent stereochemical information encoded within the chiral substrate. Finally, we obtained crystals of product **28a**, which were suitable for X-ray crystallographic analysis. This established the absolute stereochemistry of the product.

3.3.6. Mechanistic Considerations

The proposed mechanism for the β-alkylation of α,β-unsaturated aldehydes via excited-state iminium ion catalysis is shown in Scheme 3.21.[4] First, the condensation of the chiral secondary amine catalyst with the enal **3**, in the presence of an acid-cocatalyst, delivers the iminium ion intermediate **I**. Selective light excitation of the iminium ion at 420 nm (violet LED) provides access to an electronically excited state **I***, which could trigger the SET oxidation of the 4-alkyl-1,4-dihydropyridines **5**. This event affords the 5π electron-β-enaminyl radical intermediate **III** and the radical cation **X**, which upon C–C bond fragmentation decomposes to pyridine **21** and a neutral carbon-centered radical **V**. Subsequent stereoselective intermolecular coupling of **V** with the chiral β-enaminyl radical[35] **III** results in a new C–C bond while forging the stereogenic center. Finally, the hydrolysis of

[35] Radical couplings can occur between a transient and a persistent radical. In this case, the chiral β-enaminyl radical can be considered a persistent radical, since the radical is located at both a benzylic and an allylic position. Therefore, this intermediate can govern a stereoselective radical coupling with a transient alkyl radical. For a review on the persistent radical effect, see: Leifert, D., Studer, A., "The Persistent Radical Effect in Organic Synthesis", *Angew. Chem. Int. Ed.*, **2020**, *59*, 74.

the resulting enamine intermediate **VI** generates the amine catalyst while liberating the β-alkylated aldehyde **6**.

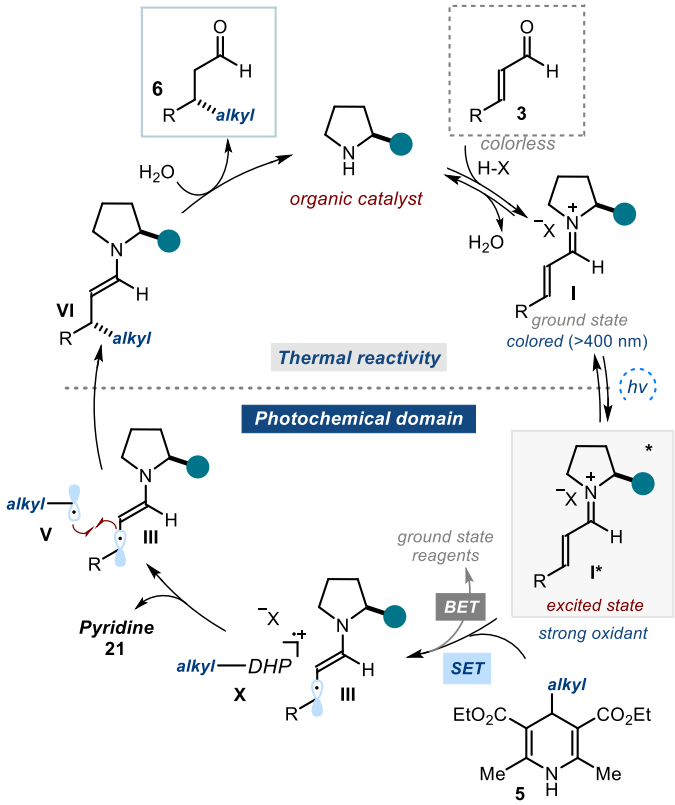

Scheme 3.21. Proposed mechanism for the excited iminium ion-mediated β-alkylation of enals.

In addition to the mechanism proposed above, we considered a self-propagating radical-chain mechanism as an alternative reaction pathway for the photochemical enantioselective β-alkylation of cinnamaldehyde (Scheme 3.22.). In this scenario, the photochemical activity of the iminium ion **I** would serve as the initiation event by inducing the SET oxidation of alkyl-DHPs **5**, which lead to the generation of the alkyl radical **V**. The self-propagating chain process would be triggered by the trapping of radical **V** by the ground-state iminium ion **I** through radical conjugate addition to deliver the α-iminyl radical cation **XII**. Subsequently, the radical cation **XII** would trigger the SET oxidation of alkyl-DHP **21**, therefore regenerating the crucial propagating alkyl radical **V**.

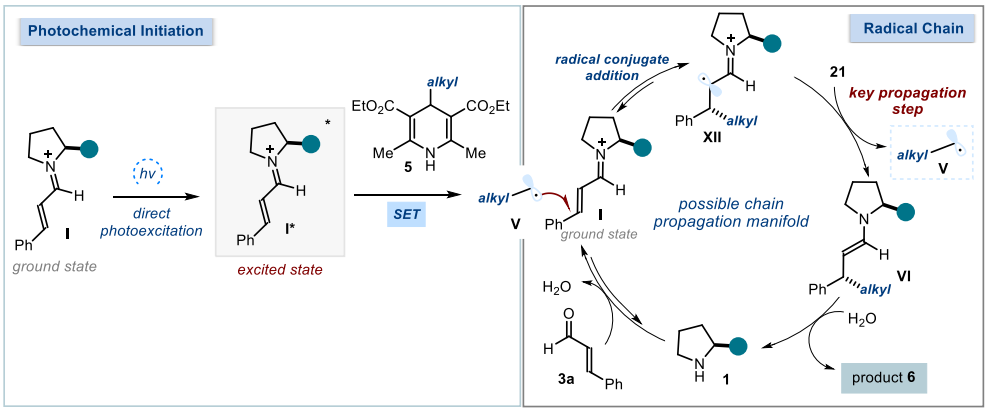

Scheme 3.22. Alternative self-propagating radical-chain mechanism.

One way to evaluate the feasibility of the key propagation step is to compare the redox potentials of α-iminyl radical intermediate **XII** and the radical precursors **5**. The redox potential of intermediate **XII** can be estimated by cyclic voltammetry study of the enamine **VI**. However, enamines of type **VI** are difficult to synthesize due to the high instability of enamines lacking an aryl substitent. We measured instead the oxidation potential of the relatively stable enamines **XIIIa** and **XIIIb**, which mimics the actual intermediate **VI** involved in the propagation step (Figure 3.10a), by cyclic voltammetry.[4] The electrochemical oxidation of enamines **XIIIa** and **XIIIb** provides access to α-iminyl radical cation of type **XII**, which is the key intermediate of the chain propagation. The oxidation potentials of **XIIIa** and **XIIIb** are reported to be +0.60 V and +0.88 *vs* Ag/Ag^+ in CH_3CN, (irreversible oxidation to give the α-iminyl radical **XIVa** and **XIVb**, respectively).[4] These values mean that the intermediate of type **XII** is incapable of oxidizing the alkyl-DHP **5** since the SET event is thermodynamically unfavorable.

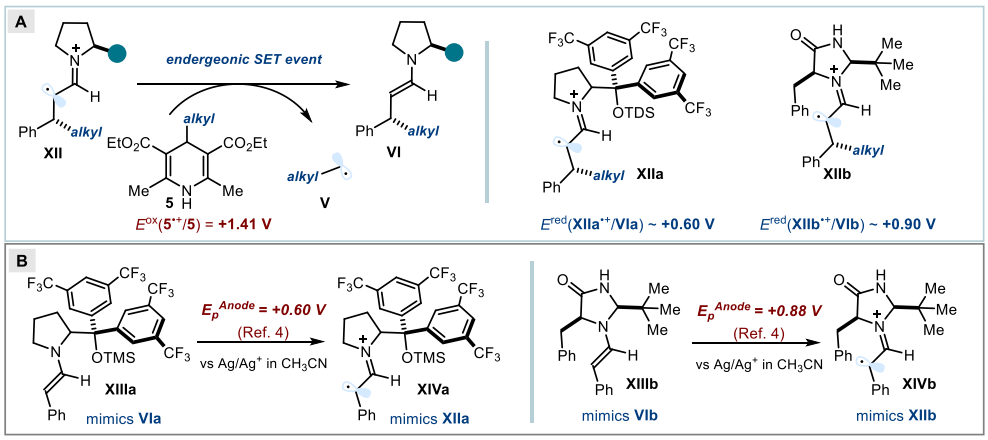

Figure 3.10. a) Endergonic SET event involving alkyl-DHP **5** and α-iminyl radical cation **XII**, a key step to regenerate propagating alkyl radical **V**. b) Estimated redox potential of α-iminyl radical cation **XIIa** and **XIIb**. TDS: thexyl-dimethylsilyl; TMS: trimethylsilyl

To exclude the possible excitation of 4-alkyl DHPs, which are known to be photo-active and might generate radicals upon light absorption (Chapter 2.2.), we recorded the UV-Vis absorption spectrum of the model substrate **25**. As depicted in Figure 3.11, the substrate presents an absorption band with a long wavelength tail (405 nm) that falls right outside of the irradiation wavelength used in the catalytic process (420 nm).

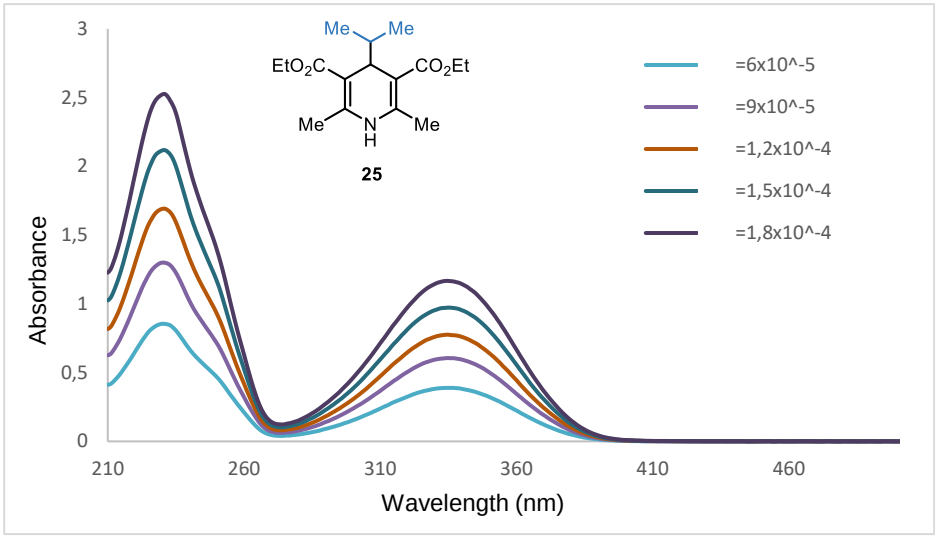

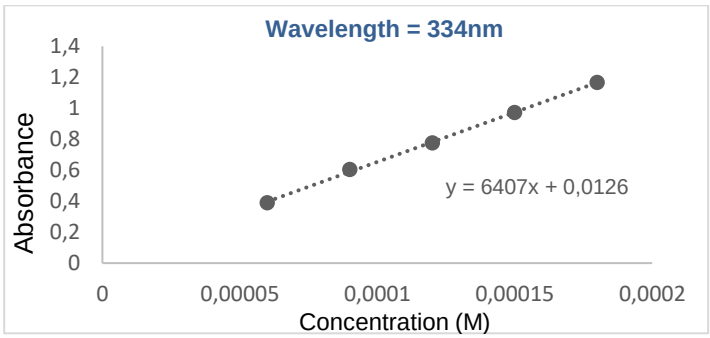

Figure 3.11. UV-Vis absorption spectra of **25** at different concentrations and Lambert-Beer linear correlation between absorbance and concentration at 334nm.

Further control experiments were conducted performing the model reaction in the absence of the catalyst, acid and light irradiation. As summarized in Table 3.5., the reaction does not proceed in the absence of the acid or the amine catalyst (entry 1 and 2). In these cases, the conversion of the DHP **25** is less than 10%, confirming the absence of a direct absorption of the DHP substrate **25**. These experiments also rule out the direct involvement of

cinnamaldehyde **3** photoactivity at this wavelength. The reaction does not proceed in the absence of light, confirming the photochemical nature of the transformation (entry 4).

Table 3.5. Control experiments

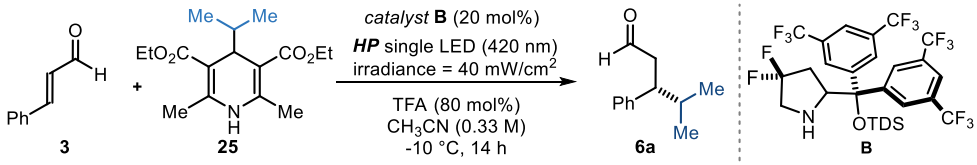

entry	TFA	Catalyst	Light	Conversion **25** (%)[a]	Yield **6a** (%)[b]
1	✗	✗	✓	< 10	0
2	✗	✓	✓	< 10	0
3	✓	✗	✓	74	8
4	✓	✓	✗	0	0

[a]Conversion of **25** was determined by ^{1}H-NMR analysis using trichloroethylene as the internal standard. [b]Yield of **6a** determined by ^{1}H-NMR analysis using trichloroethylene as the internal standard. TDS: thexyldimethyl silyl.

However, when adding TFA in the absence of amine catalyst **B**, we observed the formation of the alkylation product **6a** in 8% yield along with 74% conversion of the DHP **25** (entry 3). The rationale behind this observation could be that the presence of TFA triggers the homolytic C–C cleavage of the DHP **21a** under light irradiation and generates the *iso*-propyl radical along with the pyridine side-product. This possibility was recently corroborated by Wang and Chen, who demonstrated the decomposition of 4-cyclohexyl-DHP **29** under blue LED irradiation in the presence of stoichiometric amount of TFA (Scheme 3.23.). [36]

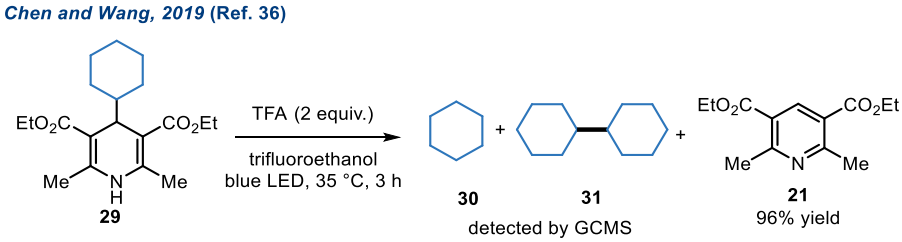

Scheme 3.23. Decomposition of DHP in the presence of TFA under LED illumination.

[36] Chen, X., Ye, F., Luo, X., Liu, X., Zhao, J., Wang, S., Zhou, Q., Chen, G., Wang, P., "Histidine-Specific Peptide Modification via Visible-Light-Promoted C-H Alkylation", *J. Am. Chem. Soc.* **2019**, 141, 18230.

3.4. Conclusions

In conclusion, we have developed a catalytic photochemical method for the direct regio- and stereoselective installation of alkyl fragments at the β-position of α,β-unsaturated aldehydes. The chemistry relies on the visible light excitation of chiral iminium ions, which turns them into strong oxidants and can trigger the generation of C(sp^3)-centered radicals from readily available alkyltrifluoroborate salts and 4-alkyl-1,4-dihydropyridines. The reaction is operationally simple and allows the preparation of a wide range of enantioenriched chiral β-alkylated aldehydes. In addition, this strategy could also be applied to the asymmetric functionalization of saccharides.

3.5. Experimental Section

General Information. The ^{1}H NMR, ^{19}F NMR, ^{13}C NMR spectra and HPLC or UPC^2 traces are available in the literature[1] and are not reported in the present dissertation.

The NMR spectra were recorded at 400 MHz and 500 MHz for 1H or at 100 MHz and 125 MHz for 13C, respectively. The chemical shifts (δ) for 1H and 13C are given in ppm relative to residual signals of the solvents (CHCl3 @ 7.27 ppm 1H NMR, 77.00 ppm 13C NMR). Coupling constants are given in Hz. The following abbreviations are used to indicate the multiplicity: s, singlet; d, doublet; t, triplet; q, quartet; m, multiplet; br s, broad signal.

High-resolution mass spectra (HRMS) were obtained from the ICIQ High Resolution Mass Spectrometry Unit on MicroTOF Focus and Maxis Impact (Bruker Daltonics) with electrospray ionization. X-ray data were obtained from the ICIQ X-Ray Unit using a Bruker-Nonius diffractometer equipped with an APPEX 2 4K CCD area detector. Optical rotations were measured on a Polarimeter Jasco P-1030 and are reported as follows: $[\alpha]_D$ rt (c in g per 100 mL, solvent).
UV-vis measurements were carried out on a Shimadzu UV-2401PC spectrophotometer equipped with photomultiplier detector, double beam optics and D2 and W light sources. Cyclic voltammetry studies were carried out on a Princeton Applied Research PARSTAT 2273 potentiostat offering compliance voltage up to ± 100 V (available at the counter electrode), ± 10 V scan range and ± 2 A current range.

General Procedures. All reactions were set up under an argon atmosphere in oven-dried glassware using standard Schlenk techniques, unless otherwise stated. Synthesis grade solvents were used as purchased. Anhydrous solvents were taken from a commercial SPS solvent dispenser. Chromatographic purification of products was accomplished using force-flow chromatography (FC) on silica gel (35-70 mesh). For thin layer chromatography (TLC) analysis throughout this work, Merck precoated TLC plates (silica gel 60 GF_{254}, 0.25 mm) were used, using UV light as the visualizing agent and and either phosphomolybdic acid in EtOH, dinitrophenylhydrazine in EtOH/H_2O or basic aqueous potassium permangante ($KMnO_4$), and heat as developing agents. Organic solutions were concentrated under reduced pressure on a Büchi rotary evaporator (in vacuo at 40 ºC, ~5 mbar).

Determination of Diastereomeric Ratio. The diastereomeric ratio was determined by ^{1}H NMR analysis of the crude reaction mixture through integration of diagnostic signals.
Determination of Enantiomeric Purity: HPLC analysis on chiral stationary phase was performed on an Agilient 1200 series HPLC, using a Daicel Chiralpak IC-3 column with *i*PrOH:hexane as the eluent. UPC^2 analysis on chiral stationary phase was performed on an Waters Acquity instrument using a CEL1, CEL2, ID3 or IE3 chiral colums. The exact conditions for the analyses are specified within the characterization section. HPLC/ UPC^2

traces were compared to racemic samples prepared by running the reaction in the presence of a catalytic amount (20 mol%) of racemic 2-tert-butyl-3-methyl-5-benzyl-4-imidazolidinone, which is commercially available form Sigma Aldrich.

Materials: Commercial grade reagents and solvents were purchased at the highest commercial quality from Sigma Aldrich, Fluka, Acros Organics, Fluorochem or Alfa Aesar and used as received, unless otherwise stated. Chiral secondary amine catalysts **B** and **C** were prepared according to the reported literature. Cinnamaldehyde **3a** and the majority of enals **3** are commercially available. All the alkyl trifluoroborate salts and the majority of 4-alkyl-1,4-dihydropyridine derivatives (Hantzsch esters) were prepared according to known literature procedures (Ref. 33). The preparation of other 4-alkyl-1,4-dihydropyridines is described in the following section.

3.5.1. Substrate Synthesis

Synthesis of 4-Alkyl-1,4-Dihydropyridines 5

Many 4-alkyl-1,4-dihydropyridines were synthesized using procedure reported in the literature (Ref. 33). The following Hantzsch esters were prepared from the corresponding aldehydes.

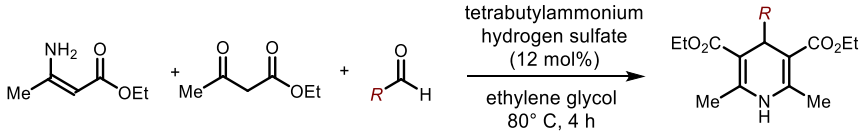

In accordance to the reported procedure[33] ethyl-3-aminocrotonate (1.0 equiv) and ethylene glycol (2.5M) were added to a flask under nitrogen. Next, ethyl acetoacetate (1.0 equiv) was added followed by aldehyde (1.0 equiv) and tetrabutylammonium hydrogen sulfate (12 mol%). The resultant solution was heated at 80 °C for 4 hours, then cooled and diluted with ethyl acetate. The solution was added to a solution of brine and separated using ethyl acetate (3 x 50 mL). The organic layers were combined, dried ($MgSO_4$) and concentrated. The crude material was purified by flash column chromatography to furnish the desired 4-alkyl-1,4-dihydropyridine.

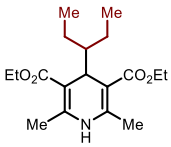

Diethyl 4-(3-pentyl)-2,6-dimethyl-1,4-dihydropyridine-3,5-dicarboxylate.

Prepared according to the procedure described above using 2-ethyl butanal (1.23 mL, 10.0 mmol). The crude material was purified by flash column chromatography (cyclohexane/ EtOAc 95:5) to give the corresponding product (1.21 g, 36% yield) as a yellow solid.

^{1}H NMR (500 MHz, $CDCl_3$) δ 5.51 (1H, s, N**H**), 4.25-4.11 (5H, m, 2 x O**C**$\mathbf{H}_2$$CH_3$ + C$\mathbf{H}_{(pyridyl)}$), 2.29 (6H, s, 2 x C$\mathbf{H}_3$), 1.31 (6H, td, *J* = 7.1, 0.5 Hz, 2 x $OCH_2C\mathbf{H}_3$), 1.23-1.02 (5H, m, C**H**($C\mathbf{H}_2CH_3$)$_2$), 0.87 (6H, t, *J* = 7.3 Hz, $CH(CH_2C\mathbf{H}_3)_2$);

^{13}C NMR (125.6 MHz, $CDCl_3$) δ 168.8 (2 x C), 144.6 (2 x C), 102.1 (2 x C), 59.6 (2 x CH_2), 49.8 (CH), 34.6 (CH), 21.2 (2 x CH_2), 19.3 (2 x CH_3), 14.3 (2 x CH_3), 11.8 (2 x CH_3).

HRMS (ESI) Exact mass calculated for $C_{18}H_{28}NO_4$ $[M-H]^-$: 322.2024, found: 322.2012.

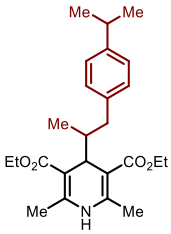

Diethyl 4-(1-(4-*iso*-propyl)phenylpropan-2-yl)-2,6-dimethyl-1,4-dihydropyridine-3,5-dicarboxylate.

Prepared according to the procedure described above using 3-(4-isopropylphenyl)isobutyraldehyde (2.00 mL, 10.0 mmol). The crude material was purified by flash column chromatography (cyclohexane/EtOAc 98:2) to give the corresponding product (1.56 g, 38% yield) as a yellow oil.

^{1}H NMR (500 MHz, $CDCl_3$) δ 7.12-7.07 (2H, m, ArH), 7.05-6.98 (2H, m, ArH), 5.57 (1H, s, NH), 4.29-4.06 (5H, m, OCH_2CH_3 + C=CCH), 2.86 (1H, app p, *J* = 6.9 Hz, $CH(CH_3)_2$), 2.77 (1H, dd, *J* = 13.3, 3.6 Hz, $CHCH_2Ar$), 2.32 (6H, app d, *J* = 1.7 Hz, 2 x $NCCH_3$), 2.09 (1H, dd, *J* = 13.3, 11.2 Hz, CH_2Ar), 1.75 (1H, ddd, *J* = 11.1, 7.5, 4.2 Hz, CH_2Ar), 1.31 (6H, dt, *J* = 12.2, 7.1 Hz, OCH_2CH_3), 1.23 (6H, d, *J* = 6.9 Hz, $CH(CH_3)_2$), 0.65 (3H, d, *J* = 6.8 Hz, $CHCH_3$).

^{13}C NMR (125.6 MHz, $CDCl_3$) δ 168.7 (C=O), 168.4 (C=O), 145.9 (C), 144.71 (C), 144.65 (C), 139.4 (C), 128.9 (2 x CH), 126.0 (2 x CH), 102.0 (C), 101.6 (C), 59.7 (2 x CH_2), 43-1 (CH), 38.84 (CH_3), 39.76 (CH_3), 33.7 (CH_2), 24.1 (2 x CH_3), 19.5 (CH), 19.4 (CH), 14.5 (CH_3), 14.44 (CH_3), 14.38 (CH_3).

HRMS (ESI) Exact mass calculated for $C_{25}H_{34}NO_4$ $[M-H]^-$: 412.2493, found: 412.2481.

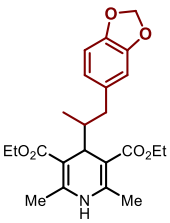

Diethyl 4-(1-(benzo[*d*][1,3]dioxol-5-yl)propan-2-yl)-2,6-dimethyl-1,4-dihydropyridine-3,5-dicarboxylate.

Prepared according to the procedure described above using 3-(benzo[*d*][1,3]dioxol-5-yl)-2-methylpropanal (1.92 g, 10.0 mmol). The crude material was purified by flash column chromatography (cyclohexane/EtOAc 80:20) to give the corresponding product (2.05 g, 49% yield) as a yellow oil.

^{1}H NMR (500 MHz, $CDCl_3$) δ 6.68 (1H, d, *J* = 7.9 Hz, ArH), 6.58 (1H, d, *J* = 1.5 Hz, ArH), 6.53 (1H, dd, *J* = 7.9, 1.5 Hz), 5.89 (2H, app q, *J* = 1.5 Hz, OCH_2O), 5.66 (1H, br s, NH), 4.28-4.13 (4H, m, OCH_2CH_3), 4.11 (1H, d, *J* = 4.8 Hz, C=CCH), 2.72 (1H, dd, *J* = 13.3, 3.5

Hz, $ArCH_2$), 2.32 (6H, app d, *J* = 1.6, $NCCH_3$), 2.03 (1H, dd, *J* = 13.3, 11.3 Hz, $ArCH_2$), 1.72-1.65 (1H, m, $CHCH_2Ar$), 1.32 (3H, t, *J* = 7.1 Hz, OCH_2CH_3), 1.30 (3H, t, *J* = 7.1 Hz, OCH_2CH_3), 0.63 (3H, d, *J* = 6.8 Hz, $CHCH_3$);

^{13}C NMR (125.6 MHz, $CDCl_3$) δ 168.6 (C=O), 168.4 (C=O), 147.3 (C), 145.2 (C), 144.8 (C), 144.7 (C), 136.0 (C), 121.7 (CH), 109.3 (CH), 107.8 (CH), 101.9 (C), 101.5 (C), 100.6 (CH_2), 59.7 (CH_2), 43.3 (CH), 39.0 (CH_2), 38.7 (CH), 19.5 (CH_3), 19.4 (CH_3), 14.4 (CH_3), 14.3 (CH_3).

HRMS (ESI) Exact mass calculated for $C_{29}H_{29}NNaO_6$ $[M+Na]^+$: 438.1887, found: 438.1885.

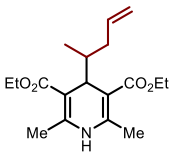

Diethyl 2,6-dimethyl-4-(pent-4-en-2-yl)-1,4-dihydropyridine-3,5-dicarboxylate

Prepared according to the procedure described above using 2-methylpent-4-enal (473 mg, 4.8 mmol). The crude material was purified by flash column chromatography (hexane/EtOAc 80:20) to give the corresponding product (713 mg, 46% yield) as a light yellow oil that solidified upon standing.

^{1}H NMR (500 MHz, $CDCl_3$) δ 5.77-5.68 (1H, m, $CH_2CH=CH_2$), 5.60 (1H, s, NH), 4.97-4.91 (2H, m, $CH=CH_2$), 4.26-4.13 (4H, m, OCH_2CH_3), 4.04 (1H, d, *J* = 4.8 Hz, C=CCH), 2.31 (6H, s, $NCCH_3$), 2.18-2.11 (1H, m, $CH_2CH=CH_2$), 1.72-1.64 (1H, m, $CH_2CH=CH_2$), 1.54-1.46 (1H, m, CCHCH), 1.30 (6H, t, *J* = 7.1 Hz, OCH_2CH_3), 0.73 (3H, d, *J* = 6.9 Hz, $CHCHCH_3$);

^{13}C NMR (125.6 MHz, $CDCl_3$) δ 168.6 (C=O), 168.4 (C=O), 144.6 (C), 138.6 (CH), 115.0 (CH_2), 102.0 (C), 101.5 (C), 59.6 (CH_2), 40.9 (CH), 38.1 (CH), 37.1 (CH_2), 19.5 (CH_3), 19.4 (CH_3), 14.9 (CH_3), 14.4 (CH_3).

HRMS (ESI) Exact mass calculated for $C_{18}H_{27}NNaO_4$ $[M+Na]^+$: 344.1832, found: 344.1834.

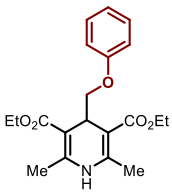

Diethyl 2,6-dimethyl-4-(phenoxymethyl)-1,4-dihydropyridine-3,5-dicarboxylate.

Prepared according to the procedure described above using 2-phenoxyacetaldehyde (1.3 g, 9.55 mmol). The crude material was purified by flash column chromatography (hexane/EtOAc 80:20) to give the corresponding product (2.2 g, 64% yield) as a light yellow solid.

^{1}H NMR (500 MHz, $CDCl_3$) δ 7.22 (dd, *J* = 8.8, 7.0 Hz, 2H, ArH), 6.90 – 6.86 (m, 3H, ArH), 5.77 (bs, 1H, NH), 4.42 (t, *J* = 5.8 Hz, 1H, C=CCH), 4.12 (qq, *J* = 10.8, 7.1 Hz, 4H, OCH_2CH_3), 3.86 (d, *J* = 5.8 Hz, 2H, OCH_2), 2.30 (s, 6H, $NCCH_3$), 1.24 – 1.18 (m, 6H, OCH_2CH_3).

^{13}C NMR (125.6 MHz, $CDCl_3$) δ 167.9 (2 x C=O), 159.4 (C), 146.2 (2 x C), 129.4 (2 x CH), 120.3 (CH), 114.6 (2 x CH), 100.1 (2 x C), 70.5 (CH_2), 60.0 (2 x CH_2), 33.9 (CH), 19.6 (2 x CH_3), 14.4 (2 x CH_3).

3.5.2. Catalyst Synthesis

Synthesis of the Chiral Amine Catalyst (*R*)-B

The chiral amine catalyst (*R*)-**B** was synthesized as shown in the following scheme according to reference 4:

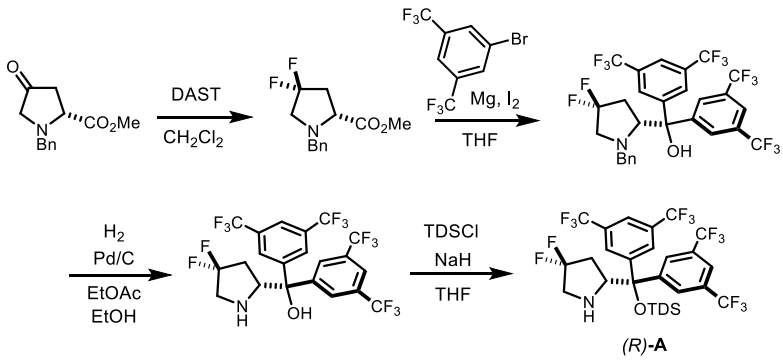

Scheme S3.1. Synthesis of chiral amine catalyst (*R*)-**B.**

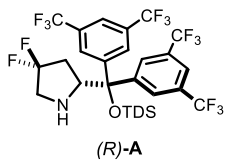

(*R*)-2-(Bis-(3,5-bis-(trifluoromethyl)-phenyl)-(((2,3-dimethylbutan-2-yl)-dimethylsilyl)-oxy)-methyl)-4,4-difluoropyrrolidine ((*R*)-B).

^{1}H NMR (400 MHz, $CDCl_3$): δ 8.10 (s, 2H, *ortho*), 8.01 (s, 2H, *para* and *para*'), 7.92 (s, 2H, *ortho*'), 4.47 (br t, *J* = 8.3 Hz, 1H, C2**H**), 3.21-3.09 (m, 1H, C5**H**H), 2.69-2.55 (m, 1H, C5H**H**), 2.31-2.11 (m, 2H, C3**H**H and N**H**), 1.95-1.69 (m, 2H, C3H**H** and SiCC**H**), 0.95 (d, *J* = 3.0 Hz, 3H, SiCCHC**H**$_3$), 0.94 (d, *J* = 3.0 Hz, 3H, SiCCHC**H**$_3$'), 0.89 (s, 3H, SiCC**H**$_3$), 0.87 (s, 3H, SiCC**H**$_3$'), -0.13 (s, 3H, SiC**H**$_3$), -0.47 (s, 3H, SiC**H**$_3$).

^{13}C NMR (101 MHz, $CDCl_3$): δ 146.3 (*ipso*), 144.8 (*ipso*'), 131.9 (2C, q, J_{CF} = 33.8 Hz, *meta*), 131.2 (2C, q, J_{CF} = 32.8 Hz, *meta'*), 128.2 (dd, J_{CF} = 249.2 Hz, 247.2 Hz, *C4*), 129.3 (2C, q, J_{CF} = 3.6 Hz, *ortho*), 128.6 (2C, q, J_{CF} = 3.9 Hz, *ortho*'), 123.4 (2C, q, J_{CF} = 273.2 Hz, Ar**C**F$_3$), 123.2 (2C, q, J_{CF} = 272.9 Hz, Ar'**C**F$_3$), 122.4 (apparent p, J_{CF} = 3.8 Hz, *para*), 122.2 (apparent p, J_{CF} = 3.8 Hz, *para*'), 82.0 (*C6*), 62.6 (dd, J_{CF} = 6.6 Hz, 1.3 Hz, *C2*), 53.7 (t, J_{CF} = 28.8 Hz, *C3*), 37.4 (t, J_{CF} = 24.9 Hz, *C5*), 33.7 (SiC**C**H), 25.8 (Si**C**CH), 20.2 (SiC**C**H$_3$), 20.0 (SiC**C**H$_3$'), 18.5 (2C, SiCCH**C**H$_3$), -0.18 (Si**C**H$_3$), -0.96 (Si**C**H$_3$').

^{19}F NMR (376 MHz, $CDCl_3$): δ -63.01 (s, 6F, $ArCF_3$), -63.05 (s, 6F, Ar'CF_3), -97.7 (dp, J_{FF} = 231.5 Hz, J_{HF} = 18.7 Hz, 1F, C4*F*F), -104.1 (br d, J_{FF} = 228.7 Hz, 1F, C4F*F*).

HRMS: calculated for $C_{29}H_{32}F_{14}NOSi$: 704.2024, found: 704.2052.

$[\alpha]_D^{26}$ = –2.2 (c= 0.62, $CHCl_3$). Lit: $[\alpha]_D^{26}$ = +1.9 (c= 0.5 $CHCl_3$, for (*S*) enantiomer.[5]

3.5.3. General Procedure for the Photochemical β-Alkylation of Enals

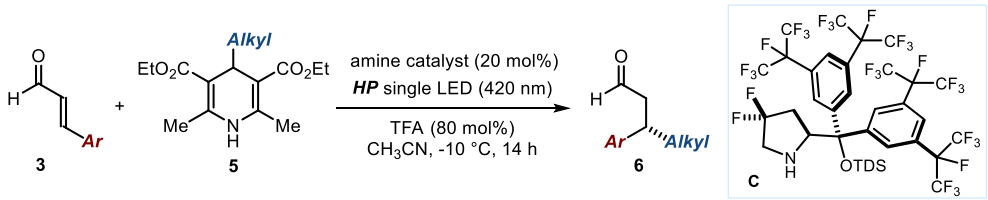

General Procedure: To a 5 mL argon-purged glass vial, containing the amine catalyst **C** (22.1 mg, 0.02 mmol, 20 mol%) and the desired 4-alkyl-1,4-dihydropyridine **5** (0.1 mmol, 1 equiv.), was added enal **3** (0.3 mmol, 3 equiv.) Then 400 µL of an argon-sparged 0.2 M acetonitrile solution of TFA (6.2 µL, 0.08 mmol, 80 mol%) and perfluorohexane (100 µL) were added. The vial was sealed with Parafilm, and then placed into an aluminium block on a 3D-printed holder, fitted with a 420 nm high-power single LED. The irradiance was fixed at 40±2 mW/cm^2, as controlled by an external power supply and measured using a photodiode light detector at the start of each reaction (Figure 3.8, Chapter 3.3.1.). The temperature was kept at -10 °C with a chiller connected to the irradiation plate. The reaction was stirred for the indicated time (generally 14 hours), then the solvent was evaporated and the crude mixture was purified by flash column chromatography on silica gel to furnish the product **6.**

The light source used for illuminating the reaction vessel consisted in a 420 nm high-power single LED (OCU-440 UE420-X-T) purchase form OSA OPTO.

3.5.4. Characterization of the β-Alkylation Products 6

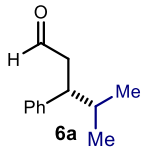

(*R*)-4-Methyl-3-phenylpentanal (6a)

Prepared according to the general procedure using cinnamaldehyde (39.6 mg, 0.3 mmol), aminocatalyst **C** (22.1 mg, 20 mol%), the corresponding dihydropyridine (29.5 mg, 0.1 mmol), trifluoroacetic acid (7.6 µL, 0.1 mmol), acetonitrile (200 µL) and perfluorohexane (100 µL). The crude material was purified by flash column chromatography (pentane/diethyl ether 99.7:0.3) to give the product **6a** (14.6 mg, 83% yield, 86% ee, average of two runs) as a colourless oil. The enantiomeric excess of the corresponding alcohol (obtained upon reduction with sodium borohydride) was determined by UPC^2 analysis using a CEL2 chiral column: after 1 min of 100% CO_2, gradient up to 60:40

CO_2/isopropanol over 5 minutes, curve 6), flow rate 2 mL/min. τ_{minor} = 3.31 min, τ_{major} = 3.51 min (86% ee); $[\alpha]_D^{26}$ = –14.3 (c = 0.57, CH_2Cl_2, 86% ee), Lit: $[\alpha]_D^{26}$ = +14.9 (c = 1.04 CH_2Cl_2, 83% ee, for (*S*) enantiomer).

^{1}H NMR (400 MHz, $CDCl_3$) δ 9.61 (1H, t, *J* = 2.2 Hz, C**H**O), 7.33-7.28 (2H, m, Ar**H**), 7.25-7.18 (1H, m, Ar**H**), 7.18-7.13 (2H, m, Ar**H**), 2.96 (1H, ddd, *J* = 9.5, 7.5, 5.5 Hz, PhC**H**), 2.84-2.71 (2H, m, CHOC**H**$_2$), 1.95-1.81 (1H, m, C**H**$(CH_3)_2$), 0.96 (3H, d, *J* = 6.7 Hz, C**H**$_3$), 0.79 (3H, d, *J* = 6.7 Hz, C**H**$_3$);

^{13}C NMR (101 MHz, $CDCl_3$) δ 202.4 (C=O), 142.5 (C), 128.3 (CH), 128.2 (CH), 126.5 (CH), 47.2 (CH_2), 46.9 (CH), 33.4 (CH), 20.5 (CH_3), 20.2 (CH_3).

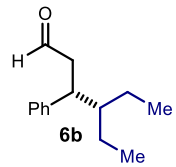

6b

(*R*)-4-ethyl-3-phenylhexanal (6b) Prepared according to the general procedure using cinnamaldehyde (39.6 mg, 0.3 mmol), aminocatalyst **C** (22.1 mg, 20 mol%), the corresponding dihydropyridine (32.3 mg, 0.1 mmol), trifluoroacetic acid (6.2 µL, 0.08 mmol), acetonitrile (400 µL) and perfluorohexane (100 µL). The crude material was purified by flash column chromatography (pentane/diethyl ether 99.7:0.3) to give the product **6b** (17.6 mg, 86% yield, 88% ee, average of two runs) as a colourless oil. The enantiomeric excess of the corresponding alcohol (obtained upon reduction with sodium borohydride) was determined by HPLC analysis on a Agilent IC-3 column, 95:05 hexane/*i*-PrOH, flow rate 0.6 mL/min, 20 °C. λ = 215 nm. τ_{minor} = 16.0 min, τ_{major} = 20.1 min (88% ee). $[\alpha]_D^{26}$ = –4.49 (c = 0.79, $CHCl_3$, 88% ee).

^{1}H NMR (500 MHz, $CDCl_3$) δ 9.60 (1H, t, *J* = 2.3 Hz, C**H**O), 7.32-7.27 (2H, m, Ar**H**), 7.23-7.18 (3H, m, Ar**H**), 3.25 (1H, q, *J* = 7.4 Hz, PhC**H**), 2.77-2.74 (2H, m, CHOC**H**$_2$), 1.51-1.39 (1H, m, CH(C**H**$_2$CH$_3$)$_2$), 1.37-1.23 (3H, m, CH(C**H**$_2$CH$_3$)$_2$), 1.11 (1H, dp, *J* = 14.5 Hz, 7.4 Hz, PhCHC**H**), 0.90 (3H, t, *J* = 7.4 Hz, CH(CH_2C**H**$_3$)$_2$), 0.83 (3H, t, *J* = CH(CH_2C**H**$_3$)$_2$);

^{13}C NMR (125.8 MHz, $CDCl_3$) δ 202.6 (C=O), 142.8 (C), 128.4 (2 x CH), 128.3 (2 x CH), 126.4 (CH), 46.7 (CH_2), 46.0 (CH), 41.9 (CH), 22.3 (CH_2), 21.9 (CH_2), 11.1 (CH_3), 10.8 (CH_3).

HRMS (ESI) Exact mass calculated for $C_{14}H_{20}NaO$ $[M+Na]^+$: 227.1406, found: 227.1399.

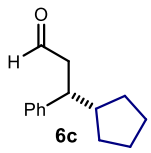

6c

(*R*)-3-cyclopentyl-3-phenylpropanal (6c)

Prepared according to the general procedure using cinnamaldehyde (39.6 mg, 0.3 mmol), aminocatalyst **C** (22.1 mg, 0.02 mmol), the corresponding dihydropyridine (32 mg, 0.1 mmol), trifluoroacetic acid (6.2 µL, 0.08 mmol), acetonitrile (400 µL) and perfluorohexane (100 µL). The crude material was purified by flash column chromatography (pentane/diethyl ether 99.7:0.3) to give the product **6c** (15.1 mg, 75% yield, 94% ee, average of two runs) as a colourless oil. The enantiomeric excess of the

corresponding alcohol (obtained upon reduction with sodium borohydride) was determined to be 94% by HPLC analysis on a Daicel Chiralpack IC-3 column: 90:10 hexane/*i*-PrOH, flow rate 0.6 mL/min, 20 °C, λ = 215 nm. τ_{minor} = 11.5 min, τ_{major} = 14.5 min. $[\alpha]_D^{26}$ = +15.1 (c= 0.40, $CHCl_3$, 94% ee).

^{1}H NMR (500 MHz, $CDCl_3$) δ 9.60 (1H, t, *J* = 2.3 Hz, C**H**O), 7.31-7.25 (2H, m, Ar**H**), 7.21-7.17 (3H, m, Ar**H**), 2.94 (1H, td, *J* = 9.7, 5.0 Hz, ArC**H**), 2.83-2.72 (2H, m, C**H**$_2$CHO), 2.10-2.02 (1H, m, C**H**CHCH$_2$CHO), 1.91-1.84 (1H, m, cyclopentyl**H**), 1.73-1.62 (1H, m, cyclopentyl**H**), 1.63-1.52 (2H, m, cyclopentyl**H**), 1.49-1.35 (2H, m, cyclopentyl**H**), 1.26-1.16 (1H, m, cyclopentyl**H**), 1.09-1.00 (1H, m, cyclopentyl**H**);

^{13}C NMR (125.8 MHz, $CDCl_3$) δ 202.4 (C=O), 143.8 (C), 128.5 (2 x CH), 127.8 (2 x CH), 126.5 (CH), 49.5 (CH_2), 46.4 (CH), 46.2 (CH), 31.4 (CH_2), 31.3 (CH_2), 25.2 (CH_2), 24.8 (CH_2);

HRMS (ESI) Exact mass calculated for $C_{15}H_{22}NaO_2$ $[M+MeOH+Na]^+$: 257.1512, found: 257.1513.

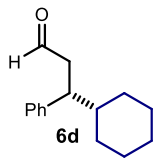

6d

(*R*)-3-cyclohexyl-3-phenyl-propanal (6d)

Prepared according to the general procedure using cinnamaldehyde (39.6 mg, 0.3 mmol), aminocatalyst **C** (22.1 mg, 0.02 mmol), the corresponding dihydropyridine (33.5 mg, 0.1 mmol), trifluoroacetic acid (6.2 µL, 0.08 mmol), acetonitrile (400 µL) and perfluorohexane (100 µL). The crude material was purified by flash column chromatography (pentane/diethyl ether 99.7:0.3) to give the product **6d** (13.8 mg, 64% yield, 87% ee, average of two runs) as a colourless oil. The enantiomeric excess of the corresponding alcohol (obtained upon reduction with sodium borohydride) was determined by HPLC analysis on a Agilent IC-3 column, 90:10 hexane/*i*-PrOH, flow rate 0.6 mL/min, 20 °C. λ = 215 nm. τ_{minor} = 12.6 min, τ_{major} = 15.3 min (87% ee). $[\alpha]_D^{26}$ = -3.7 (c= 0.66, $CHCl_3$, 87% ee).

^{1}H NMR (400 MHz, $CDCl_3$) δ 9.61 (1H, t, *J* =2,2 Hz, C**H**O), 7.32-7.26 (2H, m, Ar**H**), 7.23-7.18 (1H, m, Ar**H**), 7.16-7.12 (2H, m, Ar**H**), 3.02-2.94 (1H, m, ArC**H**), 2.87-2.68 (2H, m, C**H**$_2$CHO), 1.85- 1.71 (2H, m, cyclohexyl**H**), 1.69-1.59 (2H, m, cyclohexyl**H**), 1.54-1.44 (2H, m, cyclohexyl**H**), 1.25-1.02 (3H, m, cyclohexyl**H**), 1.00-0.77 (2H, m, cyclohexyl**H**).

^{13}C NMR (101 MHz, $CDCl_3$) δ 202.6 (C=O), 142.7 (C), 128.3 (CH), 128.2 (CH), 126.4 (CH), 47.1(CH_2), 46.1 (CH), 43.1 (CH), 31.0 (CH), 30.7 (CH_2), 26.4 (CH_2), 26.3 (CH).

(*R*)-3-cyclobutyl-3-phenyl-propanal (6e)

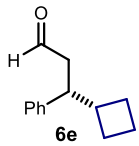

6e

Prepared according to the general procedure using cinnamaldehyde (39.6 mg, 0.3 mmol), aminocatalyst **C** (22.1 mg, 0.02 mmol), tetrabutylammonium cyclobutyltrifluoroborate (36.5 mg, 0.1 mmol), trifluoroacetic acid (3.1 µL, 0.04 mmol), acetonitrile (200 µL) and perfluorohexane (100 µL). The crude material was purified by flash column chromatography (pentane/diethyl ether 99:1) to give the product **3e** (5.5 mg, 29% yield, 72% ee, average of two runs) as a colourless oil. The enantiomeric excess of the corresponding alcohol (obtained upon reduction with sodium borohydride) was determined to be 72% by HPLC analysis on a Daicel Chiralpack IC-3 column: 90:10 hexane/*i*-PrOH, flow rate 0.6 mL/min, 20 °C, λ = 215 nm. τ_{minor} = 11.5 min, τ_{major} = 13.1 min (72% ee). $[\alpha]_D^{26}$ = -12.1 (c= 0.3,$CHCl_3$, 72%ee).

^{1}H NMR (500 MHz, $CDCl_3$) δ 9.65 (1H, t, *J* = 2.3 Hz, C**H**O), 7.32-7.27 (2H, m, Ar**H**), 7.23-7.16 (3H, m, Ar**H**), 3.13-3.06 (1H, m, ArC**H**), 2.68-2.63 (2H, m, CHOC**H**$_2$), 2.59-2.48 (1H, m, cyclobutyl**H**), 2.16-2.06 (1H, m, cyclobutyl**H**), 1.84-1.70 (3H, m, cyclobutyl**H**), 1.66-1.58 (1H, m, cyclobutyl**H**), 1.35-1.26 (1H, m, cyclobutyl**H**).

^{13}C NMR (125.8 MHz, $CDCl_3$) δ 202.2 (C=O), 142.1 (C), 128.5 (CH), 127.6 (CH), 126.6 (CH), 47.8 (CH_2), 47.0 (CH), 41.4 (CH), 27.5 (CH_2), 26.8 (CH_2), 17.3 (CH_2).

HRMS (ESI) Exact mass calculated for $C_{14}H_{20}NaO_2$ $[M+Na+MeOH]^+$: 243.1356, found: 243.1357.

This entry was performed using tetrabutylammonium cyclobutyltrifluoroborate as the radical precursor because of the photochemical inactivity of the corresponding dihydropyridine, which failed to deliver the corresponding radical upon excitation.

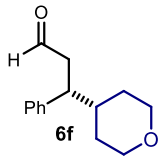

6f

(*R*)-3-phenyl-3-(tetrahydro-2H-pyran-4-yl)propanal (6f)

Prepared according to the general procedure using cinnamaldehyde (39.6 mg, 0.3 mmol), aminocatalyst **C** (22.1 mg, 0.02 mmol), the corresponding dihydropyridine (33.7 mg, 0.1 mmol), trifluoroacetic acid (6.2 µL, 0.08 mmol), acetonitrile (400 µL) and perfluorohexane (100 µL). The crude material was purified by flash column chromatography (hexane/diethyl ether, gradient from 90:10 to 70:30) to give the product **6f** (13.7 mg, 63% yield, 87% ee, average of two runs) as a yellow oil. The enantiomeric excess of the corresponding alcohol (obtained upon reduction with sodium borohydride) was determined by HPLC analysis on a Agilent IC-3 column,70:30 hexane/*i*-PrOH, flow rate 0.6 mL/min, 20 °C, λ = 215 nm. τ_{minor} = 13.8 min, τ_{major} = 15.5 min (87% ee). $[\alpha]_D^{26}$ = –17.9 (c = 0.30, $CHCl_3$, 87% ee).

^{1}H NMR (500 MHz, $CDCl_3$) δ 9.62 (1H, t, *J* =2,1 Hz, C**H**O), 7.35-7.28 (2H, m, Ar**H**), 7.22 (1H, tt, *J* = 6.7, 1.2 Hz, Ar**H**), 7.18-7.13 (2H, m, Ar**H**), 4.01 (1H, ddd, *J* = 11.4, 4.0 2.3 Hz,- C**H**$_2$OCH$_2$-), 3.92-3.84 (1H, m, - C**H**$_2$OCH$_2$-), 3.36 (1H, td, *J* = 11.9, 2.2 Hz,- CH$_2$OC**H**$_2$-),

3.26 (1H, td, *J* = 11.5, 2.9 Hz,- CH_2OCH_2-), 2.98 (1H, ddd, *J* = 9.7, 8.4, 5.2 Hz, ArC**H**), 2.85 (1H, ddd, *J* = 16.5, 5.2, 1.8 Hz, CHOCH_2), 2.75 (1H, ddd, *J* = 16.5, 9.6, 2.5 Hz, CHOCH_2), 1.78-1.66 (2H, m, CHCH_2CH_2O), 1.37 (1H, dtd, *J* = 13.1, 12.0, 11.6, 4.5 Hz, CH_2CHCH_2), 1.31-1.19 (2H, m, CHCH_2CH_2O);

^{13}C NMR (125.8 MHz, $CDCl_3$) δ 201.9 (C=O), 141.8 (C), 128.6 (2 x CH), 128.2 (2 x CH), 126.8 (CH), 68.0 (CH_2), 67.9 (CH_2), 46.8 (CH_2), 45.9 (CH), 40.5 (CH), 31.2 (CH_2), 30.9 (CH_2);

HRMS (ESI) Exact mass calculated for $C_{15}H_{22}NaO_3$ $[M+MeOH+Na]^+$: 273.1461, found: 273.1470;

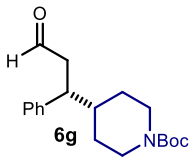

6g

3*R*, 4*RS*)-5-(benzo[*d*][1,3]dioxol-5-yl)-4-methyl-3-phenylpentanal (6g)

The compound was prepared according to the general procedure using cinnamaldehyde (39.6 mg, 0.3 mmol), aminocatalyst **B** (14 mg, 0.02 mmol), the corresponding dihydropyridine (44 mg, 0.1 mmol) trifluoroacetic acid (7.6 µL, 0.1 mmol) and dichloromethane (400 µL). The crude material was purified by flash column chromatography (hexane/diethyl ether 80:20) to give the product **6g** (11.2 mg, 35% yield, 72% ee, average of two runs) as a colourless oil. The enantiomeric excess of the corresponding alcohol (obtained upon reduction with sodium borohydride) was determined to be 72% by HPLC analysis on a Daicel Chiralpack IC-3 column: 80:20 hexane/*i*-PrOH, flow rate 0.6 mL/min, 20 °C, λ = 215 nm. τ_{minor} = 24.2 min, τ_{major} = 32.3 min (72% ee). $[\alpha]_D^{26}$ = –3.7 (c = 0.55, $CHCl_3$, 72% ee).

^{1}H NMR (500 MHz, $CDCl_3$) δ 9.61 (1H, t, *J* = 2.0 Hz, C**H**O), 7.33-7.29 (2H, m, Ar**H**), 7.23 (1H, tt, *J* = 7.3, 1.3 Hz, Ar**H**), 7.16-7.13 (2H, m, Ar**H**), 4.15 (1H, br s, NC$\mathbf{H_2}$), 4.03 (1H, br s, NC$\mathbf{H_2}$), 3.03-2.97 (1H, m, ArC**H**), 2.88-2.73 (2H, m, CHOC$\mathbf{H_2}$), 2.66 (1H, br m, NC$\mathbf{H_2}$), 2.55 (1H, br m, NC$\mathbf{H_2}$), 1.75 (1H, bd, *J* = 12.2 Hz, $NCH_2C\mathbf{H_2}$), 1.68-1.59 (1H, m, ArCHC**H**), 1.43 (9H, s, CC$\mathbf{H_3}$), 1.40-1.32 (1H, m, $NCH_2C\mathbf{H_2}$), 1.21-1.13 (1H, m, $NCH_2C\mathbf{H_2}$), 1.08-0.98 (1H, m, $NCH_2C\mathbf{H_2}$);

^{13}C NMR (125.8 MHz, $CDCl_3$) δ 201.8 (CHO), 154.7 (CO_2), 141.9 (C), 128.6 (CH), 128.2 (CH), 126.8 (CH), 79.4 (C), 47.0 (CH_2), 45.5 (CH), 41.6 (CH), 28.4 (CH_2). Due to rotamers, the N**C**H_2 carbon signal is not visible in the ^{13}C-NMR spectrum, but an HSQC signal at 44 Hz is coupled to the corresponding protons.

HRMS (ESI) Exact mass calculated for $C_{19}H_{27}NNaO_3$ $[M+Na]^+$: 340.1883, found: 340.1894.

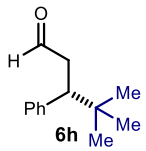

6h

(*R*)-4,4-dimethyl-3-phenylpentanal (6h)

Prepared according to the general procedure using cinnamaldehyde (39.6 mg, 0.3 mmol), aminocatalyst **C** (22.1 mg, 0.02 mmol), tetrabutylammonium *tert*-butyltrifluoroborate (36.7 mg, 0.1 mmol), trifluoroacetic acid (3.1 µL, 0.04 mmol), acetonitrile (200 µL) and perfluorohexane (100 µL). The crude material was purified by flash column chromatography (pentane/diethyl ether 99.7:0.3) to give the product **6h** (13.1 mg, 60% yield, 74 % ee, average of two runs) as a colourless oil that displayed spectroscopic data consistent with those reported previously.[4,6] The enantiomeric excess of the corresponding alcohol (obtained upon reduction with sodium borohydride) was determined by HPLC analysis on a Agilent IC-3 column, 90:10 hexane/*i*-PrOH, flow rate 0.6 mL/min, 20 °C. λ = 215 nm. τ_{minor} = 10. 5 min, τ_{major} = 11.2 min (74 % ee). $[\alpha]_D^{26}$ = –67.3 (c = 0.45, CH_2Cl_2, 74% ee); Lit: $[\alpha]_D^{26}$ = +44.0 (c = 1.29, CH_2Cl_2, 91% ee, for (*S*)-enantiomer).[6]

^{1}H NMR (500 MHz, $CDCl_3$) δ 9.54 (1H, dd, *J* = 2.9, 1.7 Hz, C**H**O), 7.31 – 7.15 (5H, m, Ar**H**), 3.05 (1H, dd, *J* = 10.7, 4.6 Hz, ArC**H**), 2.94 – 2.77 (2H, m, C**H**$_2$CHO), 0.93 (9H, s, C**H**$_3$).

^{13}C NMR (126 MHz, $CDCl_3$) δ 202.7 (C=O), 141.1 (C), 129.4 (CH), 127.9 (CH), 126.6 (CH), 50.3 (CH), 44.6 (CH_2), 33.7 (C), 27.8 (CH_3).

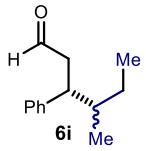

6i

(3*R*, 4*RS*)-4-methyl-3-phenylhexanal (6i)

Prepared according to the general procedure using cinnamaldehyde (39.6 mg, 0.3 mmol), aminocatalyst **C** (22.1 mg, 0.02 mmol), the corresponding dihydropyridine (30.9 mg, 0.1 mmol), trifluoroacetic acid (7.6 µL, 0.1 mmol), acetonitrile (200 µL) and perfluorohexane (100 µL). The crude material was purified by flash column chromatography (hexane/diethyl ether 99.7:0.3) to give the product **6i** (14.1 mg, 74% yield, 1:1 mixture of diastereoisomers) as a colourless oil. The enantiomeric excess of the corresponding alcohol (obtained upon reduction with sodium borohydride) was determined to be 84% for the first diastereoisomer and 83% for the second by UPC^2 analysis using CEL1 chiral column: 99.4:0.6 CO_2/ethanol, curve 6), flow rate 1.8 mL/min, λ = 215 nm. First diastereoisomer: τ_{minor} = 4.39 min, τ_{major} = 5.50 min (83% ee); second diastereoisomer: τ_{minor} = 4.75 min, τ_{major} = 5.16 min (84% ee). $[\alpha]_D^{26}$ = –4.3 (c= 0.43, $CHCl_3$, dr 1:1, 84% ee / 83% ee).

^{1}H NMR *1:1mixture of diastereoisomers* (500 MHz, $CDCl_3$) δ 9.63 (2H, q, *J* = 4.4, 2.2 Hz, 2 x C**H**O), 7.31 (4H, td, *J* = 7.6, 1.9 Hz, Ar**H**), 7.26-7.20 (2H, m, Ar**H**), 7.18 (4H, ddd, *J* = 7.9, 4.9, 1.3 Hz, Ar**H**), 3.13 (2H, dq, *J* = 21.7, 7.3 Hz, 2 x C**H**Ph), 2.84-2.76 (4H, m, 2 x C**H**$_2$CHO), 1.67 (2H, dddd, *J* = 13.0, 8.9, 6.3, 4.3 Hz, 2 x C**H**CH_3), 1.51 (1H, ddd, *J* = 13.5, 7.4, 4.4 Hz, C**H**$_2$CH3), 1.37 (1H, ddd, *J* = 13.5, 7.5, 4.0 Hz, C**H**$_2CH_3$), 1.11 (1H, dt, *J* = 13.5, 8.4, 7.2 Hz, C**H**$_2CH_3$), 1.02 (1H, dddd, *J* = 16.8, 13.6, 8.5, 7.2 Hz, C**H**$_2CH_3$), 0.96-0.92 (6H, m, CHC**H**$_3$ + CH_2C**H**$_3$), 0.87 (3H, t, *J* = 7.4 Hz, CH_2C**H**$_3$), 0.78 (3H, d, *J* = 6.8 Hz, CHC**H**$_3$);

^{13}C NMR (125.8 MHz, $CDCl_3$) δ 202.6 (C=O), 202.5 (C=O), 143.0 (C), 142.1 (C), 128.5 (2 x CH), 128.4 (2 x CH), 128.3 (2 x CH), 128.2 (2 x CH), 126.50 (CH), 126.46 (CH), 47.2 (CH_2), 46.4 (CH_2), 45.3 (CH), 44.8 (CH), 40.1 (CH), 39.7 (CH), 26.84 (CH_2), 26.76 (CH_2), 16.2 (CH_3), 16.1 (CH_3), 11.5 (CH_3), 11.4 (CH_3);

HRMS (ESI) Exact mass calculated for $C_{14}H_{22}NaO_2$ $[M+MeOH+Na]^+$: 245.1512, found: 245.1506.

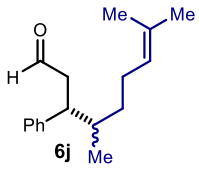

6j

(3*R*, 4*RS*)-4,8-dimethyl-3-phenylnon-8-enal (6j)

Prepared according to the general procedure using cinnamaldehyde (39.6 mg, 0.3 mmol), aminocatalyst **C** (22.1 mg, 0.02 mmol), the corresponding dihydropyridine (36 mg, 0.1 mmol), trifluoroacetic acid (6.2 µL, 0.08 mmol), acetonitrile (400 µL) and perfluorohexane (100 µL). The crude material was purified by flash column chromatography (hexane/diethyl ether 99.7:0.3) to give the product **6j** (11.5 mg, 47% yield, 1:1 mixture of diastereoisomers) as a colourless oil. The enantiomeric excess of the corresponding alcohol (obtained upon reduction with sodium borohydride) was determined to be 89% for the *major* diastereoisomer and 90% for the *minor* by UPC^2 analysis using CEL2 chiral column: 94:6 CO_2/isopropanol, curve 6), flow rate 1.8 mL/min, λ = 215 nm. *Major diastereoisomer*: τ_{minor} = 3.65 min, τ_{major} = 3.90 min (89% ee); m*inor diastereoisomer*: τ_{minor} = 3.42 min, τ_{major} = 4.60 min (90% ee). $[\alpha]_D^{26}$ = –10.6 (c = 0.40, $CHCl_3$, dr 1:1, 90% ee / 89% ee).

^{1}H NMR *1:1mixture of diastereoisomers* (400 MHz, $CDCl_3$) δ 9.61 (2H, app q, *J* = 2.2 Hz, 2x C**H**O), 7.33-7.26 (4H, m, Ar**H**), 7.24-7.13 (6H, m, Ar**H**), 5.07 (1H, ddt, *J* = 8.5, 5.6, 1.4 Hz, C**H**=C), 4.99 (1H, ddt, *J* = 8.5, 5.6, 1.4 Hz, C**H**=C), 3.12 (2H, app dq, *J* = 14.6, 7.3 Hz, 2x C**H**Ar), 2.82-2.73 (4H, m, 2x C**H**$_2$CHO), 1.97 (4H, m, 2x C**H**$_2$CH=C), 1.77-1.68 (2H, m, 2x C**H**$_2$CH$_2$CH=C), 1.68 (3H, d, *J* = 1.4 Hz, CH=C(C**H**$_3$)$_2$), 1.65 (3H, d, *J* = 1.4 Hz, CH=C(C**H**$_3$)$_2$). 1.60 (3H, d, *J* = 1.3 Hz, CH=C(C**H**$_3$)$_2$), 1.55 (3H, t, *J* = 1.3 Hz, CH=C(C**H**$_3$)$_2$), 1.50-1.39 (1H, m, C**H**$_2$CH$_2$CH=C), 1.37-1.19 (1H, m, C**H**$_2$CH$_2$CH=C), 1.12-0.97 (2H, m, 2x C**H**CHPh), 0.91 (3H, d, *J* = 7.2 Hz, CHC**H**$_3$), 0.78 (3H, d, *J* = 6.8 Hz, CHC**H**$_3$);

^{13}C NMR *Diastereomer 1* (125.8 MHz, $CDCl_3$) δ 202.5 (C=O), 142.8 (C), 131.6 (CH), 128.4 (2 x CH), 128.2 (2 x CH), 126.5 (CH), 124.3 (CH), 46.2 (CH_2), 45.4 (CH), 38.0 (CH), 34.1 (CH_2), 25.7 (CH_3), 25.5 (CH_2), 17.6 (CH_3), 16.7 (CH_3);

^{13}C NMR *Diastereomer 2* (125.8 MHz, $CDCl_3$) δ 202.4 (C=O), 141.9 (C), 131.5 (CH), 128.5 (2 x CH), 128.3 (2 x CH), 126.5 (CH), 124.3 (CH), 47.2 (CH_2), 45.0 (CH), 37.7 (CH), 34.4 (CH_2), 25.7 (CH_3), 25.6 (CH_2), 17.7 (CH_3), 16.4 (CH_3);

HRMS (ESI) Exact mass calculated for $C_{17}H_{24}NaO$ $[M+Na]^+$: 267.1719, found: 267.1711.

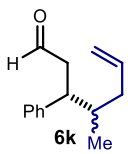

6k

(3*R*, 4*RS*)-4-methyl-3-phenylhept-6-enal (6k)

Prepared according to the general procedure using cinnamaldehyde (39.6 mg, 0.3 mmol), aminocatalyst **C** (22.1 mg, 0.02 mmol), the corresponding dihydropyridine (32.1 mg, 0.1 mmol) trifluoroacetic acid (6.2 µL, 0.08 mmol), acetonitrile (400 µL) and perfluorohexane (100 µL). The crude material was purified by flash column chromatography (pentane/diethyl ether 99:1) to give the product **6k** (9.5 mg, 47% yield, 1.4:1 mixture of diastereoisomers) as a colourless oil. The enantiomeric excess of the corresponding alcohol (obtained upon reduction with sodium borohydride) was determined to be 91% for the *major* diastereoisomer and 90% for the *minor* by UPC^2 analysis using CEL2 chiral column: 93:7 CO_2/isopropanol, curve 6), flow rate 1 mL/min, λ = 215 nm. *Major diastereoisomer*: τ_{minor} = 4.39 min, τ_{major} = 5.50 min (91% ee); *minor diastereoisomer*: τ_{minor} = 4.75 min, τ_{major} = 5.16 min (90% ee). $[\alpha]_D^{26}$ = –24.0 (c = 0.23, $CHCl_3$, dr 1.4:1, 91% ee / 90% ee).

^{1}H NMR *1.4:1mixture of diastereoisomers* (500 MHz, $CDCl_3$) δ 9.61 (2H, m, 2x C**H**O), 7.33-7.38 (4H, m, Ar**H**), 7.24-7.15 (6H, m, Ar**H**), 5.85-5.66 (2H, m, 2x H_2C=C**H**), 5.08-4.92 (4H, m, 2x **H**$_2$C=CH), 3.21-3.07 (2H, m, 2x ArC**H**), 2.84-2.76 (4H, m, 2x CHOC**H**$_2$), 2.25-2.16 (1H, m, H_2C=CHC**H**$_2$), 2.10-2.03 (1H, m, H_2C=CHC**H**$_2$), 1.90-1.79 (3H, m, 1x H_2C=CHC**H**$_2$ + 2x ArCHC**H**), 1.78-1.69 (1H, m, H_2C=CHC**H**$_2$), 0.94 (3H, d, *J* = 6.6 Hz, C**H**$_3$), 0.78 (3H, d, *J* = 6.6 Hz, C**H**$_3$).

^{13}C NMR (125.8 MHz, $CDCl_3$) δ 202.3 (CHO), 202.1 (CHO), 142.7 (C), 141.6 (C), 136.8 (CH), 128.6 (CH), 128.5 (CH), 128.3 (CH), 128.2 (CH), 126.6 (CH), 116.5 (CH_2), 116.4 (CH_2), 47.2 (CH_2), 46.4 (CH_2), 45.0 (CH), 44.3 (CH), 38.8 (CH_2), 38.7 (CH_2), 38.3 (CH), 37.9 (CH), 16.7 (CH_3), 16.4 (CH_3).

HRMS (ESI) Exact mass calculated for $C_{15}H_{22}NaO_2$ $[M+Na+MeOH]^+$: 257.1512, found: 257.1505.

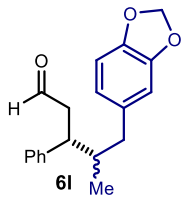

6l

(3*R*, 4*RS*)-5-(benzo[*d*][1,3]dioxol-5-yl)-4-methyl-3-phenylpentanal (6l)

Prepared according to the general procedure using cinnamaldehyde (39.6 mg, 0.3 mmol), aminocatalyst **C** (22.1 mg, 0.02 mmol), the corresponding dihydropyridine (41.5 mg, 0.1 mmol), trifluoroacetic acid (6.2 µL, 0.08 mmol), acetonitrile (400 µL) and perfluorohexane (100 µL). The crude material was purified by flash column chromatography (hexane/diethyl ether 90:10, two consecutive purifications) to give the product **6l** (15.1 mg, 51% yield, 1:1 mixture of diastereoisomers) as a colourless oil. The enantiomeric excess of the corresponding alcohol (obtained upon reduction with sodium borohydride) was determined to be 92% for the *major* diastereoisomer and 90% for the *minor* by UPC^2 analysis using ID-3 chiral column: after 1

min of 100% CO_2, gradient up to 60:40 CO_2/acetonitrile over 5 minutes, curve 6), flow rate 3 mL/min, λ = 287 nm. *Major diastereoisomer*: τ_{minor} = 5.13 min, τ_{major} = 4.47 min (92% ee); *minor diastereoisomer*: τ_{minor} = 4.73 min, τ_{major} = 4.03 min (90% ee). $[\alpha]_D^{26}$ = –7.7 (c = 0.38, $CHCl_3$, dr 1:1, 90% ee / 90% ee).

^{1}H NMR *1:1mixture of diastereoisomers* (500 MHz, $CDCl_3$) δ 9.65 (1H, t, *J* = 2.1 Hz, C**H**O), 9.63 (1H, t, *J* = 2.1 Hz, C**H**O), 7.37-7.31 (4H, m, 2x Ar**H**), 7.25-7.18 (6H, m, 2x Ar**H**), 6.74 (1H, d, *J* = 7.9 Hz, Ar**H**), 6.72 (1H, d, *J* = 7.9 Hz, Ar**H**), 6.63-6.50 (4H, m, Ar**H**), 5.92 (2H, s, OC**H**$_2$O), 5.91 (2H, s, OC**H**$_2$O), 3.26 (1H, td, *J* = 8.2, 6.8 Hz, ArC**H**), 3.13 (1H, td, *J* = 8.2, 6.8 Hz, ArC**H**), 2.91-2.87 (2H, m, CHOC**H**$_2$), 2.86-2.82 (2H, m, CHOC**H**$_2$), 2.74 (1H, dd, *J* = 13.4, 4.8 Hz, ArC**H**$_2$), 2.61 (1H, dd, *J* = 13.3, 4.2 Hz, ArC**H**$_2$), 2.16-2.03 (2H, m, ArC**H**$_2$), 2.06-1.92 (2H, m, C**H**CH_3), 0.88 (3H, d, *J* = 6.6 Hz, CHC**H**$_3$), 0.75 (3H, d, *J* = 6.6 Hz, CHC**H**$_3$);

^{13}C NMR (125.8 MHz, $CDCl_3$) δ 202.2 (C=O), 202.0 (C=O), 147.6 (C), 147.5 (C), 145.7 (C), 145.6 (C), 142.7 (C), 141.3 (C), 134.7 (C), 134.5 (C), 128.7 (CH), 128.6 (CH), 128.4 (CH), 128.2 (CH), 126.7 (CH), 121.9 (CH), 121.8 (CH), 109.3 (CH), 109.2 (CH), 108.1 (CH), 108.0 (CH), 100.8 (CH_2), 100.7 (CH_2), 47.2 (CH_2), 46.3 (CH_2), 45.2 (CH), 44.6 (CH), 41.0 (CH), 40.7 (CH_2), 40.5 (CH_2), 40.2 (CH), 16.5 (CH_3), 16.0 (CH_3);

HRMS (ESI) Exact mass calculated for $C_{19}H_{20}NaO_3$ $[M+Na]^+$: 319.1305, found: 319.1313.

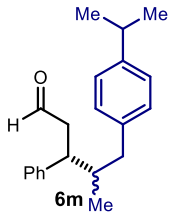

(3*R*, 4*RS*)-4,8-dimethyl-3-phenylnon-8-enal (6m)

Prepared according to the general procedure using cinnamaldehyde (39.6 mg, 0.3 mmol), aminocatalyst **C** (22.1 mg, 0.02 mmol), the corresponding dihydropyridine (41.4 mg, 0.1 mmol), trifluoroacetic acid (6.2 µL, 0.08 mmol), acetonitrile (400 µL) and perfluorohexane (100 µL). The crude material was purified by flash column chromatography (hexane/diethyl ether 96:4) to give the product **6m** (16.2 mg, 55% yield, 1:1 mixture of diastereoisomers) as a colourless oil. The enantiomeric excess of the corresponding alcohol (obtained upon reduction with sodium borohydride) was determined to be 88% for the *major* diastereoisomer and 87% for the *minor* by UPC^2 analysis on a using IE-3 chiral column: after 1 min of 100% CO_2, gradient up to 60:40 CO_2/acetonitrile over 5 minutes, curve 6), flow rate 3 mL/min, λ = 220 nm. *Major diastereoisomer*: τ_{minor} = 5.37 min, τ_{major} = 4.92 min (88% ee); *minor diastereoisomer*: τ_{minor} = 5.09 min, τ_{major} = 5.22 min (87% ee). $[\alpha]_D^{26}$ = –5.9 (c = 0.8, $CHCl_3$, dr 1:1, 88% ee/87% ee).

^{1}H NMR *1:1mixture of diastereoisomers* (500 MHz, $CDCl_3$) δ 9.63 (2H, app dt, *J* = 6.4, 2.1 Hz, 2x C**H**O), 7.37-7.30 (4H, m, Ar**H**), 7.26-7.18 (6H, m, Ar**H**), 7.16-7.11 (4H, m, Ar**H**), 7.07-7.03 (2H, m, Ar**H**), 6.99 (2H, d, *J* = 8.1 Hz, Ar**H**), 3.29-3.22 (1H, m, $CHOCH_2C$**H**), 3.18-3.11 (1H, m, $CHOCH_2C$**H**), 2.92-2.82 (6H, m, 2x CHOC**H**$_2$ + 2x ArC**H**$(CH_3)_2$), 2.78 (1H, dd, *J* = 13.6, 4.9 Hz, ArC**H**$_2$), 2.66 (1H, dd, *J* = 13.4, 4.2 Hz, ArC**H**$_2$), 2.23-2.11 (2H, m, 2x ArC**H**$_2$),

2.10-1.98 (1H, m, 2x PhCHC**H**), 1.25 (12H, dd, *J* = 6.9, 6.0 Hz, 2x CH(C**H**$_3$)$_2$), 0.88 (3H, d, *J* = 6.6 Hz, CHC**H**$_3$), 0.74 (3H, d, *J* = 6.7 Hz, CHC**H**$_3$);

^{13}C NMR (125.8 MHz, $CDCl_3$) δ 202.3 (C=O), 202.2 (C=O), 146.5 (C), 146.4 (C), 142.7 (C), 141.4 (C), 138.1 (C), 137.9 (C), 129.0 (2 x CH), 128.9 (2 x CH), 128.7 (2 x CH), 128.6 (2 x CH), 128.34 (2 x CH), 128.25 (2 x CH), 126.7 (2 x CH), 126.32 (2 x CH), 126.27 (2 x CH), 47.3 (CH_2), 46.2 (CH_2), 45.3 (CH), 44.7 (CH), 40.8 (CH), 40.6 (CH_2), 40.3 (CH_2), 40.1 (CH), 33.68 (CH), 33.66 (CH), 24.1 (4 x CH_3), 16.6 (CH_3), 16.2 (CH_3);

HRMS (ESI) Exact mass calculated for $C_{21}H_{26}NaO$ $[M+Na]^+$: 317.1876, found: 317.1877.

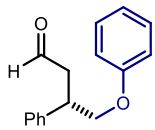

6n

(S)-4-phenoxy-3-phenylbutanal (6n)

Prepared according to the general procedure using cinnamaldehyde (39.6 mg, 0.3 mmol), aminocatalyst **C** (22.1 mg, 0.02 mmol), the correspondin dihydropyridine (35.9 mg, 0.1 mmol), trifluoroacetic acid (6.2 µL, 0.08 mmol), acetonitrile (400 µL) and perfluorohexane (100 µL). The crude material was purified by flash column chromatography (two consecutive columns, first hexane/toluene gradient from 100:0 to 0:100, then hexane/diethyl ether 9:1) to give the product **6n** (9.1 mg, 38% yield, 83 % ee, average of two runs) as a colourless oil. The enantiomeric excess was determined by HPLC analysis on a Agilent IC-3 column, 90:10 hexane/*i*-PrOH, flow rate 0.8 mL/min, 20 °C. λ = 215 nm. τ_{major} = 12. 0 min, τ_{minor} = 13.1 min (83 % ee).

^{1}H NMR (500 MHz, $CDCl_3$) δ 9.80 (t, 1H, J = 1.8 Hz C**H**O), 7.38 – 7.24 (m, 7H, Ar**H**), 6.97 – 6.93 (m, 1H, Ar**H**), 6.87 (dt, *J* = 7.8, 1.1 Hz, 2H, Ar**H**), 4.18 (dd, *J* = 9.2, 5.0 Hz, 1H, C**H**$_2$O), 4.03 (dd, *J* = 9.3, 8.3 Hz, 1H, C**H**$_2$O), 3.76 (qd, *J* = 7.4, 5.0 Hz, 1H, ArC**H**), 3.10 (ddd, *J* = 17.1, 6.9, 2.0 Hz, 1H, C**H**$_2$CHO), 2.87 (ddd, *J* = 17.1, 7.4, 1.8 Hz, 1H, C**H**$_2$CHO)

^{13}C NMR (126 MHz, $CDCl_3$) δ 200.2 (C=O), 157.6 (C), 139.6 (C), 128.7 (CH), 128.0 (CH), 127.0 (CH), 126.5 (CH), 120.3 (CH), 113.7 (CH), 70.7 (CH_2), 46.1 (CH_2), 39.11 (CH).

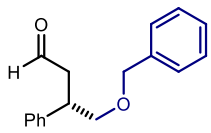

6o

(S)-4-(benzyloxy)-3-phenylbutanal (6o)

Prepared according to the general procedure using cinnamaldehyde (39.6 mg, 0.3 mmol), aminocatalyst **C** (22.1 mg, 0.02 mmol), the correspondin dihydropyridine (37.3 mg, 0.1 mmol), trifluoroacetic acid (6.2 µL, 0.08 mmol), acetonitrile (400 µL) and perfluorohexane (100 µL). The crude material was purified by flash column chromatography (two consecutive columns, first hexane/dichloromethane 1:1, then hexane /diethyl ether 9:1) to give the product **6o** (12 mg, 47% yield, 75 % ee, average of two runs) as a colourless oil. The enantiomeric excess was determined by HPLC analysis on a Agilent IC-3 column, 90:10 hexane/*i*-PrOH, flow rate 0.8 mL/min, 20 °C. λ = 215 nm. τ_{major} = 11. 8 min, τ_{minor} = 12.6 min (75 % ee).

^{1}H NMR (500 MHz, $CDCl_3$) δ 9.74 (t, 1H, J = 2Hz, C**H**O), 7.35 – 7.20 (m, 10H, Ar**H**), 4.50 (s, 2H, PhC**H$_2$**O), 3.69 – 3.65 (m, 1H, C**H$_2$**O), 3.61 – 3.52 (m, 2H, C**H$_2$**O + PhC**H**), 2.96 (ddd, *J* = 16.6, 6.8, 2.3 Hz, 2H, C**H$_2$**CHO), 2.74 (ddd, *J* = 16.7, 7.0, 1.8 Hz, 2H, C**H$_2$**CHO).

^{13}C NMR (126 MHz, $CDCl_3$) δ 200.6 (C=O), 140.2 (C), 137.2 (C), 130.5 (CH), 127.9 (CH), 127.6 (CH), 126.9 (CH), 126.8 (CH), 126.2 (CH), 73.5 (CH_2), 72.3 (CH_2), 46.4 (CH_2), 39.7 (CH).

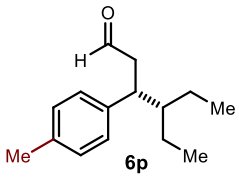

6p

(*R*)-4-ethyl-3-(*p*-tolyl)hexanal (6p)

Prepared according to the general procedure using 3-(*p*-tolyl)acrylaldehyde (44 mg, 0.3 mmol), aminocatalyst **C** (22.1 mg, 0.02 mmol), the corresponding dihydropyridine (32.3 mg, 0.1 mmol), trifluoroacetic acid (6.2 µL, 0.08 mmol), acetonitrile (200 µL) and perfluorohexane (100 µL). The crude material was purified by flash column chromatography (hexane/diethyl ether 99:1) to give the product **6p** (14.6 mg, 67% yield, 77% ee, average of two runs) as a colourless oil. The enantiomeric excess of the corresponding alcohol (obtained upon reduction with sodium borohydride) was determined to be 77% by UPC^2 analysis using CEL2 chiral column: after 1 min of 100% CO_2, gradient up to 60:40 CO_2/methanol over 5 minutes, curve 6), flow rate 2 mL/min, λ = 220 nm. τ_{minor} = 2.71 min, τ_{major} = 2.61 min.$[\alpha]_D^{26}$ = –6.3 (c = 0.7, $CHCl_3$, 77% ee).

^{1}H NMR (500 MHz, $CDCl_3$) δ 9.59 (1H, t, *J* = 2.3 Hz, C**H**O), 7.12-7.04 (4H, m, Ar**H**), 3.21 (1H, q, *J* = 7.4 Hz, ArC**H**), 2.75-2.71 (2H, m, CHOC**H$_2$**), 2.32 (3H, s, ArC**H$_3$**), 1.49-1.22 (4H, m, C**H**(CH_2CH_3)$_2$ + 3 x C**H$_2$**CH_3), 1.17-1.05 (1H, m, CH(C**H$_2$**CH_3)$_2$), 0.90 (3H, t, *J* = 7.4 Hz, CH_2C**H$_3$**), 0.83 (3H, t, *J* = 7.4 Hz, CH_2C**H$_3$**);

^{13}C NMR (125.8 MHz, $CDCl_3$) δ 202.8 (C=O), 139.6 (C), 135.9 (C), 129.1 (CH), 128.1 (CH), 46.8 (CH_2), 46.0 (CH), 41.5 (CH), 22.3 (CH_2), 21.9 (CH_2), 21.0 (CH_3), 11.1 (CH_3), 10.8 (CH_3);

HRMS (ESI) Exact mass calculated for $C_{15}H_{22}NaO$ $[M+Na]^+$: 241.1563, found: 241.1573.

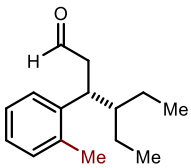

6q

(*R*)-4-ethyl-3-(*o*-tolyl)hexanal (6q)

Prepared according to the general procedure using 3-(*o*-tolyl)acrylaldehyde (44 mg, 0.3 mmol), aminocatalyst **C** (22.1 mg, 0.02 mmol), the corresponding dihydropyridine (32.3 mg, 0.1 mmol), trifluoroacetic acid (6.2 µL, 0.08 mmol), acetonitrile (200 µL) and perfluorohexane (100 µL). The crude material was purified by flash column chromatography (hexane/diethyl ether 99:1) to give the product **6q** (10.7 mg, 49% yield, 78% ee, average of two runs) as a colourless oil. The enantiomeric excess of the corresponding alcohol (obtained upon reduction with sodium borohydride) was determined to be 78% by UPC^2 analysis using

CEL2 chiral column: after 1 min of 100% CO_2, gradient up to 60:40 CO_2/isopropanol over 5 minutes, curve 6), flow rate 2 mL/min, λ = 215 nm. τ_{minor} = 3.59 min, τ_{major} = 3.35 min.$[\alpha]_D^{26}$ = +6.5 (c = 0.5, $CHCl_3$, 78% ee).

^{1}H NMR (500 MHz, $CDCl_3$) δ 9.54 (1H, t, *J* = 2.3 Hz, C**H**O), 7.19-7.08 (4H, m, Ar**H**), 3.49 (1H, q, *J* = 7.6 Hz, ArC**H**), 2.76-2.74 (2H, m, CHOC**H**$_2$), 2.38 (3H, s, ArC**H**$_3$), 1.61-1.49 (2H, m, C**H**$(CH_2CH_3)_2$ + C**H**$_2CH_3$), 1.37-1.23 (2H, m, C**H**$_2CH_3$), 1.21-1.12 (1H, m, C**H**$_2CH_3$), 0.86 (3H, t, *J* = 7.4 Hz, CH_2C**H**$_3$), 0.84 (3H, t, *J* = 7.4 Hz, CH_2C**H**$_3$);

^{13}C NMR (125.8 MHz, $CDCl_3$) δ 202.6 (CHO), 141.7 (C), 136.2 (C), 130.6 (CH), 126.8 (CH), 126.1 (CH), 126.0 (CH), 46.6 (CH_2), 45.2 (CH), 36.9 (CH), 22.3 (CH_2), 21.4 (CH_2), 20.0 (CH_3), 11.3 (CH_3), 10.3 (CH_3).

HRMS (ESI) Exact mass calculated for $C_{16}H_{26}NaO_2$ $[M+Na+MeOH]^+$: 273.1825, found: 273.1822.

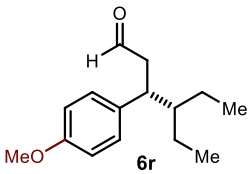

6r

(*R*)-4-ethyl-3-(4-methoxyphenyl)hexanal (6r)

Prepared according to the general procedure using 4-methoxycinnamaldehyde (48.7 mg, 0.3 mmol), aminocatalyst **C** (22.1 mg, 0.02 mmol), the corresponding dihydropyridine (32.3 mg, 0.1 mmol), trifluoroacetic acid (7.6 µL, 0.1 mmol), acetonitrile (200 µL) and perfluorohexane (100 µL). The crude material was purified by flash column chromatography (hexane/diethyl ether 90:10) to give the product **6r** (16.2 mg, 69% yield, 60% ee, average of two runs) as a colourless oil. The enantiomeric excess of the corresponding alcohol (obtained upon reduction with sodium borohydride) was determined by HPLC analysis on a Agilent IC-3 column, 90:10 hexane/*i*-PrOH, flow rate 0.6 mL/min, 20 °C. λ = 215 nm. τ_{minor} = 13.7 min, τ_{major} = 15.9 min (60% ee). $[\alpha]_D^{26}$ = –4.65 (c = 0.82, $CHCl_3$, 60% ee).

^{1}H NMR (500 MHz, $CDCl_3$) δ 9.58 (1H, t, *J* = 2.3 Hz, , C**H**O), 7.10-7.05 (2H, m, Ar**H**), 6.85-6.81 (2H, m, Ar**H**), 3.79 (3H, s, ArOC**H**$_3$), 3.20 (1H, q, *J* = 7.2 Hz, ArC**H**), 2.74-2.70 (2H, m, CHOC**H**$_2$), 1.48-1.22 (4H, m C**H**$(CH_2CH_3)_2$ + 3 x C**H**$_2CH_3$), 1.15-1.04 (1H, m, C**H**$_2CH_3$), 0.90 (3H, t, *J* = 7.3 Hz, CH_2C**H**$_3$), 0.82 (3H, t, *J* = 7.4 Hz, CH_2C**H**$_3$);

^{13}C NMR (126 MHz, $CDCl_3$) δ 202.8 (C=O), 158.0 (C), 134.6 (C), 129.1 (CH), 113.7 (CH), 55.1 (CH_3), 46.8 (CH_2), 46.1 (CH), 41.0 (CH), 22.2 (CH_2), 21.9 (CH_2), 11.1 (CH_3), 10.8 (CH_3).

HRMS (ESI) Exact mass calculated for $C_{15}H_{22}NaO_2$ $[M+Na]^+$: 257.1512, found: 257.1515.

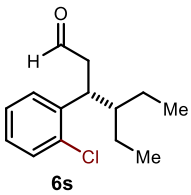

6s

(*R*)-3-(2-chlorophenyl)-4-ethylhexanal (6s)

Prepared according to the general procedure using 3-(2-chlorophenyl)acrylaldehyde (50 mg, 0.3 mmol), aminocatalyst **C** (22.1 mg, 0.02 mmol) the corresponding dihydropyridine (32.3 mg, 0.1 mmol), trifluoroacetic acid (0.08 mmol, 6.2 µL), acetonitrile (200 µL) and perfluorohexane (100 µL). The crude material was purified by flash column chromatography (hexane/diethyl ether 99:1) to give the product **6s** (13.1 mg, 55% yield, 83% ee, average of two runs) as a colourless oil. The enantiomeric excess of the corresponding alcohol (obtained upon reduction with sodium borohydride) was determined to be 83% by UPC^2 analysis using CEL2 chiral column: after 1 min of 100% CO_2, gradient up to 60:40 CO_2/ethanol over 5 minutes, curve 6), flow rate 2 mL/min, λ = 215 nm. τ_{minor} = 3.23 min, τ_{major} = 3.04 min. $[\alpha]_D^{26}$ = –12.6 (c = 0.33, $CHCl_3$, 83% ee).

^{1}H NMR (500 MHz, $CDCl_3$) δ) 9.57 (1H, dd, *J* = 3.1, 1.7 Hz, C**H**O), 7.37 (1H, dd, *J* = 7.9, 1.2 Hz, Ar**H**), 7.25-7.12 (3H, m, Ar**H**), 3.88-3.81 (1H, m, ArC**H**), 2.82-2.66 (2H, m, CHOC**H**$_2$), 1.67-1.61 (1H, m, C**H**(CH_2CH_3)$_2$), 1.57-1.46 (1H, m, C**H**$_2$$CH_3$), 1.37-1.27 (2H, m, C**H**$_2$$CH_3$), 1.25-1.14 (1H, m, C**H**$_2$$CH_3$), 0.87 (6H, t, *J* = 7.4 Hz, CH_2C**H**$_3$);

^{13}C NMR (125.8 MHz, $CDCl_3$) δ 202.1 (CHO), 140.6 (C), 134.4 (C), 129.9 (CH), 128.8 (CH), 127.6 (CH), 126.9 (CH), 45.8 (CH_2), 44.5 (CH), 37.9 (CH), 22.5 (CH_2), 21.6 (CH_2), 10.9 (CH_3), 10.6 (CH_3).

HRMS (ESI) Exact mass calculated for $C_{15}H_{23}ClNaO_2$ $[M+Na+MeOH]^+$: 293.1279, found: 293.1268.

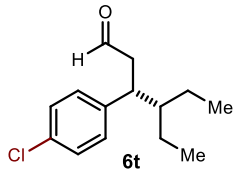

6t

(*R*)-3-(4-chlorophenyl)-4-ethylhexanal (6t)

Prepared according to the general procedure using 3-(4-chlorophenyl)acrylaldehyde (50 mg, 0.3 mmol), aminocatalyst **C** (22.1 mg, 0.02 mmol) the corresponding dihydropyridine (32.3 mg, 0.1 mmol), trifluoroacetic acid (6.2 µL, 0.08 mmol), acetonitrile (200 µL) and perfluorohexane (100 µL). The crude material was purified by flash column chromatography (hexane/diethyl ether 98.5:1.5) to give the product **6t** (10.5 mg, 44% yield, 75% ee, average of two runs) as a colourless oil. The enantiomeric excess of the corresponding alcohol (obtained upon reduction with sodium borohydride) was determined to be 74% by UPC^2 analysis using CEL2 chiral column: after 1 min of 100% CO_2, gradient up to 60:40 CO_2/isopropanol over 5 minutes, curve 6), flow rate 2 mL/min, λ = 221 nm. τ_{minor} = 3.53 min, τ_{major} = 3.42 min. $[\alpha]_D^{26}$ = +3.2 (c= 0.55, $CHCl_3$, 75% ee).

^{1}H NMR (500 MHz, $CDCl_3$) δ 9.62 (1H, t, *J* = 2.3 Hz, C**H**O), 7.30-7.26 (2H, m, Ar**H**), 7.15-7.10 (2H, m, Ar**H**), 3.28-3.22 (1H, m, ArC**H**), 2.82-2.71 (2H, m, CHOC**H**$_2$), 1.49-1.22 (4H,

m, C**H**$(CH_2CH_3)_2$ + 3 x C**H**$_2CH_3$), 1.16-1.05 (1H, m, C**H**$_2CH_3$), 0.91 (3H, t, *J* = 7.4 Hz, CH_2C**H**$_3$), 0.84 (3H, t, *J* = 7.4 Hz, CH_2C**H**$_3$);

^{13}C NMR (125.8 MHz, $CDCl_3$) δ 201.9 (CHO), 141.4 (C), 132.1 (C), 129.6 (CH), 128.5 (CH), 46.7 (CH_2), 45.9 (CH), 41.2 (CH), 22.3 (CH_2), 21.9 (CH_2), 11.0 (CH_3), 10.8 (CH_3).

HRMS (ESI) Exact mass calculated for $C_{15}H_{23}ClNaO_2$ $[M+Na+MeOH]^+$: 293.1279, found: 293.1280.

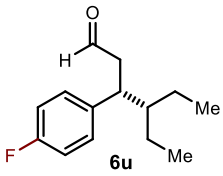

6u

(*R*)-4-ethyl-3-(4-fluorophenyl)hexanal (6u)

Prepared according to the general procedure using 4-fluoro cinnamaldehyde (45.0 mg, 0.3 mmol), aminocatalyst **C** (22.1 mg, 0.02 mmol the corresponding dihydropyridine (32.3 mg, 0.1 mmol), trifluoroacetic acid (6.2 µL, 0.08 mmol), acetonitrile (200 µL) and perfluorohexane (100 µL). The crude material was purified by flash column chromatography (hexane/diethyl ether 99:1) to give the product **6u** (10.7 mg, 48% yield, 78% ee, average of two runs) as a colourless oil. The enantiomeric excess of the corresponding alcohol (obtained upon reduction with sodium borohydride) was determined by HPLC analysis on a Agilent IC-3 column, 95:05 hexane/*i*-PrOH, flow rate 0.6 mL/min, 20 °C. λ = 215 nm. τ_{minor} = 12.9 min, τ_{major} = 13.8 min (78% ee).$[\alpha]_D^{26}$ = –3.70 (c = 0.47, $CHCl_3$, 78% ee).

^{1}H NMR (500 MHz, $CDCl_3$) δ 9.62 (1H, t, *J* = 2.6 Hz, C**H**O), 7.16-7.10 (2H, m, Ar**H**), 7.01-6.95 (2H, m, Ar**H**), 3.25 (1H, q, *J* = 7.2 Hz, ArC**H**), 2.79-2.69 (2H, m, CHOC**H**$_2$), 1.47-1.22 (4H, m, C**H**$(CH_2CH_3)_2$ + 3 x C**H**$_2CH_3$), 1.14-1.04 (1H, m, C**H**$_2CH_3$), 0.89 (3H, t, *J* = 7.3 Hz, CH_2C**H**$_3$), 0.82 (3H, t, *J* = 7.4 Hz CH_2C**H**$_3$);

^{13}C NMR (126 MHz, $CDCl_3$): δ 202.1 (CHO), 161.3 (d, J_{CF} = 244.9 Hz, Ar^{para}), 138.4 (d, J_{CF} = 3.4 Hz, Ar^{ipso}), 129.6 (2C, d, J_{CF} = 7.8 Hz, Ar^{ortho}), 115.2 (2C, d, J_{CF} = 21.2 Hz, Ar^{meta}), 46.9 (CH_2), 46.01 (CH), 41.1 (CH), 22.2 (CH_2), 21.9 (CH_2), 11.0 (CH_3), 10.8 (CH_3).

^{19}F NMR (376 MHz, $CDCl_3$): δ -116.7.

HRMS (ESI) Exact mass calculated for $C_{15}H_{23}FNaO_2$ $[M+MeOH+Na]^+$: 277.1574, found: 277.1569.

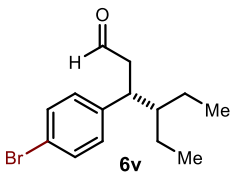

6v

(*R*)-3-(4-bromophenyl)-4-ethylhexanal (6v)

Prepared according to the general procedure using 4-bromocinnamaldehyde (63.3 mg, 0.3 mmol), aminocatalyst **C** (22.1 mg, 0.02 mmol), the corresponding dihydropyridine (32.3 mg, 0.1 mmol), trifluoroacetic acid (6.2 µL, 0.08 mmol), acetonitrile (200 µL) and perfluorohexane (100 µL). The crude material was purified by flash column chromatography (hexane/diethyl ether 99:1) to give the product **6v** (11.0 mg, 39% yield, 72%

ee, average of two runs) as a colourless oil. The enantiomeric excess of the corresponding alcohol (obtained upon reduction with sodium borohydride) was determined by UPC[2] analysis using CEL2 chiral column: after 1 min of 100% CO_2, gradient up to 60:40 CO_2/isopropanol over 5 minutes, curve 6), flow rate 2 mL/min. λ = 215 nm. τ_{minor} = 3.76 min, τ_{major} = 3.64 min (72% ee). $[\alpha]_D^{26}$ = –84.7 (c= 0.48, $CHCl_3$, 72% ee).

^{1}H NMR (500 MHz, $CDCl_3$) δ 9.60 (1H, t, *J* = 2.4 Hz, C**H**O), 7.45-7.39 (2H, m, Ar**H**), 7.09-7.02 (2H, m, Ar**H**), 3.23 (1H, q, *J* = 7.1 Hz, ArC**H**), 2.81-2.67 (2H, m, CHOC**H**$_2$), 1.49-1.18 (4H, m, C**H**(CH_2CH_3)$_2$ + 3 x C**H**$_2$$CH_3$), 1.14-1.03 (1H, m, C**H**$_2$$CH_3$), 0.89 (3H, t, *J* = 7.4 Hz, CH_2C**H**$_3$), 0.82 (3H, t, *J* = 7.4 Hz CH_2C**H**$_3$);
^{13}C NMR (101 MHz, $CDCl_3$) δ 201.8 (CHO), 141.9 (C), 131.4 (CH), 129.9 (CH), 120.19 (C), 46.6 (CH_2), 45.8 (CH), 41.2 (CH), 22.28 (CH_2), 21.88 (CH_2), 11.01 (CH_3), 10.81 (CH_3).
HRMS (ESI) Exact mass calculated for $C_{15}H_{23}BrNaO_2$ $[M+MeOH+Na]^+$: 337.0774, found: 337.0774

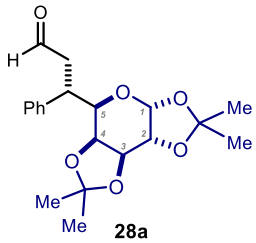

28a

(*S*)-3-phenyl-3-((3a*R*,5*R*,5a*S*,8a*S*,8b*R*)-2,2,7,7-tetramethyltetrahydro-5H-bis([1,3]dioxolo)[4,5-b:4',5'-d]pyran-5-yl)propanal (28a)

Prepared according to the general procedure using cinnamaldehyde (39.6 mg, 0.3 mmol), aminocatalyst (*S*)-**B** (14 mg, 20 mol%), and the corresponding dihydropyridine (48.2 mg, 0.1 mmol) in DCM (400 µL) . The crude material was purified by flash column chromatography (hexane/diethyl ether 4:1) to give the product (19.1 mg, 53% yield, 19:1 mixture of diastereoisomers, average of two runs) as a white solid. *Characterization of the major diastereoisomer*: ^{1}H NMR (400 MHz, $CDCl_3$) δ 9.62 (1H, t, *J* = 2.1 Hz C**H**O),7.37-7.22 (5H, m, Ar**H**), 5.56 (1H, d, *J* = 5.0 Hz, C1**H**), 4.43 (1H, dd, *J* = 8.0, 2.3 Hz, C3**H**), 4.28 (1H, dd, *J* = 5.1, 2.3 Hz, C2**H**), 3.82 (1H, dd, *J* = 10.3, 1.6 Hz, (C5**H**), 3.76 (1H, dd, *J* = 8.0, 1.6 Hz, C4**H**), 3.70 (1H, ddd, *J* = 10.3, 7.9, 6.3 Hz, ArC**H**), 3.11 (1H, ddd, *J* = 16.7, 6.3, 2.0 Hz, C**H**$_2$CHO), 2.65 (1H, ddd, *J* = 16.7, 7.9, 2.2 Hz, C**H**$_2$CHO), 1.56 (3H, s, C**H**$_3$), 1.50 (3H, s, C**H**$_3$), 1.34 (3H, s, C**H**$_3$), 1.25 (3H, s, C**H**$_3$).

^{13}C NMR (126 MHz, $CDCl_3$) δ 201.7 (CHO), 140.1 (C), 128.6 (CH), 128.4 (CH), 127.1 (CH), 109.0 (C), 108.5 (C), 96.7 (CH), 71.1 (CH), 70.8 (CH), 70.7 (CH), 70.5 (CH), 47.0 (CH_2), 40.2 (CH), 26.1 (CH_3), 26.0 (CH_3), 24.9 (CH_3), 24.3 (CH_3).

HRMS (ESI) Exact mass calculated for $C_{20}H_{26}NaO_{76}$ $[M+Na]^+$: 385.1622, found: 385.1617

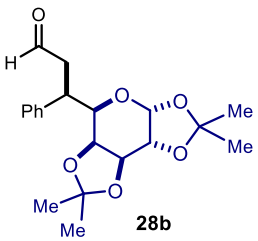

(*R*)-3-phenyl-3-((3a*R*,5*R*,5a*S*,8a*S*,8b*R*)-2,2,7,7-tetramethyltetrahydro-5H-bis([1,3]dioxolo)[4,5-b:4',5'-d]pyran-5-yl)propanal (28b)

Prepared according to the general procedure using cinnamaldehyde (39.6 mg, 0.3 mmol), aminocatalyst (*R*)-**B** (14 mg, 20 mol%), and the corresponding dihydropyridine (48.2 mg, 0.1 mmol) in DCM (400 µL). The crude material was purified by flash column chromatography (hexane/diethyl ether 4:1) to give the product (19.8 mg, 54% yield, 10:90 mixture of diastereoisomers, average of two runs) as a white solid.

C*haracterization of the major diastereoisomer*: ^{1}H NMR (400 MHz, $CDCl_3$) δ 9.62 (1H, dd, *J* = 2.6, 1.9 Hz C**H**O),7.35-7.19 (5H, m, Ar**H**), 5.47 (1H, d, *J* = 5.1 Hz, C1**H**), 4.58 (1H, dd, *J* = 8.0, 2.4 Hz, C3**H**), 4.28 (1H, dd, *J* = 5.1, 2.4 Hz, C2**H**), 4.22 (1H, dd, *J* = 8.0, 1.8 Hz, C4**H**), 4.01 (1H, dd, *J* = 8.5, 1.8 Hz, C5**H**), 3.64 (1H, td, *J* = 8.9, 5.2 Hz, ArC**H**), 3.02 (1H, ddd, *J* = 16.6, 5.2, 1.9 Hz, C$\mathbf{H}_2$CHO), 2.82 (1, ddd, *J* = 16.6, 9.2, 2.6 Hz, C$\mathbf{H}_2$CHO), 1.52 (3H, s, C$\mathbf{H}_3$), 1.49 (3H, s, C$\mathbf{H}_3$), 1.35 (3H, s, C$\mathbf{H}_3$), 1.29 (3H, s, C$\mathbf{H}_3$).

^{13}C NMR (101 MHz, $CDCl_3$) δ 201.9 (C=O), 140.3 (C), 128.5 (CH), 128.2 (CH), 126.9 (CH), 109.3 (C), 108.4 (C), 96.6 (CH), 71.0 (CH), 70.9 (CH), 70.4 (CH), 69.6 (CH), 45.30 (CH_2), 41.6 (CH), 26.0 (CH_3), 25.9 (CH_3), 24.8 (CH_3), 24.3 (CH_3).

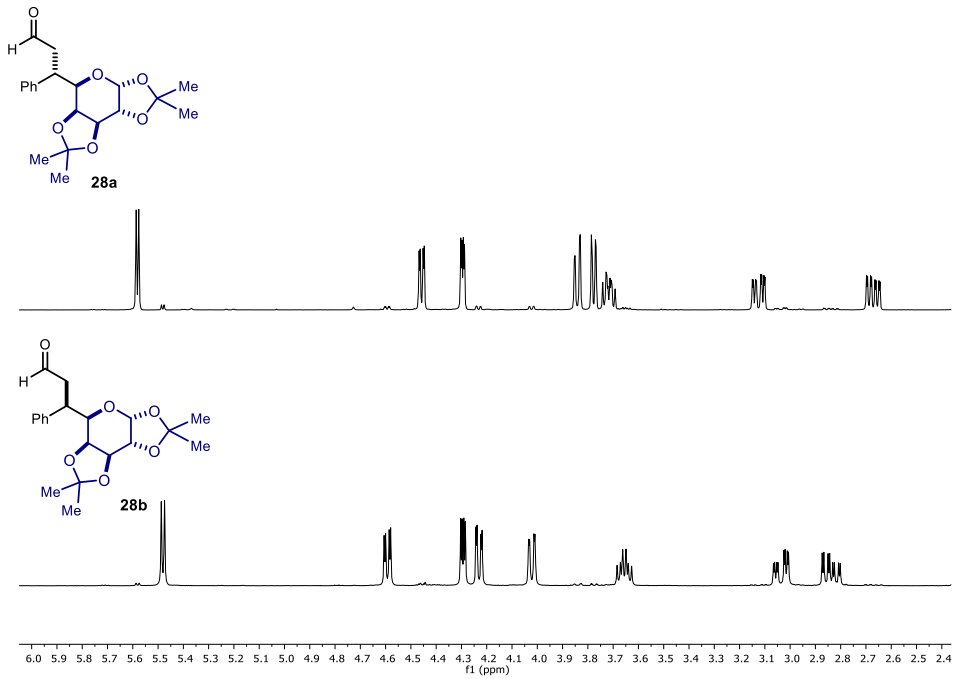

Figure S3.1. ^{1}H NMR Spectra of Diastereoisomers **28a** and **28b**

3.5.5. Cyclic Voltammetry Studies

Cyclic volmatogramm of the trifluoroborate salts 18 and 20.

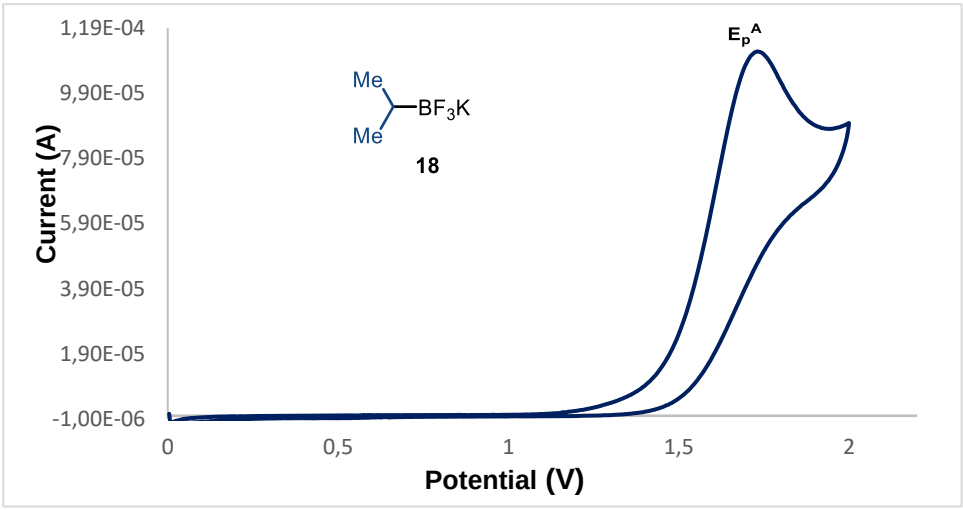

Figure S3.2. Cyclic voltammogram of potassium iso-propyl trifluoroborate **18** [0.03 M] in [0.1 M] TBAPF6 in CH_3CN. Sweep rate: 20 mV/s. Pt electrode working electrode, Ag/AgCl (KCl 3.5M) reference electrode, Pt wire auxiliary electrode. Irreversible oxidation. $E_p^A = E^{ox}$ (**18**$^{\cdot+}$/**18**) = +1.72 V; E_p^A is the anodic peak potential, while E^{ox} value describes the electrochemical properties of **18**.

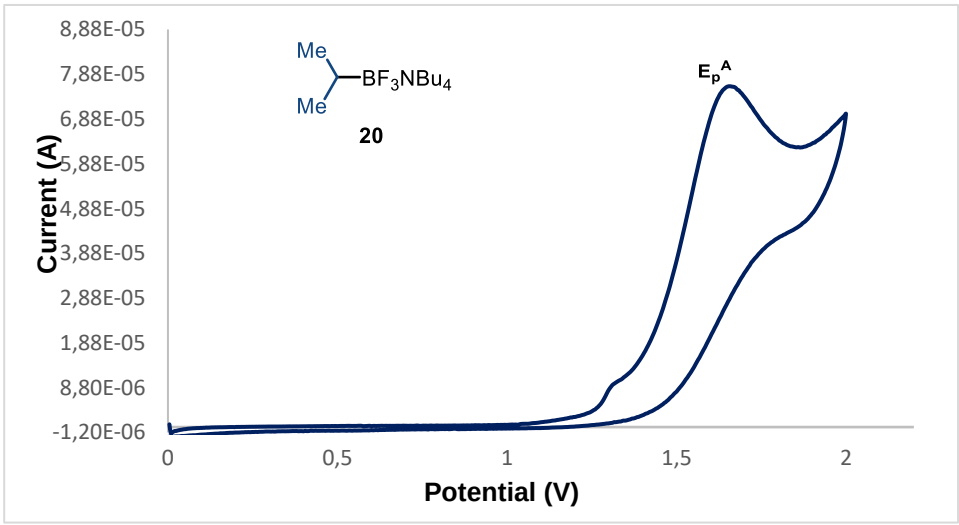

Figure S3.3. Cyclic voltammogram of tetrabutylammonium iso-propyl trifluoroborate **20** [0.02 M] in [0.1 M] $TBAPF_6$ in CH_3CN. Sweep rate: 20 mV/s. Pt electrode working electrode, Ag/AgCl (KCl 3.5M) reference electrode, Pt wire auxiliary electrode. Irreversible oxidation. $E_p^A = E^{ox}$ (**20**$^{\cdot+}$/**20**) = +1.65 V; EpA is the anodic peak potential, while Eox value describes the electrochemical properties of **20**.

The preformed chiral iminium salt **Ib**, synthesized according to the literature[4], was electrochemically characterized.

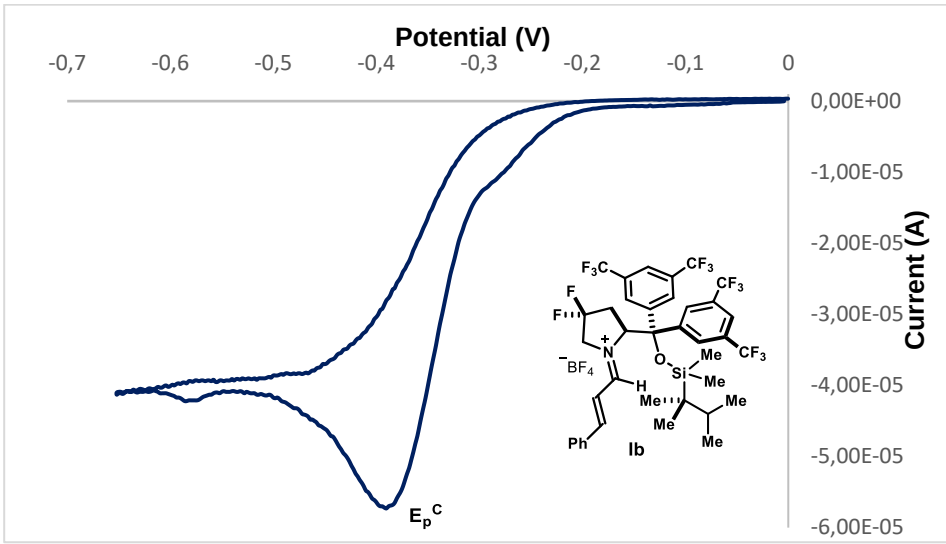

Figure S3.4. Cyclic voltammogram of the preformed iminium salt **Ib** [0.01 M] in [0.1 M] $TBAPF_6$ in CH_3CN. Sweep rate: 20 mV/s. Pt electrode working electrode, Ag/AgCl (NaCl saturated) reference electrode, Pt wire auxiliary electrode. Irreversible reduction. $E_p^C = E_{red}$ (**Ib**/**Ib**$^{\cdot-}$) = -0.38 V; E_p^C is the catodic peak potential, while E_{red} value describes the electrochemical properties of **Ib**.

3.5.6. Absorption Spectra

UV-vis absorption spectra of the Chiral Iminium salt Ib

Solutions at different concentrations of the preformed iminium salt **Ib** (obtained by opportunely diluting the original stock solution with dry acetonitrile) were introduced to a 1 cm path length quartz cuvette equipped with a Teflon® septum and analyzed using a Shimadzu 2401PC UV-Vis spectrophotometer.

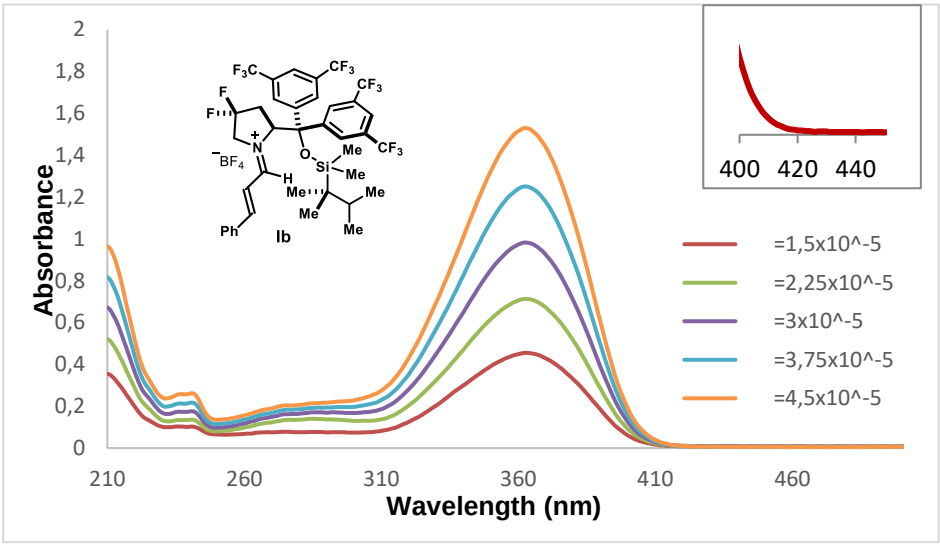

Figure S3.5. Absorption spectra of the preformed iminium salt **Ib** at different concentrations in acetonitrile. The wavelength of maximum absorbance is 363 nm. The tail wavelength was considered to be about 435 nm.

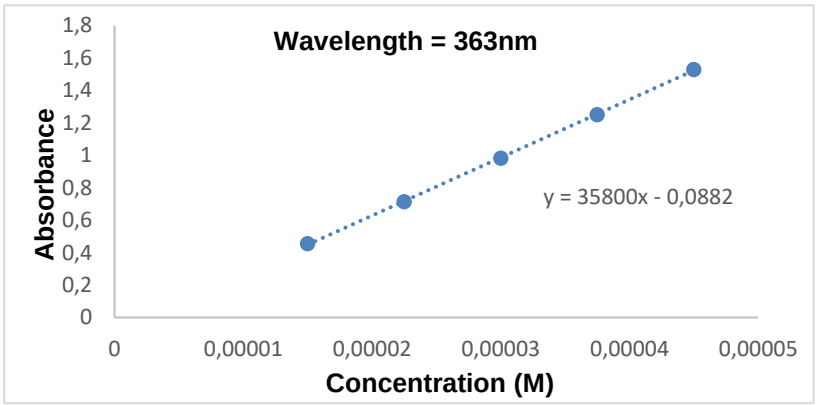

Figure S3.6. Lambert-Beer linear correlation between absorbance and concentration at 363 nm for **Ib**. The slope of the line is the molar extinction coefficient ε at 363 nm ($M^{-1}cm^{-1}$).

3.5.7. Evaluation of the Excited State Potential of the Iminium Ion Ib

Using the data collected from the cyclic voltammetry studies (Figure S3.4.) and from the absorption spectra (Figure S3.5.) of the preformed iminium ion **Ib**, we could estimate the redox potential of the excited iminium salt **Ib*** employing the following Equation 1[37]:

$$E(\mathbf{Ib^*/Ib^{\cdot-}}) = E(\mathbf{Ib/Ib^{\cdot-}}) + E_{0\text{-}0}(\mathbf{Ib^*/Ib})$$

(note that **Ib**$^{\cdot-}$ is the 5π-electron β-enaminyl radical intermediate **III** plus the counter-anion)

Since the electrochemical oxidation of the iminium salts **Ic** was irreversible (Figure S3.4.), the irreversible peak potential $E_p^{Cathode}$ was used for $E(\mathbf{Ib/Ib^{\cdot-}})$. $E_{0\text{-}0}(\mathbf{Ib^*/Ib})$, which is the excited state energy of the iminium salts **Ib**, was estimated spectroscopically from the position of the long wavelength tail of the absorption spectrum (until 435 nm, Figure S3.5.) recorded in acetonitrile, the solvent used for the electrochemical analysis.[38]

For the preformed iminium ion **Ib**, the $E_p^{cathode}$, which provides the $E(\mathbf{Ib/Ib^{\cdot-}})$, is -0.38 V (Figure S3.4.), while the position of the long wavelength tail of the absorption spectrum corresponds to 435 nm (Figure S3.5.), which translates into an $E_{0\text{-}0}(\mathbf{Ib^*/Ib})$ of 2.85 eV.

$$E(\mathbf{Ib^*/Ib^{\cdot-}}) = -0.38 + 2.85 = \mathbf{+2.45\ V}\ (\text{vs Ag/AgCl})$$

3.5.8. X-Ray Crystallographic Data

Single Crystal X-ray Diffraction Data for compound 28a

Crystals of the compound **28a** were obtained by slow evaporation of a hexane/ethyl acetate solution.

Data Collection. Measurements were made on a Bruker-Nonius diffractometer equipped with an APPEX 2 4K CCD area detector, a FR591 rotating anode with MoKα radiation. Montel mirrors and a Cryostream Plus low temperature device (T = 100K). Full-sphere data collection was used with ω and φ scans.

[37] Kavarnos, G. J. In Fundamentals of Photoinduced Electron Transfer. VCH Publishers: New York, 1993, pp 29–40.
[38] Balzani, V.; Ceroni, P.; Juris, A. In Photochemistry and Photophysics, Wiley-VCH: Weinheim, 2014, pp 103-123.

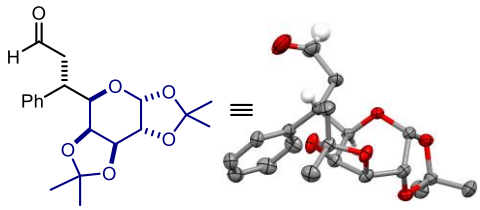

Table S3.1. Crystal data and structure refinement for 28a. ***CCDC1581199***

Empirical formula	C20 H26 O6
Formula weight	362.41
Temperature	100(2) K
Wavelength	0.71073 Å
Crystal system	Monoclinic
Space group	P2(1)
Unit cell dimensions	a = 20.0688(3)Å, α= 90°.
	b = 9.57471(12)Å, β = 113.3147(18)°.
	c = 21.8114(3)Å, γ = 90°.
Volume	3848.90(11) $Å^3$
Z	8
Density (calculated)	1.251 Mg/m^3
Absorption coefficient	0.091 mm^{-1}
F(000)	1552
Crystal size	? x ? x ? mm^3
Theta range for data collection	1.891 to 40.249°.
Index ranges	-36<=h<=36,-16<=k<=17,-39<=l<=39
Reflections collected	201662
Independent reflections	47414[R(int) = 0.0361]
Completeness to theta =40.249°	100.0%
Absorption correction	Multi-scan
Max. and min. transmission	0.995 and 0.765
Refinement method	Full-matrix least-squares on F^2
Data / restraints / parameters	47414/ 25/ 981
Goodness-of-fit on F^2	0.990
Final R indices [I>2sigma(I)]	R1 = 0.0503, wR2 = 0.1298
R indices (all data)	R1 = 0.0722, wR2 = 0.1462
Flack parameter	x =-0.08(9)
Largest diff. peak and hole	0.477 and -0.260 $e.Å^{-3}$

Chapter IV

Amide Synthesis by Nickel/Photoredox-Catalyzed Carbamoylation of (Hetero)Aryl Bromides

Target

Development of a photochemical nickel-catalyzed cross-coupling protocol for the synthesis of amides.

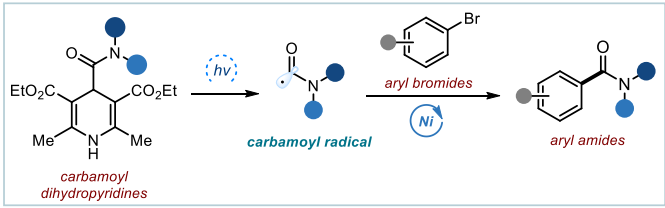

Tool

Exploiting both the ground-state and the excited-state reactivity of carbamoyl-dihydropyridines to generate carbamoyl radicals.[1]

4.1. Introduction

Amides are widespread structural units in nature, since the amide bond is the fundamental linkage of natural proteins and peptides.[2] This moiety is also widely present in polymers, agrochemicals, and pharmaceutical molecules (Figure 4.1.).[3] Among the top 50 selling small molecule drugs in 2018, more than 70% contain an amide bond linkage.[4] This explains why amide bond formation is among the most commonly performed reactions in industry and it is particularly important in drug discovery endeavors. According to an analysis by three major pharmaceutical companies in 2011, 16% of all reactions performed in pharmaceutical companies account for amide bond formations.[5]

[1] The project discussed in this chapter was conducted in the framework of an industrial collaboration with *Bayer AG Pharmaceuticals* (Mr. Tim Schulte, Dr. Lisa Candish and Dr. Karl D. Collins). I was involved, together with Dr. Luca Buzzetti and Prof. Dr. Gianfranco Favi, in the discovery of the reaction, the optimization studies and investigated the scope of the reaction. Parts of the study has been published: Alandini, N., Buzzetti, L., Favi, G., Schulte, T., Candish, L., Collins, K. D., Melchiorre, P., "Amide Synthesis by Nickel/Photoredox-Catalyzed Carbamoylation of (Hetero)Aryl Bromides" *Angew. Chem. Int. Ed.* **2020**, *59,* 5248.

[2] Greenberg, A., Breneman, C. M., Liebman, J. F., "The Amide Linkage: Structural Significance in Chemistry, Biochemistry and Materials Science", Wiley-VCH, Weinheim, **2003**.

[3] Brown D. G., Bostrom, J. "Analysis of Past and Present Synthetic Methodologies on Medicinal Chemistry: Where Have All the New Reactions Gone?", *J. Med. Chem.* **2016**, *59,* 4443.

[4] For freely accessible database, see: https://njardarson.lab.arizona.edu/content/top-pharmaceuticals-poster; McGrath, N.A., Brichacek, M., Njardarson, J. T., "A Graphical Journey of Innovative Organic Architectures That Have Improved Our Lives", *J. Chem. Educ.* **2010**, *87*, 12, 1348.

[5] Roughley, S. D., Jordan, A. M., "The Medicinal Chemist's Toolbox: An Analysis of Reactions Used in the Pursuit of Drug Candidates', *J. Med. Chem.* **2011** 54, 3451.

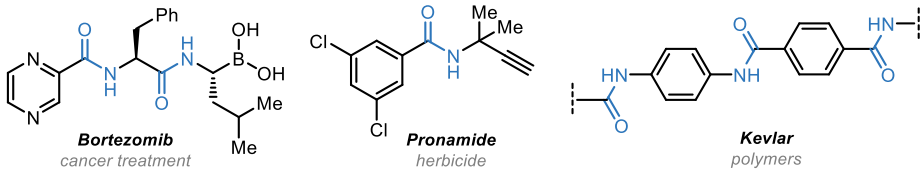

Figure 4.1. Examples of bio-relevant compounds and polymer containing an amide linkage.

Despite the prevalence and importance of the amide linkage, improved methods for amide synthesis are still sought after, especially if they can offer high efficiency and reduce the environmental impact.[6] Among the most important methods for amide synthesis, formation of C–N bonds by condensation of carboxylic acid derivatives with amines is the most common approach used both in academia and industry (Scheme 4.1.). However, this reaction requires the addition of stoichiometric amounts of high molecular weight coupling reagents, which are often expensive, toxic and/or potentially explosive.[7] While often tolerable on a small scale, this inefficiency has major implications for production of drugs or agrochemicals, which may need to be synthesized on multi-ton scale.[8]

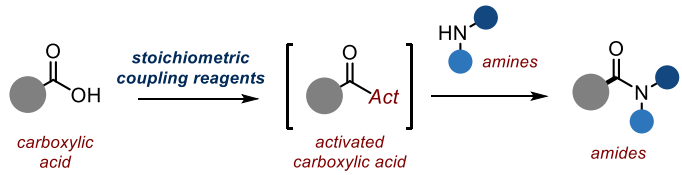

Scheme 4.1. Classical dehydrative condensation route to amide bond formation. Act: activating group.

Catalytic methods for amide formation have the potential to minimize waste, improve the environmental burden, and lower the costs of the process.[9] Recent key advances include the use of group IV metal salts or boron compounds as catalysts.[10] However, the need for

[6] Pattabiraman, V.R., Bode, J.W. "Rethinking Amide Bond Synthesis', *Nature* **2011**, *480*, 471.
[7] Selected reviews: a) Valeur, E., Bradley, M. "Amide Bond Formation: Beyond the Myth of Coupling Reagents", *Chem. Soc. Rev.* **2009**, 38, 606; b) McKnelly, K. J., Sokol, W. Nowick, J. S., "Anaphylaxis Induced by Peptide Coupling Agents: Lessons Learned from Repeated Exposure to HATU, HBTU, and HCTU", *J. Org. Chem.,* **2020**, *85*, 1764.
[8] Dunetz, J. R., Magano, J., Weisenburger, J. A., "Large-Scale Applications of Amide Coupling Reagents for the Synthesis of Pharmaceuticals", *Org. Process Res. Dev.* **2016**, *20*, 140.
[9] Sabatini, M. T., Boulton, L., T., Sneddon, H. F., Sheppard, T. D., "A Green Chemistry Perspective on Catalytic Amide Bond Formation", *Nat. Catal.* **2019**, *2*, 10.
[10] Selected examples: a) Ishihara, K., Lu, Y., "Boronic Acid–DMAPO Cooperative Catalysis for Dehydrative Condensation between Carboxylic Acids and Amines", *Chem. Sci.* **2016**, *7*, 1276; b) Sabatini, M. T., Boulton, L. T., Sheppard, T. D. "Borate Esters: Simple Catalysts for the Sustainable Synthesis of Complex Amides", *Sci. Adv.* **2017**, *3*, e1701028.

excessive amounts of drying agents and severe reaction conditions account for the low uptake of these methodologies (Scheme 4.2., left).

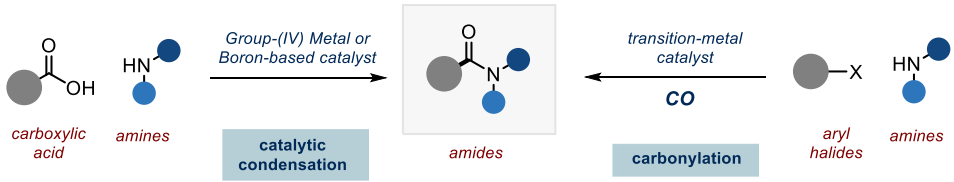

Scheme 4.2. Catalytic amide synthesis methods from the corresponding carboxylic acids (left) and aryl bromides (right).

On the other hand, Pd-catalyzed carbonylation reactions – the three-component coupling of aryl halides with an amine and carbon monoxide (CO) – offers a powerful alternative for amide synthesis (Scheme 4.2., right).[11] This C–C bond forming reaction enables the direct and selective installation of the amide moiety on an aryl halide. Whilst this reaction has significant benefits, the use of highly toxic CO gas limits its wider application in terms of safety. In addition, most of the protocols require severe reaction conditions and elevated temperatures, which limit the tolerance for substrates with sensitive functional groups. Therefore, there is still a need for catalytic amide synthesis that operates at ambient temperature, offers a broad substrate scope, and avoid the use of excessive drying agents.[12]

In this chapter, we describe the catalytic conversion of aryl and heteroaryl bromides into their corresponding amides enabled by the combination of nickel catalysis and photochemistry (Scheme 4.3.). The developed method used bench-stable and readily available 4-carbamoyl-1,4-dihydropyridines **1** (carbamoyl-DHPs) as carbamoyl radical precursors.

In particular, two different photochemical strategies have been developed, exploiting either *i*) the direct excitation of carbamoyl-DHPs **1** and its ability in the excited states to act as photoreductants and carbamoyl radical source, or *ii*) the ability of an external photoredox catalyst to facilitate the single-electron transfer (SET) oxidation of ground-state carbamoyl-DHPs **1** to afford the carbamoyl radical species. These radical generation strategies have been coupled with nickel catalysis to develop cross-coupling processes for the preparation of amides.

[11] a) Schoenberg A., Heck, R. F. "Palladium-Catalyzed Amidation of Aryl, Heterocyclic, and Vinylic Halides", *J. Org. Chem.* **1974,** *39*, 3327; b) Brennführer, A., Neumann, H., Beller, M., "Palladium-Catalyzed Carbonylation Reactions of Aryl Halides and Related Compounds", *Angew. Chem. Int. Ed.* **2009**, *48*, 4114.
[12] S. M. Mennen et al., "The Evolution of High-Throughput Experimentation in Pharmaceutical Development and Perspectives on the Future", *Org. Process Res. Dev.* **2019**, *23*, 1213.

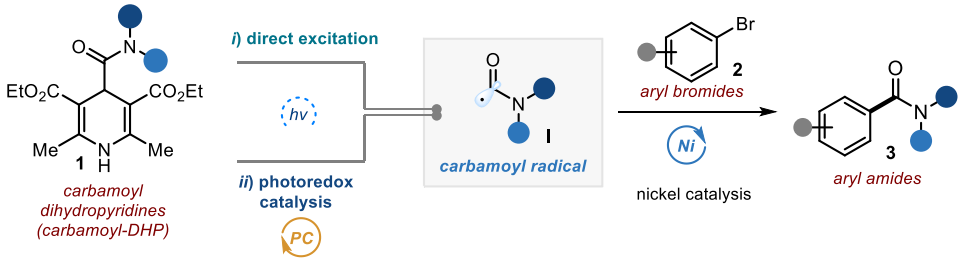

Scheme 4.3. Photochemical amide formation through Ni-catalyzed carbamoylation of aryl halides with carbamoyl-DHPs.

In the following sections, I will discuss the recent advances in transition metal-catalyzed amide synthesis using CO surrogates as well as the scientific background and the previous studies that were essential to the development of the present research project.

4.1.1. Metal-Catalyzed Routes towards Aryl Amides using CO Surrogates

Metal-catalyzed carbonylation chemistry is a powerful methodology for the installation of a carbonyl group into organic molecules.[10] This methodology concerns the incorporation of carbon monoxide (CO) to an aryl- or vinylmetal complex in the presence of nucleophiles. Aminocarbonylation reactions, where amines are used as nucleophiles, offer an alternative synthetic route towards amides through C–C bond formation (Scheme 4.4.).[13]

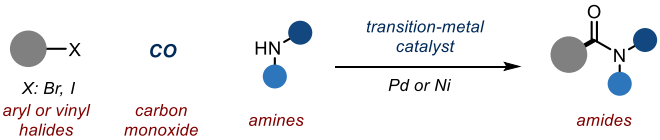

Scheme 4.4. Metal-catalyzed three-component coupling between aryl- or vinyl halides, CO and amines for the preparation of amides.

Despite the large-scale applications in industry, the necessity to handle toxic, gaseous CO limits the application in more complex organic synthesis. For this reason, numerous carbonylation methods without the use of gaseous CO have been developed over the last 30 years.[14] Pd-catalyzed aminocarbonylation in the absence of CO was realized in 2002 using *N*,*N*-dimethylformamide (DMF, **14**) as an amide source.[15] Hiyama and co-workers

[13] Roy, S., Roy, S., Gribble, G., "Metal-Catalyzed Amidation", *Tetrahedron* **2012**, *68*, 9867.
[14] Morimoto, T., Kakiuchi, K., "Evolution of Carbonylation Catalysis: No Need for Carbon Monoxide", *Angew. Chem. Int. Ed.* **2004**, *43*, 5580.
[15] Hosoi, K., Nozaki, K., Hiyama, T., "Carbon Monoxide Free Aminocarbonylation of Aryl and Alkenyl Iodides using DMF as an Amide Source", *Org. Lett.* **2002**, *4*, 2849.

demonstrated that aryl amides could be prepared from the corresponding iodides **4** through the formation of Vilsmeier iminium intermediate **II**, which required the use of phosphoryl chloride **6** as an additive (Scheme 4.5.).

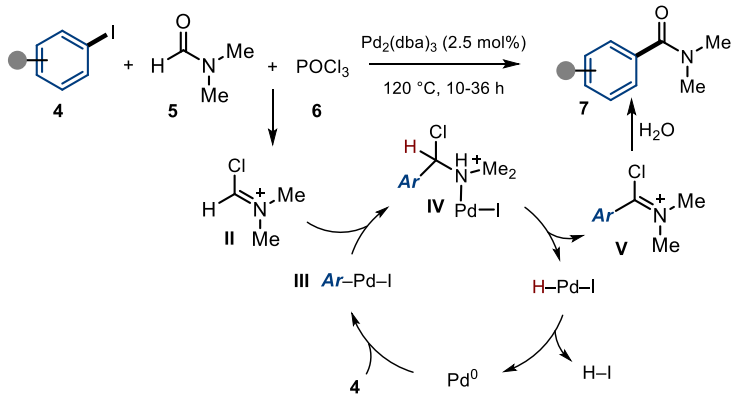

Scheme 4.5. Pd-catalyzed aminocarbonylation of aryl iodides using formamides **5** as carbamoyl source.

The reaction was proposed to proceed through a Heck-type process, where the addition of the arylpalladium species **III** to Vilsmeier intermediate **II** delivers the palladium complex **IV**. Subsequent β-hydride elimination yields the iminium ion **V**, which after hydrolysis delivers the desired amides **7**. Although both electron-rich and electron-poor aryl iodides could be used, the chemistry was limited to DMF. Lee and co-workers later demonstrated that the scope of aminocarbonylation with formamides could be expanded by using nickel-phosphite catalytic system (Scheme 4.6.).[16] The use of strong base such as NaOMe or KOMe was crucial for the reaction, which enabled the preparation of various secondary and tertiary amides.

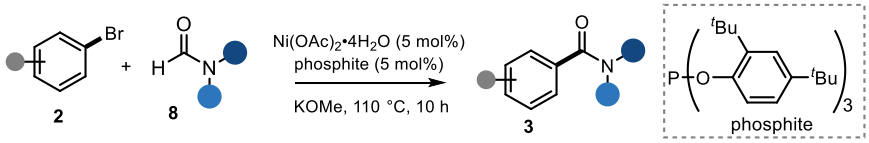

Scheme 4.6. Nickel-catalyzed aminocarbonylation with various formamides **8** as carbamoyl source.

The use of carbamoylsilane as carbamoyl sources has been reported for the synthesis of benzamides from the corresponding aryl halides. Cunico and Maity reported the direct carbamoylation of aryl halides **9** with *N*,*N*-dimethylcarbamoyl(trimethyl)silane **10** in the presence of $[Pd(PPh)_3]_4$ as catalyst (Scheme 4.7.).[17] Under these conditions, a range of aryl

[16] Ju, J., Jeong, M., Moon, J., Jung, H. M., Lee, S., "Aminocarbonylation of Aryl Halides Using a Nickel Phosphite Catalytic System", *Org. Lett.* **2007**, *9*, 4615.
[17] Cunico, R. F., Maity, B. C., "Direct Carbamoylation of Aryl Halides", *Org. Lett.* **2002**, *4*, 4357.

and heteroaryl halides could be efficiently converted to the corresponding amides. The transfer of the carbamoyl group was proposed to proceed through the complexation of the nucleophilic carbene species **VI**, generated by the rearrangement of carbamoylsilane **10**, with aryl-palladium complex **VII** to generate the complex **VIII**. Subsequent loss of trimethylsilyl halide led to the formation of the carbamoylpalladium intermediate **IX**, which undergoes reductive elimination to provide the desired product **3** and thereby restore the Pd(0) intermediate.

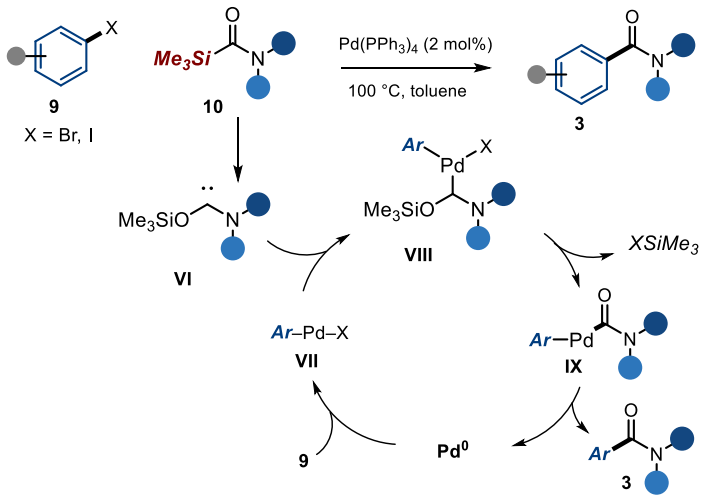

Scheme 4.7. Palladium-catalyzed aminocarbonylation using carbamoylsilane **10** as carbamoyl source.

The synthesis of aryl amides could also be achieved through decarboxylative coupling of aryl halides with oxamic acids as carbamoyl precursors. Oxamic acids are known to generate carbamoyl radicals under oxidative conditions.[18] In 2015, Shang and Fu described a Pd-catalyzed decarboxylative carbamoylation protocol, in which they use a photoredox catalyst to generate the carbamoyl radicals **I** from alkyl oxamates **20** (Scheme 4.8.).[19] Using a combination of Ir-photoredox catalyst, $[Pd(PhCN)_2Cl_2]$ and Nixantphos as ligand, various *N*,*N*-dialkylbenzamides **3** were synthesized under irradiation with blue LEDs. The carbamoylation process starts with the SET oxidation of alkyl oxamates **11** by the excited Ir^* to generate carbamoyl radicals **I**. Subsequent capture of the radical intermediates by aryl-palladium complex **X** delivers the Pd(III) complex **XI**, which oxidizes the Ir(II) to Ir(III) to

[18] Li, M., Wang, C., Fang, P., Ge, H., "Pd(II)-Catalyzed Decarboxylative Cross-Coupling of Oxamic Acids with Potassium Phenyltrifluoroborates under Mild Conditions", *Chem. Commun.* **2011**, *47*, 6587.
[19] Cheng, W. M., Shang, R., Yu, H. Z., Fu, Y., "Room-Temperature Decarboxylative Couplings of α-Oxocarboxylates with Aryl Halides by Merging Photoredox with Palladium Catalysis", *Chem. Eur. J.* **2015**, *21*, 13191.

complete the photoredox cycle. The Pd(II) intermediate **XII** undergoes reductive elimination to deliver the desired product **3** and complete the palladium catalytic cycle.

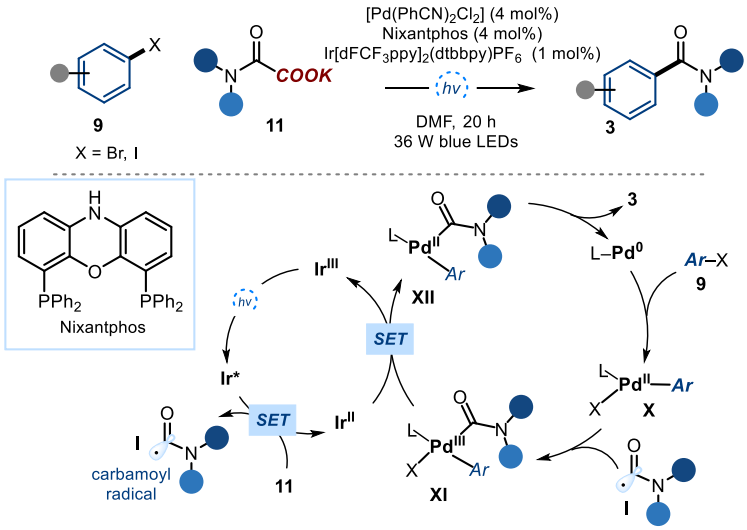

Scheme 4.8. Pd/photoredox-catalyzed decarboxylative coupling of oxamic acids for the synthesis of amides.

Isocyanates have also been frequently used as amide precursor in metal-catalyzed cross-coupling reactions.[20] In 2005, Hsieh and Cheng reported the Ni-catalyzed reductive cross-coupling of isocyanates with aryl halides (Scheme 4.9.).[21] Under the optimized conditions, aryl bromides and iodides **9** were coupled with aryl and alkyl isocyanates **12** to deliver the corresponding amides **13**. The reductive coupling reaction was proposed to start with the reduction of Ni(II) species to Ni(0) (**XIII**) by zinc powder. Oxidative addition of aryl halides **9** to the Ni(0) complex yields the intermediate **XIV**. Subsequent insertion of isocyanate **12** provides the intermediate **XV**, which after reductive elimination delivers the product **13** and Ni(II) species **XVI**. Similar transformation was later reported by the Martin group, where aryl esters and tosylates were used as coupling partner.[22] Both protocols offer a straightforward access to secondary amides under mild conditions. However, stoichiometric additives or large excess of isocyanates were required to avoid the formation of side-products derived from the metal-mediated di- and trimerization of isocyanates.

[20] Serrano, E., Martin, R., "Forging Amide Bonds via Metal-Catalyzed Cross-Coupling Reactions with Isocyanates", *Eur. J. Org. Chem.* **2018**, *24*, 3051.
[21] Hsieh, J. C., Cheng, C., H., "Nickel-Catalyzed Coupling of Isocyanates with 1,3-Iodoesters and Halobenzenes: A Novel Method for the Synthesis of Imide and Amide Derivatives", *Chem. Commun.* **2005**, *36*, 4554.
[22] Correa, A., Martin, R., "Ni-Catalyzed Direct Reductive Amidation via C–O Bond Cleavage", *J. Am. Chem. Soc.* **2014**, *136*, 7253.

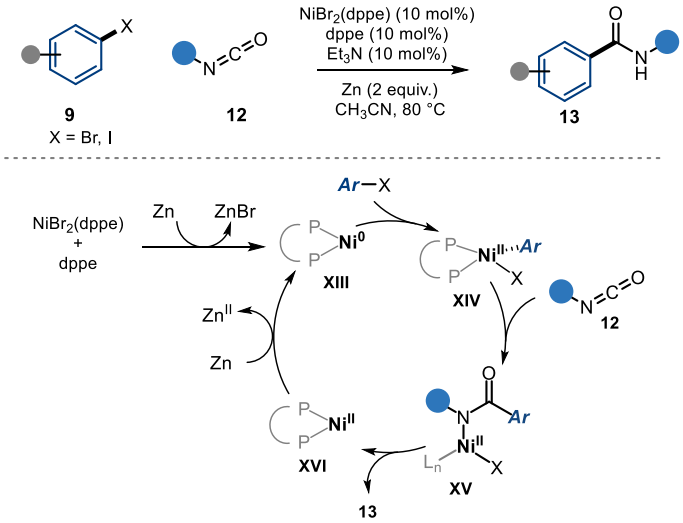

Scheme 4.9. Ni-catalyzed reductive coupling reaction of aryl halides with isocyanates **12**.

The reactions discussed above represented a few innovative strategies for addressing the drawbacks associated with the use of carbon monoxide in aminocarbonylation reactions. Although the reactions can duplicate the reactivity of carbonylation reaction with CO, considerable improvements are still needed in terms of substrate scope. In addition, the harsh reaction conditions generally required, including high temperatures and the need of additives, means that aminocarbonylation strategies which occur at ambient temperature are highly desirable.

4.1.2. C–C Bond-Forming Reactions Enabled by Photoexcitation of DHPs

1,4-Dihydropyridines (DHPs) is a versatile reagent both in thermal processes and in photoinduced transformations (see the discussion in Chapter 2).[23] The ground-state reactivity of DHPs is mainly characterized by the ability to serve as hydride donor and to play the role of NADH analogues for hydride transfer reactions.[24] The chemistry of DHPs has recently been expanded to photomediated transformations, in which the ground-state DHP derivatives play the role of SET donor to facilitate the reductive quenching cycle of photoredox

[23] Wang, P.-Z., Chen, J.-R., Xiao, W.-J. "Hantzsch Esters: An Emerging Versatile Class of Reagents in Photoredox Catalyzed Organic Synthesis", *Org. Biomol. Chem.* **2019**, *29*, 6936.
[24] Zheng, C., You, S.-L. "Transfer Hydrogenation with Hantzsch Esters and Related Organic Hydride Donors", *Chem. Soc. Rev.* **2012**, *41*, 2498.

catalysts.[25] It was later demonstrated that 4-alkyl-1,4-dihydropyridines (alkyl-DHPs), under photoredox conditions, can serve as carbon-centered radical precursors upon SET oxidation.[26]

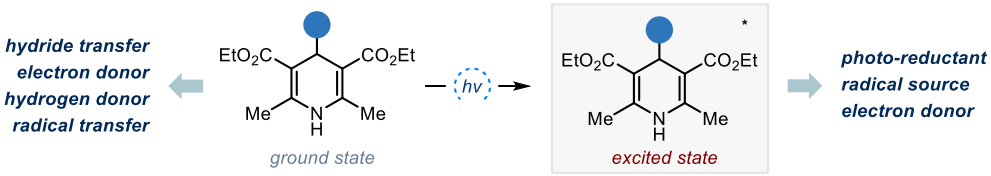

Scheme 4.10. Modes of reactivity of 1,4-dihydropyridines.

In addition to the above-mentioned reactivity modes which characterize the ground state, the direct photoexcitation of DHPs with visible light leads to a highly potent photoreductant that can productively engage in SET processes. Although the photochemical reactivity of DHPs was already identified in the 1970s,[27] it has only recently found applications in organic synthesis, mainly for the SET reduction of various organic compounds.[28] Recently, the excited-state reactivity of DHPs has been used to promote the formation of carbon–carbon bonds. In 2017, our laboratories demonstrated that alkyl-DHPs **14** exhibit a dual reactivity profile in the excited state (Scheme 4.11.), behaving as a strong SET reductant and simultaneously generating alkyl radicals **XVIII** through fragmentation of the radical cation **XVII**, which formed upon SET event.[29]

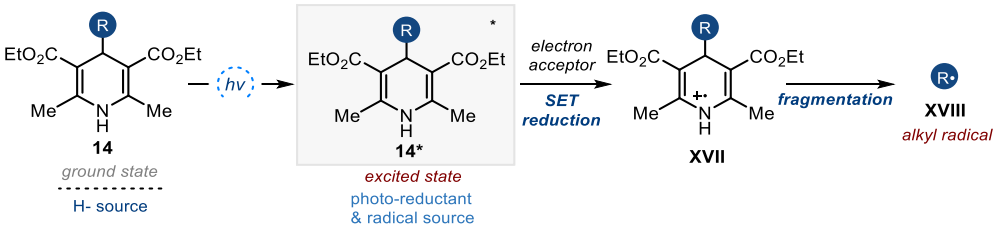

Scheme 4.11. Dual reactivity profile of excited-state alkyl-DHP **14**.

[25] Selected examples: a) Konev, M., O., McTeague, A., Johannes, J. W., "Nickel-Catalyzed Photoredox-Mediated Cross-Coupling of Aryl Electrophiles and Aryl Azides", *ACS Catal.* **2018**, *8*, 9120; b) Lackner, G., L., Quasdorf, K. W., Overman, L. E., "Direct Construction of Quaternary Carbons from Tertiary Alcohols via Photoredox-Catalyzed Fragmentation of *Tert* -Alkyl *N* -Phthalimidoyl Oxalates", *J. Am.Chem. Soc.* **2013**, *135*, 15342.

[26] Nakajima, K., Nojima, S., Sakata, K., Nishibayashi, Y., "Visible-Light-Mediated Aromatic Substitution Reactions of Cyanoarenes with 4-Alkyl-1,4-Dihydropyridines through Double Carbon–Carbon Bond Cleavage", *ChemCatChem* **2016**, *8*, 1028.

[27] Hedstrand, D. M., Kruizinga, W. H., Kellogg, R. M., "Light Induced and Dye Accelerated Reductions of Phenacyl Onium Salts by 1,4-Dihydropyridines", *Tetrahedron Lett.* **1978**, *19*, 1255.

[28] Jung, J., Kim, J., Park, G., You, Y., Cho., E. J., "Selective Debromination and α-Hydroxylation of α-Bromo Ketones Using Hantzsch Esters as Photoreductants", *Adv. Synth. Catal.* **2016**, *358*, 74.

[29] Buzzetti, L., Prieto, A., Roy, S. R., Melchiorre, P., "Radical-Based C−C Bond-Forming Processes Enabled by the Photoexcitation of 4-Alkyl-1,4-dihydropyridines", *Angew. Chem. Int. Ed.* **2017**, *56*, 15039.

These properties were confirmed by photophysical and electrochemical analysis. UV-visible absorption spectrum of 4-benzyl-1,4-dihydropyridine (Bn-DHP, **14a**) dissolved in CH_3CN established its ability to absorb light in the visible region, up to 420 nm. The photochemical reactivity of the Bn-DHP **14a** was then tested by irradiating a solution of Bn-DHP in CH_3CN using a high-power single light-emitting diode (HP single LED, λ_{max} = 405 nm, Scheme 4.12.). This experiment led to the formation of toluene **15**, 1,2-diphenylethane **16** and the corresponding Hantzsch pyridine **17**, indicating that the photoexcitation of **14a** can trigger the formation of benzyl radicals.

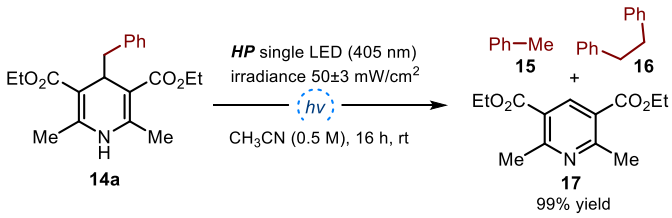

Scheme 4.12. Photodegradation of Bn-DHP **14a** to toluene **15**, diphenylethane **16** and the corresponding pyridine **17**.

To evaluate the dual propensity of **14a** to act both as a strong photoreductant and generate radicals upon light absorption, the *ipso*-substitution of cyanoarene **18** was performed using irradiation at 405 nm (Scheme 4.13.).[30] This process occurs through a radical coupling mechanism that requires the formation of the C(sp^3)-centered benzyl radical **XX** and a persistent cyanoarene radical anion **XIX**, generated upon SET reduction of **18**. The subsequent C–C bond formation affords a cyclohexadienyl anion **XXI** that is prone to rapid aromatization via elimination of cyanide to deliver the alkylated product **19**. The formation of the product **9** confirmed the ability of Bn-DHP **14a** to simultaneously act as a SET reductant and deliver the benzyl radical **XX**. Based on electrochemical and spectroscopic measurements, the excited-state reduction potential of Bn-DHP was estimated[31] to be E^{red} (**14a**$^{\bullet+}$/**14a***) = –2.0 V vs Ag/Ag$^+$, which makes the SET reduction of substrate **18** (E^{red} = –1.87 vs SCE) thermodynamically feasible.

[30] Bonesi, S. M., Fagnoni, M., "The Aromatic Carbon–Carbon *ipso*-Substitution Reaction" *Chem. Eur. J.* **2010**, *16*, 13572

[31] The excited-state oxidation potential of **14a** has been approximated on the basis of spectroscopic and electrochemical measurement and applying the Rehm-Weller theory. Rehm, D., Weller, A. "Kinetics of Fluorescence Quenching by Electron and H-Atom Transfer" *Isr. J. Chem.*, **1970**, *8*, 259

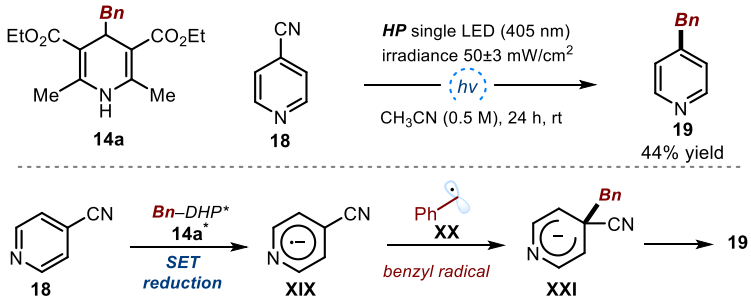

Scheme 4.13. Aromatic substitution of cyanopyridine **18**, facilitated by the radical coupling of an alkyl radical with cyanoarene radical anion **XIX**.

The dual photochemical reactivity of Bn-DHP **14a** was then combined with nickel catalysis to develop a photochemical nickel-catalyzed cross-coupling protocol. The merge of nickel and photoredox catalysis has recently emerged as a powerful platform for developing cross-coupling methods.[32] In these processes, the photoredox catalyst is responsible for modulating the oxidation potential of the nickel by SET reduction, an essential step to restore the original Ni(0) catalyst and turnover the nickel catalyst. Since the DHPs can act as both SET reductants and alkyl radical precursors upon excitation, we hypothesized that its photochemical reactivity could facilitate a nickel-catalyzed C(sp^3)-C(sp^2) cross-coupling reaction without the need of an external photoredox catalyst (Scheme 4.14.). It was proposed that the photoexcitation of alkyl-DHPs **14** generates the excited-state intermediate **14***, which can reduce the Ni(II) pre-catalyst through two discrete SET events to afford the active Ni(0) intermediate **XXIII**. The resulting radical cation **XXII** then undergoes rapid aromatization and generates the alkyl radical **XVIII**, which is intercepted by the Ni(0) complex **XXIII**. The emerging Ni(I) **XXIV** species undergoes oxidative addition with the aryl bromide **2**. Subsequent reductive elimination forges the desired C(sp^3)-C(sp^2) bond in the product **20**. Finally, SET reduction of the Ni(I) complex **XXVI** by **4*** completes the catalytic cycle and generates another alkyl radical **XVIII**.

[32] Milligan, J. A., Phelan, J. P., Badir, S. O., Molander, G. A., "Alkyl Carbon-Carbon Bond Formation by Nickel/Photoredox Cross-Coupling", *Angew. Chem. Int. Ed.* **2019**, *58*, 6152.

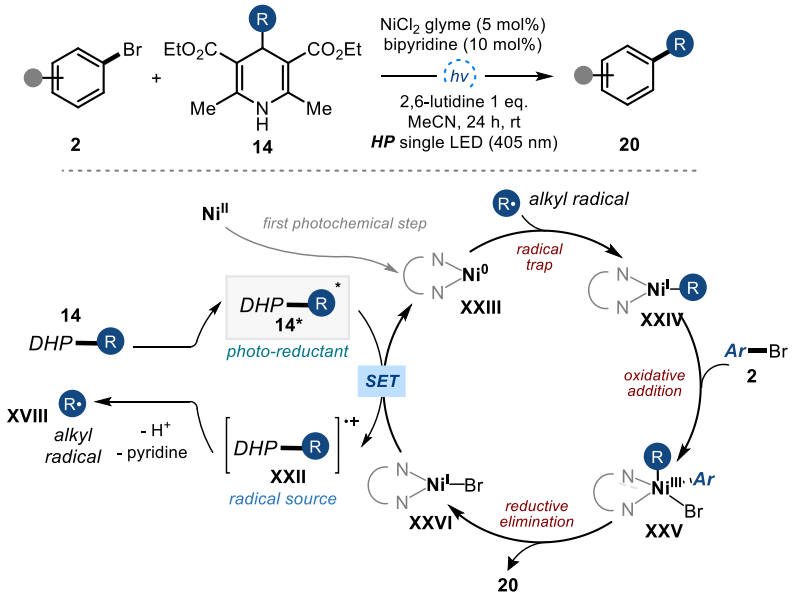

Scheme 4.14. Proposed mechanism of photochemical nickel-catalyzed cross-coupling of aryl bromide with alkyl-DHP **14.**

Under the optimized reaction conditions, a broad range of alkyl-DHPs and aryl bromides, bearing diverse functional groups, could be successfully coupled (Figure 4.2.).

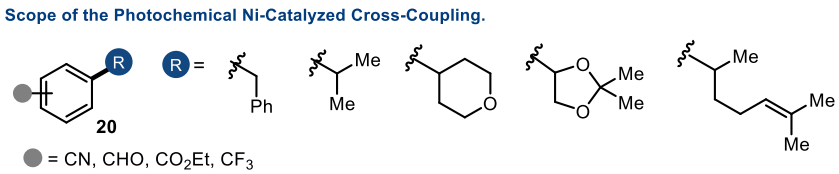

Figure 4.2. Scope of the photochemical Ni-catalyzed cross-coupling reactions with alkyl-DHPs **14.**

This photochemical strategy was also successfully applied to the stereoselective synthesis of chiral ketones under mild conditions (Scheme 4.15.).[33] Using a chiral bisoxazoline-type ligand **L1**, a wide array of anhydrides **21** was coupled with various DHPs, acting as radical precursors and SET reductants, with good yield and high enantioselectivity. The light-driven asymmetric catalytic cross-coupling method enabled the preparation of chiral ketones containing different groups at the α-stereogenic center, including an (1*H*-indol-1-yl) moiety.

[33] Gandolfo, E., Tang, X. J., Roy, S. R., Melchiorre, P., "Photochemical Asymmetric Nickel-Catalyzed Acyl Cross-Coupling", *Angew. Chem. Int. Ed.* **2019**, *58*, 16854.

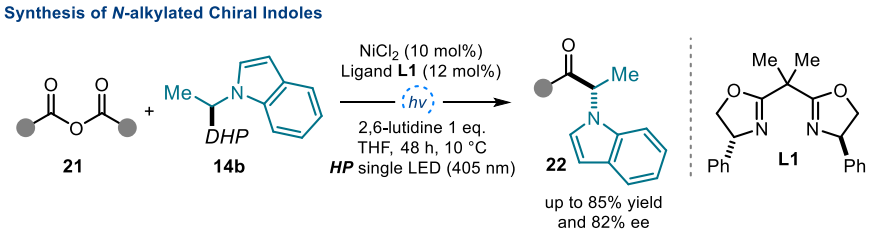

Scheme 4.15. Photochemical Ni-catalyzed asymmetric cross-coupling reaction of anhydrides **11** and alkyl-DHPs **14b.**

4.2. Design and Target of the Project (I)

The ubiquity and importance of amides in proteins, agrochemicals, pharmaceuticals and polymers prompts the continuous development of novel methods for their synthesis. Of particular interest is the development of new and alternative transformations that can effectively complement and expand the scope of conventional amidation and carbonylation chemistry.

One of the main interests of our research laboratories is the development of new methodologies based on the synergistic combination of photochemistry and metal-mediated catalysis. We have recently reported a photochemical nickel-cross coupling approach for the formation of C(sp^2)–C(sp^3) bonds, that exploits the direct excitation of 4-alkyl-1,4-dihydropyridines (alkyl-DHPs) to generate alkyl radicals (Scheme 4.16).[18]

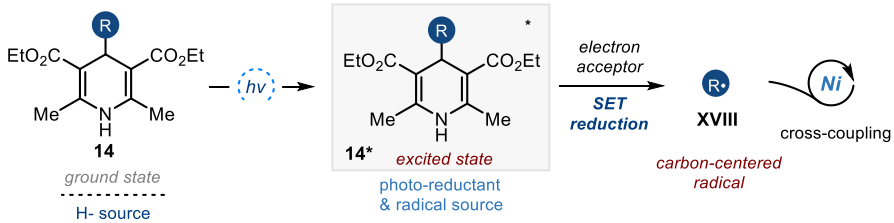

Scheme 4.16. Dual reactivity profile of the photoexcited dihydropyridines **14**.

Along this line, the main objective of the present project was to develop a mild catalytic method for the synthesis of amides by exploiting the dual reactivity profile of the excited-state dihydropyridines. Specifically, we wondered if the carbamoyl dihydropyridines (carbamoyl-DHPs **1**), adorned with a carbamoyl moiety at the C4-position, could provide the targeted carbamoyl radicals **I** upon visible-light irradiation (Scheme 4.17.).

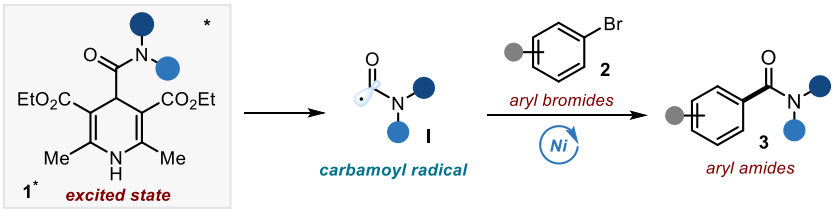

Scheme 4.17. Catalytic amide synthesis that exploits the direct excitation of carbamoyl-DHPs **1.**

Our reaction design is detailed in Scheme 4.18. The selective excitation of a sacrificial amount of carbamoyl-DHP **1** provides the excited-state intermediate **1***. This species would be responsible for the reduction of Ni(II) precatalyst to the active Ni(0) **XXIII** (E^{red} (Ni^{II}/Ni^{0})= –1.13 V vs. SCE in DMF),[34] via two discrete SET events. The resulting radical cation **XXVII** would undergo fragmentation to generate the key carbamoyl radical **I**, which is then intercepted by the Ni(0) complex to afford the Ni(I) intermediate **XXIV**. Subsequent oxidative addition onto the aryl bromide **2** would yield intermediate **XXVIII**, which upon reductive elimination may provide the desired amide product **3**. Finally, the resulting Ni(I) complex **XXVI** would undergo SET reduction by the excited carbamoyl-DHP **1***, thereby completing the nickel catalytic cycle while generating another carbamoyl radical **I**.

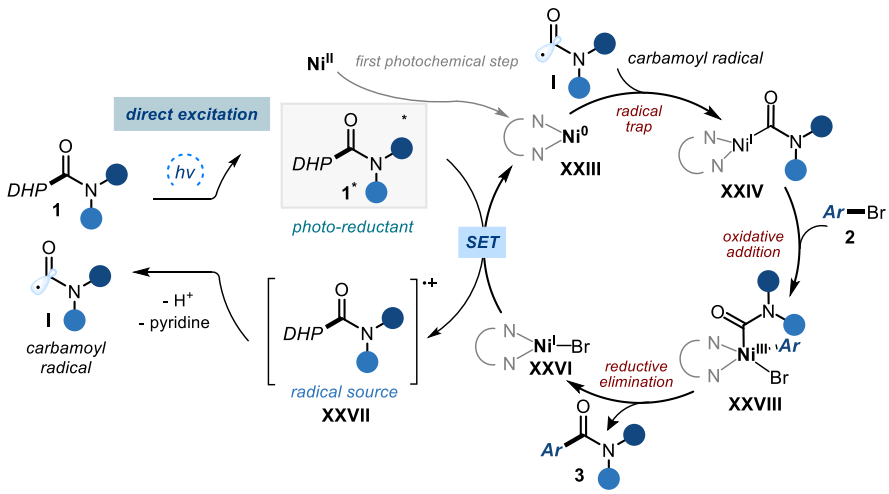

Scheme 4.18. Proposed mechanism of photochemical nickel-catalyzed cross-coupling between aryl bromides **2** and carbamoyl-DHP **1.**

[34] Börjesson, M., Moragas, T., Martin, R., "Ni-Catalyzed Carboxylation of Unactivated Alkyl Chlorides with CO_2", *J. Am. Chem. Soc.* **2016**, *138*, 7504.

4.3. Results and Discussion (I)

4.3.1. Synthesis and Photophysical Characterization of Carbamoyl-DHPs

Our investigation began with the synthesis of the carbamoyl radical precursors **1**. We identified that dihydropyridine derivatives **25** bearing a carboxylic moiety at the C4-position would represent a suitable substrate for further installation of a carbamoyl group (Scheme 4.19a). The bench-stable intermediate **25** can be easily prepared in one step and on multigram scale from cheap and commercially available amino crotonate **23** and glyoxylic acid **24**.[35] Finally, the condensation of **25** with various amines **26** in the presence of stoichiometric amounts of isobutylchloroformate **27** delivers the carbamoyl-DHPs **1** in good to excellent yields (Scheme 4.19b).

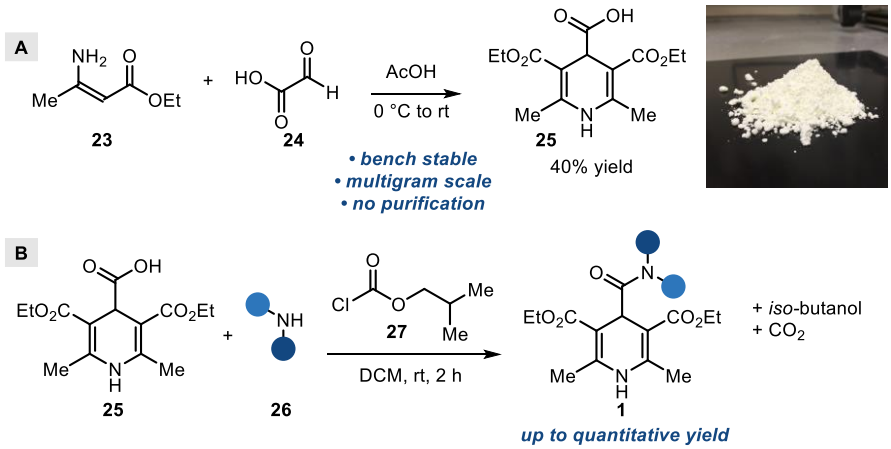

Scheme 4.19. Synthesis of carbamoyl-DHP **1.**

To gain useful insights on the photochemical reactivity of carbamoyl-DHPs, we conducted photophysical characterization of the model substrate **1a**. Firstly, we recorded the UV-visible absorption spectrum of **1a** in CH_3CN and thereby confirmed the ability of **1a** to absorb light in the visible region, until approximately 415 nm (Figure 4.3.).

[35] Dubur, G. Y., Uldrikis, Y. R. "Preparation of 3,5-Diethoxycarbonyl-2,6-Dimethyl-1,4-Dihydro-Isonicotinic Acid and 3,5-Diacetyl-2,6-Dimethyl-1,4-Dihydroisoni-Cotinic Acid and Their Salts", *Chem. Heterocycl. Compd.* **1972**, *5*, 762.

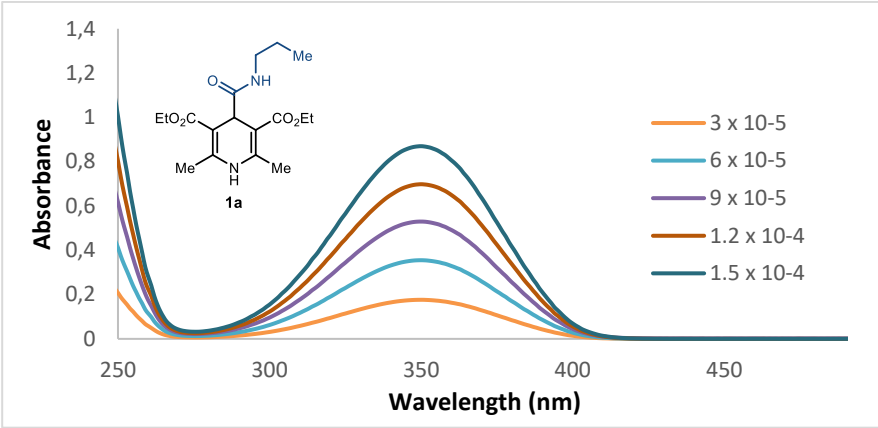

Figure 4.3. Absorption spectrum of **1a** in CH_3CN: λ_{max} = 350 nm. The tail wavelength of absorption was considered as 415 nm.

We then focused on the electrochemical characterization of substrate **1a** (Figure 4.4.). Cyclic voltammetry (CV) measurement revealed and irreversible oxidation peak with $E_p^A = E^{ox}$ (**1a**$^{\bullet+}$/**1a**) = + 1.20 V, which confirmed the propensity of carbamoyl-DHP **1a** towards SET oxidation.

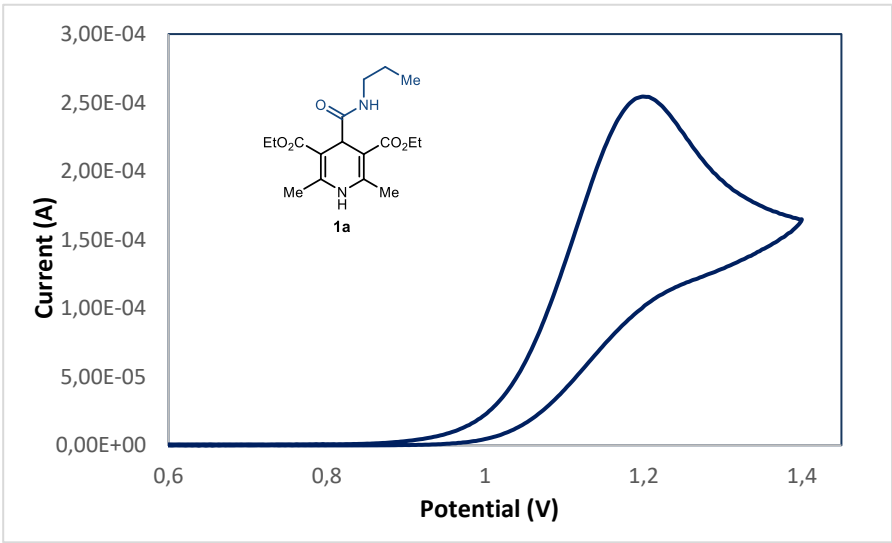

Figure 4.4. Cyclic volmmatogram of carbamoyl dihydriopyridine **1a** [0.02 M] in [0.1 M] $TBAPF_6$ in CH_3CN. Sweep rate: 30 mV/s. Glassy carbon working electrode, Ag/AgCl (satd. KCl) reference electrode, Pt wire auxiliary electrode. Irreversible oxidation. $E_p^A = E_{ox}$ (**1a**$^{\bullet+}$/**1a**) = +1.20 V; E_p^A is the anodic peak potential, while E_{ox} value describes the electrochemical properties of **1a**.

On the basis of the spectroscopic and electrochemical analysis and applying the Rehm-Weller theory,[31] we estimated the reduction potential of the excited carbamoyl-DHP **1a** to be E^{red} (**1a***/**1a**$^{\bullet-}$) = – 1.78 V vs Ag/AgCl. This value confirms that the carbamoyl-DHP is a strong reductant in the excited state.

4.3.2. Optimization of the Reaction Conditions

The feasibility of a nickel-catalyzed carbamoylation of aryl halides using the direct excitation of carbamoyl-DHPs was studied using DHP **1a** and 4-bromobenzotrifluoride **2a** as model substrates. Our first efforts focused on the identification of an optimal nickel precatalyst that could efficiently promote the cross-coupling reaction (Table 1). The screening of optimal conditions was carried out at ambient temperature, under irradiation of a violet high-power single LED (λ_{max} = 405 nm, full detail on the reaction set-up is described in the experimental section), using bipyridine as a ligand and in a 5:1 mixture of CH_3CN/*iso*-propanol (0.3 M). The presence of *iso*-propanol helped to solubilize the poorly soluble carbamoyl-DHP substrate **1a**. As summarized in Table 4.1., good yield of the target amide product **3a** was obtained when using $NiBr_2$ as the catalyst (entry 3). Other nickel sources promoted the cross-coupling reaction with lower yields (entries 1-2, 4).

Table 4.1. Screening of different nickel source.

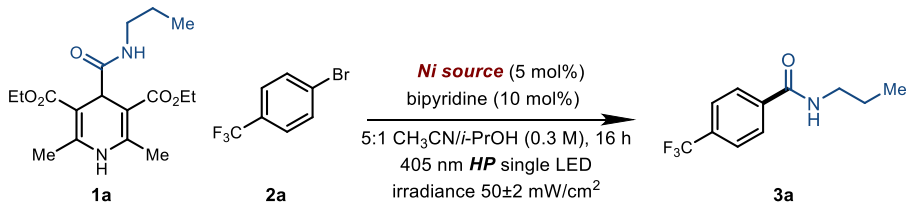

entry	Nickel source	yield (%)[a]
1	$NiCl_2$ glyme	30%
2	$NiBr_2$ glyme	36%
3	$NiBr_2$	61%
4	$NiCl_2$	45%

Reactions performed on a 0.1 mmol scale using 1.5 equiv. of **1a** under illumination by a single high-power (HP) LED (λ_{max} = 405 nm). [a] Yield of **3a** determined by ^{1}H NMR analysis of the crude mixture using trichloroethylene as the internal standard.

We then evaluated different ligands that could boost the catalytic efficiency of $NiBr_2$. Previously reported photoredox protocols for nickel cross-coupling reactions[20] suggested us to use nitrogen-based ligands (Figure 4.5.). Both bipyridine- and phenanthroline-based ligands could promote the formation of the amide product **3a**. However, the presence of

substituents *ortho* to the nitrogen did have a negative impact on the reactivity, as no desired product was observed using ligands **L5** and **L7**.

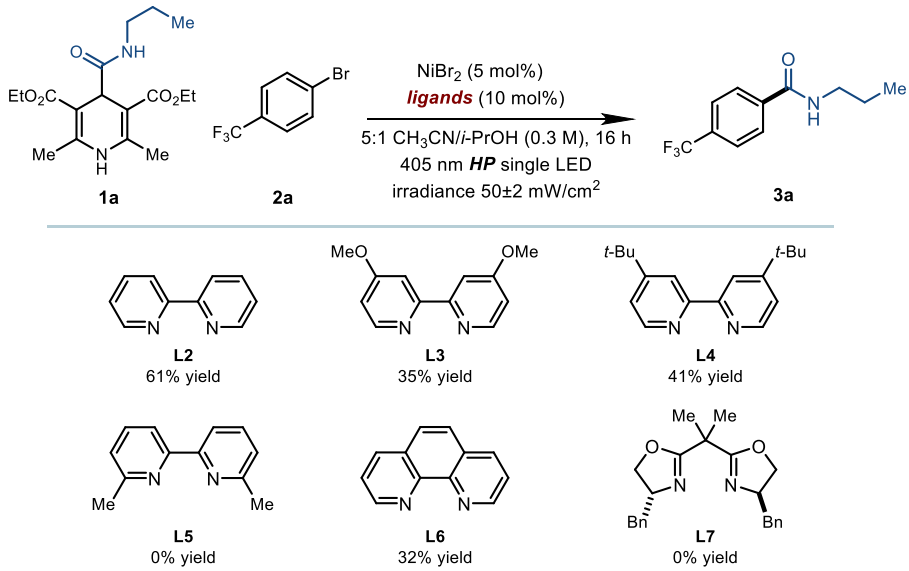

Figure 4.5. Screening of different nitrogen-based ligands. Reactions performed on a 0.1 mmol scale using 1.5 equiv. of **1a** under illumination by a single high-power (HP) LED (λ_{max} = 405 nm). [a] Yield of **3a** determined by ^{1}H NMR analysis using trichloroethylene as the internal standard.

During these experiments, and despite the moderate yield of cross-coupling product, we always noticed the full consumption of substrate **1a** to the pyridine side products **5** and **27** (Figure 4.6.). Side-product (**27**) arose from the aromatization of carbamoyl-DHP **1a**, which hindered the generation of carbamoyl radicals while affecting the efficiency of the reaction.

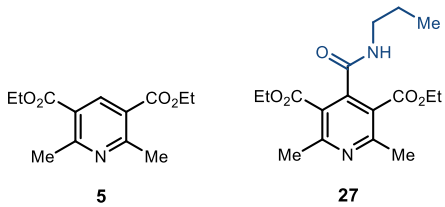

Figure 4.6. Side-products formed upon direct excitation of carbamoyl-DHP **1a**.

Unfortunately, after extensive screening of further reaction parameters, including additives and solvents, we could not improve the yield of product **3a** and circumvent the formation of the undesired side-product **27**. Nevertheless, we wanted to demonstrate that the present photochemical catalytic method could couple different carbamoyl-DHPs with electron-poor aryl bromides.

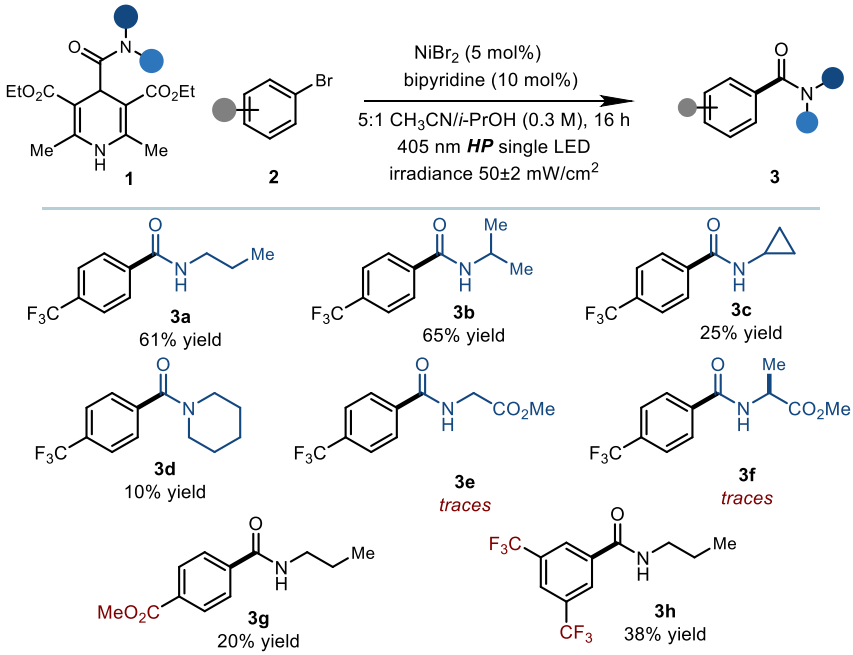

Table 4.2. Photochemical Ni-catalyzed cross-coupling between carbamoyl-DHP **1** with aryl bromides **2**. Reactions performed on a 0.1 mmol scale using 1.5 equiv. of **1** under illumination by a single high-power (HP) LED (λ_{max} = 405 nm). Yield of **3** determined by ^{1}H NMR analysis of the crude mixture using trichloroethylene as internal standard.

As depicted in Table 4.2., carbamoyl-DHP bearing *iso*-propyl and cyclopropyl groups could be used, delivering the secondary amides **3b** and **3c** in 65% and 25% yield, respectively. Tertiary amide **3d** could also be prepared, albeit in poor yield. As for the scope of aryl bromides, methyl 4-bromobenzoate and 3,5-bis(trifluoromethyl)bromobenzene afforded the corresponding amides **3g** and **3h** in 20% and 38% yield, respectively. When we used carbamoyl-DHPs bearing amino acidic residue such as glycine and (L)-alanine (adducts **3e** and **3f,** respectively), only traces amount of products were observed. In both cases, the corresponding carbamoyl-DHP did not convert to the pyridines, despite exhibiting similar absorption spectra to carbamoyl-DHP **1a** (Experimental section 4.12.7).

With the aim to develop an efficient and general protocol for catalytic amide synthesis, we surmised that the use of an external photocatalyst could efficiently deliver the desired carbamoyl radicals from carbamoyl-DHPs, avoiding the unproductive consumption of the substrates. This could significantly broaden the scope and the synthetic utility of our carbamoylation protocol. The next section provides a brief overview of the synthetic potential of combining nickel and photoredox catalysis.

4.4. The Merger of Nickel Catalysis with Photoredox Catalysis

Transition-metal-mediated cross-coupling methodologies are valuable tools for C(sp^2)–C(sp^2) and C(sp^2)–heteroatom bond formation.[36] The more electropositive character of Ni compared to Pd allows for the relative facile oxidative addition to less reactive starting materials, such as C–O and C–N electrophiles. Although Ni-catalyzed transformations based on Ni(0)/Ni(II) catalytic cycles are widespread, the easily accessible Ni(I)/Ni(III) manifold is well-suited to facilitate SET process and radical-based mechanisms.

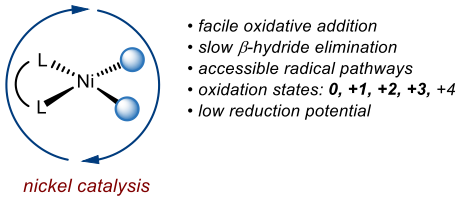

Figure 4.7. Properties of nickel for the development of cross-coupling reactions.

The ability of Ni catalysts to trigger radical pathways has been recently exploited in combination with photoredox catalysis to enable generally inaccessible cross-coupling processes.[37] Photoredox catalysis provides mild access to reactive radicals from simple precursors through SET pathways and, at the same time, facilitates Ni-catalyzed transformations by modulating the oxidation state of the transition metal.[38] These methods can efficiently activate non-traditional nucleophiles thus expanding the toolbox of coupling partners available to nickel-catalyzed cross-coupling protocols.

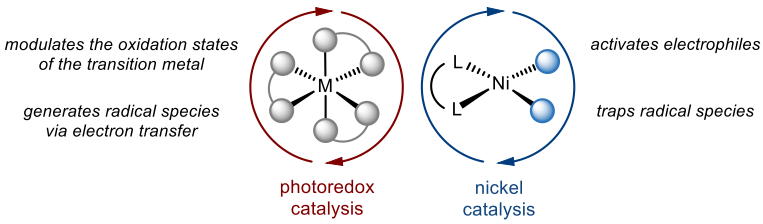

Figure 4.8. Combination of photoredox and nickel catalysis enables the development of new cross-coupling transformations.

[36] De Meijere, A. & Diederich, F., "Metal-Catalyzed Cross-Coupling Reactions", Wiley-VCH, Weinheim, **2004**.
[37] Twilton, J., Le, C., Zhang, P., Shaw, M. H., Evans, R., W., MacMillan, D. W. C., "The Merger of Transition Metal and Photocatalysis", *Nat. Rev. Chem.* **2017**, *1*, 0052.
[38] Murphy, J. J., Melchiorre, P., "Light Opens Pathways for Nickel Catalysis", *Nature*, **2015**, *524*, 297.

The field of nickel/photoredox catalysis began in 2014 with two independent works published by Molander[39] and MacMillan and Doyle.[40] The first report showed that an iridium-based photocatalyst in combination with nickel catalysis could trigger the direct coupling of aryl halides with alkyl trifluoroborate salts (Scheme 4.20.). Despite the wide use of organotrifluoroborates in classical Suzuki-Miyaura cross-coupling reactions for the formation of C(sp^2)–C(sp^2) bonds, the slow rate of transmetallation of alkyl trifluoroborate salts hampered the development of C(sp^3)–fragment coupling protocols. The Molander laboratory showed that this long-standing challenge could be addressed using a radical approach, in particular through the generation of carbon-centered radicals *via* SET oxidation of the corresponding alkyl trifluoroborate salts **28** by the photoexcited iridium catalyst.[41] Concurrently, Ni(0) complex **VIII** can undergo oxidative addition with an aryl halide **2** to form a Ni(II) complex **XXXI**, which subsequently traps the alkyl radical **XVIII** to deliver the Ni(III) complex **XXXII**. Rapid reductive elimination forges the C(sp^3)–C(sp^2) bond in the desired product **29** and the Ni(I) compex **XI**. SET reduction of complex **XI** by the reduced photocatalyst Ir(III) generates both the Ni(0) species **VIII** and the Ir photocatalyst in the original oxidation state, thus closing both catalytic cycles.

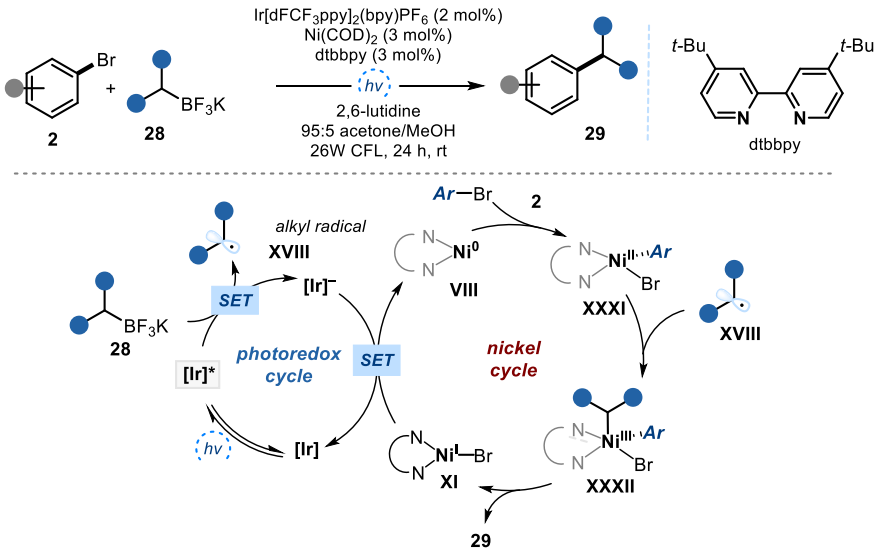

Scheme 4.20. Ni/photoredox-catalyzed cross-coupling reaction between benzyltrifluoroborate salts 28 and aryl bromides for the formation of C(sp^2)–C(sp^3) bonds.

[39] Tellis, J. C., Primer, D. N., Molander, G. A., "Single-Electron Transmetalation in Organoboron Cross-Coupling by Photoredox/Nickel Dual Catalysis", *Science* **2014**, *345*, 433.
[40] Zuo, Z., Ahneman, D. T., Chu, L., Terrett, J., Doyle, A. G., MacMillan, D. W. C., "Merging Photoredox with Nickel Catalysis: Coupling of α-Carboxyl Sp^3-Carbons with Aryl Halides", *Science* **2014**, *345*, 437.
[41] a) Primer, D. N., Karakaya, I., Tellis, J. C., Molander, G. A., "Single-Electron Transmetalation: An Enabling Technology for Secondary Alkylboron Cross-Coupling", *J. Am. Chem. Soc.* **2015**, *137*, 2195. b) Karakaya, I., Primer, D. N., Molander, G. A., "Photoredox Cross-Coupling: Ir/Ni Dual Catalysis fort he Synthesis of Benzylic Ethers", *Org. Let.*.**2015**, *17*, 3294.

In a conceptually similar approach, MacMillan and Doyle developed a cross-coupling protocol that used α-alkoxy and α-amino carboxylic acids as radical precursors (Scheme 4.21a).[40] Also in this reaction the combination of a nickel catalyst and an iridium-based photocatalyst was crucial for a successful cross-coupling transformation. In addition to metal-based photocatalysts, organic photoredox catalysts could also be used in the dual Ni/photoredox-catalyzed protocols.

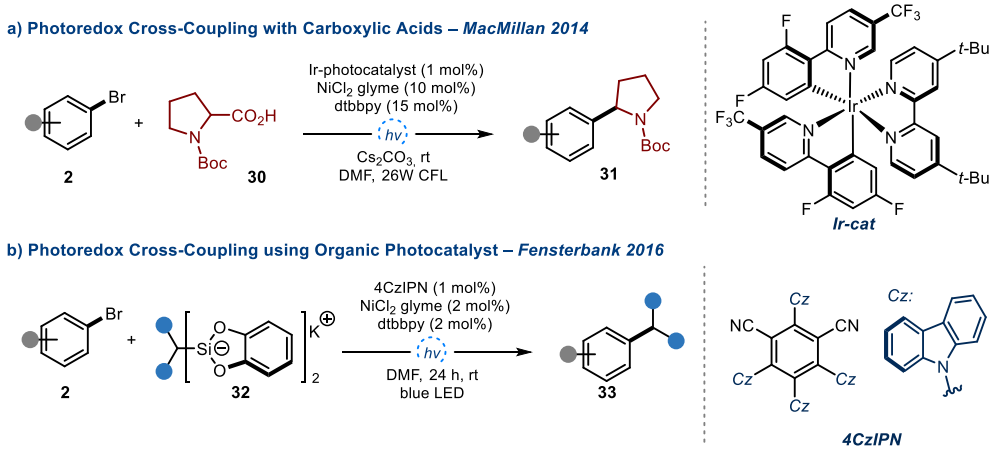

Scheme 4.21. Ni/photoredox-catalyzed cross-coupling methods using a) an iridium-based photocatalyst and carboxylic acids as radical precursors; b) an organic dye as the photocatalyst and alkylsilicates as radical precursors.

The group of Fensterbank reported that the combination of nickel and 1,2,3,5-tetrakis-(carbazole-yl-)-4,6-dicyanobenzene (4CzIPN) organic dye can facilitate the C(sp^3)–C(sp^2) bond formation (Scheme 4.21b).[42] The method uses alkyl bis(catecholato)silicates as radical precursors and couples a broad range of aryl bromides and alkyl silicates.

The mild nature of these protocols, which could be conducted at ambient temperature, enabled their application for the functionalization of molecules containing polar and heterocyclic moieties, which are often encountered in drug discovery research. Therefore, it is not surprising that this technology has been rapidly adopted by the pharmaceutical industry.[43] For instance, Knauber and co-workers at Pfizer combined nickel catalysis and ruthenium-based photocatalysis to install an alkyl fragment onto (hetero)aryl bromides (Scheme 4.22.).[44] In

[42] Lévêque, C., Chenneberg, L., Corcé, V., Ollivier, C., Fensterbank, L., "Organic Photoredox Catalysis for the Oxidation of Silicates: Applications in Radical Synthesis and Dual Catalysis", *Chem. Commun.* **2016**, *52*, 9877.
[43] Blakemore, D. C., Castro, L., Churcher, I., Rees, D. C., Thomas, A. W., Wilson, D., M., Wood, A., "Organic Synthesis Provides Opportunities to Transfor Drug Discovery", *Nat. Chem.* **2018**, *10*, 383.
[44] Thomas Knauber et al., "Ru/Ni Dual Catalytic Desulfinative Photoredox C(sp^2)–C(sp^3) Cross-Coupling of Alkyl Sulfinate Salts and Aryl Halides", *Org. Lett.* **2017**, *19*, 6566.

this transformation, alkyl sulfinate salts **35** are used as radical precursors due to their low oxidation potentials. The developed method has been applied to parallel medicinal chemistry protocols where a series of casein kinase 1δ inhibitor analogs **36** have been synthesized by reacting the advanced aryl bromide intermediate **34** with various alkyl sulfinate salts **35**.

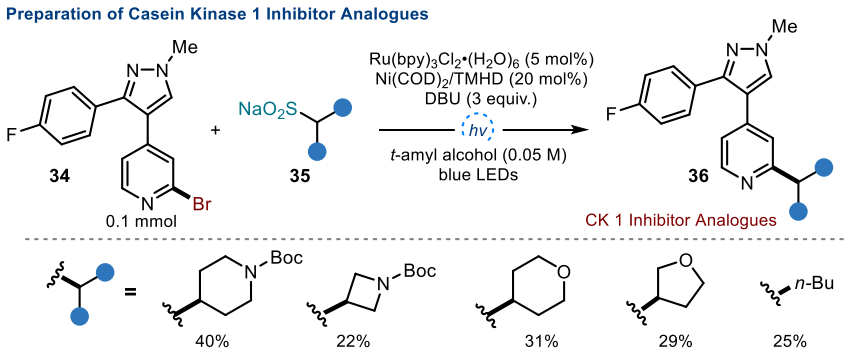

Scheme 4.22. The Preparation of Casein Kinase inhibitor analogues enabled by the combination of nickel and photoredox catalysis.

4.5. Design and Target of the Project (II)

In the previous section (Chapter 4.3.2.), we demonstrated that dihydropyridines can release carbamoyl radicals upon direct light excitation and engage in nickel-catalyzed radical cross-coupling reaction to access aryl amides. However, reactivity issues were encountered during the study of the scope for the transformation. Nevertheless, these results encouraged us to pursue other routes to efficiently access a wide array of amides under mild conditions. We envisaged that the use of an external photoredox catalyst in combination with a nickel catalyst could enable the carbamoylation of aryl bromides and overcome the limitation encountered in the previous attempts (Scheme 4.23.).

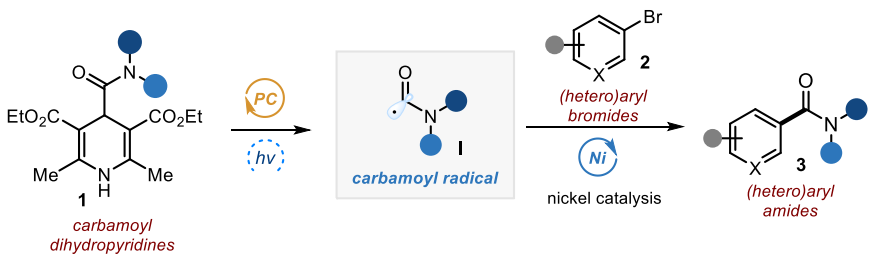

Scheme 4.23. Design of the dual nickel/photoredox-catalyzed carbamoylation of aryl halides.

In particular, we aimed to exploit the ground-state reactivity of carbamoyl-DHPs **1** to generate carbamoyl radicals **I** upon SET oxidation by visible-light activated photoredox catalyst. In agreement with previous studies, the success of this approach would rely on the ability of Ni(0) complexes to undergo oxidative addition to aryl bromides **2** while engaging in radical capture mechanisms. The resulting Ni(III) complex would undergo reductive elimination to afford the desired cross-coupled amide product **3**. More importantly, we reasoned that the use of an external photoredox catalyst, which could selectively absorb light in regions where the carbamoyl-DHP **1** could not (λ = 460 nm), could preclude the degradation of the substrates arising from their direct excitation (see Figure 4.6. for details).

4.6. Results and Discussion (II)

4.6.1. Optimization Studies

In Chapter 4.3.2., we demonstrated that several carbamoyl-DHPs can deliver carbamoyl radicals upon light excitation and can couple with electron-poor aryl bromide to obtain aryl amides. However, carbamoyl-DHPs bearing amino acidic moiety remain unreactive and gave very low conversion. Therefore, with the aim of developing a general approach for amide synthesis, we conducted the optimization study using the carbamoyl-DHP substrate **1-ala**, bearing an (L)-alanine residue, and 4-bromobenzotrifluoride **2a** (Scheme 4.24.). Initial experiments were conducted at ambient temperature, in CH_3CN, in the presence of an organic photocatalyst **4CzIPN**, $NiCl_2$ glyme and bipyridine (bpy) as the ligand, and under irradiation of a single high-power (HP) blue LED (λ_{max} = 460 nm).

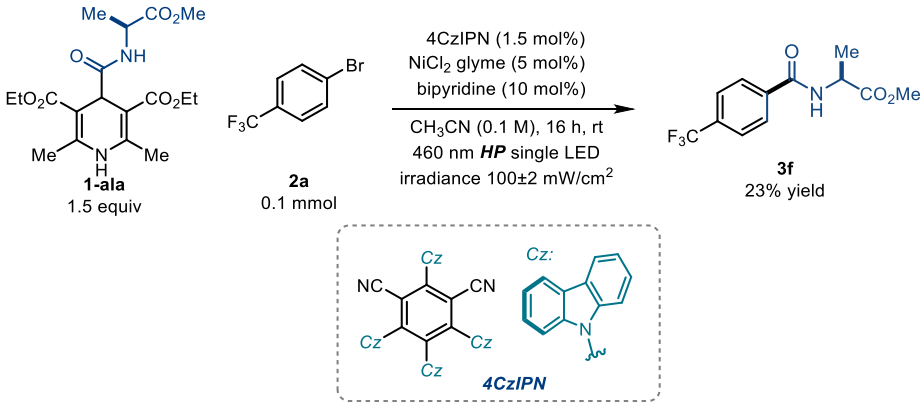

Scheme 4.24. Preliminary attempt of Ni/photoredox-catalyzed carbamoylation of aryl bromide **2a**.

The choice of the photocatalyst 4CzIPN was based on its redox properties, since the given value for the oxidative potential of the photoexcited 4CzIPN ($E_{1/2}$ (**4CzIPN***/**4CzIPN**$^-$) =

+1.43 V vs SCE)[45] is high enough to take an electron from the carbamoyl-DHP radical precursor (E_{red}(**1-ala**$^{\bullet+}$/**1-ala**) = + 1.39 V vs Ag/Ag$^+$ in CH_3CN). After 16 hours of irradiation, the reaction furnished the desired amide product **3f**, albeit in a moderate yield of 23%. Also in this case, we observed complete conversion of the substrate **1-ala** to the pyridine **5** and the undesired side product **37**, which arises from the aromatization of DHP **1-ala** (Figure 4.9.).

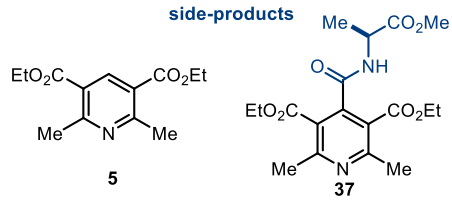

Figure 4.9. Major side-products of Ni/photoredox-catalyzed carbamoylation reaction with carbamoyl-DHP **1-ala.**

Nevertheless, this preliminary result encouraged us to investigate further reaction parameters, starting with the screening of different ligands.

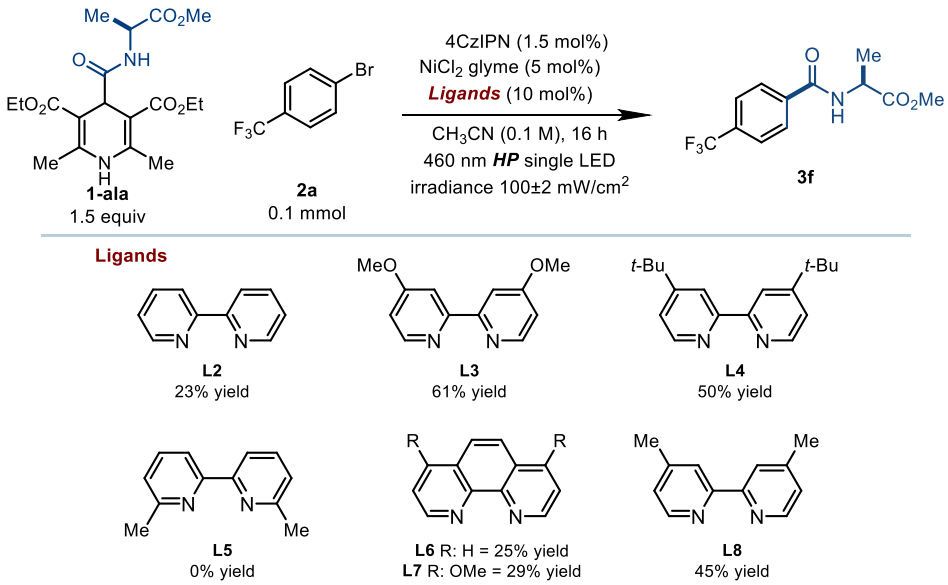

Figure 4.10. Reactions performed on a 0.1 mmol scale using 1.5 equiv. of **1-ala** under illumination by a single high-power (HP) LED (λ_{max} = 460nm). [a] Yield of the 3f determined by ^{1}H NMR analysis using trichloroethylene as internal standard.

[45] Speckmeier, E., Fischer, T. G., Zeitler, K., "A Toolbox Approach To Construct Broadly Applicable Metal-Free Catalysts for Photoredox Chemistry: Deliberate Tuning of Redox Potentials and Importance of Halogens in Donor–Acceptor Cyanoarenes", *J. Am. Chem. Soc.* **2018**, *140*, 15353.

As summarized in Figure 4.10, both bipyridine and phenanthroline-based ligands are competent for the transformation. Importantly, the presence of *para*-substituents on the ligands led to higher yields of the desired product (ligands **L3**, **L4** and **L8**). *Ortho*-substituted bipyridine ligands completely inhibited the transformation (**L5**), a trend which was already observed in the study discussed in Section 4.5.2. Finally, 4-4'-dimethoxy-2-2'-bipyridine (dMeObpy, **L3**) was identified as the optimal ligand.

Next, the influence of different solvents on the reaction outcome was investigated. As shown in Table 4.3., reactions in other solvents showed no improvement in terms of yields. Interestingly, despite providing the amide product in lower yield, ethereal solvents such as tetrahydrofuran (THF) or 1,4-dioxane produce only trace amounts of the side-product **40** (entries 1 and 5). A significant improvement was observed when conducting the reaction in THF and in the presence of an additive. The combination of this solvent and Na_2CO_3 was crucial to achieve high yields of the desired amide **3f** while decreasing side-product formation (entry 8). Finally, lowering the concentration of the reaction led to a clean reaction crude and quantitative yield of the desired cross-coupled product (entry 9).

Table 4.3. Screening with various solvents and additives.

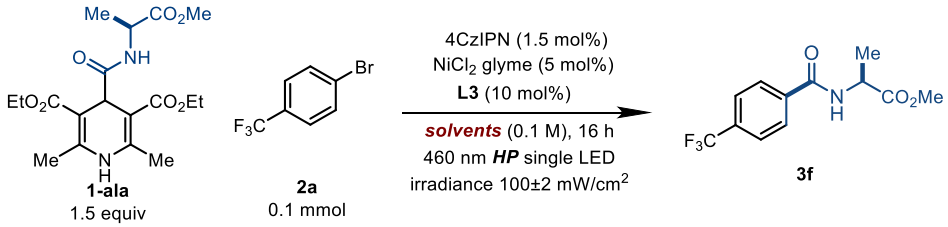

entry	solvents	additives	yield (%)[a]
1	Tetrahydrofuran (THF)	-	34
2	Acetonitrile	-	61
3	Acetone	-	34
4	DMF	-	32
5	1,4-dioxane	-	10
6	THF	2,6-Lutidine	38
7	THF	Na_2CO_3	95
8	THF (0.05 M)	Na_2CO_3	99

Reactions performed on a 0.1 mmol scale using 1.5 equiv. of **1-ala** under illumination by a single high-power (HP) LED (λ_{max} = 460nm). [a] Yield of the 3f determined by ^{1}H NMR analysis of the crude mixture using trichloroethylene as the internal standard. [b] Reactions performed in 0.05 M of the corresponding solvents.

Additionally, the reaction proceeds also in "industrially preferred" solvents (ethyl acetate (EtOAc) and acetone (Table 4.6., entries 3 and 4 respectively)), offering a good versatility to

avoid potential substrate solubility issues.[46] As a proof of the method's robustness, the reaction could be performed without degassing the solvent (entry 5) and in the presence of water (entry 6), which only marginally affected the efficiency of the process.[47] Control experiments showed that the reaction could not proceed in the absence of light, photocatalyst, or nickel catalyst (entry 7).

Importantly, as testament of the mild conditions of the system, we confirmed that no racemization of the enantiopure alanine scaffold occurred during the process.

Table 4.4. Screening of different conditions.

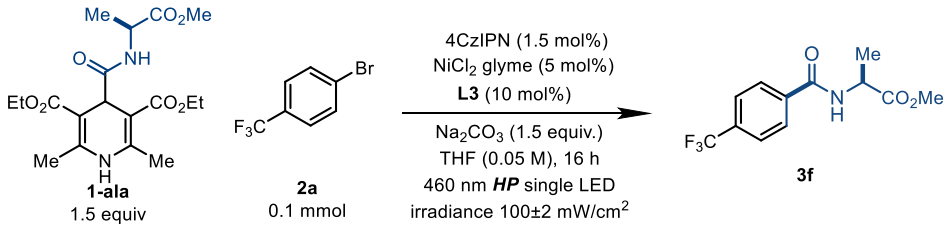

entry	Deviation from standard conditions	yield (%)[a]
1	none	99
2	1,4-dioxane instead of THF	99
3	EtOAc instead of THF	55
4	acetone instead of THF	33
5	Non-degassed THF	90
6	H_2O (10 equiv.)	87
7	No 4CzIPN, nickel or light	0

Reactions performed on a 0.1 mmol scale using 1.5 equiv. of **1-ala** under illumination by a single high-power (HP) LED (λ_{max} = 460nm). [a] Yield of 3f determined by ^{1}H NMR analysis using trichloroethylene as internal standard.

4.6.2. Scope of the Aryl and Heteroaryl Bromides[48]

The generality of the carbamoylation method was studied by applying the optimized reaction conditions (Table 4.6., entry 1) to an array of aryl bromides **2** and carbamoyl-DHPs **1** (Table

[46] Prat, D., Wells, A., Hayler, J., Sneddon, H., McElroy, C. R., Abou-Shehada, S., Dunn, P. J., "CHEM21 Selection Guide of Classical- and Less Classical-Solvents", *Green Chem.* **2016**, *18*, 288.
[47] Oderinde, M. S., Varela-Alvarez, A., Aquila, B., Robbins, D. W., Johannes, J. W., "Effects of Molecular Oxygen, Solvent and Light on Iridum-Photoredox/Nickel Dual-Catalyzed Cross-Coupling Reactions", *J. Org. Chem.* **2015**, *80,* 7642.
[48] The evaluation of the reaction scope was conducted with feedback from the collaborators in *Bayer AG*. The main aim was to prove the compatibility of the method with polar functional groups and pharmaceutically relevant scaffolds.

4.5.). The transformation allowed for the carbamoylation of a wide array of aryl bromides with L-alanine derived DHP **1-ala** and tolerated unprotected polar functional groups.

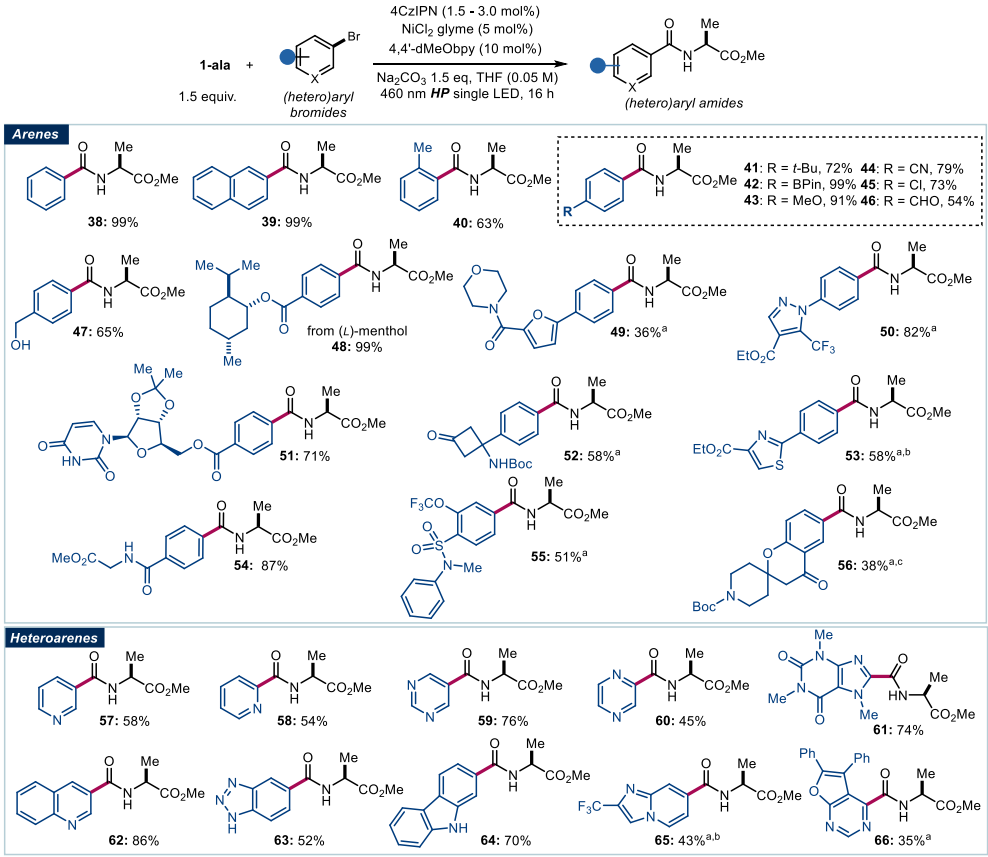

Table 4.5. Scope of (hetero)aryl bromides. Reactions performed on 0.1 mmol scale at ambient temperature for 16 h under illumination by a single blue LED (λ_{max} = 460 nm) and using dihydropyridines (1.5 equiv.), Na_2CO_3 (1.5 equiv.) in THF (0.05M). Yields of products refer to isolated material after purification (average of two runs per substrate). [a] Performed in 1,4-dioxane (0.05 M) using 3 mol% of the photocatalyst. [b] 0.2 mmol scale. [c] 0.2 mmol scale in 1,4-dioxane (0.025 M). Boc: *tert*-butyloxycarbonyl.

High yields were achieved with bromobenzene and bromonaphthalene (products **38** and **39**). An aryl bromide bearing an *ortho*-substituent was well-tolerated (**40**). The ability to tolerate aryl boronates (**42**) and chlorides (**45**) demonstrated that the protocol is orthogonal to classical metal-catalyzed cross-coupling reactions and allows further functionalization. We next evaluated the compatibility with unprotected polar functional groups, which is an important criterion for assessing a method's applicability for complex molecule synthesis and drug discovery.[42,49] Aryl bromides bearing sensitive functional groups such as aldehydes (**46**),

[49] Pitt, W. R., Parry, D. M., Perry, B. G., Groom, C. R., "Heteroaromatic Rings for the Future", *J. Med. Chem.,* **2009**, *52*, 2952.

unprotected alcohols (**47**), Boc-protected amines (**52** and **56**), amides (**49** and **54**) and sulfonamide moieties (**58**) underwent the reaction smoothly.

The carbamoylation method showed a good level of tolerance towards heterocyclic substituents containing oxygen (**49** and **56**), nitrogen (**49**-**51**), and sulfur atoms (**53** and **55**). Functionalized aryl bromides bearing L-menthol, *2'*,*3'*-*O*-isopropylideneuridine (**54**), and glycine were tolerated (**57**), highlighting the method's potential for complex molecule functionalization.

Given the prevalence of nitrogen-containing heterocycles in biologically active molecules, we then evaluated the possibility of hetero(aryl) bromides to undergo carbamoylation process. Pyridines (**57**-**58**), pyrimidines (**59**), pyrazine (**60**), quinoline (**62**), benzotriazole (**63**), imidazo[12-*a*]pyridine (**65**), imidazole in caffeine (**61**), and furo[2,3-*d*]pyrimidine (**66**) could all be functionalized. The protocol also provides a direct approach to carbamoylated carbazole (**64**), which would be difficult to access through conventional amidation methods because the carboxylic acid precursors are not readily available.

4.6.3. Scope of the Dihydropyridines

The evaluation of the carbamoyl-DHPs amenable to this protocol was performed using 4-bromobenzotrifluoride **2a** as the coupling partner. We first focused on DHPs bearing amino acidic residues other than L-alanine. Glycine (product **67**), (L)-phenylalanine (**68**) and (L)-valine (**69**) could be installed in the amide products in excellent yields. The presence of free alcohols within (L)-serine (**70**) and (L)-tyrosine (**71**) and of an unprotected nitrogen in (L)-tryptophan (**72**) was well tolerated. The reaction also proceeded efficiently when using the methionine-derived dihydropyridine, affording amide **73** bearing *S*-methyl thioether group. Peptides are generally considered poor drug candidates because of their low oral bioavailability. However, modifications, including *N*-terminal-capping, can improve their stability and bioavailability. This carbamoylation method provided the *N*-aroyl capped dipeptide **74** in high yield.

Further evaluation of the dihydropyridines revealed that a variety of *N*-alkyl carbamoyl groups could be tolerated, delivering secondary amides including the drug molecule moclobemide (**85**), in moderate to high yields. An aniline-containing carbamoyl group could be installed, although an electron-rich aryl bromide was required to secure high reactivity (**86**). Tertiary amides bearing morpholines (**88**), piperidines (**89**), pyrrolidines (**90**) and piperazines (**91**) were obtained in good yields, while the acyclic tertiary amides were achieved in moderate yields (**92**-**93**). These results suggest that our protocol can complement amide formation strategies based on isocyanates, as they are limited to the synthesis of primary and secondary amides.

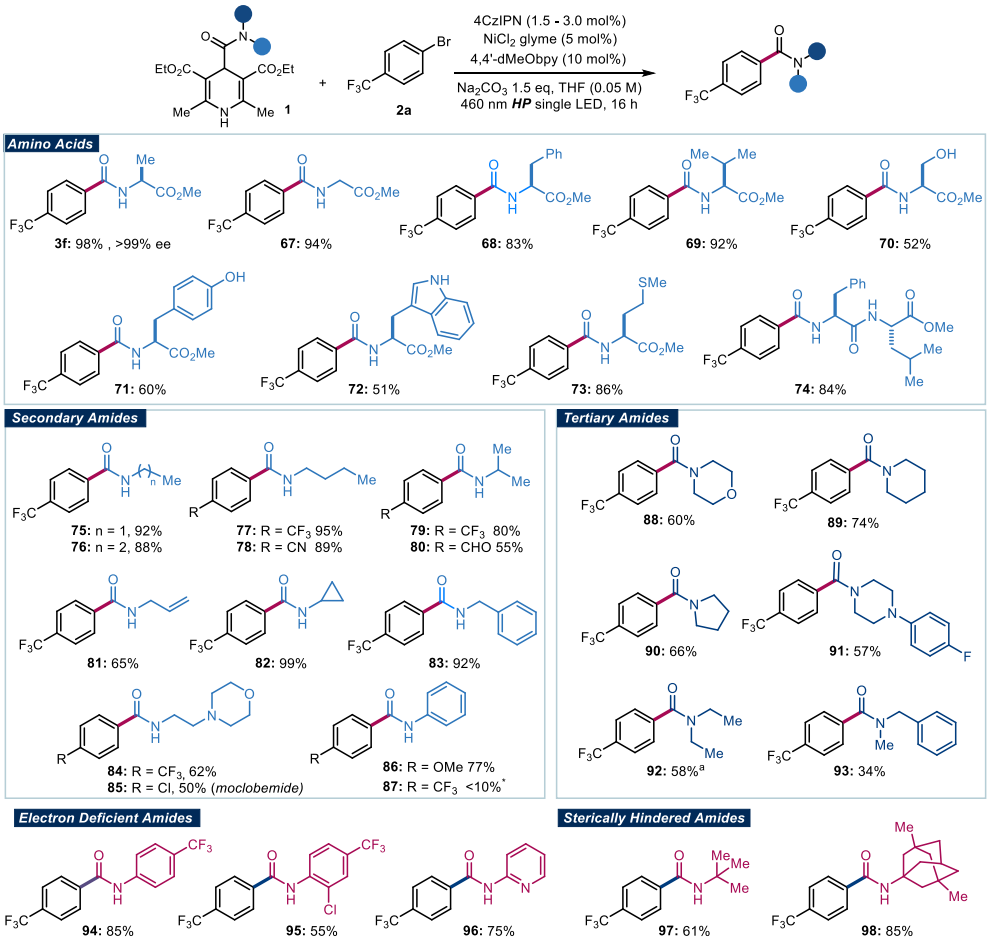

Table 4.6. Scope of carbamoyl radical precursors. Reactions performed on 0.1 mmol scale at ambient temperature for 16 h under illumination by a single blue LED (λ_{max} = 460 nm) and using dihydropyridines (1.5 equiv.), Na_2CO_3 (1.5 equiv.) in THF (0.05 M). Yields of products refer to isolated material after purification (average of two runs per substrate). [a] Performed in 1,4-dioxane (0.05 M).

Finally, we evaluated the possibility of installing amide functionalities bearing either sterically hindered or electron-poor amine moieties. Both amides bearing electron-poor anilines or pyridines (**94-96**), and hindered fragments (**97-98**) could all be efficiently prepared using this dual catalytic approach.

4.6.4. Scale-Up of Nickel/Photoredox-Catalyzed Carbamoylation Reaction

We then focused on the scalability of this protocol. Challenges in performing photoredox reactions in large scale are often associated with the decreased irradiation efficiency.[50] In principle, when using large batch reactors, light penetration is limited to the outer layer of the reaction mixture, which often leads to extended irradiation times. Moreover, overirradiation of the reaction mixture often leads to increased formation of byproducts.

Our collaborators in *Bayer AG* has recently developed a straightforward approach for the scale-up of nickel/photoredox-catalyzed cross-coupling reactions using an immersion-well (IW) batch reactor (Figure 4.11.).[51] These reactors consist of reaction vessels fitted with an immersion well that contains the light source. The efficiency of such reactor is relatively high since the light source is effectively surrounded by the reaction mixture. The IW reactors can be placed on a magnetic stirrer plate and equipped with magnetic stir bar. Thus, reactions can be carried out with both homogeneous and heterogeneous reaction mixtures.

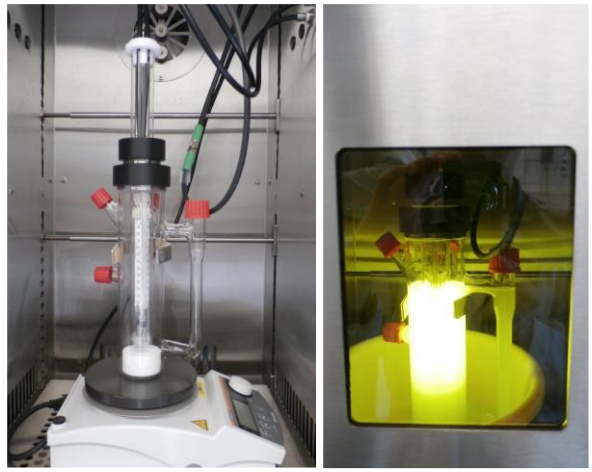

Figure 4.11. Immersion-well photoreactor fitted with 460 nm LED.

With this reaction set-up, we performed the carbamoylation reaction with carbamoyl-DHP **1-ala** and aryl bromide **2a** in 15 mmol scale (Scheme 4.25.). After 4 hours of irradiation, we observed a complete conversion of the substrate **1-ala** and the formation of the cross-coupled product **3f** in 72% yield (≈ 3 gram). Importantly, the scale-up reaction was performed without the need for significant reoptimization.

---

[50] Cambie, D., Bottecchia, C., Straathof, N. J. W., Hessel, V., Noel, T., "Applications of Continuous-Flow Photochemistry in Organic Synthesis, Material Science, and Water Treatment", *Chem. Rev.* **2016**, *116*, 10276.
[51] Grimm, I., Hauer, S., T., Schulte, T., Wycich, G., Collins, K. D., Lovis, K., Candish, L., "Upscaling Photoredox Cross-Coupling Reactions in Batch Using Immersion-Well Reactors", *Org. Process. Res. Dev.* **2020**, DOI: 10.1021/acs.oprd.0c00070.

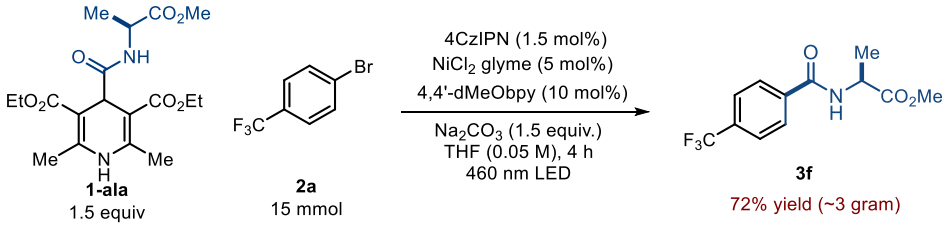

Scheme 4.25. Scale up of the model reaction to 15 mmol scale using an immersion-well reactor.

4.6.5. Limitations of the Developed Carbamoylation Approach

Figure 4.12. shows a list of carbamoyl-DHPs and aryl bromides that failed to afford the desired amide products. In the case of DHPs **1b** and **1c**, we observed conversion to the corresponding Hantzsch pyridines, however, no cross-coupled products were obtained. Unfortunately, the radical precursor **1d** bearing a free acidic moiety provided only traces of the coupling product. Aryl halides bearing bulky substituents in the *ortho* position (**2b-c**) failed to give the desired product, possibly due to steric hindrance.

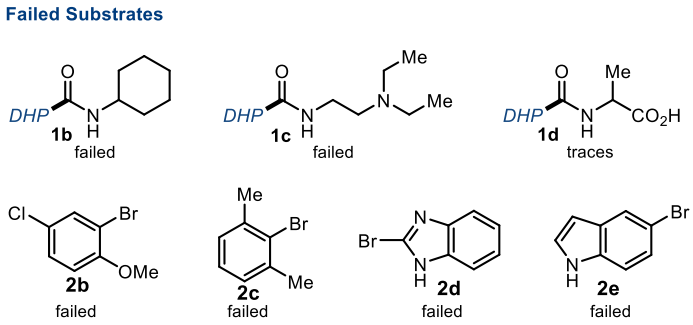

Figure 4.12. Substrate that failed to react under the reaction conditions.

4.7. Proposed Mechanism

The proposed mechanism for the nickel/photoredox-catalyzed carbamoylation process is depicted in Figure 4.13. The catalytic cycle starts with the excitation of the photocatalyst 4CzIPN (**PC**, $E_{1/2}$ (**PC***/**PC**$^{\bullet-}$) = +1.43 V vs. SCE in CH_3CN), which forms an oxidant strong enough to activate the carbamoyl-DHP **1** (E_{ox} (**1-ala**$^{\bullet+}$/**1-ala**) = +1.39 V vs. Ag/Ag+ in CH_3CN)[44] through an SET oxidation. The resulting radical cation **1**$^{\bullet+}$ would then fragment to generate a carbamoyl radical **I** and the corresponding pyridine. Simultaneously, the Ni(0) complex **VIII** undergoes oxidative addition with aryl bromide **2** affording the Ni(II) complex **XXXI**, which then intercepts the nucleophilic carbamoyl radical **I**, leading to the Ni(III)

intermediate **XXIX**. Reductive elimination provides the cross-coupling amide product **3** and Ni(I) species **XI**. The latter complex (E_{red} [Ni(I)/Ni(0)] ≈ –1.13 V vs Ag/Ag^+ in DMF)[32] undergoes an SET reduction by the reduced form of the 4CzIPN photocatalyst ($E_{1/2}$ (**4CzIPN**/**4CzIPN**$^{\bullet-}$) = -1.24 V vs. SCE in CH_3CN),[44] completing the catalytic cycle while generating both active catalysts.

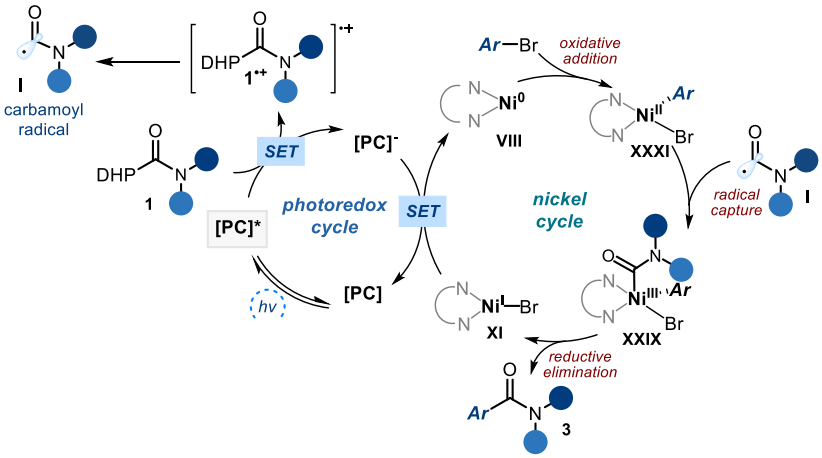

Figure 4.13. Proposed mechanism of Ni/photoredox-catalyzed carbamoylation of aryl bromides.

4.8. Attempts to Extend the Scope of the Carbamoylation Strategy

After demonstrating that the combination of photoredox and nickel catalysis can facilitate the direct carbamoylation of aryl bromides, we wondered whether the developed methodology could be applied to unactivated alkyl bromides. The cross-coupling reactions of alkyl halides is difficult because of their reluctance to undergo oxidative addition and the propensity of in-situ generated alkyl metal species for β-hydride elimination, homodimerization or protonation.[52] Recently, the right choice of catalytic systems and ligands enabled the use of alkyl bromides in cross-coupling transformations,[53] including metallaphotoredox transformations.[54]

Encouraged by the literature precedents, we evaluated the reactivity of alkyl bromides in the developed carbamoylation protocol (Scheme 4.26.). The reaction of ethyl 4-bromobutyrate

[52] Jana, R., Pathak, T. P., Sigman, M. S., "Advances in Transition-Metal (Pd, Fe, Ni)-Catalyzed Cross-Coupling Reactions Using Alkyl-organometallics as Reaction Partners", *Chem. Rev.*, **2011**, *111*, 3, 1417.
[53] Choi, J., Fu, G. C., "Transition Metal-Catalyzed Alkyl-Alkyl Bond Formation: Another Dimension in Cross-Coupling Chemistry", *Science* **2017**, *356,* eaaf7230.
[54] Selected examples: a) Johnston, C. P., Smith, R. T., Allmendinger, S., MacMillan, D. W. C., "Metallaphotoredox-Catalysed sp3-sp3 Cross-Coupling of Carboxylic Acids with Alkyl Halides", *Nature,* **2016**, *536*, 322. b) Thullen, S. M., Treacy, S. M., Rovis, T., "Regioselective Alkylative Cross-Coupling of Remote Unactivated C(sp^3)–H Bonds", *J. Am. Chem. Soc.* **2019**, *141*, 14062.

99a with the (L)-alanine-derived **1-ala** provided the corresponding amide product **100a** in 40% yield. Other alkyl bromides exhibited similar reactivities (**100b-c**). Difficulties were encountered during the isolation of the products, since the reaction crudes contained significant amounts of pyridine **37** and dimer **101** side-products. Interestingly, we did not detect side-products arising from β-hydride elimination. In general, these preliminary results highlight the possibility of using alkyl bromides as electrophile in the Ni/photoredox-catalyzed cross-coupling with carbamoyl-DHP. Further studies to develop a more effective protocol are ongoing in our laboratories.

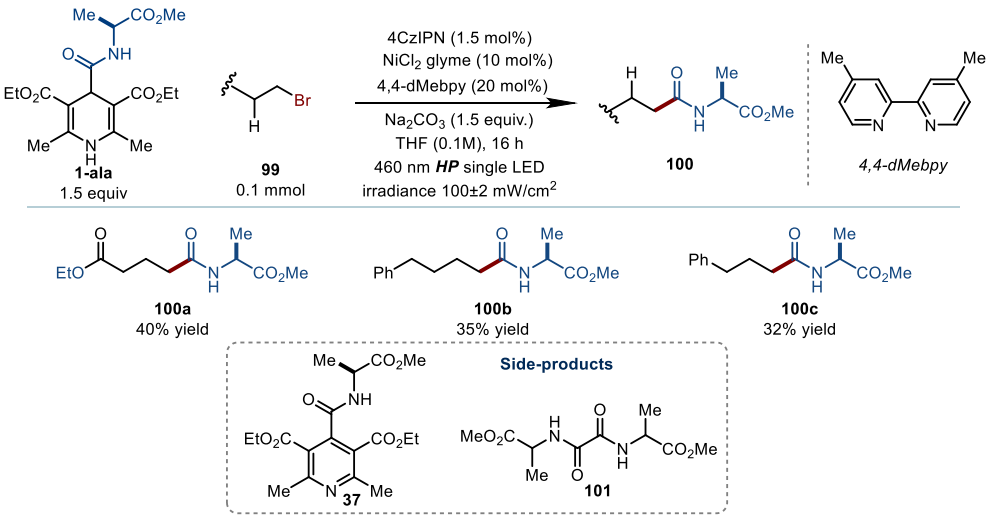

Scheme 4.26. Ni/photoredox-catalyzed carbamoylation of unactivated alkyl bromides.

4.9. Conclusions

This chapter summarizes our efforts towards the development of a protocol for catalytic amide synthesis at ambient temperature. The chemistry exploits the ability of readily available 4-carbamoyl-1,4-dihydropyridines **1** to generate carbamoyl radicals upon SET oxidation by a visible-light-activated photoredox catalyst. This carbamoyl radical generation was used to develop a nickel cross coupling process to synthesize (hetero)aryl amides from readily available aryl bromides. The mild reaction conditions secured a broad functional group tolerance and the direct functionalization of complex molecules. Moreover, we demonstrated that the process is robust and directly scalable without the need for re-optimization. In terms of atom economy, the generation of pyridine side-products can be viewed as the major drawback. Finally, preliminary results for the carbamoylation of unactivated alkyl bromides are described. The encouraging yields obtained using different ligands could potentially promote the coupling of a broader scope of alkyl bromides. In addition, the carbamoylation

of aryl halides could also be achieved through the direct excitation of carbamoyl-DHPs. These findings, along with the experimental simplicity and the low cost and the stability of the substrates, suggest that this catalytic approach to amide synthesis can effectively complement conventional carbonylation chemistry and be useful in life science endeavours.

4.10. Experimental Section

General Information. The ^{1}H NMR, ^{19}F NMR, ^{13}C NMR spectra and UPC^2 traces are available in the literature[1] and are not reported in the present dissertation.

The NMR spectra were recorded at 400 MHz and 500 MHz for ^{1}H, 100 or 125 MHz for ^{13}C and 376 MHz for ^{19}F. The chemical shift (δ) for ^{1}H and ^{13}C are given in ppm relative to residual signals of the solvents ($CHCl_3$ @ 7.26 ppm ^{1}H NMR and 77.16 ppm ^{13}C NMR, and tetramethylsilane @ 0 ppm). Coupling constants are given in Hertz. The following abbreviations are used to indicate the multiplicity: s, singlet; d, doublet; q, quartet; m, multiplet; bs, broad signal; app, apparent; quin, quintet.

High resolution mass spectra (HRMS) were obtained from the ICIQ HRMS unit on MicroTOF Focus and Maxis Impact (Bruker Daltonics) with electrospray ionization (ESI). Cyclic voltammetry (CV) studies were carried out on a Princeton Applied Research PARSTAT 2273 potentiostat offering compliance voltage up to ± 100 V (available at the counter electrode), ± 10 V scan range and ± 2 A current range.

Yields of isolated products refer to materials of >95% purity as determined by ^{1}H NMR analysis.

General Procedures. All reactions were set up under an argon atmosphere in oven-dried glassware using standard Schlenk techniques, unless otherwise stated. Synthesis grade solvents were used as purchased; anhydrous solvents were taken from a commercial SPS solvent dispenser. Chromatographic purification of products was accomplished using forced-flow chromatography (FC) on silica gel (35-70 mesh). For thin layer chromatography (TLC) analysis throughout this work, Merck pre-coated TLC plates (silica gel 60 GF_{254}, 0.25 mm) were employed, using UV light as the visualizing agent and phosphomolybdic acid in EtOH or basic aqueous potassium permanganate ($KMnO_4$) stain solutions, and heat as developing agents. Organic solutions were concentrated under reduced pressure on a Büchi rotatory evaporator.

Determination of Enantiomeric Purity: UPC^2 analysis on chiral stationary phase was performed on a Waters Acquity instrument using a CEL1 chiral columns. The exact conditions for the analyses are specified within the characterization section. UPC^2 traces were compared to racemic samples prepared by running the reaction using racemic amino esters.

Materials. Most of the starting materials used in this study are commercial and were purchased in the highest purity available from Sigma-Aldrich, Fluka, Alfa Aesar, Fluorochem, and used as received, without further purifications. The photocatalyst 2,4,5,6-Tetra(carbazol-9-yl)isophthalonitrile (4CzIPN) was synthesized according to a reported procedure.[55]

---

[55] Luo, J., Zhang, J., "Donor-Acceptor Fluorophores for Visible-Light-Promoted Organic Synthesis: Photoredox/Ni Dual Catalytic C(sp^3)-C(sp^2) Cross-Coupling", *ACS Catal.* **2016**, *6*, 2, 873.

4.10.1. Substrate Synthesis

Synthesis of 3,5-diethoxycarbonyl-3,6-dimethyl-1,4-dihydroisonicotinic acid (25)

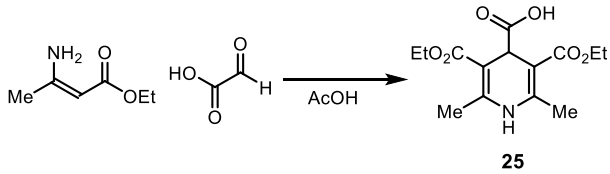

25

Scheme S4.1. Preparation of 4-carboxyl-1,4-dihydropyridine C.

In accordance to a procedure reported in the literature, glyoxylic acid (5 g, 54 mmol, 1 equiv.) was added portionwise at 0 °C to a solution of ethyl-3-aminocrotonate (13.7 mL, 109 mmol, 2.0 equiv.) in 25 mL of glacial acetic acid. The reaction mixture rapidly became yellow and a precipitate deposited. After the evolution of heat had ceased, the reaction mixture was left stirring overnight at room temperature. The solid was collected by filtration and washed with acetic acid and water. The solids were dried overnight under reduced pressure to obtain the pure acid **C** as a white powder. Yield: 37% (6 g).

^{1}H NMR (500 MHz, $CDCl_3$): δ 6.27 (s, 1H), 4.61 (s, 1H), 4.23 (q, *J* = 7.1 Hz, 4H), 2.27 (s, 6H), 1.29 (t, *J* = 7.1 Hz, 6H) ppm.

^{13}C NMR (101 MHz, MeOD): δ 176.5, 168.3, 146.8, 97.7, 59.7, 39.9, 17.0, 13.3 ppm.

Synthesis of 4-Carbamoyl-1,4-Dihydropyridines 1:

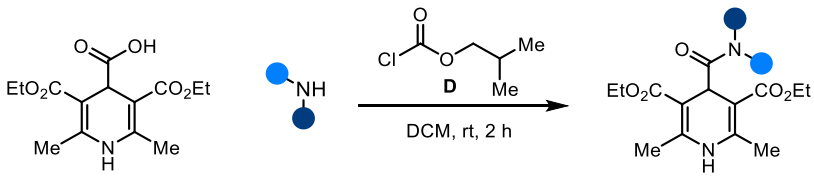

Scheme S4.2. Preparation of 4-carbamoyl-1,4-dihydropyridines **1.**

In a round bottom flask, the carboxylic acid **C** (1 equiv.) was suspended in DCM (0.2 M) followed by the addition of triethylamine (1.2 equiv. or 2 equiv. when amine hydrochloride salts are used). The resulting yellow solution was cooled down to 0 °C and isobutylchloroformate (1.2 equiv.) was then added dropwise. After 10 minutes, the mixture was allowed to warm up to ambient temperature and stirred for 20 minutes. Next, the (primary) amine (1.2-1.5 equiv.) was added and the resulting solution stirred at ambient temperature for another 60 minutes (overnight for secondary amines). After completion of the reaction (as judged by TLC, *n*-hexane/acetone 2:1), the solution was diluted with DCM,

washed with sat. $NaHCO_3$ and water. The organic layers were combined, dried ($MgSO_4$) and concentrated. The remaining residue was purified by flash column chromatography or recrystallized from diethyl ether to provide the desired 4 carbamoyl-1,4-dihydropyridines **1**.

4.10.2. Cyclic Voltammetry Study of Carbamoyl-DHP 1-ala

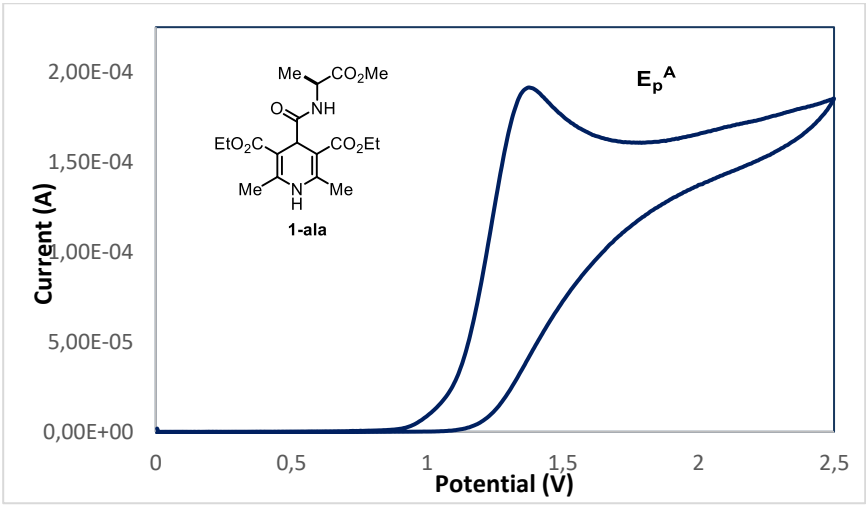

Figure S4.1. Cyclic voltammogram of carbamoyl dihydropyridine **1-ala** [0.02 M] in [0.1 M] $TBAPF_6$ in CH_3CN. Sweep rate: 30 mV/s. Glassy carbon working electrode, Ag/AgCl (satd. KCl) reference electrode, Pt wire auxiliary electrode. Irreversible oxidation. $E_p^A = E_{ox}$ (1-ala$^{\cdot+}$/1-ala) = +1.39 V; E_p^A is the anodic peak potential, while E_{ox} value describes the electrochemical properties of 1a.

4.10.3. UV-Vis Absorption Spectra of 1-ala

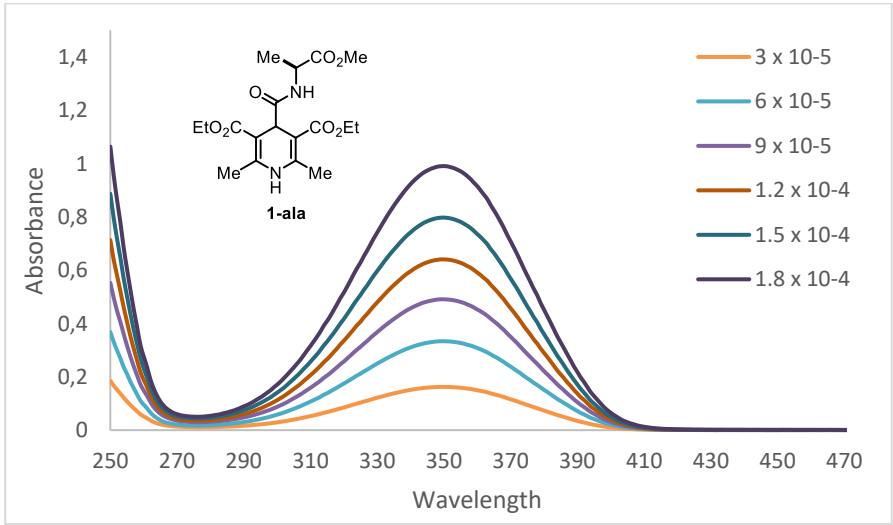

Figure S4.2. Absorption spectrum of **1-ala** at different concentrations in CH_3CN: λ_{max} = 350 nm. The tail wavelength of absorption was considered to be about 405 nm.

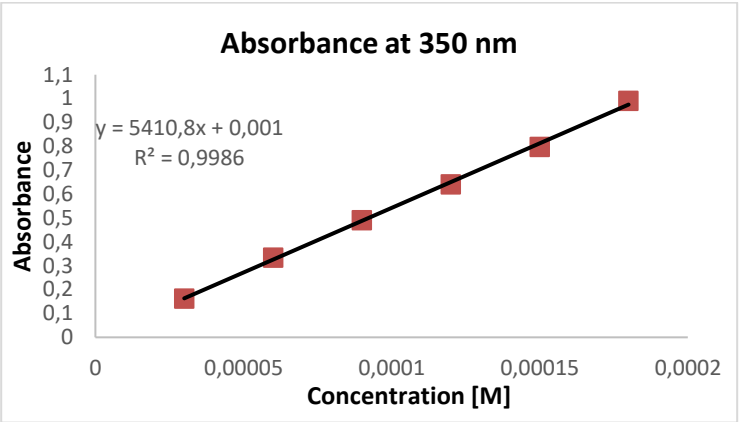

Figure S4.3. Lambert-Beer linear correlation between absorbance and concentration at 350 nm for **1-ala**. The slope of the line is the molar extinction coefficient ε at 350 nm ($M^{-1}cm^{-1}$).

4.10.4. Optimization Studies

Screening of Solvents and Ligands Using High-Throughput Experimentation (HTE)

High-throughput experimentation was performed at the CELLEX-ICIQ High Throughput Experimentation (HTE) laboratory at the ICIQ. The screens were conducted on a 5 μmol scale (relative to the aryl bromide). Yields were determined by UPLC using 4,4′-dimethylbiphenyl as the internal standard (IS).

Reactions were performed in 250 μL glass vials in 24 well LED plate and the vials were equipped with Teflon-coated magnetic stir bars. The plate was placed in a glovebox, then nickel complexes was added as a slurry in THF using micropipettes followed by addition of ligands (as solutions in THF). The solvents were then removed using centrifugal parallel evaporator. Then, other compounds (dihydropyridine, base, photocatalyst and aryl bromide) were added as solutions in the corresponding solvents using micropipettes. The plate was sealed and stirred over a bed blue LED lights with a fan to keep the reaction at room temperature. After 16 h, the plate was removed from the glovebox and unsealed. IS (1.25 μmol) was then added to the vials. The plate is then centrifuged to allow the remaining solids to settle. Aliquots (50 μL) were taken and introduced in to a 96-well UPLC analysis plate, diluted with MeCN (500 μL), and analyzed by UPLC-MS.

Screen 1. Variations of ligands and solvents using High-Throughput-Experimentation

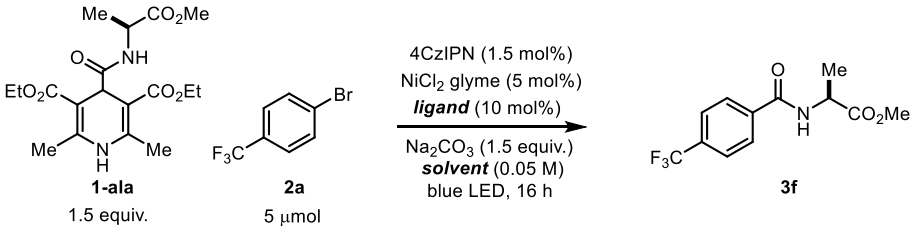

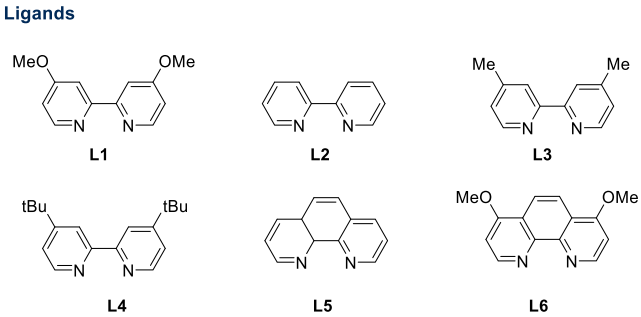

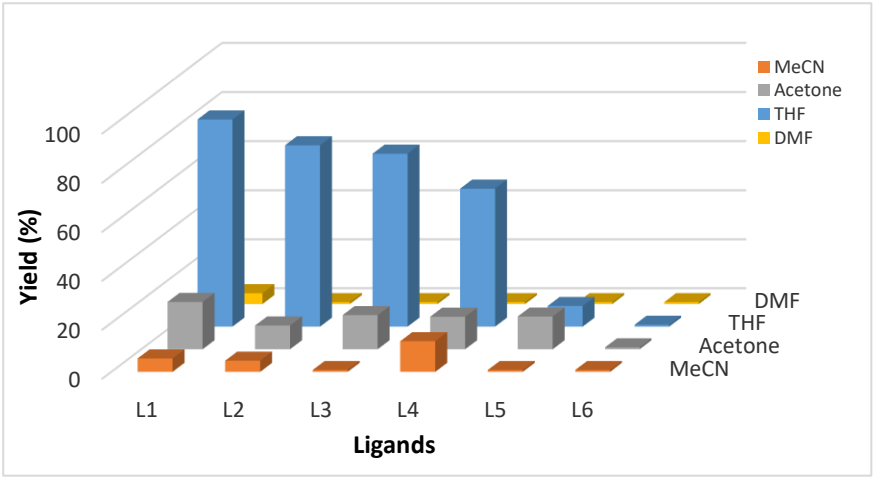

General Procedure for the Screening of Different Parameters

An oven dried Schlenk tube equipped with a stir bar was charged with dihydropyridine **1-ala** (57.4 mg, 0.15 mmol, 1.5 equiv.), nickel precatalyst (0.005 mmol, 5 mol%), 4-4′-dimethoxy-2-2′-bipyridine (2.2 mg, 0.01 mmol. 10 mol%), photocatalyst (0.0015 mmol, 1.5 mol%), base (0.15 mmol, 1.5 equiv), anhydrous organic solvents (2.0 mL, 0.05 M) and 4-bromobenzotrifluoride **2a** (14 μL, 0.1 mmol, 1.0 equiv.). The tube was sealed and the reaction mixture was degassed via freeze-pump-thaw procedure (2 cycles) and backfilled with

argon. The reaction was stirred under light irradiation at ambient temperature for 16 hours. After completion, the reaction mixture was filtered through silica gel with EtOAc, concentrated in vacuo and analyzed by ^{1}H NMR with an internal standard (trichloroethylene, 1 equiv.).

Screen 2. Variation of different parameters

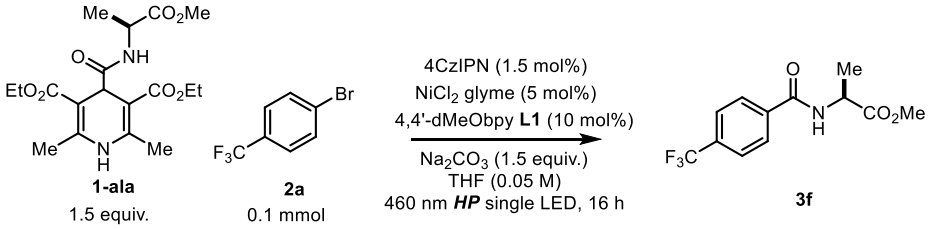

entry	Variation from the standard condition	NMR yield (%)
1	none	99
2	$NiBr_2$ glyme instead of $NiCl_2$ glyme	99
3	$NiBr_2$ instead of $NiCl_2$ glyme	57
4	$NiCl_2$ instead of $NiCl_2$ glyme	55
5	Ir1 instead of 4CzIPN	40
6	Ir2 instead of 4CzIPN	51
7	Non-degassed THF (under Ar)	99
8	Non-degassed THF (BHT stabilized)	79
9	With 10 equiv. of H_2O	87
10	Reversed stoichiometry	88
11	no 4CzIPN	0
12	no $NiCl_2$ glyme	0
13	no light	0
14	no ligand	13

Reactions performed on a 0.1 mmol scale at ambient temperature for 16 h under illumination by a single high power (HP) blue LED (λmax = 460 nm, irradiance = 100±3 mW/cm^2).Yield determined by ^{1}H NMR analysis of the crude mixture using trichloroethylene as the internal standard.

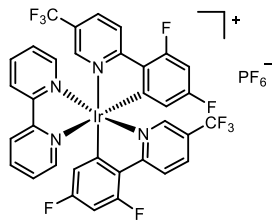

Ir1
$(Ir[dF(CF_3)ppy]_2(bpy))PF_6$

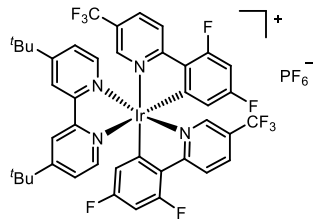

Ir2
$(Ir[dF(CF_3)ppy]_2(dtbbpy))PF_6$

Screen 3 Further variation of solvents

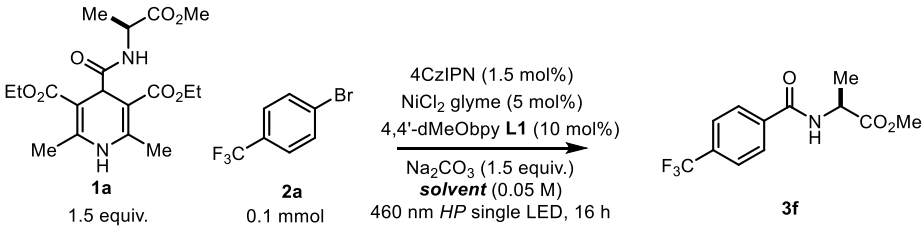

entry	solvent	NMR yield (%)
1	THF	99
2	1,4-dioxane	99
3	DME	72
4	MeCN	50
5	DMF	traces
6	Acetone	33
7	DMSO	traces
8	DCE	traces
9	DMA	20
10[a]	EtOAc	99

Reactions performed on a 0.1 mmol scale at ambient temperature for 16 h under illumination by a single high power (HP) blue LED (λmax = 460 nm, irradiance = 100±3 mW/cm²).Yield determined by ^{1}H NMR analysis of the crude mixture using trichloroethylene as the internal standard. [a] 24 hours reaction

Screen 4 Variation of bases

entry	base	NMR yield of 3f (%)
1	Na_2CO_3	99
2	NaOAc	72
3	Li_2CO_3	52
4	Cs_2CO_3	11
5	2,6-lutidine	50
6	DBU	traces
7	pyridine	36
8	Without base	33

Reactions performed on a 0.1 mmol scale at ambient temperature for 16 h under illumination by a single high power (HP) blue LED (λmax = 460 nm, irradiance = 100±3 mW/cm²).Yield determined by ^{1}H NMR analysis of the crude mixture using trichloroethylene as the internal standard.

4.10.5. General Procedure of the Carbamoylation of (Hetero)Aryl Bromides

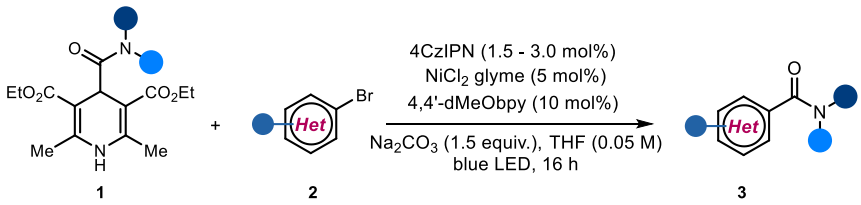

General Procedure A: An oven dried Schlenk tube equipped with a stir bar was charged with (hetero)aryl bromide **2** (*if solids*, 0.1 mmol, 1 equiv.) and dihydropyridines **1** (0.15 mmol, 1.5 equiv.) followed by addition of $NiCl_2$·dme (0.005 mmol, 5 mol%), 4-4′-dimethoxy-2-2′-bipyridine (0.01 mmol. 10 mol%), the photocatalyst 4CzIPN (0.0015 mmol, 1.5 mol%), Na_2CO_3 (0.15 mmol, 1.5 equiv), anhydrous THF or 1,4-dioxane (2 mL, 0.05 M) and (hetero)aryl bromide (*if liquids or oils*). The tube was sealed and the reaction mixture was degassed via freeze-pump-thaw procedure (2 cycles) and backfilled with argon. The reaction was placed on a 3D-printed plastic support mounted on an aluminum block fitted with a 460 nm high-power single LED (λ_{max} = 460 nm). The irradiance was fixed at 100±3 mW/cm^2, as controlled by an external power supply and measured using a photodiode light detector at the start of each reaction. This setup secured a reliable irradiation while keeping a distance of 1 cm between the reaction vessel and the light source (the full setup is detailed in Figure S2). Following the reaction, the reaction mixture was filtered through silica gel with EtOAc and concentrated in vacuo. The crude material was purified by flash column chromatography in silica gel to afford the corresponding product **3**.

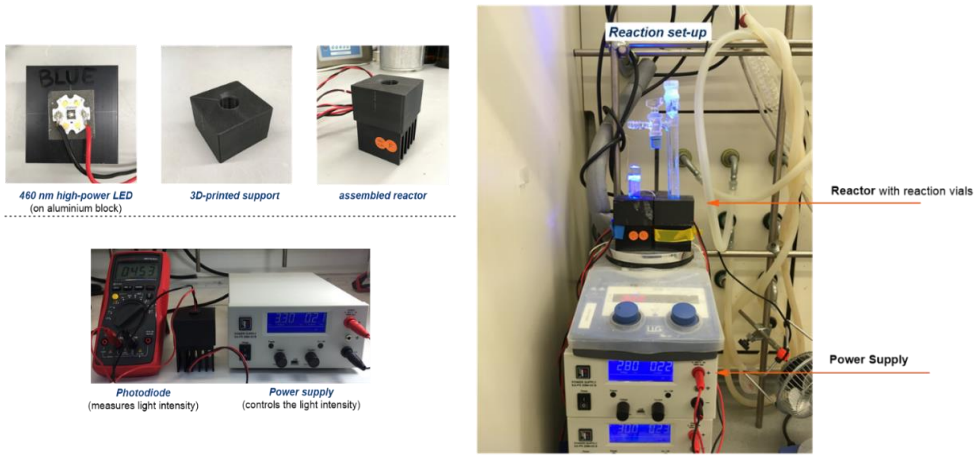

Figure S4.4. Detailed set-up and illumination system. The light source for illuminating the reaction vessel consisted of a 460 nm high-power single LED (OCU-440 UE420-X-T) purchased from OSA Opto Light.

General Procedure B (0.1 - 0.2 mmol scale): A microwave tube equipped with a stir bar was charged with (hetero)aryl bromide (*if solids* 1 equiv.) and dihydropyridines (1.5 or 3.0 equiv.) followed by addition of $NiCl_2$·dme (5 mol%), 4-4′-dimethoxy-2-2′-bipyridine (10 mol%), the photocatalyst 4CzIPN (1.5 or 3.0 mol%), Na_2CO_3 (1.5 equiv), anhydrous THF or 1,4-dioxane (0.05-0.025 M) and (hetero)aryl bromide (*if liquids or oils*). The tube was sealed and the reaction mixture was degassed via sparging with argon (3 min.). The reaction was placed in an EvoluChem™ PhotoRedOx reactor fitted with a 455 nm high-power single LED (λ_{max} = 455 nm) with an irradiance of 34 mW/cm^2 (the set-up is detailed in Figure S4.5.). Following the reaction, the reaction mixture was filtered through silica gel with EtOAc and concentrated in vacuo. The crude material was purified by flash column chromatography in silica gel or preparative HPLC to afford the corresponding product.

Figure S4.5. EvoluChemTM PhotoRedOx reactor fitted with a 455 nm high-power single LED.

4.10.6. Characterization of Products

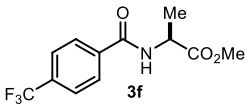

Methyl (4-(trifluoromethyl)benzoyl)-*L*-alaninate (3f)

Prepared according to the general procedure A using 4-bromobenzotrifluoride (14 µL, 0.1 mmol, 1.0 equiv.), the corresponding dihydropyridine **1a** (57.4 mg, 0.15 mmol, 1.5 equiv.), 4CzIPN (1.2 mg, 0.015 mmol, 1.5 mol%), $NiCl_2$·dme (1.1 mg, 0.005 mmol, 5 mol %), and dMeObpy (2.2 mg, 0.01 mmol, 10 mol %) in anhydrous THF (2.0 mL, 0.05 M). The crude material was purified by flash column chromatography (*n*-hexane/EtOAc gradient 8:1 to 4:1) to give the corresponding amide **3f** (27 mg, 98% yield, average of two runs) as a white solid that displayed spectroscopic data consistent with those reported previously.[5]

^{1}H NMR (400 MHz, $CDCl_3$): δ 7.90 (d, *J* = 8.1 Hz 2H), 7.68 (d, *J* = 8.1 Hz, 2H), 6.89 (d, *J* = 7.3 Hz, 1H), 4.80 (quin, *J* = 7.2 Hz, 1H), 3.80 (s, 3H), 1.53 (d, *J* = 7.2 Hz, 3H) ppm.

^{13}C NMR (101 MHz, $CDCl_3$): δ 173.5, 165.5, 137.1, 133.4 (*J* = 32 Hz), 127.5, 125.6 (q, *J* = 3.8 Hz), 123.6 (*J* = 272 Hz), 52.7, 48.6, 18.5 ppm.

^{19}F NMR (376 MHz, $CDCl_3$): δ -63.10 ppm.

$[\alpha]D^{26}$ = +25.6 (c = 0.50, $CHCl_3$). Reference compound: $[\alpha]D^{26}$ = +27.2 (c = 0.53, $CHCl_3$).

Conditions: UPC^2 (Daicel Chiralpak CEL-1 column gradient 100% CO_2 to 60:40 CO_2/acetonitrile over 6 minutes, curve 6), flow rate 2 mL/min, λ= 225 nm).

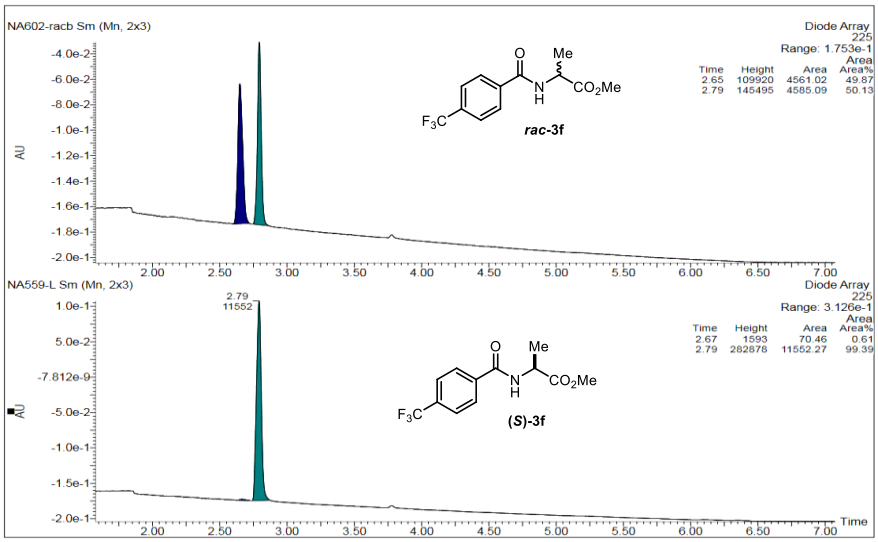

1 mmol scale reaction. The model reaction was repeated on 1 mmol scale using commercially available Kessil lamp (PR160-456, 40 W, λ_{max} = 456 nm) as the light source. An oven dried 100 mL Schlenk tube equipped with a stir bar was charged with dihydropyridine **1-ala** (574 mg,1.5 mmol, 1.5 equiv.) followed by addition of NiCl2·dme (11 mg, 0.05 mmol, 5 mol%), 4-4′-dimethoxy-2-2′-bipyridine (22 mg, 0.1 mmol. 10 mol%), photocatalyst 4CzIPN (12 mg, 0.015 mmol, 1.5 mol%), Na_2CO_3 (159 mg, 1.5 mmol, 1.5 equiv), anhydrous THF (20 mL, 0.05 M) and 4-bromobenzotrifluoride **2a** (138 µL, 1 mmol, 1 equiv.). The tube was sealed and the reaction mixture was degassed via freeze-pump-thaw procedure (2 cycles) and backfilled with argon. The reaction mixture was stirred under irradiation with a 40 W 456 nm blue LED Kessil lamp (100% intensity, 5 cm

distance from the Schlenk tube, using fans to cool down the reaction temperature) for 24 hours. After completion, the reaction mixture was filtered through silica gel with EtOAc, concentrated in vacuo and analyzed by ^{1}H NMR with an internal standard (trichloroethylene, 1 equiv., NMR yield: 99%). The crude material was purified by flash column chromatography (n hexane/EtOAc 4:1) to yield product 4 (251 mg, 91%).

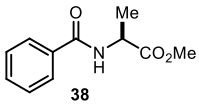

38

Methyl benzoyl-*L*-alaninate (38)

Prepared according to the general procedure A using bromobenzene (15.7 mg, 0.1 mmol, 1.0 equiv.), the corresponding dihydropyridine **1-ala** (57.4 mg, 0.15 mmol, 1.5 equiv.), 4CzIPN (1.2 mg, 0.015 mmol, 1.5 mol%), $NiCl_2$·dme (1.1 mg, 0.005 mmol, 5 mol %), and dMeObpy (2.2 mg, 0.01 mmol, 10 mol %) in anhydrous THF (2.0 mL, 0.05 M). The crude material was purified by flash column chromatography (*n*-hexane/EtOAc gradient 6:1 to 4:1) to give the corresponding amide **38** (27 mg, 98% yield, average of two runs) as a white solid that displayed spectroscopic data consistent with those reported previously.[6]

^{1}H NMR (400 MHz, $CDCl_3$): δ 7.82 – 7.77 (m, 2H), 7.55 – 7.38 (m, 3H), 6.77 (d, *J* = 7.0 Hz, 1H), 4.80 (quin, *J* = 7.2 Hz, 1H), 3.78 (s, 3H), 1.52 (d, *J* = 7.2 Hz, 3H) ppm.

^{13}C NMR (101 MHz, $CDCl_3$): δ 174.1, 167.2, 134.3, 132.1, 128.9, 127.4, 52.9, 48.8, 19.0 ppm.

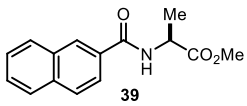

39

Methyl (2-naphthoyl)-*L*-alaninate (39)

Prepared according to the general procedure A using 2-bromonaphthalene (20.7 mg, 0.1 mmol, 1.0 equiv.), the corresponding dihydropyridine **1-ala** (57.4 mg, 0.15 mmol, 1.5 equiv.), 4CzIPN (1.2 mg, 0.015 mmol, 1.5 mol%), $NiCl_2$·dme (1.1 mg, 0.005 mmol, 5 mol %), and dMeObpy (2.2 mg, 0.01 mmol, 10 mol %) in anhydrous THF (2.0 mL, 0.05 M). The crude material was purified by flash column chromatography (*n*-hexane/EtOAc gradient 4:1) to give the corresponding amide **39** (26 mg, 99% yield, average of two runs) as a white solid.

^{1}H NMR (400 MHz, $CDCl_3$): δ 8.32 (s, 1H), 7.92 – 7.83 (m, 4H), 7.58 – 7.50 (m, 2H),6.96 (d, *J* = 7.2 Hz, 1H) 4.87 (quin, *J* = 7.2 Hz, 1H), 3.80 (s, 3H), 1.57 (d, *J* = 7.2 Hz, 3H) ppm.

^{13}C NMR (126 MHz, $CDCl_3$): δ 174.2, 167.2, 135.2, 132.9, 129.3, 128.8, 128.1, 128.0, 127.1, 123.94, 52.9, 48.9, 19.1.ppm.

HRMS (ESI, m/z) calcd. for $C_{15}H_{16}NO_3$ ($[M+H]^+$): 258.1125, found 258.1124.

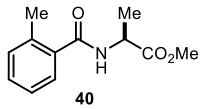

40

Methyl (2-methylbenzoyl)-*L*-alaninate (40)

Prepared according to the general procedure A using 2-bromotoluene (17.1 mg, 0.1 mmol, 1.0 equiv.), the corresponding dihydropyridine **1-ala** (57.4 mg, 0.15 mmol, 1.5 equiv.), 4CzIPN (1.2 mg, 0.015 mmol, 1.5 mol%), $NiCl_2$·dme (1.1 mg, 0.005 mmol, 5 mol %), and dMeObpy (2.2 mg, 0.01 mmol, 10 mol %) in anhydrous THF (2.0 mL, 0.05 M). The crude material was purified by flash column chromatography (*n*-hexane/EtOAc 3:1) to give the corresponding amide **40** (14 mg, 63% yield, average of two runs) as a white solid.

^{1}H NMR (400 MHz, $CDCl_3$): δ 7.40 (d, *J* = 7.5, 1H), 7.34 – 7.28 (m,1H), 7.24 – 7.17 (m, 2H), 6.34 (d, *J* = 7.4 Hz, 1H), 4.79 (quin, *J* = 7.2 Hz, 1H), 3.79 (s, 3H), 2.45 (s, 3H), 1.51 (d, *J* = 7.2 Hz, 3H) ppm.

^{13}C NMR (75 MHz, $CDCl_3$): δ 173.5, 169.5, 136.3, 135.7, 131.1, 130.1, 126.8, 125.7, 52.5, 48.3, 19.7, 18.6.ppm.

HRMS (ESI, m/z) calcd. for $C_{12}H_{14}NO_3$ ($[M-H]^-$): 220.0979, found 220.0970.

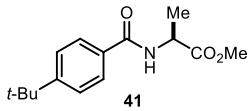

41

Methyl (4-(tert-butyl)benzoyl)-*L*-alaninate (41)

Prepared according to the general procedure A using 1-Bromo-4-tert-butylbenzene (21.3 mg, 0.1 mmol, 1.0 equiv.), the corresponding dihydropyridine **1-ala** (57.4 mg, 0.15 mmol, 1.5 equiv.), 4CzIPN (1.2 mg, 0.015 mmol, 1.5 mol%), $NiCl_2$·dme (1.1 mg, 0.005 mmol, 5 mol %), and dMeObpy (2.2 mg, 0.01 mmol, 10 mol %) in anhydrous THF (2.0 mL, 0.05 M). The crude material was purified by flash column chromatography (*n*-hexane/EtOAc 6:1) to give the corresponding amide **7** (19 mg, 72% yield, average of two runs) as a white solid.

^{1}H NMR (400 MHz, $CDCl_3$) δ 7.74 (d, *J* = 8.5 Hz 2H), 7.45 (d, *J* = 8.5 Hz, 2H), 6.73 (d, *J* = 7.3 Hz, 1H), 4.80 (quin, *J* = 7.2 Hz, 1H), 3.78 (s, 3H), 1.51 (d, *J* = 7.2 Hz, 3H), 1.33 (s, 9H) ppm.

^{13}C NMR (101 MHz, $CDCl_3$) δ 173.7, 166.7, 155.3, 131.1, 126.9, 125.1, 52.5, 48.4, 34.9, 31.1, 18.7.ppm.

HRMS (ESI, m/z) calcd. for $C_{15}H_{22}NO_3$ ($[M+H]^+$): 264.1594, found 264.1596.

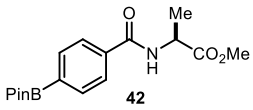

42

Methyl [4-(4,4,5,5-tetramethyl-1,3,2-dioxaborolan-2-yl)benzoyl]-*L*-alaninate (42)

Prepared according to the general procedure A using 2-(4-bromophenyl)-4,4,5,5-tetramethyl-1,3,2-dioxaborolane (28.3 mg, 0.1 mmol, 1.0 equiv.), the corresponding dihydropyridine **1-ala** (57.4 mg, 0.15 mmol, 1.5 equiv.), 4CzIPN (1.2 mg, 0.015 mmol, 1.5 mol%), $NiCl_2$·dme (1.1 mg, 0.005 mmol, 5 mol %), and dMeObpy (2.2 mg,

0.01 mmol, 10 mol %) in anhydrous THF (2.0 mL, 0.05 M). The crude material was purified by flash column chromatography (*n*-hexane/EtOAc 1:1) to give the corresponding amide **42** (32 mg, 96% yield, average of two runs) as a white solid.

^{1}H NMR (300 MHz, $CDCl_3$) δ 7.87 (d, J = 8.2 Hz, 2H), 7.78 (d, J = 8.3 Hz, 2H), 6.75 (d, J = 7.3 Hz, 1H), 4.81 (quin, J = 7.2 Hz, 1H), 3.80 (s, 3H), 1.53 (d, J = 7.2 Hz, 3H), 1.36 (s, 12H) ppm.

^{13}C NMR (75 MHz, $CDCl_3$) δ 166.7, 136.1, 134.9, 126.2, 84.2, 48.5, 24.9, 18.7 ppm.

HRMS (ESI, m/z) calcd. for $C_{17}H_{25}NO_5B$ ($[M+H]^+$): 333.1857, found 333.1853.

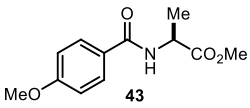

43

Methyl (4-methoxybenzamido)-*L*-alaninate (43)

Prepared according to the general procedure A using 4-bromo anisole (13 µL, 18.7 mg, 0.1 mmol, 1.0 equiv.), the corresponding dihydropyridine **1-ala** (57.4 mg, 0.15 mmol, 1.5 equiv.), 4CzIPN (1.2 mg, 0.015 mmol, 1.5 mol%), $NiCl_2$·dme (1.1 mg, 0.005 mmol, 5 mol %), and dMeObpy (2.2 mg, 0.01 mmol, 10 mol %) in anhydrous THF (2.0 mL, 0.05 M). Multiple purification by column chromatography (n-hexane/EtOAc 1:1) resulted in poor separation from oxamide by-product. An analytical amount of the pure compound was isolated for characterization (HPLC-MS on Zorbax Eclipse C18 100 x 4.6mm, 3.5µm, H_2O / MeOH 60:40, flow rate: 1 mL/min, Ionization mode: APCI +/-), which displayed spectroscopic data consistent with those reported previously.[7] The yield (91%) of **43** were inferred by ^{1}H NMR analysis of the crude reaction mixture using trichloroethylene as the internal standard.

^{1}H NMR (500 MHz, $CDCl_3$) δ 7.77 (d, *J* = 9.0 Hz, 2H), 6.93 (d, *J* = 8.9 Hz, 2H), 6.63 (d, *J* = 7.2 Hz, 1H), 4.79 (quin, *J* = 7.2 Hz, 1H), 3.85 (s, 3H), 3.79 (s, 3H), 1.51 (d, *J* = 7.2 Hz, 3H) ppm.

^{13}C NMR (126 MHz, $CDCl_3$) δ 174.2, 166.7, 162.8, 129.2, 126.6, 114.1, 55.8, 52.9, 48.8, 19.1 ppm.

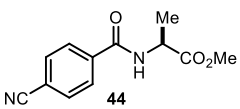

44

Methyl (4-cyanobenzoyl))-*L*-alaninate (44)

Prepared according to the general procedure A using 1-bromo-4-cyanobenzene (18.2 mg, 0.1 mmol, 1.0 equiv.), the corresponding dihydropyridine **1-ala** (57.4 mg, 0.15 mmol, 1.5 equiv.), 4CzIPN (1.2 mg, 0.015 mmol, 1.5 mol%), $NiCl_2$·dme (1.1 mg, 0.005 mmol, 5 mol %), and dMeObpy (2.2 mg, 0.01 mmol, 10 mol %) in anhydrous THF (2.0 mL, 0.05 M). Multiple purification by column chromatography (n-hexane/EtOAc 1:1) resulted in poor separation from oxamide byproduct. An analytical amount of the pure compound was isolated for characterization (HPLC-MS on Zorbax Eclipse C18 100 x 4.6mm, 3.5µm, 75:25 H_2O/MeCN, 25% MeOH hold 15', flow rate:

1 mL/min, Ionization mode: APCI +/-). The yield (79%) of **44** were inferred by ^{1}H NMR analysis of the crude reaction mixture using trichloroethylene as the internal standard.

^{1}H NMR (400 MHz, $CDCl_3$) δ 7.91 (d, *J* = 8.7 Hz, 2H), 7.75 (d, *J* = 8.7 Hz, 2H), 6.80 (d, *J* = 7.1 Hz, 1H), 4.79 (quin, *J* = 7.2 Hz, 1H), 3.81 (s, 3H), 1.54 (d, *J* = 7.1 Hz, 3H). ppm.

^{13}C NMR (101 MHz, $CDCl_3$) δ 173.4, 165.0, 137.8, 132.5, 127.8, 117.9, 115.4, 52.8, 48.7, 18.6 ppm.

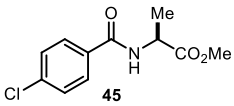

45

Methyl (4-chlorobenzamido)-*L*-alaninate (45)

Prepared according to the general procedure A using 1-Bromo-4-chlorobenzene (19.1 mg, 0.1 mmol, 1.0 equiv.), the corresponding dihydropyridine **1-ala** (57.4 mg, 0.15 mmol, 1.5 equiv.), 4CzIPN (1.2 mg, 0.015 mmol, 1.5 mol%), $NiCl_2$·dme (1.1 mg, 0.005 mmol, 5 mol %), and dMeObpy (2.2 mg, 0.01 mmol, 10 mol %) in anhydrous THF (2.0 mL, 0.05 M). The crude material was purified by flash column chromatography (*n*-hexane/EtOAc gradient 8:1 to 4:1) to give the corresponding amide **45** (18 mg, 73% yield, average of two runs) as a white solid.

^{1}H NMR (400 MHz, $CDCl_3$): δ 7.73 (d, *J* = 8.6 Hz, 2H), 7.38 (d, *J* = 8.8 Hz, 2H), 6.83 (d, *J* = 7.3 Hz, 1H), 4.70 (quin, *J* = 7.2 Hz, 1H), 3.78 (s, 3H), 1.50 (d, *J* = 7.2 Hz, 3H) ppm.

^{13}C NMR (101 MHz, $CDCl_3$): δ 173.6, 165.7, 137.9, 132.2, 128.8, 128.5, 52.6, 48.5, 18.5 ppm.

HRMS (ESI, m/z) calcd. for $C_{11}H_{11}ClNO_3$ ($[M-H]^-$): 240.0433, found 240.0436.

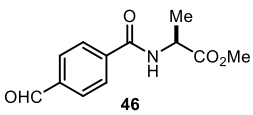

46

Methyl (4-formylbenzoyl)-*L*-alaninate (46)

Prepared according to the general procedure A using 4-bromobenzaldehyde (18.5 mg, 0.1 mmol, 1.0 equiv.), the corresponding dihydropyridine **1-ala** (57.4 mg, 0.15 mmol, 1.5 equiv.), 4CzIPN (1.2 mg, 0.015 mmol, 1.5 mol%), $NiCl_2$·dme (1.1 mg, 0.005 mmol, 5 mol %), and dMeObpy (2.2 mg, 0.01 mmol, 10 mol %) in anhydrous THF (2.0 mL, 0.05 M). Multiple purification by column chromatography resulted in poor separation from several unidentified byproducts. The yield (54%) of **46** were inferred by ^{1}H NMR analysis of the crude reaction mixture using trichloroethylene as the internal standard. An analytical amount of the pure compound was isolated by preparative TLC (*n*-hexane/acetone 4:1) to obtain a white solid.

^{1}H NMR (400 MHz, $CDCl_3$): δ 10.09 (s, 1H), 7.96 (s, 4H), 6.80 (br s, 1H), 4.82 (quin, *J* = 7.2 Hz, 1H), 3.81 (s, 3H), 1.55 (d, *J* = 7.2 Hz, 3H) ppm.

^{13}C NMR (101 MHz, $CDCl_3$) δ 191.5, 173.5, 165.7, 139.1, 138.4, 129.9, 127.8, 52.7, 48.7, 18.6 ppm.

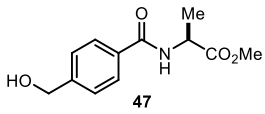

47

Methyl [4-(hydroxymethyl)benzoyl]-*L*-alaninate (47)

Prepared according to the general procedure A using 4-Bromobenzyl alcohol (18.7 mg, 0.1 mmol, 1.0 equiv.), the corresponding dihydropyridine **1-ala** (57.4 mg, 0.15 mmol, 1.5 equiv.), 4CzIPN (1.2 mg, 0.015 mmol, 1.5 mol%), $NiCl_2$·dme (1.1 mg, 0.005 mmol, 5 mol %), and dMeObpy (2.2 mg, 0.01 mmol, 10 mol %) in anhydrous THF (2.0 mL, 0.05 M). The crude material was purified by flash column chromatography (DCM/acetone 4:1) to give the corresponding amide **47** (15.5 mg, 65% yield, average of two runs) as a white solid.

^{1}H NMR (400 MHz, $CDCl_3$): δ 7.71 (d, *J* = 8.4 Hz, 2H), 7.34 (d, *J* = 7.9 Hz, 2H), 6.85 (d, *J* = 7.3 Hz, 1H), 4.76 (quin, *J* = 7.2 Hz, 1H), 4.69 (s, 2H), 3.77 (s, 3H), 2.76 (br, 1H), 1.50 (d, *J* = 7.2 Hz, 3H) ppm.

^{13}C NMR (101 MHz, $CDCl_3$) δ 166.8, 145.1, 132.7, 127.2, 126.7, 64.4, 52.6, 48.5, 18.5 ppm.

HRMS (ESI, m/z) calcd. for $C_{12}H_{14}NO_4$ ($[M-H]^-$): 236.0928, found 236.0931.

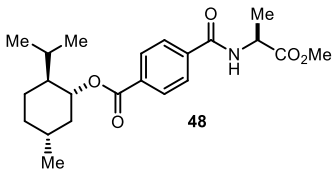

48

(1*R*,2*S*,5*R*)-2-isopropyl-5-methylcyclohexyl 4-[(1-methoxy-1-oxopropan-2-yl)carbamoyl]benzoate (48)

Prepared according to the general procedure A using (1*R*,2*S*,5*R*)-2-isopropyl-5-methylcyclohexyl 4-bromobenzoate (33.9 mg, 0.1 mmol, 1.0 equiv.), the corresponding dihydropyridine **1-ala** (57.4 mg, 0.15 mmol, 1.5 equiv.), 4CzIPN (1.2 mg, 0.015 mmol, 1.5 mol%), $NiCl_2$·dme (1.1 mg, 0.005 mmol, 5 mol %), and dMeObpy (2.2 mg, 0.01 mmol, 10 mol %) in anhydrous THF (2.0 mL, 0.05 M). The crude material was purified by flash column chromatography (*n*-hexane/EtOAc 4:1) to give the corresponding amide **48** (39 mg, 99% yield, average of two runs) as a white solid.

^{1}H NMR (400 MHz, $CDCl_3$): δ 8.08 (d, *J* = 8.5 Hz, 2H), 7.85 (d, *J* = 8.8 Hz, 2H),), 6.87 (d, *J* = 7.3 Hz, 1H), 4.94 (td, *J* = 10.9, 4.4 Hz, 1H), 4.80 (quin, *J* = 7.2 Hz, 1H), 3.79 (s, 3H), 2.16 – 2.08 (m, 1H), 1.97 – 1.87 (m, 1H), 1.76 – 168 (m, 2H), 1.62 – 1.52 (m, 2H), 1.53 (d, *J* = 7.2 Hz, 3H), 1.18 – 1.06 (m, 2H), 0.92 (dd, *J* = 6.8, 5.4 Hz, 7H), 0.79 (d, *J* = 7.0 Hz, 3H) ppm.

^{13}C NMR (101 MHz, $CDCl_3$): δ 173.5, 165.9, 165.2, 137.6, 133.7, 129.8, 127.1, 75.4, 52.6, 48.6, 47.2, 40.9, 34.3, 31.4, 26.6, 23.7, 22.0, 20.7, 18.5, 16.5 ppm.

HRMS (ESI, m/z) calcd. for $C_{22}H_{32}NO_5$ ($[M+H]^+$): 390.2275, found 390.2262.

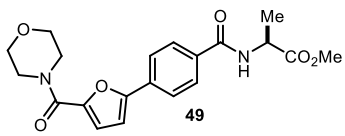

49

Methyl *N*-{4-[5-(morpholine-4-carbonyl)furan-2-yl]benzoyl}-*L*-alaninate (49)

Prepared according to the general procedure B using [5-(4-bromophenyl)-2-furyl](morpholin-4-yl)methanone (33.6

mg, 0.1 mmol, 1.0 equiv.), the corresponding dihydropyridine **1-ala** (57.4 mg, 0.15 mmol, 1.5 equiv.), 4CzIPN (2.37 mg, 0.03 mmol, 3 mol%), $NiCl_2$·dme (1.1 mg, 0.005 mmol, 5 mol %), dMeObpy (2.2 mg, 0.01 mmol, 10 mol %) and Na_2CO_3 (15.9 mg, 0.15 mmol, 1.5 equiv.) in anhydrous 1,4-dioxane (1.7 mL, 0.058 M). The crude material was purified by preparative HPLC (Method: Column: Reprosil C18; 10 µm; 125x30 mm / Flow rate: 75 ml/min / Eluent: A = H_2O (0,01% formic acid), B = acetonitrile / Gradient: 0.00-5.00 min = 10% B, 6.50 min = 20% B, 17.0-19.75 min = 100% B, 19.75.00-23.00min = 90% B) to give the corresponding amide **49** (13.8 mg, 39% yield) as a white solid.

^{1}H NMR (500 MHz, $CDCl_3$) δ 7.86 (d, *J* = 8.5 Hz, 2H), 7.75-7.71 (m, 2H), 7.12 (d, *J* = 3.4 Hz, 1H), 6.88-6.81 (m, 2H), 4.81 (quin, *J* = 7.2 Hz, 1H), 3.98-3.83 (m, 4H), 3.81 (s, 3H), 3.80-3.77 (m, 4H), 1.54 (d, *J* = 7.0 Hz, 3H) ppm.

^{13}C NMR (126 MHz, $CDCl_3$) δ 173.69, 166.02, 158.92, 154.05, 147.42, 133.45, 132.63, 127.80, 124.27, 118.93, 108.14, 66.98, 52.67, 48.57, 18.64 ppm (one signal overlapping).

HRMS (ESI, m/z) calcd. for $C_{20}H_{23}N_2O_6$ ($[M+H]^+$): 387.1556, found 387.1556.

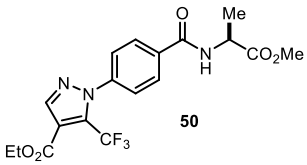

50

Ethyl 1-(4-{[(2*S*)-1-methoxy-1-oxopropan-2-yl]carbamoyl}phenyl)-5-(trifluoromethyl)-1H-pyrazole-4-carboxylate (50)

Prepared according to the general procedure B using ethyl 1-(4-bromophenyl)-5-(trifluoromethyl)-1H-pyrazole-4-carboxylate (72.6 mg, 0.2 mmol, 1.0 equiv.), the corresponding dihydropyridine **1-ala** (115 mg, 0.3 mmol, 1.5 equiv.), 4CzIPN (4.73 mg, 0.03 mmol, 3 mol%), $NiCl_2$·dme (2.20 mg, 0.01 mmol, 5 mol %), dMeObpy (4.33 mg, 0.02 mmol, 10 mol %) and Na_2CO_3 (31.8 mg, 0.3 mmol, 1.5 equiv.) in anhydrous 1,4-dioxane (4 mL, 0.05 M). The crude material was purified by preparative HPLC (Method: Column: Reprosil C18; 10 µm; 125x30 mm / Flow rate: 75 ml/min / Eluent: A = H_2O (0,01% formic acid), B = acetonitrile / Gradient: 0.00-5.00 min = 10% B, 6.50 min = 20% B, 17.0-19.75 min = 100% B, 19.75.00-23.00min = 90% B) to give the corresponding amide **50** (67.4 mg, 82% yield) as a white solid.

^{1}H NMR (500 MHz, DMSO-d_6) δ 9.03 (d, *J* = 7.0 Hz, 1H), 8.35 (s, 1H), 8.08-8.03 (m, 2H), 7.69 (d, *J* = 8.2 Hz, 2H), 4.52 (quin, *J* = 7.2 Hz, 1H), 4.33 (q, *J* = 7.0 Hz, 2H), 3.67 (s, 3H), 1.43 (d, *J* = 7.2 Hz, 3H), 1.31 (t, *J* = 7.0 Hz, 3H) ppm.

^{13}C NMR (126 MHz, DMSO-d_6) δ 172.91, 165.12, 160.18, 142.34, 140.98, 135.11, 131.51 (q, *J* = 39 Hz) 128.44, 126.10, 118.85 (q, *J* = 272 Hz), 116.37, 61.04, 51.89, 48.34, 16.61, 13.88 ppm.

HRMS (ESI, m/z) calcd. for $C_{18}H_{19}N_3O_5F_3$ ($[M+H]^+$): 414.1277, found 414.1274.

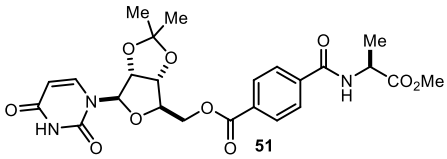

51

((3a*R*,4*R*,6*R*,6a*R*)-6-(2,4-dioxo-3,4-dihydropyrimidin-1(2H)-yl)-2,2-dimethyltetrahydrofuro[3,4-d][1,3]dioxol-4-yl)methyl 4-(((*S*)-1-methoxy-1-oxopropan-2-yl)carbamoyl)benzoate (51)

Prepared according to the general procedure A using the aryl bromide **2c** (46.7 mg, 0.1 mmol, 1.0 equiv.), the corresponding dihydropyridine **1-ala** (57.4 mg, 0.15 mmol, 1.5 equiv.), 4CzIPN (1.2 mg, 0.015 mmol, 1.5 mol%), $NiCl_2$·dme (1.1 mg, 0.005 mmol, 5 mol %), and dMeObpy (2.2 mg, 0.01 mmol, 10 mol %) in anhydrous THF (2.0 mL, 0.05 M). The crude material was purified by flash column chromatography (*first purification*: DCM/acetone 8:1, *second purification*: DCM/MeOH 98:2) to give the corresponding amide **51** (36 mg, 70% yield, average of two runs) as a white solid.

^{1}H NMR (300 MHz, $CDCl_3$): δ 9.22 (s, 1H), 8.07 (dd, *J* = 8.5, 2.8 Hz, 2H), 7.85 (dd, *J* = 8.5, 2.0 Hz, 2H), 7.24 (d, *J* = 7.9 Hz, 2H), 6.94 (app t, *J* = 7.9 Hz, 1H), 5.66 (dt, *J* = 8.1, 2.5 Hz, 1H), 5.60 (s, 1H), 5.09 (d, *J* = 6.4 Hz, 1H), 4.95 (dd, *J* = 6.4, 4.1 Hz, 1H), 4.80 (quin, *J* = 7.2 Hz, 1H), 4.65 – 4.50 (m, 2H), 4.51 – 4.43 (m, 1H), 3.79 (s, 3H), 1.58 (s, 3H), 1.53 (d, *J* = 6.2 Hz, 3H), 1.37 (s, 3H) ppm.

^{13}C NMR (101 MHz, $CDCl_3$): δ 173.6, 166.0, 165.3, 163.1, 149.8, 142.5, 138.2, 132.4, 129.9, 127.2, 114.7, 102.6, 95.7, 85.6, 84.6, 81.2, 64.8, 52.7, 48.6, 27.2, 25.3, 18.5 ppm.

HRMS (ESI, m/z) calcd. for $C_{24}H_{28}N_3O_{10}$ ($[M+H]^+$): 518.1769, found 518.1765.

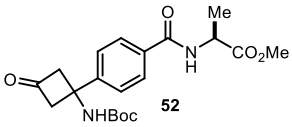

52

Methyl *N*-(4-{1-[(tert-butoxycarbonyl)amino]-3-oxocyclobutyl}benzoyl)-*L*-alaninate (52)

Prepared according to the general procedure B using *tert*-butyl [1-(4-bromophenyl)-3-oxocyclobutyl]carbamate (34.0 mg, 0.1 mmol, 1.0 equiv.), the corresponding dihydropyridine **1-ala** (57.4 mg, 0.15 mmol, 1.5 equiv.), 4CzIPN (2.37 mg, 0.03 mmol, 3 mol%), $NiCl_2$·dme (1.1 mg, 0.005 mmol, 5 mol %), dMeObpy (2.2 mg, 0.01 mmol, 10 mol %) and Na_2CO_3 (15.9 mg, 0.15 mmol, 1.5 equiv.) in anhydrous 1,4-dioxane (2.0 mL, 0.05 M). The crude material was purified by preparative HPLC (Method: Column: Reprosil C18; 10 µm; 125x30 mm / Flow rate: 75 ml/min / Eluent: A = H_2O (0,01% formic acid), B = acetonitrile / Gradient: 0.00-5.00 min = 10% B, 6.50 min = 20% B, 17.0-19.75 min = 100% B, 19.75.00-23.00min = 90% B) to give the corresponding amide **52** (22.5 mg, 58% yield) as a white solid.

^{1}H NMR (500 MHz, $CDCl_3$) δ 7.82 (d, *J* = 8.2 Hz, 2H), 7.50 (br d, *J* = 8.2 Hz, 2H), 6.78 (br d, *J* = 5.2 Hz, 1H), 5.39 (br s, 1H), 4.85-4.75 (m, 1H), 3.80 (s, 3H), 3.69-3.53 (m, 4H), 1.53 (d, *J* = 7.3 Hz, 3H), 1.47-1.30 (br s, 9 H) ppm. Rotamers.

^{13}C NMR (126 MHz, $CDCl_3$) δ 203.51, 173.72, 166.20, 154.47, 147.39, 133.06, 127.53, 125.85, 80.55, 59.94, 52.67, 50.53, 48.54, 28.30, 18.66 ppm.

HRMS (ESI, m/z) calcd. for $C_{20}H_{27}N_2O_6$ ([M+H]$^+$): 391.1864, found 391.1862.

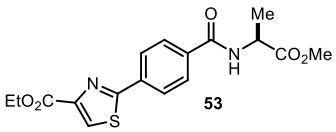

Ethyl 2-(4-{[(2*S*)-1-methoxy-1-oxopropan-2-yl]carbamoyl}phenyl)-1,3-thiazole-4-carboxylate (53)

Prepared according to the general procedure B using ethyl 2-(4-bromophenyl)-1,3-thiazole-4-carboxylate (62.4 mg, 0.2 mmol, 1.0 equiv.), the corresponding dihydropyridine **1-ala** (115 mg, 0.3 mmol, 1.5 equiv.), 4CzIPN (4.73 mg, 0.03 mmol, 3 mol%), $NiCl_2$·dme (2.20 mg, 0.01 mmol, 5 mol %), dMeObpy (4.33 mg, 0.02 mmol, 10 mol %) and Na_2CO_3 (31.8 mg, 0.3 mmol, 1.5 equiv.) in anhydrous 1,4-dioxane (8 mL, 0.025 M). The crude material was purified by preparative HPLC (Method: Column: Reprosil C18; 10 µm; 125x30 mm / Flow rate: 75 ml/min / Eluent: A = H_2O (0,01% formic acid), B = acetonitrile / Gradient: 0.00-5.00 min = 10% B, 6.50 min = 20% B, 17.0-19.75 min = 100% B, 19.75.00-23.00min = 90% B) to give the corresponding amide **53** (42.2 mg, 58% yield) as a white solid.

^{1}H NMR (500 MHz, $CDCl_3$) δ 8.21 (s, 1H), 8.12-8.08 (m, 2H), 7.91-7.88 (m, 2H), 6.81-6.75 (m, 1H), 4.82 (quin, *J* = 7.2 Hz, 1H), 4.46 (q, *J* = 7.2 Hz, 2H), 3.81 (s, 3H), 1.55 (d, *J* = 7.2 Hz, 3H), 1.44 (t, *J* = 7.1 Hz, 3H) ppm.

^{13}C NMR (126 MHz, $CDCl_3$) δ 173.62, 167.47, 165.84, 161.33, 148.49, 135.64, 135.60, 127.81, 127.73, 127.14, 61.69, 52.72, 48.64, 18.70, 14.40 ppm.

HRMS (ESI, m/z) calcd. for $C_{17}H_{19}N_2O_5$ ([M+H]$^+$): 363.1015, found 363.1017.

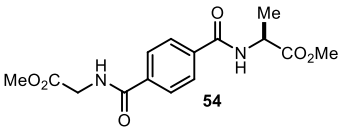

Methyl(4-((2-methoxy-2-oxoethyl) carbamoyl) benzoyl)-*L*-alaninate (54)

Prepared according to the general procedure A using methyl (4-bromobenzoyl)glycinate (27.2 mg, 0.1 mmol, 1.0 equiv.), the corresponding dihydropyridine **1-ala** (57.4 mg, 0.15 mmol, 1.5 equiv.), 4CzIPN (1.2 mg, 0.015 mmol, 1.5 mol%), $NiCl_2$·dme (1.1 mg, 0.005 mmol, 5 mol %), and dMeObpy (2.2 mg, 0.01 mmol, 10 mol %) in anhydrous THF (2.0 mL, 0.05 M). The crude material was purified by flash column chromatography (*n*-hexane/EtOAc 4:1) to give the corresponding amide **54** (28 mg, 87% yield, average of two runs) as a white solid. ^{1}H NMR (400 MHz, $CDCl_3$): δ 7.79 (s, 4H), 7.12 – 6.92 (m, 2H), 4.79 (quin, *J* = 7.2 Hz, 1H), 4.22 (qd, *J* = 18.3, 5.2 Hz, 2H), 3.79 (s, 3H), 3.78 (s, 3H), 1.52 (d, *J* = 7.2 Hz, 3H) ppm.

^{13}C NMR (101 MHz, $CDCl_3$): δ 173.7, 170.6, 166.7, 166.1, 136.6, 136.3, 127.4, 52.6, 52.5, 48.6, 41.7, 18.3 ppm.

HRMS (ESI, m/z) calcd. for C15H19N2O6 ([M+H]$^+$): 323.1238, found 323.1233.

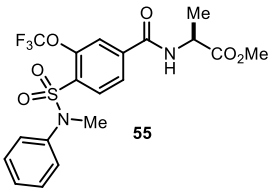

Methyl N-{4-[methyl(phenyl)sulfamoyl]-3-(trifluoromethoxy)benzoyl}-*L*-alaninate (55)

Prepared according to the general procedure B using 4-bromo-N-methyl-N-phenyl-2-(trifluoromethoxy)benzenesulfonamide (41.0 mg, 0.1 mmol, 1.0 equiv.), the corresponding dihydropyridine **1-ala** (57.4 mg, 0.15 mmol, 1.5 equiv.), 4CzIPN (1.2 mg, 0.015 mmol, 1.5 mol%), $NiCl_2$·dme (1.1 mg, 0.005 mmol, 5 mol %), dMeObpy (2.2 mg, 0.01 mmol, 10 mol %) and Na_2CO_3 (15.9 mg, 0.15 mmol, 1.5 equiv.) in anhydrous THF (2.0 mL, 0.05 M). The crude material was purified by flash column chromatography (cyclohexane/EtOAc 8:2) to give the corresponding amide **55** (24 mg, 52% yield) as a white solid.

^{1}H NMR (500 MHz, $CDCl_3$) δ 7.88-7.85 (m, 1H), 7.83-7.79 (m, 1H), 7.59 (dd, *J* = 8.2 Hz, 1H), 7.31-7.21 (m, 3H), 7.16-7.11 (m, 2H), 6.86 (br d, *J* = 7.0 Hz, 1H), 4.76 (quin, *J* = 7.0 Hz, 1H), 3.81 (s, 3H), 3.41 (s, 3H), 1.54 (d, *J* = 7.0 Hz, 3H) ppm.

^{13}C NMR (126 MHz, $CDCl_3$) δ 164.11, 146.37, 140.31, 139.81, 133.59, 132.55, 129.30, 127.78, 126.81, 124.00, 120.11, 52.83, 48.87, 39.18, 18.37 ppm.

HRMS (ESI, m/z) calcd. for $C_{19}H_{20}F_3N_2O_6$ ([M+H]$^+$): 461.0916, found 461.0996.

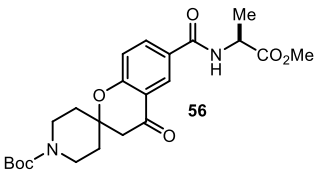

***tert*-Butyl 6-{[(2*S*)-1-methoxy-1-oxopropan-2-yl]carbamoyl}-4-oxo-3,4-dihydrospiro[[1]benzopyran-2,4'-piperidine]-1'-carboxylate (56)**

Prepared according to the general procedure B using *tert*-butyl 6-bromo-4-oxo-3,4-dihydro-1'H-spiro[chromene-2,4'-piperidine]-1'-carboxylate (79.3 mg, 0.2 mmol, 1.0 equiv.), the corresponding dihydropyridine **1-ala** (115 mg, 0.3 mmol, 1.5 equiv.), 4CzIPN (4.73 mg, 0.03 mmol, 3 mol%), $NiCl_2$·dme (2.20 mg, 0.01 mmol, 5 mol %), dMeObpy (4.33 mg, 0.02 mmol, 10 mol %) and Na_2CO_3 (31.8 mg, 0.3 mmol, 1.5 equiv.) in anhydrous 1,4-dioxane (3.5 mL, 0.057 M). The crude material was purified by flash column chromatography (cyclohexane/EtOAc 8:2) to give the corresponding amide **56** (33.4 mg, 38% yield) as a white solid.

^{1}H NMR (500 MHz, $CDCl_3$) δ 8.23 (d, *J* = 2.1 Hz, 1H), 8.06 (dd, *J* = 8.8, 2.4 Hz, 1H), 7.05 (d, *J* = 8.8 Hz, 1H), 6.91 (d, *J* = 7.3 Hz, 1H), 4.79 (quin, *J* = 7.2 Hz, 1H), 4.00-3.81 (m, 2H), 3.79 (s, 3H), 3.22 (br s, 2H), 2.76 (s, 2H), 2.06-1.96 (m, 2H), 1.71-1.58 (m, 2H), 1.53 (d, *J* = 7.0 Hz, 3H), 1.46 (s, 9H) ppm.

^{13}C NMR (126 MHz, $CDCl_3$) δ 173.63, 165.37, 161.38, 154.67, 135.96, 126.97, 124.99, 119.82, 118.95, 79.94, 78.79, 52.61, 48.55, 47.77, 34.07, 33.90, 28.43, 18.47 ppm (one signal overlapping).

HRMS (ESI, m/z) calcd. for $C_{23}H_{31}N_2O_7$ ([M+H]$^+$): 447.2131, found 447.2124.

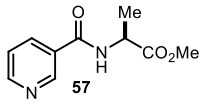

57

N-nicotinylalanine methyl ester (57)

Prepared according to the general procedure A using methyl 3-bromopyridine (9.63 µL, 15.8 mg, 0.1 mmol, 1.0 equiv.), the corresponding dihydropyridine **1-ala** (47.8 mg, 0.125 mmol, 1.25 equiv.), 4CzIPN (1.2 mg, 0.015 mmol, 1.5 mol%), $NiCl_2$·dme (1.1 mg, 0.005 mmol, 5 mol %), and dMeObpy (2.2 mg, 0.01 mmol, 10 mol %) in anhydrous THF (2.0 mL, 0.05 M). The crude material was purified by flash column chromatography (DCM/acetone 4:1) to give the corresponding amide **57** (12 mg, 58% yield) as a white solid that displayed spectroscopic data consistent with those reported previously.[8]

^{1}H NMR (400 MHz, $CDCl_3$) δ 9.02 (d, *J* = 2.1 Hz, 1H), 8.73 (dd, *J* = 5.0, 1.7 Hz, 1H), 8.12 (td, *J* = 7.9, 2.3 Hz, 1H), 7.39 (dd, *J* = 8.0, 4.9 Hz, 1H), 6.87 (d, *J* = 7.1 Hz, 1H), 4.80 (quin, *J* = 7.2 Hz, 1H), 3.80 (s, 3H), 1.54 (d, *J* = 7.2 Hz, 3H) ppm.

^{13}C NMR (101 MHz, $CDCl_3$) δ 173.4, 164.9, 152.5, 148.1, 135.1, 129.6, 123.45, 52.7, 48.60, 18.54 ppm.

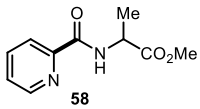

58

2-(*N*-(*1'*-Methoxycarbonyl-ethyl)-carboxamido)-pyridine (58)

Prepared according to the general procedure A using methyl 2-bromopyridine (9.54 µL, 15.8 mg, 0.1 mmol, 1.0 equiv.), the corresponding dihydropyridine **1-ala** (57.4 mg, 0.125 mmol, 1.25 equiv.), 4CzIPN (1.2 mg, 0.015 mmol, 1.5 mol%), $NiCl_2$·dme (1.1 mg, 0.005 mmol, 5 mol %), and dMeObpy (2.2 mg, 0.01 mmol, 10 mol %) in anhydrous THF (2.0 mL, 0.05 M). The crude material was purified by flash column chromatography (*n*-hexane/EtOAc 2:1) to give the corresponding amide **58** (11 mg, 54% yield, average of two runs) as a yellow oil that displayed spectroscopic data consistent with those reported previously.[8]

^{1}H NMR (300 MHz, $CDCl_3$) δ 8.58 (d, J = 4.8, 1H), 8.48 (br s, 1H), 8.18 (d, J = 7.8 Hz, 1H), 7.84 (td, J = 7.7, 1.7 Hz, 1H), 7.44 (dt, J = 4.8, 1.2 Hz, 1H), 4.80 (quin, J = 7.3 Hz, 1H), 3.78 (s, 3H), 1.55 (d, J = 7.2 Hz, 3H) ppm.

^{13}C NMR (75 MHz, $CDCl_3$) δ 173.2, 163.9, 149.4, 148.2, 137.3, 126.3, 122.3, 52.5, 48.1, 18.5 ppm.

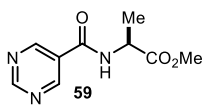

59

Methyl (pyrimidine-5-carbonyl)-*L*-alaninate (59)

Prepared according to the general procedure A using 5-bromopyrimidine (15.9 mg, 0.1 mmol, 1.0 equiv.), the corresponding dihydropyridine **1-ala** (57.4 mg, 0.15 mmol, 1.5 equiv.), 4CzIPN (1.2 mg, 0.015 mmol, 1.5

mol%), $NiCl_2$·dme (1.1 mg, 0.005 mmol, 5 mol %), and dMeObpy (2.2 mg, 0.01 mmol, 10 mol %) in anhydrous THF (2.0 mL, 0.05 M). The crude material was purified by flash column chromatography (DCM/EtOAc 2:3) to give the corresponding amide **59** (16 mg, 76% yield, average of two runs) as a white solid.

^{1}H NMR (400 MHz, $CDCl_3$): δ 9.30 (s, 1H), 9.12 (s, 2H), 7.07 (d, *J* = 7.3 Hz, 1H), 4.79 (quin, *J* = 7.2 Hz, 1H), 3.79 (s, 3H), 1.52 (d, *J* = 7.2 Hz, 3H) ppm.

^{13}C NMR (101 MHz, $CDCl_3$): δ 173.2, 162.9, 160.7, 155.7, 127.4, 52.8, 48.6, 18.4 ppm.

HRMS (ESI, m/z) calcd. for $C_9H_{10}N_3O_3$ ([M-H]$^-$): 208.0728, found 208.0735.

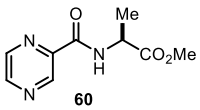

60

Methyl(pyrazine-2-carbonyl)-*L*-alaninate (60)

Prepared according to the general procedure A using 2-bromopyrazine (9.0 µL, 15.9 mg, 0.1 mmol, 1.0 equiv.), the corresponding dihydropyridine **1-ala** (57.4 mg, 0.15 mmol, 1.5 equiv.), 4CzIPN (1.2 mg, 0.015 mmol, 1.5 mol%), $NiCl_2$·dme (1.1 mg, 0.005 mmol, 5 mol %), and dMeObpy (2.2 mg, 0.01 mmol, 10 mol %) in anhydrous THF (2.0 mL, 0.05 M). Multiple purification by column chromatography resulted in poor separation from several byproducts. The yield (45%) of **60** were inferred by ^{1}H NMR analysis of the crude reaction mixture using trichloroethylene as the internal standard. An analytical amount of the pure compound was isolated by preparative TLC (n hexane/EtOAc 1:1) to obtain as a yellow oil that displayed spectroscopic data consistent with those reported previously.[23]

^{1}H NMR (300 MHz, $CDCl_3$): δ 9.39 (d, J = 1.5 Hz, 1H), 8.76 (d, J = 2.5 Hz, 1H), 8.56 (t, J = 1.3 Hz, 1H), 8.26 (br s, 1H), 4.81 (quin, J = 7.3 Hz, 1H), 3.80 (s, 3H), 1.56 (d, J = 7.1 Hz, 3H) ppm.

^{13}C NMR (75 MHz, $CDCl_3$): δ 172.9, 162.6, 147.5, 144.4, 144.1, 142.7, 52.6, 48.1, 18.4 ppm.

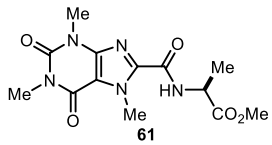

61

Methyl(1,3,7-trimethyl-2,6-dioxo-2,3,6,7-tetrahydro-1H-purine-8-carbonyl)-*L*-alaninate (61)

Prepared according to the general procedure A using 8-bromocaffeine (27.0 mg, 0.1 mmol, 1.0 equiv.), the corresponding dihydropyridine **1-ala** (57.4 mg, 0.15 mmol, 1.5 equiv.), 4CzIPN (1.2 mg, 0.015 mmol, 1.5 mol%), $NiCl_2$·dme (1.1 mg, 0.005 mmol, 5 mol %), and dMeObpy (2.2 mg, 0.01 mmol, 10 mol %) in anhydrous THF (2.0 mL, 0.05 M). The crude material was purified by flash column chromatography (DCM/EtOAc 9:1) to give the corresponding amide **61** (24 mg, 74% yield, average of two runs) as a white solid.

^{1}H NMR (400 MHz, $CDCl_3$) δ 7.82 (d, *J* = 7.8 Hz, 1H), 4.71 (quintet, *J* = 7.3 Hz, 1H), 4.37 (s, 3H), 3.79 (s, 3H), 3.57 (s, 3H), 3.40 (s, 3H), 1.54 (d, *J* = 7.2 Hz, 3H) ppm.

^{13}C NMR (101 MHz, $CDCl_3$) δ 172.7, 157.5, 155.6, 151.5, 146.2, 140.4, 110.3, 52.7, 48.0, 34.5, 29.8, 28.1, 18.2 ppm.

HRMS (ESI, m/z) calcd. for $C_{13}H_{16}N_5O_5$ ($[M-H]^-$): 322.1157, found 322.1155.

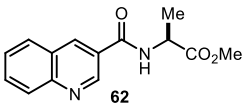

62

Methyl (quinoline-3-carbonyl)-*L*-alaninate (62)

Prepared according to the general procedure A using 3-bromoquinoline (14 μL, 21 mg, 0.1 mmol, 1.0 equiv.), the corresponding dihydropyridine **1-ala** (57.4 mg, 0.15 mmol, 1.5 equiv.), 4CzIPN (1.2 mg, 0.015 mmol, 1.5 mol%), $NiCl_2$·dme (1.1 mg, 0.005 mmol, 5 mol %), and dMeObpy (2.2 mg, 0.01 mmol, 10 mol %) in anhydrous THF (2.0 mL, 0.05 M). The crude material was purified by flash column chromatography (dichloromethane/acetone 5:1) to give the corresponding amide **62** (22 mg, 86% yield, average of two runs) as a white solid.

^{1}H NMR (400 MHz, $CDCl_3$): δ 9.29 (d, *J* = 2.3 Hz, 1H), 8.58 (dd, *J* = 2.3, 0.8 Hz, 1H), 8.13 (d, *J* = 8.6 Hz, 1H), 7.79 (ddd, *J* = 8.4, 6.9, 1.5 Hz, 1H), 7.59 (ddd, *J* = 8.1, 6.9, 1.2 Hz, 1H), 7.14 (d, *J* = 7.3 Hz, 1H), 4.87 (quin, *J* = 7.2 Hz, 1H), 3.81 (s, 3H), 1.57 (d, *J* = 7.2 Hz, 3H).ppm.

^{13}C NMR (101 MHz, $CDCl_3$): δ 173.6, 165.1, 149.3, 148.2, 135.7, 131.4, 129.3, 128.8, 127.56, 126.8, 126.4, 52.7, 48.7, 18.5.ppm.

HRMS (ESI, m/z) calcd. for $C_{14}H_{15}N_2O_3$ ($[M+H]^+$): 259.1077, found 259.1072.

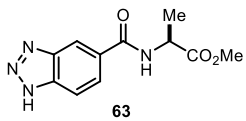

63

Methyl (1H-benzo[d][1,2,3]triazole-5-carbonyl)-*L*-alaninate (63)

Prepared according to the general procedure A using 5-bromo-1H-benzo[d][1,2,3]triazole (20 mg, 0.1 mmol, 1.0 equiv.), the corresponding dihydropyridine **1-ala** (57.4 mg, 0.15 mmol, 1.5 equiv.), 4CzIPN (1.2 mg, 0.015 mmol, 1.5 mol%), $NiCl_2$·dme (1.1 mg, 0.005 mmol, 5 mol %), and dMeObpy (2.2 mg, 0.01 mmol, 10 mol %) in anhydrous THF (2.0 mL, 0.05 M). The crude material was purified by flash column chromatography (n hexane/EtOAc 2:1) to give the corresponding amide **63** (13 mg, 52% yield, average of two runs) as a white solid.

^{1}H NMR (400 MHz, ($CDCl_3$): δ 8.07 (s, 1H), 7.89 (d, *J* = 8.2 Hz, 1H), 7.82 (d, *J* = 8.8 Hz, 1H), 7.55 (dd, *J* = 8.8, 1.7 Hz, 1H), 4.59 (quin, *J* = 7.3 Hz, 1H), 3.77 (s, 3H), 1.49 (d, *J* = 7.2 Hz, 3H)ppm.

^{13}C NMR (101 MHz, MeOD): δ 172.4, 159.6, 128.9, 119.2, 117.0, 116.2, 51.6, 48.29, 16.0 ppm.

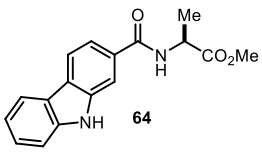

64

Methyl (9H-carbazole-2-carbonyl)-*L*-alaninate (64)

Prepared according to the general procedure A using 2-bromo-9H-carbazole (24.6 mg, 0.1 mmol, 1.0 equiv.), the corresponding dihydropyridine **1-ala** (57.4 mg, 0.15 mmol, 1.5 equiv.), 4CzIPN (1.2 mg, 0.015 mmol, 1.5 mol%), $NiCl_2$·dme (1.1 mg, 0.005 mmol, 5 mol %), and dMeObpy (2.2 mg, 0.01 mmol, 10 mol %) in anhydrous THF (2.0 mL, 0.05 M). Multiple purification by column chromatography (n-hexane/acetone 4:1) resulted in poor separation from several unidentified byproducts. An analytical amount of the pure compound was isolated for characterization (HPLC-MS on SunFire C18 column 100 x 4.6mm, 5µm, 50:50 H2O/MeCN, flow rate: 1 mL/min). The yield (70%) of **64** were inferred by ^{1}H NMR analysis of the crude reaction mixture using trichloroethylene as the internal standard.

^{1}H NMR (400 MHz, (CD_3CN): δ 9.55 (s, 1H), 8.17 – 8.13 (m, 2H), 8.00 – 7.99 (m, 1H), 7.66 (dd, *J* = 8.2, 1.5 Hz, 1H), 7.57 – 7.53 (m, 1H), 7.50 – 7.44 (m, 1H), 7.32 (s, 1H), 7.24 (ddd, *J* = 8.0, 7.1, 1.0 Hz, 1H), 4.63 (quin, *J* = 7.2 Hz, 1H), 3.72 (s, 3H), 1.50 (d, *J* = 7.3 Hz, 3H) ppm.

^{13}C NMR (101 MHz, MeOD): δ 173.7, 169.7, 141.3, 139.5, 130.6, 126.3, 125.8, 122.2, 120.2, 119.4, 118.8, 117.4, 110.6, 110.1, 51.4, 48.8, 15.9 ppm.

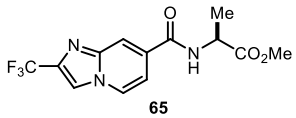

65

Methyl *N*-[2-(trifluoromethyl)imidazo[1,2-a]pyridine-7-carbonyl]-*L*-alaninate (65)

Prepared according to the general procedure B using 7-bromo-2-(trifluoromethyl)imidazo[1,2-a]pyridine (53.1 mg, 0.2 mmol, 1.0 equiv.), the corresponding dihydropyridine **1-ala** (115 mg, 0.3 mmol, 1.5 equiv.), 4CzIPN (4.73 mg, 0.03 mmol, 3 mol%), $NiCl_2$·dme (2.20 mg, 0.01 mmol, 5 mol %), dMeObpy (4.33 mg, 0.02 mmol, 10 mol %) and Na_2CO_3 (31.8 mg, 0.3 mmol, 1.5 equiv.) in anhydrous 1,4-dioxane (4 mL, 0.05 M). The crude material was purified by preparative HPLC (Method: Column: Reprosil C18; 10 µm; 125x30 mm / Flow rate: 75 ml/min / Eluent: A = H_2O (0,01% formic acid), B = acetonitrile / Gradient: 0.00-5.00 min = 10% B, 6.50 min = 20% B, 17.0-19.75 min = 100% B, 19.75.00-23.00min = 90% B) to give the corresponding amide **65** (27.4 mg, 43% yield) as a white solid.

^{1}H NMR (600 MHz, $CDCl_3$) δ 8.21 (d, *J* = 7.0 Hz, 1H), 8.10 (s, 1H), 7.97 (s, 1H), 7.40 (dd, *J* = 7.0, 1.6 Hz, 1H), 6.94 (br d, *J* = 5.7 Hz, 1H), 4.79 (quin, *J* = 7.1 Hz, 1H), 3.82 (s, 3H), 3.79-3.65 (m, 1H), 1.56 (d, *J* = 7.1 Hz, 3H) ppm.

^{13}C NMR (126 MHz, $CDCl_3$) δ 173.38, 164.42, 144.25, 137.56 (q, *J* = 39 Hz), 132.19, 126.34, 122.29 (q, *J* = 269 Hz), 117.34, 112.56, 112.43 (q, *J* = 3.8 Hz), 52.71, 48.84, 18.13 ppm.

HRMS (ESI, m/z) calcd. for $C_{13}H_{13}N_3O_3$ ($[M+H]^+$): 316.0904, found 316.0900.

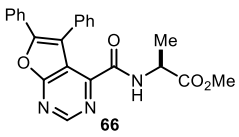

66

Methyl *N*-(5,6-diphenylfuro[2,3-d]pyrimidine-4-carbonyl)-*L*-alaninate (66)

Prepared according to the general procedure B using 4-chloro-5,6-diphenylfuro[2,3-d]pyrimidine (30.7 mg, 0.1 mmol, 1.0 equiv.), the corresponding dihydropyridine **1-ala** (57.4 mg, 0.15 mmol, 1.5 equiv.), 4CzIPN (2.37 mg, 0.03 mmol, 3 mol%), $NiCl_2$·dme (1.1 mg, 0.005 mmol, 5 mol %), dMeObpy (2.2 mg, 0.01 mmol, 10 mol %) and Na_2CO_3 (15.9 mg, 0.15 mmol, 1.5 equiv.) in anhydrous 1,4-dioxane (2.0 mL, 0.05 M). The crude material was purified by preparative HPLC (Method: Column: Reprosil C18; 10 µm; 125x30 mm / Flow rate: 75 ml/min / Eluent: A = H_2O (0,01% formic acid), B = acetonitrile / Gradient: 0.00-5.00 min = 10% B, 6.50 min = 20% B, 17.0-19.75 min = 100% B, 19.75.00-23.00min = 90% B) to give the corresponding amide **66** (13.9 mg, 35% yield) as a white solid.

^{1}H NMR (500 MHz, $CDCl_3$) δ 8.98 (s, 1H), 8.08 (br d, *J* = 7.9 Hz, 1H), 7.55-7.51 (m, 2H), 7.48-7.43 (m, 3H), 7.38-7.33 (m, 2H), 7.33-7.27 (m, 3H), 4.60 (quin, *J* = 7.3 Hz, 1H), 3.74 (s, 3H), 1.41 (d, *J* = 7.3 Hz, 3H) ppm.

^{13}C NMR (126 MHz, $CDCl_3$) δ 173.05, 167.33, 162.17, 153.33, 151.84, 150.93, 132.70, 130.13, 129.83, 128.68, 128.57, 128.45, 128.19, 127.82, 118.84, 116.32, 52.52, 47.94, 18.59 ppm.

HRMS (ESI, m/z) calcd. for $C_{23}H_{20}N_3O_4$ ($[M+H]^+$): 402.1448, found 402.1444.

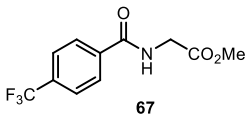

67

Methyl N-(4-trifluoromethylbenzoyl)glycine (67)

Prepared according to the general procedure A using 4-bromobenzotrifluoride (14 µL, 0.1 mmol, 1.0 equiv.), the corresponding dihydropyridine **1b** (55.3 mg, 0.15 mmol, 1.5 equiv.), 4CzIPN (1.2 mg, 0.015 mmol, 1.5 mol%), $NiCl_2$·dme (1.1 mg, 0.005 mmol, 5 mol %), and dMeObpy (2.2 mg, 0.01 mmol, 10 mol %) in anhydrous THF (2.0 mL, 0.05 M). The crude material was purified by flash column chromatography (*n*-hexane/EtOAc gradient 8:1 to 4:1) to give the corresponding amide **67** (25 mg, 94% yield, average of two runs) as a white solid that displayed spectroscopic data consistent with those reported previously.[9]

^{1}H NMR (400 MHz, $CDCl_3$): δ 7.92 (d, *J* = 8.3 Hz 2H), 7.71 (d, *J* = 8.3 Hz, 2H), 6.77 (bs, 1H), 4.26 (d, *J* = 5.0 Hz, 2H), 3.82 (s, 3H) ppm.

^{13}C NMR (101 MHz, $CDCl_3$): δ 170.3, 166.1, 136.9, 133.5 (q, *J*= 32 Hz), 127.6, 125.7 (q, *J* = 3.7 Hz), 123.6 (d, *J* = 272.5 Hz), 52.6, 41.8 ppm.

^{19}F NMR (376 MHz, $CDCl_3$): δ -63.12 ppm.

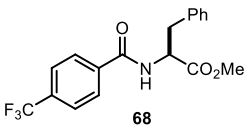

68

N-(4-trifluoromethylbenzoyl)phenylalanine methyl ester (68)

Prepared according to the general procedure A using 4-bromobenzotrifluoride (14 µL, 0.1 mmol, 1.0 equiv.), the corresponding dihydropyridine **1c** (68.7 mg, 0.15 mmol, 1.5 equiv.), 4CzIPN (1.2 mg, 0.015 mmol, 1.5 mol%), $NiCl_2$·dme (1.1 mg, 0.005 mmol, 5 mol %), and dMeObpy (2.2 mg, 0.01 mmol, 10 mol %) in anhydrous THF (2.0 mL, 0.05 M). The crude material was purified by flash column chromatography (*n*-hexane/DCM 1:1 to pure DCM) to give the corresponding amide **68** (29 mg, 83% yield, average of two runs) as a white solid.

^{1}H NMR (400 MHz, $CDCl_3$): δ 7.80 (d, *J* = 8.1 Hz 2H), 7.66 (d, *J* = 8.4 Hz, 2H), 7.32 – 7.23 (m, 3H), 7.16 – 7.11 (m, 2H), 6.73 (d, *J* = 7.2 Hz, 1H) 5.09 (d, *J* = 7.6, 5.7 Hz, 1H), 3.79 (s, 3H), 3.34 – 3.19 (m, 2H) ppm.

^{13}C NMR (101 MHz, $CDCl_3$): δ 171.9, 165.6, 137.1, 135.7, 133.5 (q, *J*= 32 Hz), 129.3, 128.7, 127.5, 127.3, 125.6 (q, *J* = 3.8 Hz), 123.62 (d, *J* = 272.5 Hz) 53.6, 52.5, 37.7 ppm.

^{19}F NMR (376 MHz, $CDCl_3$): δ -63.12 ppm.

HRMS (ESI, m/z) calcd. for $C_{18}H_{15}F_3NO_3$ ($[M-H]^-$): 350.1010, found 350.1010.

$[\alpha]D^{26}$ = +77.8 (c = 0.50, $CHCl_3$). Reference compound: $[\alpha]D^{26}$ = +78.2 (c = 0.50, $CHCl_3$).

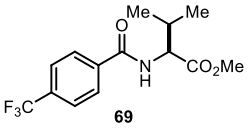

69

Methyl-3-methyl-2-[4(trifluoromethyl)benzamido] butanoate (69)

Prepared according to the general procedure A using 4-bromobenzotrifluoride (14 µL, 0.1 mmol, 1.0 equiv.), the corresponding dihydropyridine **1d** (49.3 mg, 0.12 mmol, 1.2 equiv.), 4CzIPN (1.2 mg, 0.015 mmol, 1.5 mol%), $NiCl_2$·dme (1.1 mg, 0.005 mmol, 5 mol %), and dMeObpy (2.2 mg, 0.01 mmol, 10 mol %) in anhydrous THF (2.0 mL, 0.05 M). The crude material was purified by flash column chromatography (*n*-hexane/DCM 1:1 to pure DCM) to give the corresponding amide **69** (28 mg, 92% yield. average of two runs) as a white solid that displayed spectroscopic data consistent with those reported previously.[10]

^{1}H NMR (400 MHz, $CDCl_3$): δ 7.91 (d, *J* = 8.5 Hz, 1H), 7.70 (d, *J* = 8.3 Hz, 1H), 6.73 (d, *J* = 8.6 Hz, 1H), 4.80 (dd, *J* = 8.6, 4.9 Hz, 1H), 3.81 (s, 3H), 2.31 (m, 1H), 1.01 (d, *J* = 6.9 Hz, 3H), 1.01 (d, *J* = 6.9 Hz, 3H) ppm.

^{13}C NMR (101 MHz, $CDCl_3$): δ 172.5, 166.0, 137.4, 133.5 (q, *J*= 32 Hz), 127.6, 125.7 (q, *J*= 3.8 Hz), 123.6 (q, *J*= 274 Hz), 57.6, 52.4, 31.6, 18.9, 17.9 ppm.

^{19}F NMR (376 MHz, $CDCl_3$): δ -63.11 ppm.

$[\alpha]D^{26}$ = +28.1 (c = 0.50, CH_2Cl_2). Reference compound: $[\alpha]D^{26}$ = +29.5 (c = 0.51, CH_2Cl_2).

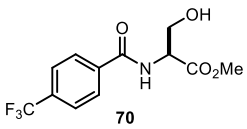

70

N-(4-trifluoromethylbenzoyl)serine methyl ester (70)

Prepared according to the general procedure A using 4-bromobenzotrifluoride (14 µL, 0.1 mmol, 1.0 equiv.), the corresponding dihydropyridine **1e** (59.8 mg, 0.15 mmol, 1.5 equiv.), 4CzIPN (1.2 mg, 0.015 mmol, 1.5 mol%), $NiCl_2$·dme (1.1 mg, 0.005 mmol, 5 mol %), and dMeObpy (2.2 mg, 0.01 mmol, 10 mol %) in anhydrous THF (2.0 mL, 0.05 M). The crude material was purified by flash column chromatography (*n*-hexane/EtOAc 1:1) to give the corresponding amide **70** (15 mg, 52% yield, average of two runs) as a white solid.

^{1}H NMR (400 MHz, $CDCl_3$): δ 7.94 (d, *J* = 8.1 Hz, 2H), 7.71 (d, *J* = 8.3 Hz, 2H), 7.17 (d, *J* = 7.3 Hz, 1H), 4.88 (dt, *J* = 7.1, 3.5 Hz, 1H), 4.12 (dd, *J* = 11.2, 3.6 Hz, 1H), 4.06 (dd, *J* = 11.2, 3.4 Hz, 1H), 3.84n(s, 3H).

^{13}C NMR (101 MHz, $CDCl_3$): δ 170.8, 166.3, 136.8, 133.7 (q, *J* = 33 Hz), 127.7, 125.7 (q, *J*= 3.7 Hz), 123.6 (q, *J*= 272 Hz), 63.3, 55.1, 53.0 ppm.

^{19}F NMR (376 MHz, $CDCl_3$): δ -63.13 ppm.

HRMS (ESI, m/z) calcd. for $C_{12}H_{11}F_3NO_4$ ($[M-H]^-$): 290.0646, found 290.0652.

$[\alpha]D^{26}$ = +37.7 (c = 0.36, CH_2Cl_2). Reference compound: $[\alpha]D^{26}$ = +33.8 (c = 0.49, CH_2Cl_2).

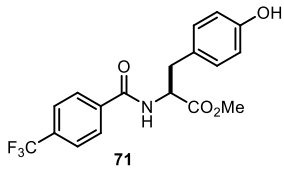

71

Methyl 3-(4-hydroxyphenyl)-2-{[4-(trifluoromethyl) benzoyl]amino}propanoate (71)

Prepared according to the general procedure using A 4-bromobenzotrifluoride (14 µL, 0.1 mmol, 1.0 equiv.), the corresponding dihydropyridine **1f** (71.2 mg, 0.15 mmol, 1.5 equiv.), 4CzIPN (1.2 mg, 0.015 mmol, 1.5 mol%), $NiCl_2$·dme (1.1 mg, 0.005 mmol, 5 mol %), and dMeObpy (2.2 mg, 0.01 mmol, 10 mol %) in anhydrous THF (2.0 mL, 0.05 M). Multiple purification by column chromatography (*n*-hexane/EtOAc 2:1) resulted in poor separation from several unidentified byproducts. An analytical amount of the pure compound was isolated for characterization (HPLC-MS on SunFire C18 column 100 x 4.6mm, 5µm, 40:60 H_2O/MeOH, flow rate: 1 mL/min, APCI +/-). The yield (60%) of **71** were inferred by ^{1}H NMR analysis of the crude reaction mixture using trichloroethylene as the internal standard.

^{1}H NMR (400 MHz, CD_3CN): δ 7.88 (d, *J* = 7.5 Hz, 1H), 7.76 (d, *J* = 8.5 Hz, 1H), 7.29 (d, *J* = 7.9 Hz, 1H), 7.08 (d, *J* = 8.6 Hz, 1H), 6.72 (d, *J* = 8.5 Hz, 1H), 4.78 (td, J = 8.3, 5.6 Hz, 1H), 3.69 (s, 3H), 3.16 (dd, *J* = 14.0, 5.6 Hz, 1H), 3.02 (dd, *J* = 14.0, 8.6 Hz, 1H) ppm.

^{13}C NMR (101 MHz, MeOD): δ 172.2, 167.5, 156.0, 137.6, 129.8, 127.8, 127.6, 125.1 (q, *J* = 3.9 Hz), 114.9, 54.8, 51.4, 35.9 ppm.

^{19}F NMR (376 MHz, $CDCl_3$): δ -63.11 ppm.

HRMS (ESI, m/z) calcd. for $C_{18}H_{15}F_3NO_4$ ([M-H]$^-$): 366.0959, found 366.0955.

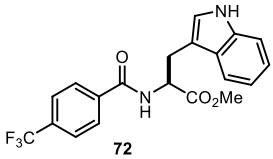

72

Methyl (4-(trifluoromethyl)benzoyl)-*L*-tryptophanate (72)

Prepared according to the general procedure using A 4-bromobenzotrifluoride (14 µL, 0.1 mmol, 1.0 equiv.), the corresponding dihydropyridine **1g** (75 mg, 0.15 mmol, 1.5 equiv.), 4CzIPN (1.2 mg, 0.015 mmol, 1.5 mol%), $NiCl_2$·dme (1.1 mg, 0.005 mmol, 5 mol %), and dMeObpy (2.2 mg, 0.01 mmol, 10 mol %) in anhydrous THF (2.0 mL, 0.05 M). The crude material was purified by flash column chromatography (*n*-hexane/EtOAc 2:1) to give the corresponding amide **72** (20 mg, 51% yield, average of two runs) as a pale yellow solid.

^{1}H NMR (400 MHz, $CDCl_3$): δ 8.18 (s, 1H), 7.78 (d, *J* = 8.3 Hz, 2H), 7.66 (d, *J* = 8.2 Hz, 2H), 7.56 (d, *J* = 8.1 Hz, 1H), 7.39 (d, *J* = 8.4 Hz, 1H), 7.23 (t, *J* = 7.5 Hz, 1H), 7.11 (t, *J* = 7.4 Hz 1H), 7.03 (d, *J* = 2.4 Hz, 1H), 6.71 (d, *J* = 7.7 Hz, 1H), 5.17 (dt, *J* = 7.7, 5.1 Hz, 1H), 3.78 (s, 3H), 3.57 – 3.43 (m, 2H) ppm.

^{13}C NMR (101 MHz, $CDCl_3$): δ 172.1, 165.6, 137.1, 136.1, 133.4 (d, *J*= 33 Hz), 127.7, 127.6, 125.6 (q, *J* = 3.7 Hz), 122.8, 122.5, 119.9, 118.6, 111.4, 109.9, 53.7, 52.6, 27.5 ppm.

^{19}F NMR (376 MHz, $CDCl_3$): δ -63.08 ppm.

HRMS (ESI, m/z) calcd. for $C_{20}H_{16}F_3N_2O_3$ ([M-H]$^-$): 389.1119, found 389.1121

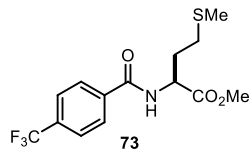

73

N-(4-trifluoromethylbenzoyl)methionine methyl ester (73)

Prepared according to the general procedure A using 4-bromobenzotrifluoride (14 µL, 0.1 mmol, 1.0 equiv.), the corresponding dihydropyridine **1h** (66 mg, 0.15 mmol, 1.5 equiv.), 4CzIPN (1.2 mg, 0.015 mmol, 1.5 mol%), $NiCl_2$·dme (1.1 mg, 0.005 mmol, 5 mol %), and dMeObpy (2.2 mg, 0.01 mmol, 10 mol %) in anhydrous THF (2.0 mL, 0.05 M). The crude material was purified by flash column chromatography (*n*-hexane/EtOAc 4:1, average of two runs) to give the corresponding amide **73** (29 mg, 86% yield) as a white solid.

^{1}H NMR (400 MHz, $CDCl_3$): δ 7.92 (d, *J* = 8.1 Hz, 2H), 7.70 (d, *J* = 8.1 Hz, 2H), 7.11 (d, *J* = 7.6 Hz, 1H), 4.93 (td, *J* = 7.2, 4.9 Hz, 1H), 3.80 (s, 3H), 2.60 (t, *J* = 7.2, 2H), 2.30 (m, 1H), 2.20 – 2.10 (m, 1H) 2.11 (s, 3H) ppm.

^{13}C NMR (101 MHz, $CDCl_3$): δ 172.4, 166.7, 136.9, 133.5 (q, *J* = 32 Hz), 127.6, 125.7 (q, *J* = 3.7 Hz), 123.6 (q, *J* = 273 Hz), 52.8, 52.3, 31.3, 30.1, 15.6 ppm.

^{19}F NMR (376 MHz, $CDCl_3$): δ -63.11 ppm.

HRMS (ESI, m/z) calcd. for $C_{14}H_{15}F_3NO_3S$ ([M-H]$^-$): 334.0730, found 334.0740.

[α]D^{26} = +23.8 (c = 0.48, CH_2Cl_2). Reference compound: [α]D^{26} = +23.2 (c = 0.50, CH_2Cl_2).

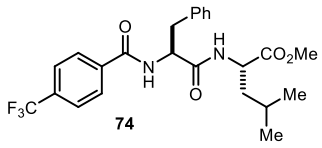

74

N-(4-trifluoromethylbenzoyl)-L-phenylalanine-L-leucine methyl ester (74)

Prepared according to the general procedure A using 4-bromobenzotrifluoride (14 µL, 0.1 mmol, 1.0 equiv.), the corresponding dihydropyridine **1i** (86 mg, 0.15 mmol, 1.5 equiv.), 4CzIPN (1.2 mg, 0.015 mmol, 1.5 mol%), $NiCl_2$·dme (1.1 mg, 0.005 mmol, 5 mol %), and dMeObpy (2.2 mg, 0.01 mmol, 10 mol %) in anhydrous THF (2.0 mL, 0.05 M). The crude material was purified by flash column chromatography (*n*-hexane/EtOAc 4:1) to give the corresponding amide **74** (39 mg, 84% yield, average of two runs) as a white solid.

^{1}H NMR (400 MHz, $CDCl_3$): δ 7.81 (d, *J* = 7.9 Hz, 2H), 7.62 (d, *J* = 8.2 Hz, 2H), 7.41 (d, *J* = 7.7 Hz, 1H), 7.29 – 7.19 (m, 5H), 6.62 (d, *J* = 7.9 Hz, 1H), 4.98 (q, *J* = 7.1 Hz, 1H), 4.55 (td, *J* = 8.3, 5.3 Hz, 1H), 3.71 (s, 3H), 3.27 – 3.13 (m, 2H), 1.66 – 1.43 (m, 3H), 0.86 (d, *J* = 6.2 Hz, 6H) ppm.

^{13}C NMR (101 MHz, $CDCl_3$) δ 172.7, 170.9, 165.8, 136.9, 136.4, 133.4 (q, *J* = 32.8 Hz), 129.4, 128.6, 127.6, 127.1, 125.5 (q, *J* = 3.7 Hz), 123.6 (q, *J* = 272.6 Hz), 54.9, 52.3, 51.1, 41.3, 38.4, 24.8, 22.6, 21.8 ppm.

^{19}F NMR (376 MHz, $CDCl_3$) δ -63.14 ppm.

HRMS (ESI, m/z) calcd. for $C_{24}H_{26}F_3N_2O_4$ ($[M-H]^-$): 463.1850, found 463.1849.

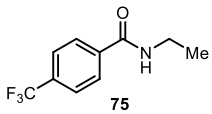

75

N-ethyl-4-(trifluoromethyl)benzamide (75)

Prepared according to the general procedure A using 4 bromobenzotrifluoride (14 µL, 0.1 mmol, 1.0 equiv.), the corresponding dihydropyridine **1j** (48.7 mg, 0.15 mmol, 1.5 equiv.), 4CzIPN (1.2 mg, 0.015 mmol, 1.5 mol%), $NiCl_2$·dme (1.1 mg, 0.005 mmol, 5 mol %), and dMeObpy (2.2 mg, 0.01 mmol, 10 mol %) in anhydrous THF (2.0 mL, 0.05 M). The crude material was purified by flash column chromatography (*n*-hexane/EtOAc 4:1) to give the corresponding amide **75** (20 mg, 92% yield, average of two runs) as a white solid that displayed spectroscopic data consistent with those reported previously.[11]

^{1}H NMR (400 MHz, $CDCl_3$): δ 7.86 (d, *J* = 8.2 Hz, 2H), 7.67 (d, *J* = 8.3 Hz, 2H), 6.27 (s, 1H), 3.50 (qd, *J* = 7.3, 5.6 Hz, 2H), 1.26 (t, *J* = 7.3 Hz, 3H) ppm.

^{13}C NMR (101 MHz, $CDCl_3$): δ 166.2, 138.1, 133.1 (q, *J* = 32.8 Hz), 127.3, 125.6 (q, *J* = 3.8 Hz), 123.7 (q, *J* = 273 Hz), 35.1, 14.8 ppm.

^{19}F NMR (376 MHz, $CDCl_3$): δ -63.05 ppm.

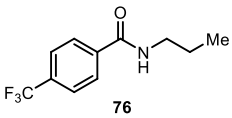

76

N-propyl-4-(trifluoromethyl)benzamide (76)

Prepared according to the general procedure A using 4 bromobenzotrifluoride (14 µL, 0.1 mmol, 1.0 equiv.), the corresponding dihydropyridine **1k** (50.8 mg, 0.15 mmol, 1.5 equiv.), 4CzIPN (1.2 mg, 0.015 mmol, 1.5 mol%), $NiCl_2$·dme (1.1 mg, 0.005 mmol, 5 mol %), and dMeObpy (2.2 mg, 0.01 mmol, 10 mol %) in anhydrous THF (2.0 mL, 0.05 M). The crude material was purified by flash column chromatography (*n*-hexane/EtOAc 6:1 to 4:1) to give the corresponding amide **76** (20mg, 88% yield, average of two runs) as a white solid.

^{1}H NMR (400 MHz, $CDCl_3$): δ 7.86 (d, *J* = 8.1 Hz, 2H), 7.68 (d, *J* = 8.2 Hz, 2H), 6.27 (s, 1H), 3.46 – 3.39 (m, 2H), 1.65 (dq, *J* = 13.7, 6.9, 6.5 Hz, 2H), 0.99 (t, *J* = 7.4 Hz, 3H).

^{13}C NMR (126 MHz, $CDCl_3$): δ 166.7, 138.5, 133.4 (q, *J* = 32.5 Hz), 127.3, 125.9 (q, *J* = 3.7 Hz), 124.0 (q, *J* = 273 Hz), 42.3, 23.2, 11.7 ppm.

^{19}F NMR (376 MHz, $CDCl_3$): δ -63.05 ppm.

HRMS (ESI, m/z) calcd. for $C_{11}H_{13}F_3NO$ ($[M+H]^+$): 232.0944, found 232.0939.

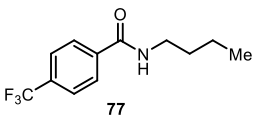

77

N-butyl-4-(trifluoromethyl)benzamide (77)

Prepared according to the general procedure A using 4-bromobenzotrifluoride (14 µL, 0.1 mmol, 1.0 equiv.), the corresponding dihydropyridine **1l** (52.9 mg, 0.15 mmol, 1.5 equiv.), 4CzIPN (1.2 mg, 0.015 mmol, 1.5 mol%), $NiCl_2$·dme (1.1 mg, 0.005 mmol, 5 mol %), and dMeObpy (2.2 mg, 0.01 mmol, 10 mol %) in anhydrous THF (2.0 mL, 0.05 M). The crude material was purified by flash column chromatography (*n*-hexane/DCM 1:1 to pure DCM) to give the corresponding amide **77** (23.2 mg, 95% yield, average of two runs) as a white solid that displayed spectroscopic data consistent with those reported previously.[12]

^{1}H NMR (400 MHz, $CDCl_3$): δ 7.85 (d, *J* = 8.1 Hz, 2H), 7.67 (d, *J* = 8.2 Hz, 2H), 6.31 (s, 1H), 3.46 (td, *J* = 7.2, 5.7 Hz, 2H), 1.65 – 1.55 (m, 2H), 1.46 – 1.35 (m, 2H), 0.96 (t, *J* = 7.3 Hz, 3H) ppm.

^{13}C NMR (101 MHz, $CDCl_3$): δ 165.3, 138.2, 133.1 (q, *J* =32.7 Hz), 127.3, 125.6 (q, *J* = 3.7 Hz), 123.7 (q, *J* = 273 Hz), 42.0, 31.6, 20.1, 13.7 ppm.

^{19}F NMR (376 MHz, $CDCl_3$): δ -63.06 ppm.

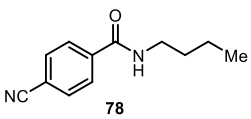

78

N-butyl-4-cyanobenzamide (78)

Prepared according to the general procedure A using 1-bromo-4-cyanobenzene (18.2 mg, 0.1 mmol, 1.0 equiv.), the corresponding dihydropyridine **78** (52.9 mg, 0.15 mmol, 1.5 equiv.), 4CzIPN (1.2 mg, 0.015 mmol, 1.5 mol%), $NiCl_2$·dme (1.1 mg, 0.005 mmol, 5 mol %), and dMeObpy (2.2

mg, 0.01 mmol, 10 mol %) in anhydrous THF (2.0 mL, 0.05 M). The crude material was purified by flash column chromatography (*n*-hexane/EtOAc 4:1 to 2:1) to give the corresponding amide **78** (18 mg, 89% yield) as a white solid that displayed spectroscopic data consistent with those reported previously.[13]

^{1}H NMR (500 MHz, ($CDCl_3$) δ 7.85 (d, *J* = 8.6 Hz, 1H), 7.71 (d, *J* = 8.6 Hz, 1H), 6.30 (s, 1H), 3.45 (td, *J* = 7.2, 5.7 Hz, 2H), 1.63 – 1.56 (m, 2H), 1.45 – 1.36 (m, 2H), 0.95 (t, *J* = 7.4 Hz, 2H) ppm.

^{13}C NMR (126 MHz, $CDCl_3$) δ 166.1, 139.1, 132.8, 127.9, 118.4, 115.3, 40.5, 31.9, 20.5, 14.1 ppm.

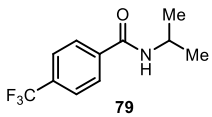

79

N-isopropyl-4-(trifluoromethyl)benzamide (79)

Prepared according to the general procedure A using 4-bromobenzotrifluoride (14 µL, 0.1 mmol, 1.0 equiv.), the corresponding dihydropyridine **1m** (40.6 mg, 0.12 mmol, 1.2 equiv.), 4CzIPN (1.2 mg, 0.015 mmol, 1.5 mol%), $NiCl_2$·dme (1.1 mg, 0.005 mmol, 5 mol %), and dMeObpy (2.2 mg, 0.01 mmol, 10 mol %) in anhydrous THF (2.0 mL, 0.05 M). The crude material was purified by flash column chromatography (n-hexane/DCM 1:1 to pure DCM) to give the corresponding amide **79** (19 mg, 80% yield, average of two runs) as a white solid that displayed spectroscopic data consistent with those reported previously.[14]

^{1}H NMR (400 MHz, $CDCl_3$): δ 7.85 (d, *J* = 8.2 Hz, 1H), 7.67 (d, *J* = 8.3 Hz, 2H), 6.01 (br s, 1H), 4.35 – 4.22 (m, 1H), 1.28 (d, *J* = 6.6 Hz, 6H).

^{13}C NMR (101 MHz, $CDCl_3$): δ 165.4, 138.3, 133.04 (q, *J* = 32.7 Hz), 127.3, 125.6 (q, *J* = 3.8 Hz), 123.6 (q, *J* = 273 Hz), 42.2, 22.8 ppm.

^{19}F NMR (376 MHz, $CDCl_3$): δ -63.03 ppm.

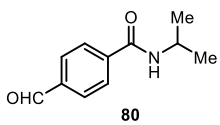

80

4-formyl-N-isopropyl-benzamide (80)

Prepared according to the general procedure A using 4-bromobenzaldehyde (18.5 mg, 0.1 mmol, 1.0 equiv.), the corresponding dihydropyridine **1m** (50.8 mg, 0.15 mmol, 1.5 equiv.), 4CzIPN (1.2 mg, 0.015 mmol, 1.5 mol%), $NiCl_2$·dme (1.1 mg, 0.005 mmol, 5 mol %), and dMeObpy (2.2 mg, 0.01 mmol, 10 mol %) in anhydrous THF (2.0 mL, 0.05 M). Multiple purification by column chromatography resulted in poor separation from several byproducts. The yield (55%) of **80** were inferred by 1H NMR analysis of the crude reaction mixture using trichloroethylene as the internal standard. An analytical amount of the pure compound was isolated by preparative TLC (n hexane/EtOAc 4:1) to obtain a white solid that displayed spectroscopic data consistent with those reported previously.[15]

^{1}H NMR (400 MHz, $CDCl_3$): δ 10.07 (s, 1H), 7.92 (q, *J* = 8.5 Hz, 4H), 6.00 (s, 1H), 4.37 – 4.23 (m, 1H), 1.29 (d, *J* = 6.6 Hz, 6H) ppm.

^{13}C NMR (101 MHz, $CDCl_3$): δ 191.5, 165.6, 140.2, 138.1, 129.8, 127.6, 42.3, 22.8 ppm.

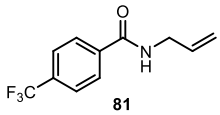

81

N-isopropyl-4-(trifluoromethyl)benzamide (81)

Prepared according to the general procedure A using 4-bromobenzotrifluoride (14 μL, 0.1 mmol, 1.0 equiv.), the corresponding dihydropyridine **1n** (40.4 mg, 0.12 mmol, 1.2 equiv.), 4CzIPN (1.2 mg, 0.015 mmol, 1.5 mol%), $NiCl_2$·dme (1.1 mg, 0.005 mmol, 5 mol %), and dMeObpy (2.2 mg, 0.01 mmol, 10 mol %) in anhydrous THF (2.0 mL, 0.05 M). The crude material was purified by flash column chromatography (*n*-hexane/EtOAc 4:1)) to give the corresponding amide **81** (15 mg, 65% yield) as a white solid.

^{1}H NMR (400 MHz, $CDCl_3$): δ 7.91 – 7.87 (m, 2H), 7.72 – 7.67 (m, 2H), 6.29 (br s, 1H), 5.94 (m, 1H), 5.35 – 5.17 (m, 2H), 4.10 (tt, *J* = 5.8, 1.5 Hz, 2H).

^{13}C NMR (101 MHz, $CDCl_3$): δ 166.0, 137.7, 133.7, 133.3 (q, *J* = 32.9 Hz), 127.4, 125.7 (q, *J* = 3.7 Hz), 123.7 (q, *J* = 271 Hz), 117.1, 42.6 ppm.

^{19}F NMR (376 MHz, $CDCl_3$): δ -63.07 ppm.

HRMS (ESI, m/z) calcd. for $C_{11}H_9F_3NO$ ($[M-H]^-$): 228.0642, found 228.0638.

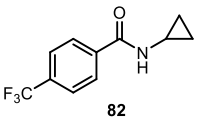

82

N-cyclopropyl 4-trifluoromethylbenzamide (82)

Prepared according to the general procedure A using 4-bromobenzotrifluoride (14 μL, 0.1 mmol, 1.0 equiv.), the corresponding dihydropyridine **1o** (50.5 mg, 0.15 mmol, 1.5 equiv.), 4CzIPN (1.2 mg, 0.015 mmol, 1.5 mol%), $NiCl_2$·dme (1.1 mg, 0.005 mmol, 5 mol %), and dMeObpy (2.2 mg, 0.01 mmol, 10 mol %) in anhydrous THF (2.0 mL, 0.05 M). The crude material was purified by flash column chromatography (*n*-hexane/EtOAc 4:1) to give the corresponding amide **82** (22.5 mg, 99% yield, average of two runs) as a white solid

^{1}H NMR (400 MHz, $CDCl_3$): δ 7.86 (d, *J* = 8.1 Hz, 2H), 7.67 (d, *J* = 8.4 Hz, 2H), 6.56 (s, 1H), 2.92 (tq, *J* = 7.2, 3.7 Hz, 1H), 0.94 – 0.84 (m, 2H), 0.70 – 0.62 (m, 1H).

^{13}C NMR (101 MHz, $CDCl_3$): δ 167.7, 137.7, 133.2 (q, *J* = 32.8 Hz), 127.4, 125.4 (q, *J* = 3.7 Hz), 123.6 (q, *J* = 273 Hz), 23.3, 6.7 ppm.

^{19}F NMR (376 MHz, $CDCl_3$): δ -63.09 ppm.

HRMS (ESI, m/z) calcd. for C11H9F3NO ($[M-H]^-$): 228.0642, found 228.0643.

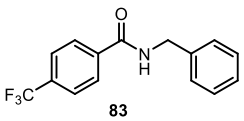

83

N-benzyl 4-trifluoromethylbenzamide (83)

Prepared according to the general procedure A using 4-bromobenzotrifluoride (14 µL, 0.1 mmol, 1.0 equiv.), the corresponding dihydropyridine **1p** (58.0 mg, 0.15 mmol, 1.5 equiv.), 4CzIPN (1.2 mg, 0.015 mmol, 1.5 mol%), $NiCl_2$·dme (1.1 mg, 0.005 mmol, 5 mol %), and dMeObpy (2.2 mg, 0.01 mmol, 10 mol %) in anhydrous THF (2.0 mL, 0.05 M). The crude material was purified by flash column chromatography (*n*-hexane/DCM 1:1 to pure DCM) to give the corresponding amide **83** (26 mg, 92% yield, average of two runs) as a white solid that displayed spectroscopic data consistent with those reported previously.[16]

^{1}H NMR (400 MHz, $CDCl_3$) δ 7.89 (d, *J* = 7.2 Hz, 2H), 7.68 (d, *J* = 8.4 Hz, 2H), 7.39 – 7.28 (m, 5H), 6.58 (s, 1H), 4.64 (d, *J* = 5.7 Hz, 2H) ppm.

^{13}C NMR (101 MHz, $CDCl_3$) δ 166.1, 137.7, 133.2 (q, *J* = 32.5 Hz), 128.9, 127.9, 127.8, 127.5, 125.7 (q, *J* = 3.7 Hz), 123.6 (q, *J* = 273 Hz), 44.3 ppm.

^{19}F NMR (376 MHz, $CDCl_3$) δ -63.07 ppm.

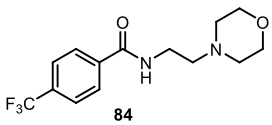

84

N-(2-morpholinoethyl)-4-(trifluoromethyl)benzamide (84)

Prepared according to the general procedure A using 4-bromobenzotrifluoride (14 µL, 0.1 mmol, 1.0 equiv.), the corresponding dihydropyridine **1q** (49.1 mg, 0.12 mmol, 1.2 equiv.), 4CzIPN (1.2 mg, 0.015 mmol, 1.5 mol%), $NiCl_2$·dme (1.1 mg, 0.005 mmol, 5 mol %), and dMeObpy (2.2 mg, 0.01 mmol, 10 mol %) in anhydrous THF (2.0 mL, 0.05 M). The crude material was purified by flash column chromatography (DCM/MeOH 98:2) to give the corresponding amide **84** (18 mg, 62% yield, average of two runs) as a white solid.

^{1}H NMR (500 MHz, $CDCl_3$): δ 7.88 (d, *J* = 8.1 Hz, 2H), 7.70 (d, *J* = 8.1 Hz, 2H), 6.88 (s, 1H), 3.73 (t, *J* = 4.7 Hz, 4H), 3.61 – 3.52 (m, 2H), 2.62 (t, *J* = 6.0 Hz, 2H), 2.52 (t, *J* = 4.6 Hz, 4H).

^{13}C NMR (101 MHz, $CDCl_3$): δ 166.1, 137.8, 133.2 (q, *J* = 32.7 Hz), 127.4, 125.6 (q, *J* = 3.8 Hz), 123.7 (q, *J* = 272.6 Hz), 66.9, 56.8, 53.3, 36.1 ppm.

^{19}F NMR (376 MHz, $CDCl_3$): δ -62.66 ppm.

HRMS (ESI, m/z) calcd. for $C_{14}H_{16}F_3N_2O_2$ ($[M-H]^-$): 301.1169, found 301.1164.

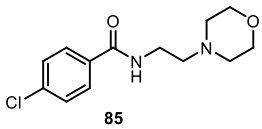

85

4-Chloro-N-(2-morpholinoethyl)benzamide (Moclobemide) (85)

Prepared according to the general procedure A using 1-bromo-4-chlorobenzene (19 mg, 0.1 mmol, 1.0 equiv.), the corresponding dihydropyridine **1q** (61.4 mg, 0.15 mmol, 1.5 equiv.), 4CzIPN (1.2 mg, 0.015 mmol, 1.5

mol%), $NiCl_2$·dme (1.1 mg, 0.005 mmol, 5 mol %), and dMeObpy (2.2 mg, 0.01 mmol, 10 mol %) in anhydrous THF (2.0 mL, 0.05 M). The crude material was purified by flash column chromatography (DCM/acetone 2:1) to give the corresponding amide **85** (18 mg, 67% yield, average of two runs) as a white solid that displayed spectroscopic data consistent with those reported previously.[17]

^{1}H NMR (400 MHz, $CDCl_3$): δ 7.71 (d, *J* = 8.6 Hz, 2H), 7.42 (d, *J* = 8.5 Hz, 2H), 6.74 (br s, 1H), 3.73 (t, *J* = 4.7 Hz, 4H), 3.55 (q, *J* = 5.8 Hz, 2H), 2.61 (t, *J* = 6.0 Hz, 12H), 2.51 (t, *J* = 4.3, 4H) ppm.

^{13}C NMR (101 MHz, $CDCl_3$): δ 166.3, 137.7, 132.9, 128.8, 128.3, 66.9, 56.8, 53.3, 36.1 ppm.

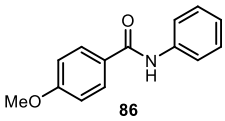

86

4-methoxy-N-phenylbenzamide (86)

Prepared according to the general procedure A using 1-bromo-4-methoxybenzene (18.7 mg, 0.1 mmol, 1.0 equiv.), the corresponding dihydropyridine **1r** (55.9 mg, 0.15 mmol, 1.5 equiv.), 4CzIPN (1.2 mg, 0.015 mmol, 1.5 mol%), $NiCl_2$·dme (1.1 mg, 0.005 mmol, 5 mol %), and dMeObpy (2.2 mg, 0.01 mmol, 10 mol %) in anhydrous THF (2.0 mL, 0.05 M). The crude material was purified by flash column chromatography (*n*-hexane/EtOAc 4:1 to 2:1) to give the corresponding amide **86** (17.5 mg, 77% yield, average of two runs) as a white solid that displayed spectroscopic data consistent with those reported previously.[18]

^{1}H NMR (500 MHz, $CDCl_3$): δ 7.84 (d, *J* = 8.8 Hz, 2H), 7.74 (br s, 1H), 7.63 (d, *J* = 8.2 Hz, 2H), 7.39 – 7.34 (m, 2H), 7.18 – 7.10 (m, 1H), 6.98 (d, *J* = 8.8 Hz, 2H), 3.88 (s, 3H).

^{13}C NMR (126 MHz, $CDCl_3$): δ 165.6, 162.9, 138.5, 129. 5, 129.3, 127.5, 124.7, 120.5, 114.4, 55.8 ppm.

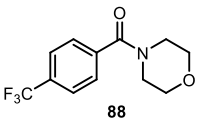

88

N-(4-Trifluoromethylbenzoyl)morpholine (88)

Prepared according to the general procedure A using 4-bromobenzotrifluoride (14 µL, 0.1 mmol, 1.0 equiv.), the corresponding dihydropyridine **1s** (44 mg, 0.12 mmol, 1.2 equiv.), 4CzIPN (1.2 mg, 0.015 mmol, 1.5 mol%), $NiCl_2$·dme (1.1 mg, 0.005 mmol, 5 mol %), and dMeObpy (2.2 mg, 0.01 mmol, 10 mol %) in anhydrous THF (2.0 mL, 0.05 M). The crude material was purified by flash column chromatography (*n*-hexane/EtOAc 2:1) to give the corresponding amide **88** (16 mg, 62% yield, average of two runs) as a white solid that displayed spectroscopic data consistent with those reported previously.[19]

^{1}H NMR (400 MHz, $CDCl_3$): δ 7.71 (d, J = 8.0 Hz, 2H), 7.55 (d, J = 8.1 Hz, 2H), 4.15 – 3.07 (m, 8H).

^{13}C NMR (126 MHz, $CDCl_3$): δ 169.3, 139.2, 132.3 (q, *J* = 32.8 Hz), 127.84, 126.07 (q, *J* = 3.8 Hz), 124.02 (q, *J* = 272.4 Hz), 67.17, 48.47, 42.91 ppm.

^{19}F NMR (376 MHz, $CDCl_3$): δ -63.05 ppm.

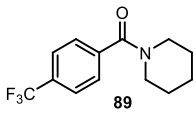

89

Piperidin-1-yl(4-(trifluoromethyl)phenyl)methanone (89)

Prepared according to the general procedure A using 4-bromobenzotrifluoride (14 µL, 0.1 mmol, 1.0 equiv.), the corresponding dihydropyridine **1t** (54,7 mg, 0.15 mmol, 1.5 equiv.), 4CzIPN (1.2 mg, 0.015 mmol, 1.5 mol%), $NiCl_2$·dme (1.1 mg, 0.005 mmol, 5 mol %), and dMeObpy (2.2 mg, 0.01 mmol, 10 mol %) in anhydrous THF (2.0 mL, 0.05 M). The crude material was purified by flash column chromatography (*n*-hexane/EtOAc 2:1) to give the corresponding amide **89** (19 mg, 74% yield, average of two runs) as a pale yellow solid that displayed spectroscopic data consistent with those reported previously.[20]

^{1}H NMR (400 MHz, $CDCl_3$): δ 7.66 (d, *J* = 8.1 Hz, 2H), 7.50 (d, *J* = 8.0 Hz, 2H), 3.72 (s, 2H), 3.29 (s, 2H), 1.69 (s, 4H), 1.52 (s, 2H) ppm.

^{13}C NMR (101 MHz, $CDCl_3$): δ 169.1, 140.5, 131.7 (q, *J* = 32.6 Hz), 127.5, 125.9 (q, *J* = 3.8 Hz), 124.1 (q, *J* = 272 Hz), 49.0, 43.5, 26.9, 25.9, 24.9 ppm.

^{19}F NMR (376 MHz, $CDCl_3$): δ -62.96 ppm.

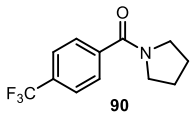

90

Pyrrolidin-1-yl(4-(trifluoromethyl)phenyl)methanone (90)

Prepared according to the general procedure A using 4-bromobenzotrifluoride (14 µL, 0.1 mmol, 1.0 equiv.), the corresponding dihydropyridine **1u** (53 mg, 0.15 mmol, 1.5 equiv.), 4CzIPN (1.2 mg, 0.015 mmol, 1.5 mol%), $NiCl_2$·dme (1.1 mg, 0.005 mmol, 5 mol %), and dMeObpy (2.2 mg, 0.01 mmol, 10 mol %) in anhydrous THF (2.0 mL, 0.05 M). The crude material was purified by flash column chromatography (*n*-hexane/EtOAc 1:1) to give the corresponding amide **90** (16 mg, 66% yield, average of two runs) as a pale yellow solid that displayed spectroscopic data consistent with those reported previously.[21]

^{1}H NMR (400 MHz, $CDCl_3$): δ 7.67 (d, *J* = 8.5 Hz, 2H), 7.62 (d, *J* = 8.5 Hz, 2H), 3.66 (t, *J* = 6.9 Hz, 2H), 3.39 (t, *J* = 6.6 Hz, 2H), 2.01 – 1.94 (m, 2H), 1.93 – 1.86 (m, 1H) ppm.

^{13}C NMR (101 MHz, $CDCl_3$): δ 168.3, 140.7, 131.7 (q, *J* = 32.7 Hz), 127.5, 125.4 (q, *J* = 3.8 Hz), 123.8 (q, *J* = 272 Hz), 49.5, 46.3, 26.4, 24.4 ppm.

^{19}F NMR (376 MHz, $CDCl_3$): δ -62.60 ppm.

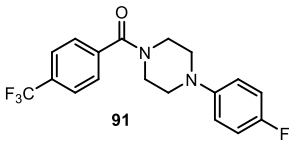

91

[4-(4-fluorophenyl)piperazin-1-yl]-[4-(trifluoromethyl)phenyl]methanone (91)

Prepared according to the general procedure A using 4-bromobenzotrifluoride (14 µL, 0.1 mmol, 1.0 equiv.), the corresponding dihydropyridine **1v** (68.9 mg, 0.15 mmol, 1.5 equiv.), 4CzIPN (1.2 mg, 0.015 mmol, 1.5 mol%), $NiCl_2$·dme (1.1 mg, 0.005 mmol, 5 mol %), and dMeObpy (2.2 mg, 0.01 mmol, 10 mol %) in anhydrous THF (2.0 mL, 0.05 M). Irradiation time: 36 hours. The crude material was purified by flash column chromatography (*n*-hexane/EtOAc 3:2) to give the corresponding amide **91** (20 mg, 57% yield, average of two runs) as a white solid.

^{1}H NMR (400 MHz, $CDCl_3$): δ 7.72 (d, *J* = 7.9 Hz, 1H), 7.57 (d, *J* = 8.3 Hz, 1H), 7.04 – 6.97 (m, 2H), 6.96 – 6.89 (m, 2H), 3.98 (br s, 2H), 3.58 (br s, 2H), 3.21 (br s, 2H), 3.07 (br s, 2H) ppm.

^{13}C NMR (101 MHz, $CDCl_3$): δ 168.9, 159.0, 156.7, 147.3, 139.1, 131.8 (q, *J* = 32.8 Hz), 127.5, 125.7 (q, *J* = 3.8 Hz), 123.7 (q, *J* = 272.4 Hz), 118.9, 118.8, 115.9, 115.7, 50.8, 47.6, 42.2, 29.7ppm.

^{19}F NMR (376 MHz, $CDCl_3$): δ -62.62, -122.55 ppm.

HRMS (ESI, m/z) calcd. for $C_{18}H_{16}F_4N_2NaO$ ($[M+Na]^+$): 375.1091, found 375.1092.

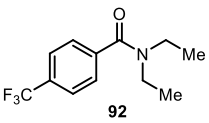

92

N,N-diethyl-4-(trifluoromethyl)benzamide (92)

Prepared according to the general procedure A using 4-bromobenzotrifluoride (14 µL, 0.1 mmol, 1.0 equiv.), the corresponding dihydropyridine **1w** (52.9 mg, 0.15 mmol, 1.5 equiv.), 4CzIPN (1.2 mg, 0.015 mmol, 1.5 mol%), $NiCl_2$·dme (1.1 mg, 0.005 mmol, 5 mol %), and dMeObpy (2.2 mg, 0.01 mmol, 10 mol %) in anhydrous 1,4-dioxane (2.0 mL, 0.05 M). Irradiation time: 36 hours. The crude material was purified by flash column chromatography (*n*-hexane/EtOAc 4:1) to give the corresponding amide **92** (14 mg, 58% yield, average of two runs) as a white solid that displayed spectroscopic data consistent with those reported previously.[22]

^{1}H NMR (400 MHz, $CDCl_3$): δ 7.65 (d, *J* = 8.2 Hz, 2H), 7.48 (d, *J* = 8.5 Hz, 2H), 3.56 (q, *J* = 6.9 Hz, 2H), 3.21 (q, *J* = 6.7 Hz, 2H), 1.25 (t, *J* = 6.1 Hz, 3H), 1.11 (t, *J* = 6.1 Hz, 3H) ppm.

^{13}C NMR (101 MHz, $CDCl_3$): δ 169.81, 131.17 (q, *J* = 32.8 Hz), 126.68, 125.54 (q, *J* = 3.8 Hz), 123.80 (q, *J* = 272.2 Hz), 43.25, 39.38, 14.19, 12.86 ppm.

^{19}F NMR (376 MHz, $CDCl_3$): -62.93 ppm.

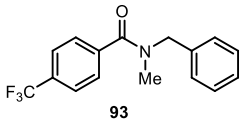

93

N-benzyl-N-methyl-4-(trifluoromethyl)benzamide (93)

Prepared according to the general procedure A using 4-bromobenzotrifluoride (14 µL, 0.1 mmol, 1.0 equiv.), the corresponding dihydropyridine **1x** (60.1 mg, 0.15 mmol, 1.5 equiv.), 4CzIPN (1.2 mg, 0.015 mmol, 1.5 mol%), $NiCl_2$·dme (1.1 mg, 0.005 mmol, 5 mol %), and dMeObpy (2.2 mg, 0.01 mmol, 10 mol %) in anhydrous THF (2.0 mL, 0.05 M). The crude material was purified by flash column chromatography (*n*-hexane/EtOAc 4:1) to give the corresponding amide **93** (10 mg, 34% yield, average of two runs) as a yellow oil.[23]

^{1}H NMR (300 MHz, $CDCl_3$): δ 7.78 – 7.52 (m, 4H), 7.44 – 7.30 (m, 5H), 7.17 (s, 1H), 4.79 (s, 1H), 4.49 (s, 1H), 2.98 (d, J = 65.4 Hz, 3H) ppm.

^{13}C NMR (101 MHz, $CDCl_3$): δ 170.9, 170.1, 139.9, 136.6, 136.1, 131.8, 129.0, 128.8, 128.3, 127.9, 127.74, 127.4, 127.2, 126.6, 125.6, 125.1, 122.37, 55.04, 50.86, 36.84, 33.31 ppm.

^{19}F NMR (376 MHz, $CDCl_3$): δ -62.98 ppm.

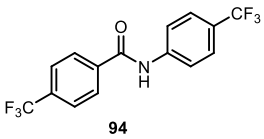

94

4-(trifluoromethyl)-N-(4-(trifluoromethyl)phenyl)-benzamide (94)

Prepared according to the general procedure A using 4-bromobenzotrifluoride (14 µL, 0.1 mmol, 1.0 equiv.), the corresponding dihydropyridine **1y** (66 mg, 0.15 mmol, 1.5 equiv.), 4CzIPN (1.2 mg, 0.015 mmol, 1.5 mol%), $NiCl_2$·dme (1.1 mg, 0.005 mmol, 5 mol %), and dMeObpy (2.2 mg, 0.01 mmol, 10 mol %) in anhydrous THF (2.0 mL, 0.05 M). The crude material was purified by flash column chromatography (*n*-hexane/EtOAc 20:1) to give the corresponding amide **94** (28 mg, 85% yield) as white solid that displayed spectroscopic data consistent with those reported previously.[25]

^{1}H NMR (500 MHz, $(CD_3)_2CO$): δ 10.05 (s, 1H), 8.22 (d, *J* = 8.1 Hz, 1H), 8.07 (d, *J* = 0.6 Hz, 1H), 7.9 (d, *J* = 8.1 Hz, 1H), 7.7 (d, *J* = 8.2 Hz, 2H) ppm.

^{13}C NMR (101 MHz,$(CD_3)_2CO$): δ 164.7, 138.6, 132.8, 132.5, 128.5, 125.9 (q, *J* = 3.8 Hz), 125.5 (q, *J* = 3.8 Hz), 125.1 (d, *J* = 32.1 Hz), 122.9 (d, *J* = 48.5 Hz), 120.4, 120.1, 120.0 ppm.

^{19}F NMR (376 MHz, $(CD_3)_2CO$): δ -62.22, -63.17 ppm.

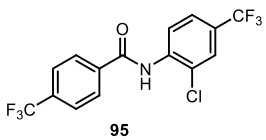

95

N-(2-chloro-4-(trifluoromethyl)phenyl)-4-(trifluoromethyl)benzamide (95)

Prepared according to the general procedure A using 4-bromobenzotrifluoride (14 µL, 0.1 mmol, 1.0 equiv.), the corresponding dihydropyridine **1z** (71 mg, 0.15 mmol, 1.5 equiv.), 4CzIPN (1.2 mg, 0.015 mmol, 1.5 mol%), $NiCl_2$·dme (1.1

mg, 0.005 mmol, 5 mol %), and dMeObpy (2.2 mg, 0.01 mmol, 10 mol %) in anhydrous THF (2.0 mL, 0.05 M). The crude material was purified by flash column chromatography (*n*-hexane/EtOAc 10:1) to give the corresponding amide **95** (20 mg, 55% yield) as white solid.

^{1}H NMR (500 MHz, $CDCl_3$):δ 8.75 (d, *J* = 9.2 Hz, 1H), 8.56 (s, 1H), 8.04 (d, *J* = 7.7 Hz, 1H), 7.82 (d, *J* = 7.9 Hz, 1H), 7.72 (dd, *J* = 2.2, 0.8 Hz, 1H), 7.62 (d, *J* = 8.5 Hz, 1H) ppm.

^{13}C NMR (126 MHz, $CDCl_3$): δ 164.4, 137.7, 137.6, 134.67 (q, *J* = 33.1 Hz), 128.0, 127.4 (q, *J* = 33.7 Hz), 126.7 (q, *J* = 3.8 Hz), 126.5 (q, *J* = 3.7 Hz), 125.6 (q, *J* = 3.7 Hz), 124.8 (d, *J* = 32.1 Hz), 123.3, 122.6 (q, *J* = 31.4 Hz), 121.5 ppm.

^{19}F NMR (376 MHz, $CDCl_3$): δ -62.09, -62.81 ppm.

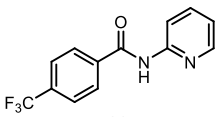

96

N-(pyridin-2-yl)-4-(trifluoromethyl)benzamide (96)

Prepared according to the general procedure A using 4-bromobenzotrifluoride (14 µL, 0.1 mmol, 1.0 equiv.), the corresponding dihydropyridine **1aa** (56 mg, 0.15 mmol, 1.5 equiv.), 4CzIPN (1.2 mg, 0.015 mmol, 1.5 mol%), $NiCl_2$·dme (1.1 mg, 0.005 mmol, 5 mol %), and dMeObpy (2.2 mg, 0.01 mmol, 10 mol %) in anhydrous THF (2.0 mL, 0.05 M). The crude material was purified by flash column chromatography (*n*-hexane/EtOAc 10:1) to give the corresponding amide **96** (20 mg, 75% yield) as white solid that displayed spectroscopic data consistent with those reported previously.[26]

^{1}H NMR (400 MHz, $CDCl_3$): δ 8.88 (s, 1H), 8.38 (d, *J* = 8.4 Hz, 1H), 8.25 (dt, *J* = 4.1, 1.0 Hz, 1H), 8.04 (d, *J* = 8.1 Hz, 2H), 7.83 – 7.72 (m, 3H), 7.09 (ddd, *J* = 7.4, 4.9, 1.0 Hz, 1H) ppm

^{13}C NMR (101 MHz, $CDCl_3$): δ 164.5, 151.2, 147.9, 138.7, 137.6, 133.9 (d, *J* = 32.8 Hz), 127.8, 125.9 (q, *J* = 3.7 Hz), 123.6 (q, *J* = 272.7 Hz), 120.3, 114.4 ppm.

^{19}F NMR (376 MHz, $CDCl_3$): δ -62.74 ppm.

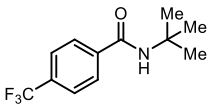

97

N-(*tert*-butyl)-4-(trifluoromethyl)benzamide (97)

Prepared according to the general procedure A using 4-bromobenzotrifluoride (14 µL, 0.1 mmol, 1.0 equiv.), the corresponding dihydropyridine **1ab** (53 mg, 0.15 mmol, 1.5 equiv.), 4CzIPN (1.2 mg, 0.015 mmol, 1.5 mol%), $NiCl_2$·dme (1.1 mg, 0.005 mmol, 5 mol %), and dMeObpy (2.2 mg, 0.01 mmol, 10 mol %) in anhydrous THF (2.0 mL, 0.05 M). The crude material was purified by flash column chromatography (*n*-hexane/Et_2O 10:1) to give the corresponding amide **97** (15 mg, 61 % yield) as white solid that displayed spectroscopic data consistent with those reported previously.[27]

^{1}H NMR (400 MHz, $CDCl_3$): δ 7.82 (d, *J* = 8.2 Hz, 1H), 7.67 (d, *J* = 7.9 Hz, 1H), 5.94 (br s, 1H), 1.48 (s, 9H) ppm.

^{13}C NMR (126 MHz, $CDCl_3$): δ 165.9, 139.6, 133.2 (q, *J* = 32.7 Hz), 127.6, 125.9 (q, *J* = 3.8 Hz), 124.1 (d, *J* = 272.8 Hz), 52.4, 29.2 ppm.

^{19}F NMR (376 MHz, $CDCl_3$): δ -63.00 ppm.

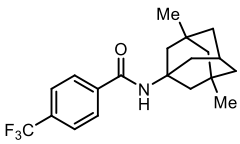

98

N-(3,5-dimethyladamant-1-yl)-4-(trifluoromethyl)benzamide (98)

Prepared according to the general procedure A using 4-bromobenzotrifluoride (14 μL, 0.1 mmol, 1.0 equiv.), the corresponding dihydropyridine **1ac** (67 mg, 0.15 mmol, 1.5 equiv.), 4CzIPN (1.2 mg, 0.015 mmol, 1.5 mol%), $NiCl_2$·dme (1.1 mg, 0.005 mmol, 5 mol %), and dMeObpy (2.2 mg, 0.01 mmol, 10 mol %) in anhydrous THF (2.0 mL, 0.05 M). The crude material was purified by flash column chromatography (*n*-hexane/DCM 1:1) to give the corresponding amide **98** (30 mg, 85 % yield) as white solid that displayed spectroscopic data consistent with those reported previously.[28]

^{1}H NMR (400 MHz, $CDCl_3$): δ7.80 (d, J = 8.2 Hz, 2H), 7.66 (d, *J* = 8.2 Hz, 2H), 5.83 (s, 1H), 2.20 (p, *J* = 3.2 Hz, 1H), 1.96 (d, *J* = 3.3, 2H), 1.84 – 1.71 (m, 4H), 1.48 – 1.11 (m, 6H), 0.89 (s, 6H) ppm.

^{13}C NMR (101 MHz, $CDCl_3$): δ 165.4, 139.3, 132.8 (d, *J* = 32.6 Hz), 127.2, 125.5 (q, *J* = 3.8 Hz), 123.7 (q, *J* = 272.5 Hz), 54.3, 50.6, 47.6, 42.6, 40.2, 32.5, 30.2, 30.03 ppm.

^{19}F NMR (376 MHz, $CDCl_3$): δ -62.99 ppm.

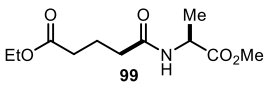

99

Ethyl (S)-5-((1-methoxy-1-oxopropan-2-yl)amino)-5-oxopentanoate (99)

Prepared according to the general procedure A using ethyl 4-bromobutanoate (14 μL, 0.1 mmol, 1.0 equiv.), the dihydropyridine **1-ala** (57 mg, 0.15 mmol, 1.5 equiv.), 4CzIPN (1.2 mg, 0.015 mmol, 1.5 mol%), $NiCl_2$·dme (2.2 mg, 0.01 mmol, 10 mol %), and 4,4'-dimethyl bipyridine (2.2 mg, 0.012 mmol, 12 mol %) in anhydrous THF (2.0 mL, 0.1 M). The crude material was purified by flash column chromatography (*n*-hexane/EtOAc 2:1) to give the corresponding amide **98** (10 mg, 40 % yield) as colorless oil.
^{1}H NMR (400 MHz, $CDCl_3$): δ 6.13 (d, *J* = 7.6 Hz, 1H), 4.62 (p, *J* = 7.2 Hz, 1H), 4.15 (q, *J* = 7.1 Hz, 2H), 3.77 (s, 3H), 2.48 – 2.36 (m, 2H), 2.35 – 2.26 (m, 2H), 2.06 – 1.93 (m, 2H), 1.42 (d, *J* = 7.2 Hz, 3H), 1.32 – 1.24 (m, 3H) ppm.

^{13}C NMR (101 MHz, $CDCl_3$): δ 173.6, 173.2, 171.70, 60.4, 52.5, 47.9, 35.2, 33.2, 20.8, 18.5, 14.2 ppm.

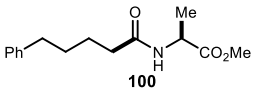

100

Methyl (5-phenylpentanoyl)-L-alaninate (100)

Prepared according to the general procedure A using ethyl 4-bromobutyl benzene (17 µL, 0.1 mmol, 1.0 equiv.), the dihydropyridine **1-ala** (57 mg, 0.15 mmol, 1.5 equiv.), 4CzIPN (1.2 mg, 0.015 mmol, 1.5 mol%), $NiCl_2$·dme (2.2 mg, 0.01 mmol, 10 mol %), and 4,4'-dimethyl bipyridine (2.2 mg, 0.012 mmol, 12 mol %) in anhydrous THF (2.0 mL, 0.1 M). The crude material was purified by flash column chromatography (*n*-hexane/EtOAc 2:1) to give the corresponding amide **100** (10 mg, 35 % yield) as colorless oil.

^{1}H NMR (400 MHz, $CDCl_3$): δ 7.32 – 7.25 (m, 2H), 7.22 – 7.15 (m, 3H), 5.98 (br s, 1H), 4.66 – 4.53 (m, 1H), 3.76 (s, 3H), 2.65 (t, *J* = 7.2 Hz, 2H), 2.25 (t, *J* = 7.1 Hz, 2H), 1.78 – 1.64 (m, 4H), 1.41 (d, *J* = 7.2 Hz, 3H) ppm.

4.10.7. 15 mmol Scale Reaction

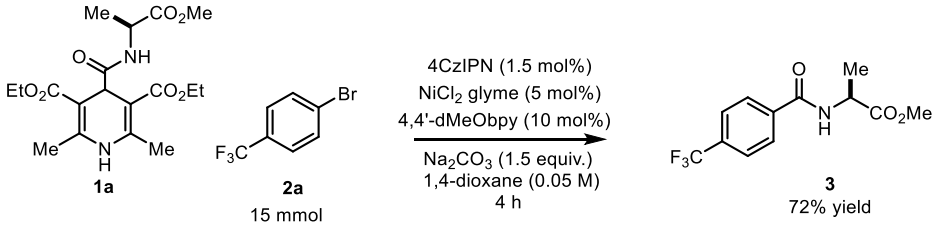

The scale-up was performed in an immersion-well reactor purchased from Peschl Ultraviolet GmbH. Reactor specifications:

Reactor volume: 350 mL
Optical path length: 14 mm
Wavelength: λ_{max} = 460 nm
Radiant flux: 27 W

Procedure

To the reaction flask fitted with stirring magnet was added 1-bromo-4-(trifluoromethyl)benzene **2a** (3.38 g, 15.0 mmol, 1.0 equiv.), diethyl 4-{[(2*S*)-1-methoxy-1-oxopropan-2-yl]carbamoyl}-2,6-dimethyl-1,4-dihydropyridine-3,5-dicarboxylate **1-ala** (8.60 g, 22.5 mmol, 1.5 equiv.), and 4CzIPN (178 mg, 0.225 mmol, 0.015 equiv.), $NiCl_2$·dme (165 mg, 0.75 mmol, 5 mol %), dMeObpy (324 mg, 1.5 mmol, 10 mol %) and Na_2CO_3 (2.38 g, 22.5 mmol, 1.5 equiv.), followed by anhydrous 1,4-dioxane (300 mL). The mixture was degassed by bubbling argon through the solution for 20 minutes, then and the flask was sealed (!! IMPORTANT – this set-up is not gas-tight, the CO_2 generated is released through the seals preventing pressure buildup!!). The immersion tube was fitted and the the reaction was

irradiated with for 4 h, then the crude reaction mixture was analyzed by LCMS. Following the reaction, water was added to the reaction (200 mL) and the mixture was extracted with EtOAc (3 x 200 mL). The combined organic phases were washed with water and brine, dried with Na_2SO_4 and filtered. The reaction mixture was concentrated and purified by silica gel column chromatography gradient column to provide the pure product (2.97 g, 72%).

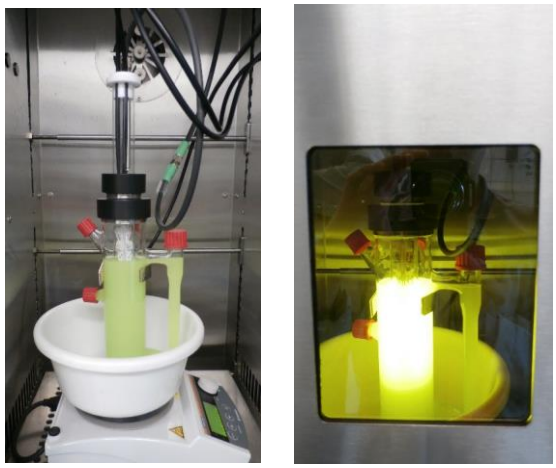

Figure S4.6. Immersion-well photoreactor fitted with a 460 nm high-power LED.

4.10.8. Evaluation of the Excited State Potential of Carbamoyl-DHP 1a

Using the data collected from the cyclic voltammetry studies and from the absorption spectra of the carbamoyl-DHP **1a** (Chapter 4.3.1.), we could estimate the redox potential of the excited carbamoyl-DHP **1a*** employing the following Equation 1[56]:

$$E(\mathbf{1a}^{\cdot+}/\mathbf{1a^*}) = E(\mathbf{1a}^{\cdot+}/\mathbf{1a}) + E_{0\text{-}0}(\mathbf{1a^*/1a}) \quad [\text{Eq. 1}]$$

Since the electrochemical oxidation of the DHP **1a** was irreversible (Figure 4.4.), the irreversible peak potential E_p^{Anode} was used for $E(\mathbf{1a}^{\cdot+}/\mathbf{1a})$. $E_{0\text{-}0}(\mathbf{1a^*/1a})$, which is the excited state energy of the carbamoyl-DHP **1a**, was estimated spectroscopically from the position of the long wavelength tail of the absorption spectrum (until 415 nm, Figure 4.3.) recorded in acetonitrile, the solvent used for the electrochemical analysis.[57]

[56] Kavarnos, G. J. In Fundamentals of Photoinduced Electron Transfer. VCH Publishers: New York, 1993, pp 29–40.
[57] Balzani, V.; Ceroni, P.; Juris, A. In Photochemistry and Photophysics, Wiley-VCH: Weinheim, 2014, pp 103-123.

For the carbamoyl-DHP **1a**, the E_p^{anode}, which provides the E(**1a**$^{\cdot+}$/**1a**), is 1.20 V (Figure 4.4.), while the position of the long wavelength tail of the absorption spectrum corresponds to 415 nm (Figure 4.3.), which translates into an $E_{0\text{-}0}$(**1a***/**1a**) of 2.98 eV.

$$E(\mathbf{1a^*}/\mathbf{1a}^{\cdot-}) = 1.20 - 2.98 = \mathbf{-1.78\ V}\ (\text{vs Ag/AgCl})$$

4.10.9. General Procedure for the Carbamoylation of Aryl Bromide *via* Direct Excitation of Carbamoyl-DHPs

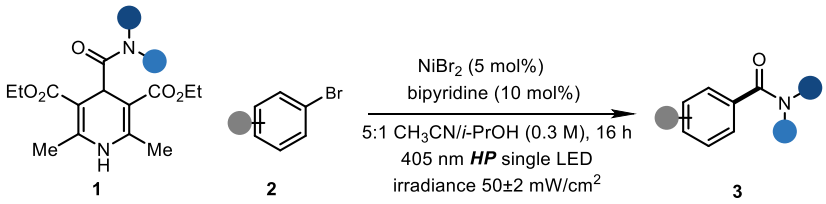

General procedure C: An oven dried Schlenk tube equipped with a stir bar was charged with (hetero)aryl bromide **2** (*if solids*, 0.1 mmol, 1 equiv.) and dihydropyridines **1** (0.15 mmol, 1.5 equiv.) followed by addition of $NiCl_2$·dme (0.005 mmol, 5 mol%), bipyridine (0.01 mmol. 10 mol%), anhydrous CH_3CN (250 µL) and *iso*-propanol (50 µL) and (hetero)aryl bromide (*if liquids or oils*). The tube was sealed and the reaction mixture was degassed via freeze-pump-thaw procedure (2 cycles) and backfilled with argon. The reaction was placed on a high-power single LED (λ_{max} = 405 nm, irradiance = 50 ± 2 mW/cm^2, as controlled by an external power supply). Following the reaction, the reaction mixture was filtered through silica gel with EtOAc and concentrated in vacuo. The crude material was purified by flash column chromatography in silica gel to afford the corresponding product

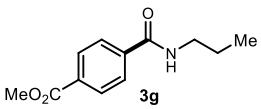

Methyl 4-(propylcarbamoyl)benzoate (3g)

Prepared according to the general procedure C using methyl 4-bromobenzoate (22 mg, 0.1 mmol, 1.0 equiv.), the corresponding dihydropyridine (51 mg, 0.15 mmol, 1.5 equiv.), $NiBr_2$ (1.1 mg, 0.005 mmol, 5 mol %), and bipyridine (1.6 mg, 0.01 mmol, 10 mol %). The crude material was purified by flash column chromatography (*n*-hexane/EtOAc 2:1) to give the corresponding amide **3g** (5 mg, 20 % yield) as white solid.

^{1}H NMR (400 MHz, $CDCl_3$): δ 8.08 (d, *J* = 8.5 Hz, 2H), 7.85 (d, *J* = 8.8 Hz, 2H), 6.37 (s, 1H), 3.46 – 3.39 (m, 2H), 1.65 – 1.55 (m, 2H), 0.99 (t, *J* = 7.2 Hz, 3H).

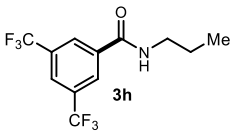

***N*-propyl-3,5-bis(trifluoromethyl)benzamide (3h)**

Prepared according to the general procedure C using methyl 1,3-bis(trifluoromethyl)-5-bromobenzene (17.3 µL, 0.1 mmol, 1.0 equiv.), the corresponding dihydropyridine (51 mg, 0.15 mmol, 1.5 equiv.), $NiBr_2$ (1.1 mg, 0.005 mmol, 5 mol %), and bipyridine (1.6 mg, 0.01 mmol, 10 mol %). The crude material was purified by flash column chromatography (*n*-hexane/EtOAc 2:1) to give the corresponding amide **3h** (11.5 mg, 38 % yield) as white solid.

^{1}H NMR (400 MHz, $CDCl_3$): δ 7.97 (t, *J* = 2.5 Hz, 1H), 7.81 (dd, *J* = 2.2, 2.0 Hz, 2H), 6.40 (s, 1H), 3.48 – 3.31 (m, 2H), 1.63 – 1.53 (m, 2H), 0.96 (t, *J* = 7.3 Hz, 3H).

Chapter V

General Conclusions

During my doctoral studies, I have explored the potential of dihydropyridine derivatives to serve as versatile reagents in different photochemical processes. Chapter III describes the use of 4-alkyl-1,4-dihydropyridines (alkyl-DHPs) as electron donors and radical precursors in the photochemical enantioselective β-alkylation of α,β-unsaturated aldehydes. The chemistry exploits the ability of excited-state chiral iminium ions to behave as strong oxidants, triggering the generation of C(sp^3)-centered radicals from the readily available alkyl-DHPs. This transformation provides a strategy for the direct regio- and stereoselective installation of various alkyl fragments at the β-carbon of enals under mild conditions.

In Chapter IV, we demonstrated that 4-carbamoyl-1,4-dihydropyridines (carbamoyl-DHPs) are useful carbamoyl precursors for photochemical catalytic amide synthesis. In a first approach, we showed that selective absorption of violet light turned carbamoyl-DHPs into strong reducing agents that can modulate the oxidation state of a nickel catalyst through single-electron transfer while undergoing homolytic cleavage to deliver carbamoyl radicals. This photochemical reactivity was combined with a nickel catalytic cross-coupling mechanism to enable the carbamoylation of aryl bromides. This approach afforded aryl amides. We later showed that the catalytic photochemical amide formation strategy could be improved using an external photoredox catalyst. The developed strategy tolerates sensitive functional groups and allows the installation of amide scaffolds within substrates of pharmaceutical relevance. In addition, we demonstrated that the reaction can be performed in 15 mmol scale without the need for reoptimization using an immersion-well batch reactor.

UNIVERSITAT ROVIRA I VIRGILI
1,4-DIHYDROPYRIDINES AS VERSATILE REAGENTS IN PHOTOCHEMICAL CARBON-CARBON BOND-FORMING PROCESSES
Nurtalya Alandini

UNIVERSITAT ROVIRA I VIRGILI
1,4-DIHYDROPYRIDINES AS VERSATILE REAGENTS IN PHOTOCHEMICAL CARBON-CARBON BOND-FORMING PROCESSES
Nurtalya Alandini

UNIVERSITAT
ROVIRA i VIRGILI